Sustainable Drinking Water Treatment:

Using Weak Base Anion Exchange Sorbents Embedded With Metal Oxide Nanoparticles

to Simultaneously Remove Multiple Oxoanions

by

James McKay Gifford

A Dissertation Presented in Partial Fulfillment
of the Requirements for the Degree
Doctor of Philosophy

Approved November 2015 by the
Graduate Supervisory Committee:

Paul Westerhoff, Co-Chair
Kiril Hristovski, Co-Chair
Mikhail Chester

ARIZONA STATE UNIVERSITY

May 2016

ABSTRACT

Ion exchange sorbents embedded with metal oxide nanoparticles can have high affinity and high capacity to simultaneously remove multiple oxygenated anion contaminants from drinking water. This research pursued answering the question, "Can synthesis methods of nano-composite sorbents be improved to increase sustainability and feasibility to remove hexavalent chromium and arsenic simultaneously from groundwater compared to existing sorbents?" Preliminary nano-composite sorbents outperformed existing sorbents in equilibrium tests, but struggled in packed bed applications and at low influent concentrations. The synthesis process was then tailored for weak base anion exchange (WBAX) while comparing titanium dioxide against iron hydroxide nanoparticles (Ti-WBAX and Fe-WBAX, respectively). Increasing metal precursor concentration increased the metal content of the created sorbents, but pollutant removal performance and usable surface area declined due to pore blockage and nanoparticle agglomeration. An acid-post rinse was required for Fe-WBAX to restore chromium removal capacity. Anticipatory life cycle assessment identified critical design constraints to improve environmental and human health performance like minimizing oven heating time, improving pollutant removal capacity, and efficiently reusing metal precursor solution. The life cycle environmental impact of Ti-WBAX was lower than Fe-WBAX as well as a mixed bed of WBAX and granular ferric hydroxide for all studied categories. A separate life cycle assessment found the total number of cancer and non-cancer cases prevented by drinking safer water outweighed those created by manufacture and use of water treatment materials and energy. However, treatment relocated who bore the health risk, concentrated it in a sub-population, and changed the primary manifestation from

cancer to non-cancer disease. This tradeoff was partially mitigated by avoiding use of pH control chemicals. When properly synthesized, Fe-WBAX and Ti-WBAX sorbents maintained chromium removal capacity while significantly increasing arsenic removal capacity compared to the parent resin. The hybrid sorbent performance was demonstrated in packed beds using a challenging water matrix and low pollutant influent conditions. Breakthrough curves hint that the hexavalent chromium is removed by anion exchange and the arsenic is removed by metal oxide sorption. Overall, the hybrid nano-sorbent synthesis methods increased sustainability, improved sorbent characteristics, and increased simultaneous removal of chromium and arsenic for drinking water.

DEDICATION

I dedicate my life and this dissertation to my amazing wife, Alisa. She inspires me to be my best, supports me through the hard days and long nights, all while spectacularly balancing being a mother, physician assistant, and disciple. She knows the content of this dissertation as well as I do, which is a comment to both her intelligence and her selfless interest in understanding what I care about.

This dissertation is the fourth best thing I have helped create over the last six years. I also dedicate it the first three: our incredible children, Blaine, Christine, and Dustin. The ways and extent to which they will impact the world eclipse anything that can be contained herein.

Thank you to my mother Carrie who taught me to love to learn, and my father Brent who taught me to love engineering. Thank you to Debbie who showed me how to simultaneously be a successful graduate student and parent young children, Ron who showed me to simultaneously be scientific and laugh, and Trudy who showed me to simultaneously handle professional pressure and excel in personal endeavors.

ACKNOWLEDGMENTS

Thank you to my research advisor Paul Westerhoff whose outstanding mentorship and willingness to challenge me forever changed the direction of my life, and whose ideas inspired the direction of this research. Thank you to Kiril Hristovski and Mikhail Chester whose input was vital to reaching the impactful findings. Thank you to professional mentors Bruce Rittmann, Brad Allenby, Jim Elser, and Helen Rowe who strongly influenced the way this research was carried out and interpreted.

Funding for this research has been provided by the United States Environmental Protection Agency under EPA-G2011-STAR-G1 and EPA-F2013-STAR-E1 Graduate Fellowship for Environmental Studies. Personal financial support has been provided by Ron & Sharon Thomas, Irene Douglas through the Achievement Reward for College Scientist Foundation, and the AZ Water Professional Association.

TABLE OF CONTENTS

LIST OF TABLES

LIST OF FIGURES

Figure Page

CHAPTER 1

INTRODUCTION AND BACKGROUND

IDENTIFYING THE NEED FOR SIMULTANEOUS TREATMENT

An easily overseen dirt road lined with saguaro cactus and sage brush cuts through the Sonoran Desert about an hour south of Phoenix. It ends in a small, quiet community that has about 10 sporadically placed houses. The community water comes from a single well that pumps into a pneumatic tank for storage and pressure. Hypochlorite is added for disinfection, but no further treatment is provided before distribution. This town is typical of many very small drinking water systems throughout the state of Arizona and the nation. The Environmental Protection Agency (EPA) defines very small drinking water systems as serving between 25 and 500 people, and estimates that 84% of water utilities fall into this category. These systems face unique challenges due to their size, which is why they account for 79% of all maximum contaminant level (MCL) violations, including 87% of all arsenic MCL violations (Impellitteri et al. 2007). Despite the challenges, they serve people who are still equally entitled to a clean water supply.

Challenges for water treatment in small systems. Small systems face challenges that current treatment technologies do not address because of limited access to resources such as capital and operational expertise. Communities must therefore try to meet multiple treatment goals with only few resources available. Few customers means there is limited capital and therefore difficult to afford installation of multiple treatment processes to address multiple treatment goals. Access to water must be less than 2.5% of total income to be considered affordable (Baird 2010) and significant capital expenditure

by the utility may cause rates to exceed this threshold. For example, 500 people with an American average income of $52,250 per year (Noss 2014) could therefore only afford a maximum utility operational cost of $653,000 per year, including amortized capital spending. Without economy of scale resultant from large-scale equipment purchases, this is very difficult to attain. Additionally, with low operational budget comes limited access to and ability to pay for expert operators.

Traditional approaches to simultaneous pollutant removal are limited in their applicability for small systems, indicating new technologies need to be developed. Sorption vessels with beds of mixed media or different media in series are limited in their pollutant removal capacity as only a fraction of the sorbent material is working for any given pollutant. Regeneration of such a system requires cost and operational effort to separate the media, apply a mixed regeneration solution, and to remix the bed. Reverse osmosis is effective at removing multiple contaminants, but is extremely energy intensive, often involves pre-treatment, and fouls quickly requiring operator attention. Coagulation processes require precise dosing, creates many residuals that may be difficult to handle in remote locations, and is operationally intensive. It is clear that current technology does not address the needs of small systems for simultaneous removal of drinking water pollutants.

The main water quality concern for small systems is inorganic contaminants that pose chronic exposure problems such as chromium, arsenic, nitrate, fluoride, and perchlorate. This is because 95% of very small systems operate on groundwater, 60% of which have no additional treatment beyond disinfection (Impellitteri et al. 2007). The disinfection mitigates acute health risks stemming from bacterial and viral contaminants,

but does not address inorganic contaminants. This research focuses on two prevalent inorganic groundwater pollutants: hexavalent chromium (Cr(VI)) and arsenic (As). Cr(VI) is an oxidized metal that is under enhanced monitoring and toxicology review by the EPA (USEPA 2010a, Register 2012). California recently enacted a public health goal of 0.02 µg/L for Cr(VI), treating it as a possible ingested human carcinogen, with an enforceable MCL of 10 µg/L (CCR 2014). Cr(VI) is more soluble and more toxic than its trivalent form, and one of the leading treatment technologies is anion exchange (Brandhuber et al. 2004b). As went through similar regulation when its MCL was lowered to 10 µg/L in 2006. It has a variety of human ailments including cancer of the bladder, lungs, and skin (USEPA 2010b). Treatment processes including adsorption to iron (Westerhoff et al. 2005) have been extensively studied but many small systems still struggle to comply. For example, one utility authority serving small systems in Arizona reported 36% of service locations averaged 10 to 32 µg/L of As in 2010 (TOUA 2010). These two inorganic contaminants are the focus of this study due to current regulatory relevance, MCL violation frequency by small systems, common occurrence in groundwater, and similar divalent oxygenated anionic state in pH ranges relevant to drinking water.

Opportunities to improve water treatment technology for small systems. The solution to providing small communities safe drinking water is not to downsize traditional water treatment methods, but create novel paradigms specifically designed to meet their needs. Instead of multiple processes optimized for individual pollutant removal, a single process that removes multiple pollutants concurrently would be simple to operate, as illustrated in Figure 1.1. This approach can reduce cost and complexity,

which is necessary due to lack of specialized personnel and a small funding base. Such a process may not be concerned with optimizing the removal of each pollutant as much as having a single step treatment that can meet multiple treatment goals.

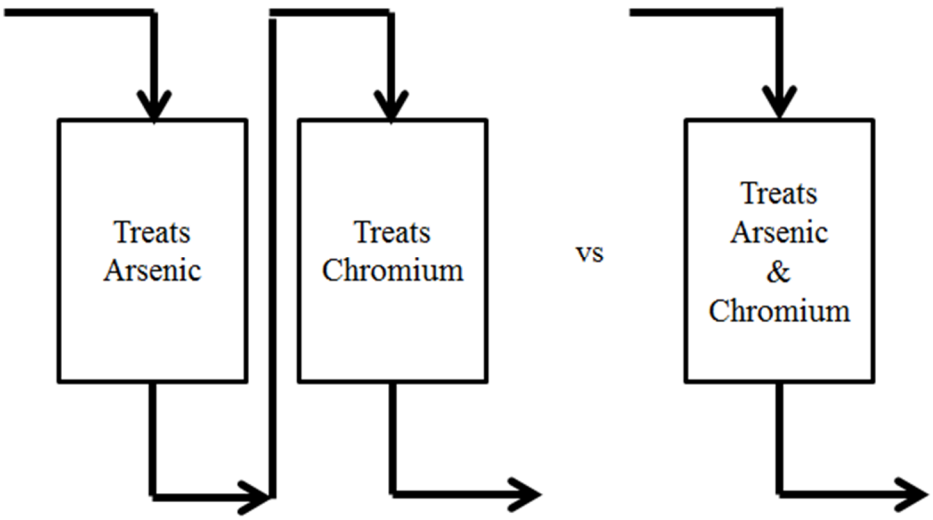

Figure 1.1. A single process that can remove multiple pollutants concurrently may be more simple to operate for small drinking water systems, and use less material with a smaller environmental footprint compared to multiple processes optimized for individual pollutant removal.

Sorption processes have potential to remove each of the identified inorganic contaminants and may be delivered in simple to use and replace cartridges. The cost of sorbent is lower than the salary required for an expert operator with a complicated process. Regeneration may not be necessary if the utility prefers to simply replace a single sorbent cartridge when indicated. Sorbents do not require sensitive chemical dosing or mixing. They do not generate continuous waste streams. Sorbents such as weak base anion exchange resins (WBAX) and metal oxides (MOx) have shown high capacity and affinity for the target pollutants (McGuire et al. 2007, Westerhoff et al. 2005). Hybrids of the other materials have shown promise for simultaneous removal of multiple pollutants (Elton et al. 2013, Hristovski et al. 2008b). An opportunity now exists to develop a new nano-enabled hybrid sorbent using MOx and WBAX (MOx-WBAX) for the simultaneous treatment of the target pollutants.

This research develops the science and technology of sorption processes for simultaneous removal of inorganic pollutants by nano-enabled hybrid sorbents. The focus is on inorganic pollutants due to their occurrence and toxicity in groundwater. The context is small drinking water systems due to the disproportional health risk people served by these systems face. It is novel since it develops simultaneous removal of multiple pollutants instead of viewing multiple constituents as competitive. The broader impact is to develop water treatment technology and scientific understanding to influence how decision makers and technology developers carry out their work, and disseminate the research results for widespread benefit to human health. This impetus is illustrated in Figure 1.2.

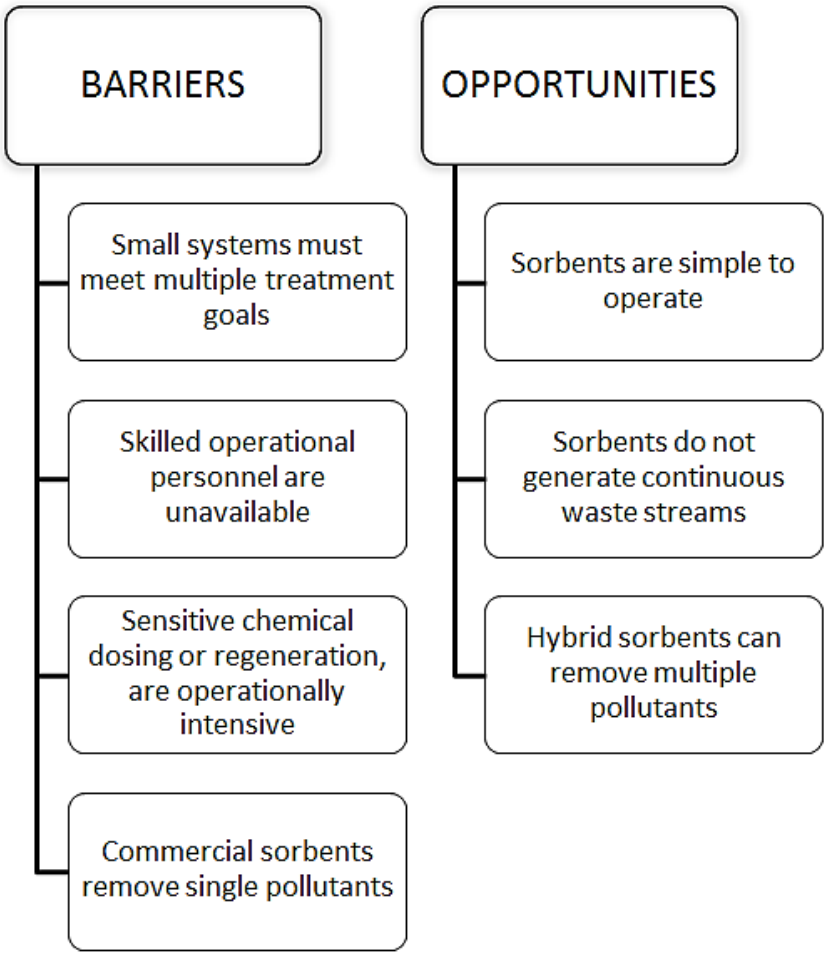

Figure 1.2. The impetus for developing sustainable hybrid nano-sorbents is to address the barriers and take advantage of the opportunities that exist for treating drinking water in small systems.

RESEARCH OBJECTIVE

The objective of the research was to address the overarching question: *Can synthesis methods of hybrid nano-sorbents be improved to increase sustainability and feasibility to remove multiple inorganic contaminants simultaneously from groundwater compared to existing sorbents?*

Answers to the overarching question were sought through conducting a literature review, performing extensive original research, and synthesizing the findings. The literature review is included in chapter 2. Original research addressing the hypotheses is in chapters 3-8. Chapter 9 synthesizes the findings to address the overarching question.

RESEARCH QUESTIONS AND HYPOTHESES

This research addressed five research questions that encompassed seven research hypotheses. Each question and the correlated hypotheses are illustrated in Figure 1.3. Each box represents a research question and the contents show the associated hypotheses with each question. The arrows demonstrate how the answers to the questions help inform other answers, and the interconnectedness of them all. The justification and approach to testing each one are then briefly described. Subsequently, each question then has a dedicated chapter (chapters 3-8) presenting research intended to test the associated hypotheses, and the important findings. Each research chapter is ultimately intended to become a journal manuscript.

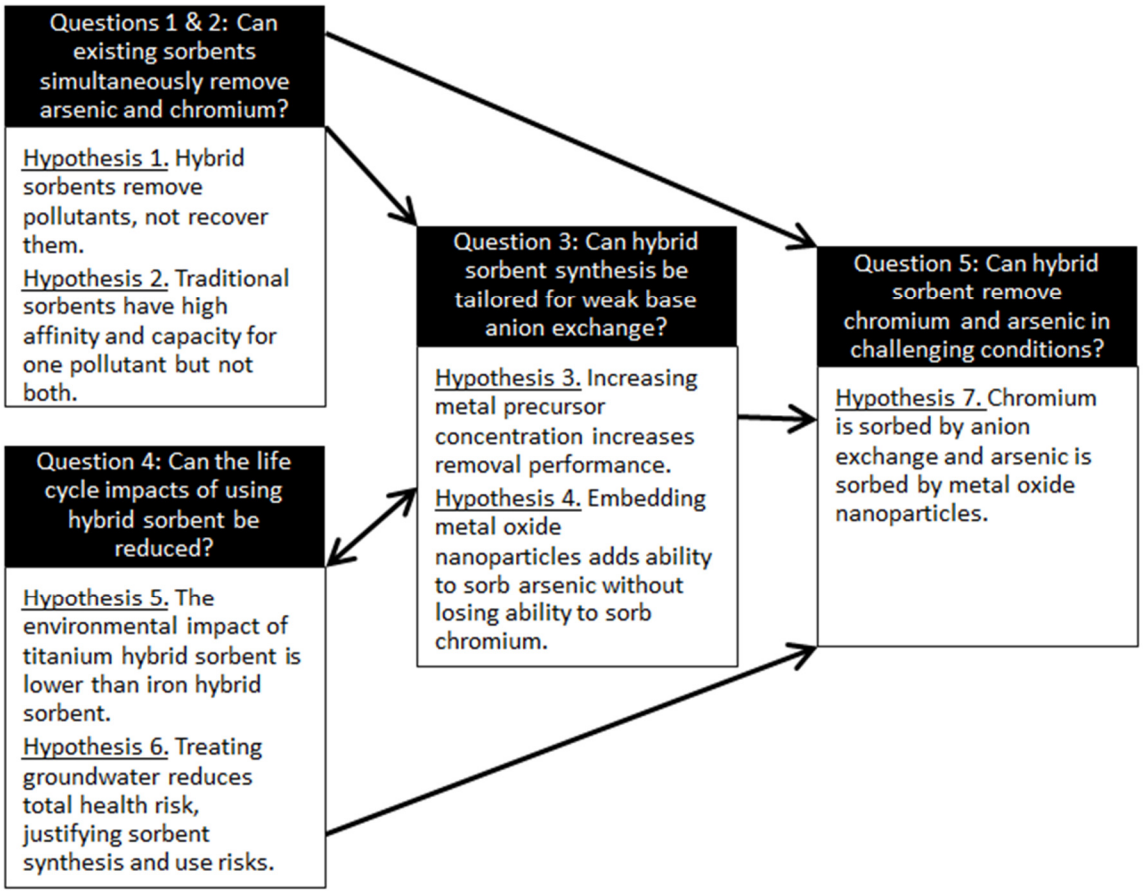

Figure 1.3. Each heading is a research project, correlating to one dissertation chapter and a future journal manuscript. Subheadings are research hypotheses that are explored within that project. Arrows indicate how each project informs the others.

Question 1: Can hybrid sorbents recover phosphate from microbial biofuel residual? The initial work investigated if a hybrid sorbent is better employed in a removal or a recovery paradigm compared to a traditional sorbent. It studied whether the hybrid sorbent can remove a target oxygenated anion and how well it can subsequently release it for reuse. The target oxyanion was phosphate since it is a limited nutrient that can be beneficially reused for microbial biostock growth. It was hypothesized that:

> *1. A hybrid iron nanoparticle embedded strong base anion exchange resin has higher sorption capacity for phosphate from microbial biofuel residual compared to a strong base anion exchange resin, but releases less for reuse.*

Column testing was conducted for the nano-iron embedded strong base anion exchange resin and a traditional strong base anion exchange resin, both of which had been used for phosphate removal. Both deionized water and challenging oxidized organic matrix were tested to compare the mass of phosphate sorbed and released by regeneration. This demonstrated that hybrid sorbents are in fact good sorbents for removal of oxygenated anions from challenging water matrices.

This question and a preliminary form of the associated chapter were used as a masters thesis. After further collaboration and refinement it was published in a peer reviewed scientific journal (Gifford et al. 2015). It is presented in this dissertation as chapter 3 to document its development and present it in light of the other research projects and how it supports the overarching research question.

Question 2: Can Existing Sorbents Simultaneously Remove Arsenic and Chromium? Using sorbents that are already commercially available, chapter 4 identified

if multiple goal treatment was already feasible or if new technologies needed to be developed. It was hypothesized:

> *2. Current market-available drinking water treatment sorbents have a high affinity and capacity to remove either arsenate or hexavalent chromium, but very low capacity to remove both oxo-anions simultaneously.*

Multiple commercially available sorbents were selected, such as metal oxides that are currently considered leading technologies for As treatment, and weak base anion exchange resins that are considered leading technology for Cr removal. The sorption capacity and affinity to remove both pollutants simultaneously was tested. The effects of water testing matrix and pollutant concentration were identified, which enables development of an equilibrium testing protocol to screen many sorbents. Further verification was obtained through column testing. In order to compare quantitatively the performance of the various sorbents, a novel ranking system was developed that weighs sorption capacity for simultaneous removal. This quantitative index was used throughout the research to compare sorbents.

Question 3: Can Hybrid Synthesis be Tailored for WBAX? Iron hydroxide and titanium dioxide nanoparticles have been formed in-situ within strong base anion exchange and granular activated carbon for simultaneous removal of various pollutants (Sarkar et al. 2012, Zhao et al. 2011). This is usually accomplished by soaking the sorbent in strong metal precursor solution, then forming the metal nanoparticle with heat hydrolysis or a strong base precipitation. Hybridization with metal nanoparticles has been only sparsely employed in WBAX. WBAX is a leading treatment for hexavalent

chromium due to its selectivity for the chromate molecule in low concentrations and very long run life in column operation (Brandhuber et al. 2004b). WBAX differs from strong base anion exchange because the functional group is a ternary amine instead of a quartenary amine, it typically has a smaller average pore diameter, and has highest pollutant removal efficiency in a lower pH range. It was hypothesized that:

3. Increasing metal precursor concentration increases the pollutant removal performance of hybrid MOx-WBAX.

4. Embedding WBAX resins with iron or titanium oxide nanoparticles adds the ability to sorb arsenate with only small (<10%) decrease in the ion exchange capacity for chromate.

Chapter 5 explored tailoring the hybridization process for WBAX. The concentration of the metal precursor solution was important to the characteristics of the final sorbent. A high metal content provided a higher concentration gradient to drive the metal deeper into the parent resin pores, as well as provided a higher mass of metal available for precipitation. However, excess metal content may have blocked access to ion exchange sites through surface coating or pore clogging, thus reducing both surface area and removal capacity. It was sought to maximize hybrid sorbent pollutant removal capacity by identifying the precursor concentration that balanced having metal available and avoided clogging pores. It also established a basis for conducting sustainability analysis, making them more accessible for small drinking water systems.

Three different weak base anion exchange resins that are commonly used for treatment of groundwater pollutants were used in the metal nanoparticle impregnation in conjunction with various metal precursor concentrations. The impregnated resins were

then characterized for surface area and pore size distribution using nitrogen gas deposition, metal content using acid digestion and gravimetric analysis, and metal hydroxide form using XRD. Surface area analysis of ion exchange resins required developing a new protocol because the resin could melt and collapse the pores during heat drying. The same impregnation and characterization methods were employed on a macroporous strong base anion exchange resin as a control to compare results of impregnation efficacy to existing literature. This impregnation and characterization determined if pollutants targeted by weak base anion exchange resins could be included in simultaneous treatment, if the weak base anion exchange resins could withstand the synthesis protocol, and how/if the synthesis protocol must have been adapted.

Basic performance testing was evaluated to establish if simultaneous removal was additive or competitive. This as done by developing full isotherms at the relevant contaminant/foulant/sorbent ratios under conditions relevant to groundwater treatment. It was tested in lab synthesized groundwater and also in a real world well water to demonstrate to utilities the real world application. Short bed adsorber tests and packed bed column tests were conducted to capture the sorption kinetics and bed life duration. These determined if the synthesis indeed augmented removal capacity for a second pollutant or diminished the original target pollutant removal capacity. Results established if simultaneous removal of pollutants must be competitive or if co-treatment may be additive or even synergistic.

Question 4: Can the life cycle impacts of using hybrid sorbents be reduced?

If metal nanoparticle impregnated resins are to become widely adopted, the environmental and human health impacts of their manufacture, use, and disposal should

be considered. Chapters 6 presents life cycle assessment of the iron impregnated and the titanium impregnated sorbents to determine impacts including embodied energy, carbon footprint, and human toxicity. The system boundary included resin synthesis (including raw material extraction and chemical production), resin use (normalized to removal capacity and ability to be regenerated), and resin disposal (including hazardous waste handling). This was benchmarked to the environmental impacts of the current technology and to not treating the water at all. Chapter 7 presents a life cycle assessment focusing specifically on the human health impacts associated with wellhead treatment by comparing the embedded risks associated with producing and using treatment materials to the benefits of drinking treated water. It was hypothesized that:

> *5. The life cycle environmental impact of titanium impregnated WBAX is lower than iron impregnated WBAX.*
>
> *6. Removal of hexavalent chromium and arsenic from groundwater reduces the total public health risk, justifying the risk assumed during sorbent synthesis and disposal.*

Testing was accomplished following LCA methods, using impact assessment data from EcoInvent database, and present results in terms of TRACI environmental impact categories. The results of these analyses justified if the produced resins could be employed in a single use cartridge or needed to be regenerated and reused multiple times to justify the environmental impact of synthesis. Opportunities to decrease the environmental impact of their life cycle were identified, increasing the overall sustainability of the nano-enabled sorbents. Conducting this analysis before and during

the development of the synthesis protocol maximized the opportunity to incorporate the results into the final product.

Question 5: Can MOx-WBAX remove hexavalent chromium and arsenic from water in challenging flow through conditions, and if so what is the removal mechanism? The next question addressed in Chapter 8 focused on verifying the pollutant removal performance of the created hybrid sorbent. The culminating test was to demonstrate the ability of the new sorbents to meet the challenge previously identified, including removing pollutant from a challenging water matrix in packed bed flow through mode with minimal operational intervention. This column testing also hoped to elucidate mechanistic understanding of how the hybrid sorbents remove pollutants, which in turn perhaps informed how they may be regenerated. Previous studies speculate that Cr(VI) is reduced to Cr(III) on the surface of WBAX because visual observations show the spent resin takes on a green color characteristic of solid Cr(III) (McGuire et al. 2007). The mechanism of removal for arsenic removal and for chromium removal is important to understand in order to maximize performance and inform overcoming limitations hybrid resins may have. One limitation with WBAX and MOx-WBAX is that it unknown how they can be regenerated. This research hypothesized:

> *7. During treatment of co-occuring pollutants using MOx-WBAX, the hexavalent chromium is removed by anion exchange and the arsenic is removed by metal oxide sorption.*

Understanding the pollutant removal mechanism and unlocking the ability to regenerate the sorbents built upon knowledge gained from testing in previous chapters,

since observing competitive removal capacity could indicate the same mechanism is at work for the two pollutants but additive removal would indicate different mechanisms.

CHAPTER 2

LITERATURE REVIEW

An ongoing critical review of published literature and patent applications is vital to the proposed research endeavor. Its purpose is to place the proposed research in the context of other work being conducted, and to identify gaps in knowledge that will aid in developing the research hypotheses.

1.0 POLLUTANTS OF CONCERN

1.1 Hexavalent chromium. Chromium (Cr) is a metallic element that is tasteless and odorless. It occurs naturally in rocks and dirt. It is used industrially for making steel and alloys, chrome plating, pigments, and leather and wood preservatives.(USEPA 2013)

Cr in water is found primarily in two oxidation states (Schweitzer and Pesterfield 2010). Under oxidized conditions it exists as hexavalent chromium (Cr(VI)). Cr (VI) can be a monovalent anion, $HCrO_4^{1-}$, or a divalent anion, CrO_4^{2-}, with predominance switching at the pKa of 6.4. These forms have a yellow or orange color. Under reduced conditions, Cr exists in a trivalent form (Cr(III)). It can be cationic, Cr^{3+}, or uncharged as Cr_2O_3 with pKa of 4.0. The Cr_2O_3 form is only sparingly soluble. Cr(III) forms have a green color.

Cr(VI) has long been known to be a human carcinogen and non-carcinogenic toxin through inhalation exposure (USEPA 1998a). The current USEPA toxicology report also reported a non-carcinogenic health hazard by oral exposure reference dose (RfD) of $3x10^{-3}$ mg/kg-day. However it reports “no data suggested that Cr(VI) is carcinogenic by the oral route of exposure.” The carcinogenic and non-carcinogenic

toxicology associated with oral exposure are currently being revised and the updated report has been released for public comment (USEPA 2010a). This draft version generally finds increased health risk. The non-carcinogenic RfD is reduced to $9x10^{-4}$ mg/kg-day. Chronic oral exposure to Cr(VI) is connected to gastrointestinal effects including oral ulcers, diarrhea, abdominal pain, and vomiting. It is identified as "likely to be carcinogenic to humans" by chronic oral exposure. The proposed slope factor is 0.5 $(mg/kg\text{-}day)^{-1}$, which is equivalent to a unit risk of $1.4x10^{-5}$ $(ppb)^{-1}$ using standard assumptions for body mass, water intake, and lifespan. This is due to observations of neoplasms in the small intestines of mice and tumors in the oral cavity of rats exposed to high doses of Cr(VI). The mutagenicity of Cr(VI) is thought to be mediated through the generation of highly reactive chromium intermediates, like Cr(IV) and Cr(V), formed during the intracellular reduction of Cr(VI) to Cr(III).

National occurrence of Cr(VI) is being investigated as part of the USEPA Unregulated Contaminant Monitoring Rule (UCMR) 3 (USEPA 2015c). This monitoring will take place through 2016, but results reported as of August 2015 were downloaded and analyzed to produce Figure 2.1. It shows that 19% of the nationwide utilities participating in UCMR3 have greater than 1 ppb Cr(VI) in the raw water source, and 30% have total Cr above 1 ppb. Nationally, 2% of utilities have greater than 10 ppb Cr(VI). If only systems that use groundwater are considered, 4% of them exceed 10 ppb Cr(VI) influent. This is consistent with findings that generally Cr(VI) is more prevalent in groundwater sources, and Cr(III) is more prevalent in surface water sources where it has been reduced by natural organic matter (Frey et al. 2004, McNeill et al. 2012). If only small systems that serve less than 10,000 people are included, very similar occurrence

patterns are observed as the total occurrence. For instance, 1% have greater than 10ppb Cr(VI). However most small systems are exempt from UCMR3 monitoring (as evidenced by the fact that small systems comprise 4% of the total reporting systems, but nationally comprise 93% of all systems (Impellitteri et al. 2007)) and thus the sample size is much smaller and may not be representative. It is noted that Cr(III) can be oxidized to Cr(VI) in water distribution from interaction with disinfectants (Lindsay et al. 2012). A previous occurrence survey found the highest level of Cr(VI) in source water was 53 ppb (Frey et al. 2004).

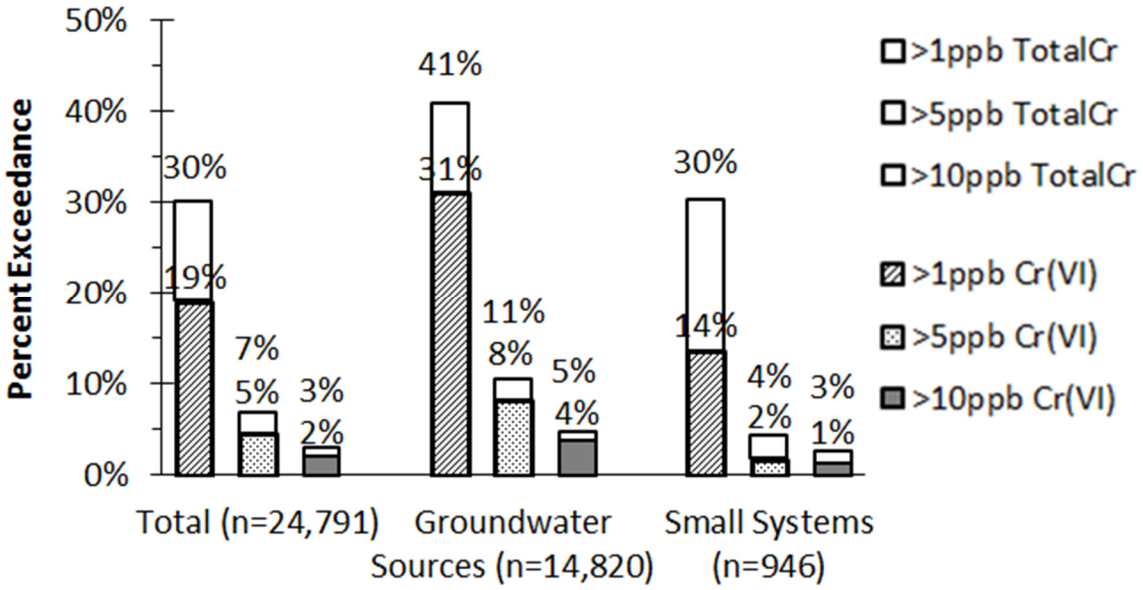

Figure 2.1. UCMR3 Chromium Occurrence. Percent of water utilities that report a raw water level of total Cr (hollow boxes) and Cr(VI) (patterned boxes) greater than certain thresholds. Total data is further split out by primarily use groundwater sources, and by systems that serve less than 10,000 people. Data analyzed August 2015, but UCMR3 monitoring will be continued through 2016.

Cr is federally regulated in drinking water at a maximum contaminant level (MCL) of 100 ppb of total Cr (USEPA 2013). This regulation is being reviewed and may possibly be lowered in the near future after UCMR3 monitoring and updated toxicology reporting are finalized. The state of California has recently adopted an MCL of 10 ppb Cr(VI) (CCR 2014). This regulation was issued in April 2014 and compliance monitoring started in July 2014.

Multiple analysis methods to determine total Cr or Cr(VI) exist (McNeill et al. 2012). Two primary methods will be used in this research that are available at ASU. The first is by inductively coupled plasma mass spectrometry following EPA standard method 200.8 (USEPA 1994). This method has method detection limit of 0.08 µg/L for total Cr. Second, Cr(VI) is determined using ion chromatography to isolate the anion then measured spectrally by reacting with 1,5-diphenylcarbazide to produce a pink color following EPA standard method 218.7 (USEPA). This method has a method detection limit of 0.018 µg/L Cr(VI).

There are three primary methods of treating chromium in water: sorption with weak base anion exchange (WBAX), sorption with strong base anion exchange (SBAX), and reducing Cr(VI) to Cr(III) followed by coagulation and filtration (RCF). Many extensive reviews of these treatment options have been published (Blute et al. 2012, Brandhuber et al. 2004b, Malaviya and Singh 2011, McGuire et al. 2007, Mohan and Pittman 2006, Najm et al. 2014, Owlad et al. 2009).

WBAX has a very high affinity for Cr(VI) and a very high removal capacity. Both bench scale and pilot scale column tests have demonstrated long run times up to 100,000 to 300,000 bed volumes before breakthrough (McGuire et al. 2007, Najm et al.

2014). In order to achieve maximum sorption capacity with WBAX, the influent water must be acidified to pH 6 (Brandhuber et al. 2004b, McGuire et al. 2007). WBAX is a single pass sorbent, meaning it is unknown how to regenerate it and is disposed of after a single exhaustion. Hazardous waste classifications of spent sorbent indicate it is not TCLP or RCRA waste, but may be STLC and TTLC waste (Najm et al. 2014). Uranium is often sorbed by WBAX with one study indicating it may classify as TENORM (Najm et al. 2014) and another indicating it would not (McGuire et al. 2007). The difficulty in regenerating the spent sorbent is because Cr(VI) is reduced to Cr(III) after sorption to WBAX as confirmed by XANES (McGuire et al. 2007), causing it to take on a green color.

Treatment of Cr(VI) using SBAX is another common technology. Compared to WBAX, the SBAX resins generally have much lower affinity for Cr(VI) showing greater competition from nitrate and sulfate. Generally, SBAX also has a much lower capacity than WBAX, with bench scale and pilot scale column tests only lasting 10,000 to 15,000 bed volumes (Brandhuber et al. 2004b, Najm et al. 2014). It can be regenerated and reused multiple times by a strong salt solution (Najm et al. 2014). It is generally the cheapest treatment option for Cr(VI) compared to WBAX or RCF, with possible costs ranging from $0.66-0.81 per 1,000 gallons for large systems and $6.8-6.9 per 1,000 gallons for small systems (Najm et al. 2014).

Several other novel methods of Cr(VI) treatment have been proposed. Removal can be achieved by sorption to carbon-based sorbents such as activated carbon (Mohan and Pittman 2006), wheat bran (Nameni et al. 2008), and iron-modified biochar (Liu et al. 2010). Removal by sorption to natural materials is reported including weathered basalt

andesite (Shah et al. 2009) or clino-pyrrhotite (Lu et al. 2006). Reduction of Cr(VI) to Cr(III) can also be achieved by zero-valent iron followed by sorption to iron coated sand (Mak et al. 2011a), by zero-valent magnesium (Lee et al. 2013), by zero-valent iron nanoparticles (Singh et al. 2012), and by glow discharge plasma generated by a platinum anode (Wang and Jiang 2008).

1.2 Arsenic. Arsenic (As) is a naturally occurring element in rocks, soil, water, air, animals, and plants (USEPA 2012). Industrially it is used for hardening copper and lead alloys, glass manufacturing to decolorize, leather preservative, pesticides, and in wood preservative. Over 90% of domestic use is for the wood preservative chromate copper arsenate (USEPA 2010b), but use is being phased out.

As in water is colorless, tasteless, and odorless in environmental aqueous conditions. It can be found primarily in one of two oxidation states. It is most often pentavalent arsenic (As(V)), but under very reduced acqueous conditions can be trivalent (As(III)). As(V) can be associated with the divalent anion $HAsO_4^{2-}$ or the monovalent anion $H_2AsO_4^{1-}$. The pKa between these two species is 6.8 (Schweitzer and Pesterfield 2010).

Inorganic As is classified as “carcinogenic to humans”. There is vast epidemiological evidence associating it with cancer of skin, bladder, kidney, lung, liver, and prostate. Mode of Action has not been established, but does involve mutagenisis, and is thought to be connected to the highly reactive metabolite monomethylarsonous acid (MMA(III)) (USEPA 2010b). The EPA IRIS toxicological study reports a drinking water Unit Risk of 0.00005 $(ppb)^{-1}$, equivalent to an oral slope factor of 1.5 $(mg/kg/day)^{-1}$ (29). An updated draft of the IRIS study was released in 2010 and generally found

increased cancer risk. Drinking water unit risk increased to 0.00073 $(ppb)^{-1}$, equivalent to oral slope factor of 25.7 $(mg/kg/day)^{-1}$ (USEPA 2010b).

As is also associated with a variety of non-cancer human health maladies. Chronic exposure symptoms include hyperpigmentation, keratosis, burning eyes, leg swelling, liver fibrosis, and lung disease (30). Acute exposure leads to dry mouth, dysphasia, projectile vomiting, profuse diarrhea (Choong et al. 2007). This is why As has historically been used as a poison, tied to 237 murders in England during the 19th century (Hempel 2013). Even Napoleon Bonaparte's death has been speculated to be the result of accidental or intentional arsenic poisoning (Parascandola 2012). For these reasons the EPA IRIS study from 1998 reported human non-cancer toxicity at reference dose of 0.0003 mg/kg/day. The non-cancer toxicity reference dose was unchanged in the 2010 update (USEPA 2010b).

Food is typically the highest exposure to As. Many common foods contain 20-140 ppb As (USEPA 2010b). The predominant dietary source of As is seafood, followed by rice, mushrooms, and cereal (ATSDR 2007). High levels of aqueous arsenic exposure are typically associated with groundwater (USEPA 2012). As is found naturally in soil, particularly in the western US (USEPA 2010b). 12% of surface water sources in the central US and 12% of groundwater sources in the western US contain >20ppb As. (USEPA 2010b). Globally, the highest exposures are in West Bengal, Bangladesh, and Chile, where up to 12% of the population manifests adverse effects. Other countries with high exposures include Taiwan, Mexico, China, and the USA (Choong et al. 2007).

Due to its frequent occurrence and toxicity, As has a regulatory limit by USEPA and recommended limit by WHO of 10 ppb. The compliance deadline for this total As

USEPA limit was January 2006 (USEPA 2012). However, many systems are still non-compliant, with 67% of noncompliant systems serving less than 500 people (McGavisk et al. 2013).

The most common treatment technology for removing As(V) from water is sorption, which works well at low ppb levels. The most common adsorbents include are hydrous ferrous oxide and granular ferric hydroxide. Reported sorption capacity includes 280 (Westerhoff et al. 2005), 402 (Lipps et al. 2010), 2362 (Bang et al. 2011), and 3902 µgAs/g (Speitel Jr. et al. 2010). No pretreatment is required, and the packed bed has simple operation. Other less common sorbents that have been tested include activated carbon, activated alumna, and zeolites. Novel, low cost adsorbents that may have application in the developing world include coconut husk, rice husk, and sawdust (Choong et al. 2007). All of these adsorbents exhibit considerable competition from silica and sulfate. They are generally considered single use, but periodic backwashing to restore flow rate from filtered particulates can account for 2-10% of production water. Solid resin can be disposed in a hazardous waste landfill. Activated alumina (AA) can be regenerated using caustic and neutralization by acid. This regeneration process produces a dissolved AA/As sludge.

Other As treatment methods include coagulation/flocculation, membranes, and precipitation. For coagulation/flocculation, the most common coagulant is alum followed by chlorine disinfection. This requires a 6-8:1 ratio of Al/As (Choong et al. 2007). Sulfate or chloride followed by sand filtration can also be used. Membranes must be nanofiltration (0.001-0.003 µm pores) or reverse osmosis (0.0005 um pores) for arsenic removal. Pre-oxidation or pre-coagulation must be used for membranes with larger

pores. This technology exhibits little interference from source water composition and no preference for As(III) or As(V), indicating removal is through size exclusion and not charge interaction (Choong et al. 2007). As with all membrane processes, it exhibits very high energy and cost demand, has high water loss, and produce a challenging residual. Reject water containing high As and high TDS is often subject to disposal requirements. These challenges can be mitigated if co-treatment of other pollutants is needed. Removal using precipitation can be achieved. Alum requires the As to be oxidized and at a low pH, with the residuals remaining in the clarifier. Ferric chloride or ferric sulfate is simple and versatile, but works best at high As (ppm) As levels. Lime softening can contribute to some As removal, but also requires oxidized As and low pH such that it is only viable if soft water is required anyway (Choong et al. 2007). In any case, the precipitated solids require hazardous waste disposal.

1.3 Co-Occurrence of hexavalent chromium and arsenic. This dissertation seeks to develop the science and understanding of simultaneous treatment of both chromium and arsenic, and verification that co-occurrence exists is vital to the possible implementation of the findings. These two contaminants are found to co-occur in at least three places: natural groundwater, anthropogenically polluted groundwater, and within distribution system scale.

Groundwater to serve as a drinking water source is a possible scenario for co-occurrence of As and Cr. Data from a co-occurrence study (Brandhuber et al. 2004b) has been plotted and included as Figure 2.2. The bar-and-whisker chart shows, for a given total Cr or Cr(VI) level, the minimum, lower quartile, median, upper quartile and maximum level of As. It shows that the quality of groundwater supplies containing

elevated levels of total Cr is not appreciably different from that of supplies containing little or no total chromium (Brandhuber et al. 2004b). Therefore, given that one pollutant is present in groundwater, co-occurrence is no more or less likely to occur than in any other source. However, there is higher levels of As found in groundwaters that contain high levels of Cr(VI). The median concentration of As (14 µg/L) in waters with more than 5 µg/L of Cr(VI) is significantly higher than the upper quartile concentration of As (8.6 µg/L) for waters with less than 5 µg/L of Cr(VI).

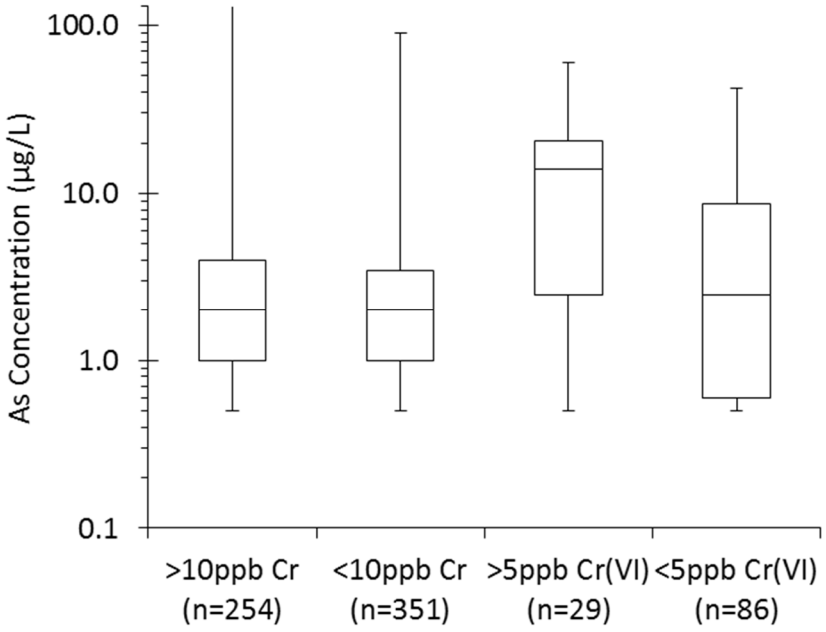

Figure 2.2. Co-Occurrence of As and Cr. The minimum, lower quartile, median, upper quartile and maximum level of As are grouped according to the total Cr or Cr(VI) level for groundwaters. New graphic from published data (Brandhuber et al. 2004b).

In contrast, a separate study conducted by a utility company in southern California found that high As levels were not correlated with or against high Cr(VI) levels (ARCADIS 2013). Of 106 wells maintained by the Coachella Valley Water District, 39 have Cr(VI) between 5-10 µg/L. Of those, 3 (8%) also have high levels of As (7.9-15.8 µg/L). Of the 37 wells with more than 10 µg/L of Cr(VI), 3 (8%) wells have high levels of As (2.5-11.9 µg/L). When the two studies are taken together, occurrence of As may or may not be more likely to co-occur with As(V), but it may be concluded that presence of one contaminant does not preclude presence of the other.

Another location where co-occurrence can occur is in anthropogenically contaminated groundwaters. After lead, Cr and As are the two most common metals found at superfund sites (USEPA 1996). The two pollutants have been found together in over 200 of the 1,000 federally designated contaminant areas. Treatment in such a scenario would likely be pump-and treat with high levels of both contaminant and very amenable to packed bed reactors that have high throughput and little energy demand.

A third scenario with observed co-occurrence is from distribution pipe corrosion. Scale sampled from inside many water distribution pipes was found to contain 13 µg/g of As and 7.3 µg/g of Cr on average (0.7 to 206 µg/g As, 1.4 to 118 µg/g Cr, 10^{th} and 90^{th} percentiles respectively) (Peng 2012). Such solids can be released into water with such events as change in water alkalinity, or flow reversal due to pipe looping, demand changes, or fire hydrant flow. Systems that change water sources, or small systems where small demand changes can drastically alter flow patterns are at particular risk.

2.0 HYBRID SORBENTS

For the purposes of this review, hybrid sorbents are defined as media composed of two materials that each adsorb pollutants from water. Literature also refers to them as nano-composite sorbents. Hybrid sorbents in which one material is present as nanoparticles within the porous structure of the other macro-material are of particular interest. The two materials may have different affinities for different pollutants, and therefore give the hybrid sorbent unique properties and abilities.

These unique properties make hybrid sorbents preferable over standard sorbents for simultaneous removal of pollutants. Standard inorganic granular sorbents like MO exhibit a number of operational challenges including low physical strength of aggregates leading to pressure increases, channeling, and poor hydraulic flow (Moller 2008). Standard anion exchange sorbents can exhibit high competition from other anions such as nitrate (Smith 2010) or sulfate (Cumbal and Sengupta 2005). Nanoparticles themselves can have high sorption capacity due to high surface area, but are very difficult to remove from water after dosing.

Hybrid sorbents overcome many of these challenges. The polymeric parent resin provides high mechanical strength for use in packed beds. It provides a fixed surface to which the nanoparticles may attach, taking advantage of their high sorption capacity without being lost into the bulk solution. This is actually a synergistic relationship as Donnan exclusion provides a higher pollutant concentration within the pores and hybrid resin therefore has higher capacity than the parent resin (Cumbal and Sengupta 2005). The hybrid resin can exhibit high removal capacity for two pollutants on a single sorbent (Cumbal and Sengupta 2005, Elton et al. 2013, Hristovski et al. 2008b), maintaining the

ability to remove the same pollutant as the parent macro-sorbent and adding ability to also remove another.

Anion exchange resin will be reviewed as a potential macro-material, then iron hydroxides and titanium dioxide will be reviewed as potential nanoparticle material.

2.1 Ion exchange sorbents. A variety of porous materials can be used as the macromaterial for a hybrid sorbent. Ion exchange resin is of particular interest as it has been widely applied for treatment of both As and Cr. A rich body of literature exists for ion exchange resin, and only a basic review for fundamental understanding is presented here.

An ion exchange sorbent is characterized by an electrostatic charge than is neutralized by a weakly held ion of the opposite charge by an ionic bond. This ion can be displaced by another ion that is more preferable due to either material or aqueous properties. The two broad classes of ion exchange are anion exchange, that have a positive surface charge and exchange anions, and cation exchange, that has a negative surface charge to exchange cations (MWH 2005). This review focuses on anion exchange as both As and Cr exist as anions in the aqueous conditions of interest.

A number of natural materials exhibit ion exchange properties, including some clays such as clinoptilolite. It has been speculated (Kunin 1958) that this phenomenon contributed to the miracle of making salt water fresh after being stored in clay jugs as recorded in the Bible. Modern day ion exchange sorbents are synthetic, composed of polymer backbone that is held together by a cross-linking agent and then functionalized. The polymer is often polystyrene or polysulphone, either of which create straight chains of inert material. The most common cross-linking agent is divinylbenzene (DVB). The

cross-linker makes connections between different chains and in different parts of the chain, giving it three-dimensional structural rigidity. The amount of cross-linking agent used therefore strongly influences properties of the resulting resin including pore structure, surface area, and degree of hydration. Resin with high cross linking creates a gel-type resin with very small pores. Less cross linking creates microreticular resin, and even less creates a macroreticular resin (Kunin 1958). The pore structure in turn influences final charge density and molecular size exclusion, and therefore can be optimized for selectivity/affinity for specific adsorbate.

Recipes for synthesizing resin are as numerous as the number of commercial resins available. Most follow the pattern of creating a cross-linked skeleton, then adding functional groups. One is reviewed here as an example of anion exchanger (Kunin 1958). Styrene-DVB copolymer is made with 400 mL water and a dispersing agent like carboxymethyl cellulose, 90 g of styrene, 10g of DVB, and 1 g of benzoyl peroxide. The mixture is heated at 90°C for one to two hours, the resin is removed from solution, and dried at 125°C for 2 hours. The copolymer is next chloromethylated. 50 g of copolymer is mixed with 100 g of chloromethyl ether in 115 mL petroleum ether and 30 g of anhydrous aluminum chloride to catalyze. It is then dried at 125°C for 2 hours. Functionalization is then accomplished by immersing in 115 mL benzene, saturating with either trimethylamine or dimethylamine gas, and drying at 50°C for 4 hours (Kunin 1958).

The two main types of anion exchange resin are strong base anion exchange (SBAX) and weak base anion exchange (WBAX). SBAX is synthesized using the trimethylamine gas, which produces a quarternary amine functional group. This

counterion held by this functional group easily dissociates at a broad range of pH. WBAX is synthesized using dimethylamine gas that produces a ternary amine functional group. The electron pair associated with the nitrogen in the amine group is more tightly held, and only takes on a positive charge at a depressed pH (<6).

2.2 Iron hydroxide nanoparticles in hybrid sorbents. Two synthesis methods and one patent for creating iron nanoparticles inside the pores structure of anion exchange resin are reviewed. First, permanganate oxidizes ferrous which then precipitates as iron (hydr)oxide (Hristovski et al. 2008b). 67 g of a perchlorate-selective SBAX resin are soaked in 800 mL of either 1.3% or 2.5% $KMnO_4$ solution. The soaked resin is rinsed then reacted with 800 mL of either 11% or 17% $FeSO_4$ for 15 or 45 minutes. It is then rinsed to remove excess protons and precipitate. Iron nanoparticles are amorphous ferric (hydr)oxide. The hybrid sorbent is found to be able to remove both perchlorate and arsenic from water. The formulations using higher permanganate and higher iron precursor solutions were found to produce higher final metal content (Hristovski et al. 2008b).

In the second method, ferric is precipitated under alkaline conditions (Hristovski et al. 2008b). 50 mL of SBAX resin is soaked in 200 mL of $FeCl_3$, then rinsed. It is then soaked in a 10% NaOH solution for 30 minutes. It is rinsed to neutralize pH and remove excess precipitate, then the entire process is repeated. The hybrid sorbent is found to be able to remove both the anion originally targeted by the parent SBAX resin as well as arsenic. This method resulted in high metal content that were evenly distributed across the resin cross section. It is concluded that parent SBAX characterized by high porosity is more amenable to being embedded with iron nanoparticles (Hristovski et al. 2008b).

Comparing these two methods, the permanganate method is unique in that the resin is soaked in the precipitation solution first and the metal solution second. This might have the effect of precipitating the nanoparticles more superficially since the metal would not have time to permeate deep into the pores before reacting. That could be why the nanoparticles were more evenly distributed through the resin depth via the hydroxide methods. The hydroxide method is unique in that the synthesis process is repeated, likely giving more opportunity for precipitation. The second contact with metal solution would be able to use the nanoparticles formed in the first contact as seeds, and may therefore form larger particles than would otherwise be possible.

A patent for synthesizing iron nanoparticles inside anion exchange resin is reviewed (Moller 2008). It claims to apply to any type of any type of anion exchange sorbent, including gel or macroporous, as well as Type 1 SBAX or Type 2 SBAX or WBAX. The resin is soaked in 7 to 50% weight by volume iron salt solution for 0.5 to 8 hours, then rinsed and filtered. It is then exposed to a 1% to 20% base solution for 15 to 60 minutes and rinsed. This process can be repeated as needed, then finally rinsed with 5% NaCl and sparged with CO_2 to reduce pH. It is found that increased precursor concentration increased resultant metal content of resin. Two cycles of 21% precursor made a final hybrid sorbent with 128 mgFe/g, whereas two cycles of 28.5% precursor made 206 mgFe/g. Shortening precursor contact time from 60 minutes to 45 or 30 minutes did not reduce final metal content. It is claimed that As removal capacity increases with iron content (Moller 2008).

Three critiques of this patent are offered. It is claimed that the process works on any type of anion exchange material, however it was not performed nor tested on WBAX.

Functional groups on WBAX are fundamentally different that those of SBAX and may react differently to the process, meaning that broad claims across all types of anion exchange should be verified. Next, the patent claims to apply to any type of metal for creating nanoparticles including iron, titanium, and others. While the use of iron is demonstrated, no attempt to demonstrate other metals is made. Titanium does not precipitate when exposed to a strong base the same way iron does, indicating a different synthesis process would be preferred. Last, it is concluded that As capacity increases with increased metal content. However this is only explored up to a 50% precursor solution concentration, and it is unknown if this trend continues indefinitely.

Various studies have shed light on important operational conditions for iron nanoparticle embedded hybrid sorbents. It is found that even for a hybrid sorbent, the adsorption of Cr, As, and phosphorus could be inhibited by presence of bicarbonate, silicon, nitrate (Smith 2010), and sulfate (Cumbal and Sengupta 2005). In packed bed column configuration, longer hybrid sorbent life is observed at lower pH (Cumbal and Sengupta 2005). Comparing the As removal capacity of the parent anion exchange resin to the iron hybrid sorbent it was used to make, the parent sorbent had only small amounts of As removal capacity (Cumbal and Sengupta 2005). Even this small capacity was limited by competition with sulfate, and the As effluent concentration exceeded the influent concentration after breakthrough as new sulfate displaces previously sorbed As.

Important insights to the removal mechanism for iron embedded hybrid resin have been made. One study has observed that double and triple layer equilibrium surface complexation models for iron hydroxide adsorption do not accurately predict pollutant removal by nanocomposite sorbents at high counterion concentrations (Smith 2010).

This suggests that more than only sorption to the metal nanoparticles contributes to As removal. A model that could accurately predict removal would need to include anion exchange as well as metal oxide sorption. Another study noted that hybrid sorbent in packed bed column tests showed an increased capacity for As removal after operational interruption (Cumbal and Sengupta 2005). This suggests that sorption is limited by intraparticle diffusion. Adequate contact time is therefore required to fully access the sorbent capacity found on nanoparticles deep inside pores. This study also quantified the benefits of the Donnan co-ion exclusion effect for hybrid sorbents. The parent anion exchange sorbent has fixed positive charges on the surface that cannot diffuse into the bulk solution. This draws increased negative charges to it, resulting in 100-times higher concentration of anions within the resin than in the bulk solution (Cumbal and Sengupta 2005). This applies to both the original counter-anion and the target anion. This high concentration provides a high energy gradient that leads to high sorption capacity of both the anion exchange and metal nanoparticle sorbents. It further excludes other positive charges from entering, resulting in 100-times lower concentration of cations in the water within the pores than in the bulk. That is why no competition from cationic species is observed.

2.3 Titanium dioxide nanoparticles in hybrid sorbents. Titanium materials can be used in a number of applications for the treatment of drinking water. For instance, titanium dioxide can photocatalyze organic-As and As(III) to As(V), which is much then much easier to treat (Guan et al. 2012). This review focuses on the use of titanium dioxide as a sorbent, and particularly as a nanoparticle embedded inside an ion exchange resin. It has previously been observed that sorption and removal of As by TiO_2 is

enhanced when combined with other sorbents like GAC, activated alumina, rare earth oxides, or even polyethylene terephthalate bottles (Guan et al. 2012). Combination with WBAX seems to be unexplored.

Titanium dioxide can be found in one of three mineral forms: anatase, brookite, and rutile. Amorphous TiO_2 is the absence of a clearly abundant form. Rutile is the most abundant TiO_2 polymorph in nature (Dadachov 2006). If being obtained commercially, Hombikat TiO_2 is an anatase form with a point of zero charge of 6.2. These have a smaller particle size with higher surface area compared to Degussa TiO_2, which contains a combination of both anatase and rutile and a higher point of zero charge of 6.9 PZC. (Dutta et al. 2004) At pH 9, sorption of As(V) onto Hombicat had Fruendlich isotherm parameters of K=16±3, n=3.1±0.4, with R^2=0.94. Sorption onto Degussa was K=1.8±0.7, n=2.5±0.4, with R^2=0.90. (Dutta et al. 2004) This infers a higher sorption capacity by the purely anatase Hombikat.

When synthesizing TiO2 nanoparticles, conditions can be controlled to prefer one mineral form over another. Generally anatase and brookite can be formed at lower hydrolysis temperatures, and rutile is formed with higher temperatures and longer heating times. In fact, anatase was formed after 10 minutes of heating in 250°C, but transitioned to rutile after 6 hours. (Kolen'ko et al. 2003). Another study found that hydrolysis temperatures below 600°C result in porous anatase. Higher temperatures result in solid rutile with concomitant drop in pore volume and surface area. (Ismagilov et al. 2009). However, an increase in temperature and heating duration has also resulted in increased anatase crystal size (Guan et al. 2012, Kolen'ko et al. 2003). Therefore, if large anatase

particles are desired, the heating time and temperature must be balanced to grow the crystals but avoid transformation to solid rutile.

Synthesis methods to create hydrous titanium dioxide nanoparticles usually involve the hydrolysis and/or precipitations of salts via heating or addition of sodium hydroxides. For example, a solution of $TiOSO_4$ can be thermostated at 120°C for 8 hours to create a TiO_2 powder (Kolen'ko et al. 2003). Many methods exist for forming these particles inside other sorbents using various precursor compositions and hydrolysis conditions exist and can be found elsewhere (Ismagilov et al. 2009). Two methods are reviewed as examples of temperature hydrolysis and chemical hydrolysis. One patent will also be reviewed.

As an example of a heating hydrolysis method, one study soaks 100 mL of SBAX in a 100% w/v solution of TiOSO4 for either 5 or 60 minutes. The soaked resin was or was not decanted, then heated for 24 hours at 80°C. After synthesis it was regenerated with 5% sodium chloride and repeatedly rinsed (Elton et al. 2013). Decanting was found to lower the final sorbent metal content by 1 – 3%. Little difference was observed between the contact times. Nanoparticles were between 50 and 90 nanometers in diameter and largely amorphous, but tend toward anatase (Elton et al. 2013).

In another study used as an example of chemical hydrolysis method, 21 grams of resin were soaked in a solution of titanium ethoxide $Ti(OC_2H_5)_4$ for 15 minutes. It was then refluxed in a 200 mL solution of 1M ammonium hydroxide at 70°C for 5 hours. It was then rinsed and dried at 65°C (Balaji and Matsunaga 2002). It was found that this process increased the Ti content from 0 to 3.5%. However it also reduced the surface area from 574 to 209 m^2/g. This is attributed to pore blockage for pores 300-600 Å in

diameter (Balaji and Matsunaga 2002). XPS analysis shows that the Ti is present in a +4 oxidation state consistent with TiO_2. In column testing, 1 g of hybrid sorbent with 1 mgAs/L influent a flowrate of 0.5 mL/min broke through for As(V) nearly immediately. The poor performance is attributed to short contact time (Balaji and Matsunaga 2002).

Comparing the two hydrolysis methods, it is interpreted that the chemical hydrolysis largely takes place on the superficial resin structure and not down into the pores, leading to low metal content, pore blockage, and ergo low pollutant removal capacity. This lends preference to temperature driven hydrolysis procedures.

At least one very general patent exists in this realm. It claims to cover making TiO_2 as a powder, grain, or coating for the purpose of sorbing any inorganic water contaminant in a vessel of any size (Dadachov 2006). The process soaks GAC in a precursor solution, filters, then heats at 110°C for several hours. The process can possibly be repeated if desired (Dadachov 2006). It claims to produce a powder precipitated in aqueous solution. This powder is stated to have a surface area of 290 m^2/g, a pore volume of 0.36 cm^3/g, and use 30% of the Ti provided in the precursor solution (Dadachov 2006). Though the patent broadly claims to work for any sorbent, it does not mention and does not demonstrate applicability to embedding inside WBAX. It broadly claims to work for removal of any pollutant but does not demonstrate effectiveness for As or for Cr removal, let alone both pollutants at once.

In almost all studies of TiO_2 nanoparticles, higher surface area leads to higher pollutant sorption capacity (Dutta et al. 2004, Guan et al. 2012). Increased sorption capacity is also coordinated with decreased crystallinity (Guan et al. 2012). Arsenic forms bidentate inner sphere complexes when sorbed to TiO_2 surfaces (Guan et al. 2012).

Low pH is preferred for sorption of As onto TiO_2. Sorption capacity of TiO_2 nanoparticles decreases with increasing pH (Guan et al. 2012). The isoelectric point of TiO_2 is between 6 and 6.7, so at low pH it takes on a positive surface charge. This is favorable to attract anionic As (Balaji and Matsunaga 2002, Dutta et al. 2004). In contrast, As(III) sorbs better at high pH (Dutta et al. 2004). As(V) is removed best at pH below 5, and As(III) is removed preferentially at pH between 5 and 10 (Balaji and Matsunaga 2002). However, in the presence of competing anions like silicate, phosphate, sulfate, bicarbonate, and NOM, most sorbents exhibit the highest As sorption capacity near neutral pH. Competing constituents inevitably reduce the overall capacity though (Guan et al. 2012). Non-competing cations such as Ca^{2+} and Mg^{2+} may enhance As sorption onto TiO_2 (Guan et al. 2012). In bottle testing, equilibrium is observed within 4 hours (Balaji and Matsunaga 2002).

3.0 LIFE CYCLE ASSESSMENT

Life cycle assessment is a critical tool for this dissertation in exploring the human health impacts of Cr and As water treatment as well as maximizing the environmental performance of the developed hybrid sorbent. This section explores previous sustainability analysis of drinking water in order to establish critical assumptions and comparative results.

3.1 Energy embedded in water supply. Water related energy use in the United States is at least 521 million MWh annually. This equates to 13% of national electricity demand. Over 85% of this demand is for pumping into the pressurized distribution system (Plappally and Lienhard 2012). This energy use results in carbon footprint of 290

million metric tons annually, which is 5% of all national carbon emissions (Griffiths-Sattenspiel and Wilson 2009). This is higher than the global average, for which 7% of electricity is used for production and distribution of drinking water and treating wastewater (Plappally and Lienhard 2012). This speaks to the higher per capita use of water by residents of the United States. In fact, WHO defines the average water requirement for human survival to be 0.0025 m^3/day/capita (0.66 gal/day/capita), but residential areas in the US use 0.35 m^3/day/capita (92 gal/day/capita) (Plappally and Lienhard 2012).

Nationally, 63% of drinking water is supplied from surface water sources (Hutson et al. 2004). Embedded energy in drinking water from surface water sources varies widely according to plant size and the required treatment processes. The national average energy consumption for surface water treatment and supply is 0.079 kWh/m^3 (Plappally and Lienhard 2012), but this average includes many small systems with minimal treatment and small distribution areas. More standard treatment plants have been observed to use 0.37 kWh/m^3 (Burton 1996), or 0.11 to 0.66 kWh/m^3 (Arpke and Hutzler 2006). Complex drinking water treatment might have embedded up to 1 kWh/m^3 (Crettaz et al. 1999). For a large surface water utility serving 1 million people producing 250 billion liters per year (180 MGD), embedded energy of 1.5 kWh/m^3 was observed which produces 390 kg CO_2-eq (Stokes and Horvath 2011).

Groundwater is the primary water source for 37% of public water systems (Hutson et al. 2004). One study of a 20 MGD groundwater plant uses 0.48 kWh/m^3 for well pumping, chlorination, and distribution pumping (Elliott et al. 2003). Similar variability observed in surface water's embedded energy depending on plant size and

treatment would also be expected for groundwater treatment. Groundwater pumping energy required to lift, provide outlet pressure, overcome pipe friction, and account for pump efficiency can be estimated as 0.004 to 0.006 kWh/m^3 per meter of well depth (Plappally and Lienhard 2012).

For comparison, wastewater treatment can vary from 0.21 kWh/m^3 for lagoons to 0.77 kWh/m^3 for extended aeration (Arpke and Hutzler 2006, Cantwell et al. 2002). A biological filter WWTP use 56% less energy and produces 35% fewer airborn toxins than an activated sludge WWTP (Emmerson et al. 1995).

Desalination uses twice as much energy and produces twice as much emissions than importing water. It uses five times more energy with 18 times more emissions than recycling water (Stokes and Horvath 2006).

3.2 Critical processes in water supply. Energy is the main resource expended during each stage of water use, and assumptions about energy mix are critical to assessing environmental impacts (Arpke and Hutzler 2006). That is why nearly all water related life cycle assessments report results in terms of embodied energy.

The largest amount of energy spent in the domestic urban water cycle is in the use phase, nearly all of which is associated with water heating (Plappally and Lienhard 2012). Energy demand during the use phase is 6.3 to 36 kWh/m3, which is 93% to 97% of energy compared to treatment and disposal (Arpke and Hutzler 2006). Reducing hot water use by 20% would save 4.4 billion gallons of water, 41 million MWh of energy, and 38.3 million metric tons of emitted CO_2 per year in heating energy. It would also reduce energy use in water supply and treatment by 9.1 million MWh and 5.6 million metric tons CO_2 per year (Griffiths-Sattenspiel and Wilson 2009).

When only looking at the water supply, studies found that the energy demand is dominated (85%) by pumping to pressurize the distribution system (Burton 1996, Plappally and Lienhard 2012) but may be as low as 37% (Stokes and Horvath 2011). System operation used 56% to 90% (Stokes and Horvath 2006) or 94% (Racoviceanu et al. 2007) of total energy demand and production. On-site pumping is responsible for 60% of the operational burden (Racoviceanu et al. 2007).

Comparatively, treatment may contribute 42% (Stokes and Horvath 2011) or 44% (Crettaz et al. 1999). Water supply contributes 21% (Stokes and Horvath 2011) to 38% (Crettaz et al. 1999).

Consumption of treatment products and chemical production is generally found to be small, contributing 6% to 10% of total impacts (Arpke and Hutzler 2006, Crettaz et al. 1999, Racoviceanu et al. 2007, Tarantini and Federica 2001). However, one study found energy used by material production for treatment chemicals to be as high as 37%. Manufacturing treatment chemicals is the largest part (73%) of that material production (Stokes and Horvath 2011).

The construction and disposal phases of water treatment facilities are found to range from negligible when compared to the operational stage (Raluy et al. 2005), up to 4% to 9% of total environmental impact (Stokes and Horvath 2006). When only looking at the construction materials, the materials used (such as the iron) contributed more impact than the manufacture (such as processing into a pipe) (Dennison et al. 1999). Maintenance may cause 5-36% of total environmental impacts (Stokes and Horvath 2006)

3.3 Energy demand of individual treatment processes. Environmental impact studies of individual treatment processes, products, and chemicals are sparse, but some exist. Studies that do exist report results in terms of embedded energy in the finished water. This has the fallacy of hiding variation based on dosage.

Ozone uses 0.03 to 0.15 kWh/m^3 (Elliott et al. 2003).

Microfiltration uses 0.18 kWh/m^3 (Elliott et al. 2003).

Surface water chlorination uses 0.000021 to 0.00053 kWh/m^3. Groundwater chlorination uses 0.002 kWh/m^3 (Burton 1996). Another study found chlorine treatment has an average embedded energy of 0.003 kWh/m^3 (Kroschwitz 1995).

Alum treatment has an average embedded energy of 0.04 kWh/m3 (Kroschwitz 1995). Alum (aluminum sulfate) is made by reacting bauxite with sulfuric acid, producing very low toxicity and little waste products.

Lime treatment has an average embedded energy of 0.42 kWh/m^3 (Kroschwitz 1995). Lime (CaO) is produced by heating limestone to drive off CO_2.

Energy consumption associated with utilization of polymers for coagulation ranges from 0.4 to 0.7 kWh/m^3 (Tripathi 2007).

Energy associated with removal of industrial pollutants and anthropogenic materials, which require advanced treatment processes, has not been evaluated (Plappally and Lienhard 2012).

4.0 RESEARCH NEEDS

After detailed review of the existing body of knowledge regarding this topic, a few knowledge gaps and research needs can be identified.

Metal (hydr)oxide nanoparticle precipitation into weak base anion exchange resin has not been explored. This has been done on many other parent materials, including strong base anion exchange, activated carbon, and natural minerals. WBAX differs from other sorbents in that its tertiary amine is a unique functional group, it has different pore structure and pore size distribution, is functional in a unique pH range, and has high selectivity with high capacity for Cr(VI).

A clear correlation between synthesis procedures for a metal oxide nanoparticle embedded WBAX and the resultant sorbent characteristics has therefore not been explored either. The effects of variables such as metal precursor concentration and hydrolysis time on resultant metal content and surface area and pollutant removal efficiency is unknown.

It has not been proven what the mechanism for removal of Cr(VI) on the surface of WBAX is. It has been shown that Cr(VI) is ultimately reduced to Cr(III), but it is unknown how this happens, whether it happens before or after sorption, what the electron donor/reducing agent is, and whether the ion exchange functional group becomes available again after the Cr(III) precipitates.

No studies were found that use life cycle assessment to inform treatment technology selection. Only few use LCA to describe the treatment technology at all, with most focusing on the water supply or distribution. Almost all studies use energy demand as the final reported result, meaning there is opportunity to evaluate environmental impacts of water treatment beyond just energy use. No studies were found that evaluate ion exchange resins, and only few that include other sorbents such as activated carbon. There is a good understanding of other chemicals like alum. Further opportunity exists to

explore the embodied energy in a groundwater use if treatment beyond only chlorination is required.

CHAPTER 3

PHOSPHORUS RECOVERY FROM MICROBIAL BIOFUEL RESIDUAL USING MICROWAVE PEROXIDE DIGESTION AND ANION EXCHANGE

ABSTRACT

Sustainable production of microalgae for biofuel requires efficient phosphorus (P) utilization, which is a limited resource and vital for global food security. This research tracks the fate of P through biofuel production and investigates P recovery from the biomass using the cyanobacterium *Synechocystis* sp. PCC 6803. Our results show that *Synechocystis* contained 1.4% P dry weight. After crude lipids were extracted (e.g., for biofuel processing), 92% of the intracellular P remained in the residual biomass, indicating phospholipids comprised only a small percentage of cellular P. We estimate a majority of the P is primarily associated with nucleic acids. Advanced oxidation using hydrogen peroxide and microwave heating released 92% of the cellular P into orthophosphate. We then recovered the orthophosphate from the digestion matrix using two different types of anion exchange resins. One resin impregnated with iron nanoparticles adsorbed 98% of the influent P through 20 bed volumes, but only released 23% during regeneration. A strong-base anion exchange resin adsorbed 87% of the influent P through 20 bed volumes and released 50% of it upon regeneration. This recovered P subsequently supported growth of *Synechocystis*. This proof-of-concept recovery process reduced P demand of biofuel microalgae by 54%.

1. INTRODUCTION

There is an urgent need to find energy replacements for fossil fuels, whose combustion releases known and suspected human carcinogens and greenhouse gases into the atmosphere. One promising alternative is biofuel, which provides renewable energy with net greenhouse gas emissions significantly lower than fossil fuel (Batan et al. 2010). Biofuel derived from microalgae offers several advantages over biofuel from terrestrial plants: it does not compete with food crops for arable land, it can be continuously harvested, and it provides a much higher areal yield (Rittmann 2008, Schenk et al. 2008).

Microalgae biofuel production requires several inputs, including water, sunlight, carbon dioxide, and nutrients – particularly nitrogen (N) and phosphorus (P). During lipid extraction from microalgae biomass for liquid fuels, most of the N and P are discarded, requiring new nutrients for subsequent growth. Should microalgae become a significant replacement for fossil fuel in the future, the requirements for biomass growth would create a huge nutrient demand, rivaling that of agriculture (Erisman et al. 2010). Thus, capturing and recycling nutrients represents a significant opportunity for making large-scale cultivation of microalgae more sustainable (Clarens et al. 2010).

Nutrient recycling is particularly essential for P. Unlike N, which can be fixed from the atmosphere through the Haber-Bosch method (Huo et al. 2012), P is mined from

---

Abbreviations: ATP, adenosine triphosphate, DI, deionized water; EBCT, empty bed contact time; FAME, fatty acid methyl esters; HAX, hybrid anion exchange; ortho-PO_4^{3-}, orthophosphate; P, phosphorus; PG, phosphatidylglycerol; SBAX, strong base anion exchange.

ore that has finite stocks. World reserves of accessible P are estimated as 65,000 million metric tons (USGS 2011), and these are non-renewable and not substitutable. Depletion of economically affordable P may bring about international crises due to the essential role of P fertilizer for global food production (Cordell et al. 2009). Farmers in developing countries could be disproportionately harmed (Childers et al. 2011). Sustainable microbial biofuel production demands efficient nutrient recycling to prevent biofuel from becoming an enormous P demand competing with food production.

This research develops a proof-of-concept process for P-recovery from microalgae after extraction of lipids. The research objective is to track P through biofuel production and then recover P from residual biomass in a reusable form by using advanced oxidation to release the P for efficient ion exchange capture. The reusable form provides bioavailable P that supports microalgae growth.

We selected the cyanobacteria for this work because it is an excellent candidate for future utilization in large-scale biomass cultivation, particularly when energy efficiency in biosynthesis of fatty acids is crucial (Wijffels et al. 2013). Specifically we use *Synechocystis* sp. PCC 6803, which is a prokaryotic autotroph, Gram negative and able to withstand a wide range of environmental conditions. Lipids in the form of diacylglycerols are available in an extensive network of thylakoid membranes (van de Meene et al. 2006, Vermaas 2001). It may be genetically manipulated for specific traits favorable for biofuel production such as high lipid content (Vermaas 1996) because the entire genome has been sequenced (Kaneko et al. 1996).

1.1. P Recovery

To recover P from microbial biomass we first release organic-bound P as inorganic orthophosphate (ortho-PO_4^{3-}). This is necessary to improve the efficiency of the subsequent capture since ortho-PO_4^{3-} is more reactive. It also mitigates heterotrophic contamination of the biomass culture, which can occur after long run periods or with accumulation of inactive cells (Mata et al. 2010). Subsequently, we selectively capture the ortho-PO_4^{3-} from the liquid in a usable form. This is necessary to isolate and purify the ortho-PO_4^{3-}, allowing accurate and controlled dosing into the aqueous growth media during reuse. It also concentrates the ortho-PO_4^{3-} solution to minimize handling or hauling. This subsection gives the impetus for the technologies we selected to accomplish those goals.

Many P-recovery methods are available (de-Bashan and Bashan 2004, Morse et al. 1998, Rittmann et al. 2011). We selected an advanced oxidation process using hydrogen peroxide and microwave heating to release organic P from the residual biomass. Advanced oxidation creates hydroxyl free radicals that are highly effective for attacking organic matter to release ortho-PO_4^{3-} (Liao et al. 2005). This transformation may involve oxidation and hydrolysis reactions. While it may be possible to find technologies that are less energy-intensive, such as enzymatic hydrolysis or microbial fuel cells (Rittmann et al. 2011), or that do not dilute the biomass with additional liquid such as supercritical carbon dioxide (Blocher et al. 2012, Soh and Zimmerman 2011), advanced oxidation demonstrates the principle for releasing PO_4^{3-}.

We capture ortho-PO_4^{3-} using ion exchange since it recovers a liquid concentrate that is preferable for nutrient reuse during aquatic microalgae production. Other common

recovery techniques such as aluminum adsorption or struvite precipitation (de-Bashan and Bashan 2004) produce complex or low solubility solids which may be better suited for agricultural application. We evaluated two anion-exchange resins having distinctly different properties. The first was a hybrid anion exchange resin (HAX) impregnated with iron (hydr)oxide nanoparticles (Layne RT, Layne Christensen). It is reported to have a high sorption capacity and selectivity for ortho-PO_4^{3-} (Sengupta 2013) and the ability to release a high concentration ortho-PO_4^{3-} solution upon regeneration (Blaney et al. 2007, Midorikawa et al. 2008). The second was a type-1 strong-base anion exchange resin (SBAX) with quaternary amine functional groups in chloride ion form (21K-XLT, Dowex). It has a general anion-exchange capacity of 1.4 equivalents/L. It has previously been used for uranium (Stucker et al. 2011) and chromium (Rees-Nowak et al. 2005) removal, but has yet to be tested for phosphate recovery.

While the individual P recovery technologies employed in this study are not novel by themselves, their usage together such that the P completes an entire use and reuse cycle is. It is also the first study we know of to apply these technologies in the context of microbial biofuel production. Thus this study serves as a proof-of-concept that proposes an approach and can inform future optimization.

1.2. Microbial P

To focus the recovery efforts properly, this subsection estimates where P in *Synechocystis* is located based on literature review. Others have done this for several marine microalgae (Geider and La Roche 2002, Sterner and Elser 2002) but not specifically for *Synechocystis*. Biochemical fractions in cells can vary based on growth

conditions (Sheng et al. 2011a) but this provides clues for understanding the fate of P after lipid processing. Figure 3.1 summarizes the expected location of P in a *Synechocystis* cell. P may be located within adenosine triphosphate (ATP), lipids, and nucleic acid. The following three paragraphs individually analyze them.

ATP contains over 18% P by weight ($C_{10}H_{16}N_5O_{13}P_3$), but comprises less than 30 µg per g of cell mass. P associated with ATP is therefore 5 µg per g of the cell mass, which is a negligible contributor of the total cell P. The diphosphate form ADP and monophosphate form AMP are smaller fractions of the cell mass with less incorporated P and are also negligible contributors of cellular P storage.

The P content associated with lipid is a function of the fraction of lipid that is phospholipid and the fraction of phospholipid that is P. The predominant phospholipid head within cyanobacteria is phosphatidylglycerol (PG), which is the only phospholipid associated with thylakoid membranes in *Synechocystis* sp. PCC 6803 (Hajime and Murata 2007). PG has an elemental composition of $C_8H_{12}O_{10}P$. The most prevalent fatty acid chain in *Synechocystis* is C16:0, or palmitic acid (Sheng et al. 2011b), which has an elemental composition of $C_{16}H_{32}O_2$. Assuming that all phospholipids within *Synechocystis* are the diacylglycerol PG with two palmitic acid molecules, the overall elemental formula for a phospholipid molecule is $C_{40}H_{76}O_{14}P$. That means phospholipid is approximately 3.8% P by weight. PG-based lipids comprise approximately 14% of all lipids in *Synechocystis* (Sakurai et al. 2006), and lipids represent approximately 10% of the biological makeup of the overall cell (Shastri and Morgan 2005). Combining these estimates gives the theoretical amount of P associated with lipid in *Synechocystis* sp. PCC 6803 as 0.05% of the total cell weight, or 2% of the total cell P. A genetically altered

high lipid strain containing 50% crude lipids could then have as high as 0.3% of the total cell weight be P associated with lipid. For this reason, we do not expect much P in the lipids.

We estimate the P content associated with DNA and RNA by comparing its biological composition with its elemental composition. *Synechocystis* sp. PCC 6803 is approximately 3% DNA and 17% RNA by weight (Shastri and Morgan 2005). DNA and RNA are 10% P by weight (Sterner and Elser 2002). Therefore, P associated with DNA comprises 0.3% of the total cell weight, and P associated with RNA is 1.7% of the total cell weight. This is respectively 15% and 83% of the total cellular P. We consequently expect that most of the cellular P will be in nucleic acid. This was also observed in other studies on lake bacteria where P associated with RNA comprised a majority of the total cell P (Elser et al. 2003, Geider and La Roche 2002).

2. MATERIALS AND METHODS

2.1. Strain, Growth Conditions, and Biomass Production

We grew *Synechocystis* sp. PCC 6803 in BG-11 growth media (Rippka et al. 1979) modified to have five times the normal amount of phosphate (added as K_2HPO_4) (Kim et al. 2010) in a bench-top photobioreactor in semi-continuous growth mode. We separated biomass from the growth medium by means of centrifugation at 1,500 g for 20 min in 50-mL plastic tubes. We resuspended the cell pellet in 1 mM sodium bicarbonate (Sigma-Aldrich) to rinse away residual medium. We repeated centrifuging and rinsing two times before freeze-drying the final pellet (Labconco Freezone 6) for 2 days at 0.013 mbar and -50ºC in order to obtain an accurate starting dry weight (Sheng et al. 2011b).

We collected enough biomass to perform all lipid extraction and P recovery experiments at least in duplicate.

2.2. Lipid Extraction and Transesterification

We extracted lipids from the freeze-dried biomass using the Folch Method (Folch et al. 1957) using a 2:1 (V:V) mixture of chloroform (Mallinckrodt) and methanol (Fisher Scientific), since it has a high extraction efficiency for *Synechocystis* lipids (Sheng et al. 2011b). We ground a 300-mg (all weights given as dry weight) sample with agate mortar and pestle, suspended it in 60 mL of Folch solvent, and placed it on a shaker table at 175 rpm for 2 days. We filtered the suspension with a glass fiber filter (Whatman GF/B) and then a 0.2-µm polytetrafluoroethylene filter (Whatman). The biomass retained on both filters was the primary residual, and the filtrate contained the extracted crude lipid. For samples undergoing transesterification, we evaporated the solvent from the crude lipid under N_2 gas to avoid oxidation of lipids. For samples where no further lipid processing was necessary, we evaporated the solvent by heating on hot plate.

We transesterified the crude lipid (Sheng et al. 2011b) by adding 1 mL of methanolic hydrochloric acid (Supelco) and heating the mixture in an 85ºC water bath for 2 h. After cooling the mixture to room temperature, we added 0.5 mL of deionized (DI) water and 1 mL of hexane, shook the mixture by hand for 30 s, and allowed the phases to separate. We repeated all transesterification steps two additional times, and then pooled all the hexane. The extracted hexane contained the fatty acid methyl esters (FAME), and the remaining water contained the secondary residual.

For experiments tracking the fate of P, we analyzed total P for each biomass, primary residual, crude lipid, secondary residual, and transesterified FAME (at least duplicate samples).

2.3. Advanced Oxidation

We scraped primary residual from the dried filters and added it to 60 mL (giving 3.6 gVSS/L) of 30% ultrapure H_2O_2 solution (JT Baker Ultrex II) diluted 1:10. We let this mixture stand for 1 hr of pre-digestion under fume-hood ventilation. We digested the mixtures in a microwave (CEM MARS XPress) at 400 W by ramping the temperature up to 170ºC over 10 min and then holding at 170ºC for 10 min per method SW846-3015 (USEPA 2008). Others have observed the highest fraction of P release by this peroxide dose and microwave heating temperature (Liao et al. 2005, Wong et al. 2006), and future work may explore varying other conditions to optimize P release. We employed high-pressure microwave vessels to avoid breakage that the high rate of gas evolution could cause. We analyzed duplicate samples before and after oxidation for total P and ortho-PO_4^{3-}.

2.4. Phosphate Separation

We did preliminary investigation of the P separation capacity of each of the two anion exchange resins by placing 3.5 g of fresh resin in a 1.5-cm inner diameter glass column, giving a bed depth of 3.0 cm. We supported the resin with glass beads to ensure even flow distribution. We flushed 100 mL of DI water through the column and allowed air bubbles to escape. Then, we pumped a solution of monobasic sodium phosphate

(Mallinkrodt ACS grade) in DI water (concentration 80 mgP/L) through the column at 3.2 mL/min to give an empty bed contact time (EBCT) of approximately 2 min (loading rate of 4.4 mgP/s/g resin). We periodically took effluent samples for P analysis, and continued the experiment until the effluent P concentration stabilized near the influent P concentration. We then desorbed the P using a strong regeneration solution at a pump rate of 0.5 mL/min (EBCT of approximately 10 min) until the effluent P concentration stabilized at nearly zero. The strong regeneration solution used for the HAX resin was 0.1 N potassium hydroxide (EMD), and for the SBAX resin was 0.1 N sodium chloride (Sigma Aldrich). We later varied influent P concentration, EBCT, P loading rate, influent pH, and elute contact time in order to optimize column operation.

We then tested each resin with biomass after advanced oxidation by pumping the 60 mL of digested sample through 2.0 g of fresh resin having a bed depth of 1.7 cm. The flow rate was 1.4 mL/min, giving an EBCT of approximately 2 min. We collected the effluent and pumped it through the column two more times to ensure complete capture of phosphate onto the resin. We then recovered retained ortho-PO_4^{3-} by removing the resin from the column and placing it in 33 mL (11 bed volumes) of strong regeneration solution, which was heated on a 95ºC hot plate, shaken for 24 h, and then decanted. Elution and decanting were repeated two times, and the elution solutions were pooled so that the serial batch elution mimicked a continually stirred tank mixer (CSTM) in series (n = 3). We analyzed the total volume of 100 mL (33 bed volumes) for pH, total P, and ortho-PO_4^{3-}.

We obtained the total mass of P sorbed to each resin by summing the difference between the influent concentration and the effluent concentration for each sample

multiplied by the volume treated in the time segment (area above the curve times flow rate).

2.5. Phosphorus Reuse

As a confirmatory experiment, recovered P solution was used to culture wild-type *Synechocystis* sp. PCC 6803 cells. We diluted the recovered P solution to P concentration prescribed by standard BG-11, spiked the other nutrients to standard levels, then added additional bicarbonate to compensate for low aeration in small samples. We inoculated plastic tubes containing 20 mL of the growth media with fresh *Synechocystis* cells in duplicate. We placed these on a shake table under constant light conditions for one week, and regularly monitored optical density by absorbance at 730 nm.

2.6. Phosphorus Analysis

We determined ortho-PO_4^{3-} colorimetrically with a spectrophotometer (HACH DR5000) using the PhosVer 3 Method (HACH), which is equivalent to *Standard Methods* 4500-P.E (Miner 2006). It directs to add reagent powder to 5 mL of sample and give 2 min of reaction time, then measure results at 880 nm.

We assayed total P by persulfate digestion (*Standard Method* 4500-P.B.5) (Miner 2006) followed by inductively coupled plasma optical emission spectrometry (ICP-OES). To do this we suspended samples in 50 mL DI water plus 1 mL of concentrated sulfuric acid (JT Baker ultrapure). We then added 0.4 mg of ammonium persulfate (Malinckrodt) to each sample. We autoclaved the sample for 30 min at a pressure of 1.05 kg/cm^2 and a

temperature of 122ºC. We measured total P by ICP-OES (Thermo iCAP6300) at a wavelength of 213.6 nm.

3. RESULTS & DISCUSSION

3.1. Fate of P through lipid extraction

Freeze dried *Synechocystis* sp. PCC 6803 biomass contained 1.39%±0.28% total P by dry mass. (All weights given by dry weight. ± indicates half standard deviation.) This is consistent with previous findings that P is 1.5% of dry cell mass (Kim et al. 2010). In lipid-extracted biomass samples, primary residual contained 1.50%±0.36% total P by dry mass. Figure 3.2 summarizes the fate of P through lipid extraction normalized to 100 mg of total P in the starting biomass. The primary residual contained 92±4.3 mg total P. Crude lipid contained 7.3±4.2 mg total P. For transesterified samples, total P in the FAME was 0.5±0.1 mg total P. Total P in the secondary residual was 9.5±5.3 mg. Thus, nearly all of the starting organic P was in the primary residual after lipid extraction. Of the small amount in the crude lipids, nearly all of it was in the secondary residual. Essentially no P (<1% of the starting P) was in the transesterified FAME.

These findings support our expectation that nucleic acid is the primary storage of total cell P, with only small amounts stored in phospholipids. P associated with phospholipid partitions to the crude lipid during extraction, while P associated with nucleic acid remains in the primary residual. This explains the large fraction of P found experimentally in the primary residual. The observed increase in P content from dry cells to primary residual (1.39±0.28% to 1.50±0.36%) was not statistically significant, but any increase would demonstrate the disproportional storage of P in non-lipid structures. The

92±4% of P found experimentally in the residual correlates with the expected 98% P associated with nucleic acid. We attribute the small amount of P found in the fatty acids to impurities from incomplete partitioning and analytical margin of error.

3.2. Oxidation of Organic P to Release Ortho-PO_4^{3-}

Since only small amounts of the starting P were in the crude lipid and subsequent lipid processing, the primary residual became the focus for P recovery. Prior to treatment with H_2O_2 and microwave heating, this primary residual contained 82±1 mg total P with 0.2 mg of it as ortho-PO_4^{3-}. After H_2O_2 and microwave treatment, samples contained 90±12 mg total P, including 75±6 mg as ortho-PO_4^{3-}. Therefore, H_2O_2 oxidation recovered 106±17% of the total P (analytical error accounts for recovery over 100%) and released most of it as ortho-PO_4^{3-}, which was the objective.

3.3. Recovery of Ortho-PO_4^{3-} by Resins from DI Water

Figure 3.3A shows the ability of the two resins to absorb P in DI water. Both resins were able to capture nearly all of the influent P up to 30 bed volumes. At this point, the capacity of the resins was 5.0 mgP/g resin and 4.7 mgP/g resin for the HAX and SBAX resins, respectively. The HAX resin then began a sharp breakthrough and reached complete saturation near 80 bed volumes. The SBAX resin began a gradual breakthrough, reaching 50% saturation around 200 bed volumes and 80% saturation around 500 bed volumes. At the end of the experiments, the HAX resin sorbed a total mass of 38 mg of P, giving a sorption capacity of 11 mgP/g resin, and the SBAX resin sorbed a total mass of 140 mg of P, giving a sorption capacity of 40 mgP/g resin.

Both resins released all of the P that would be eluted within the first 20 bed volumes of regeneration. They did not release any additional P with 10 additional bed volumes of regeneration (Figure 3.3B). The fastest rate of P elution for the SBAX resin occurred around 5 bed volumes, and around 8 bed volumes for the HAX resin. A total of 19 mg of P was eluted from the HAX resin, or 51% of the total sorbed P was recovered. A total of 167 mg of P was eluted from the SBAX resin, or 119% of the total sorbed was recovered (the lack of mass-balance closure was due to analytical error from high dilution required for analysis of concentrated elute). The pH of the HAX elute containing the recovered P was 12, and of the SBAX elute it was 6.

The HAX resin had higher selectivity for P as demonstrated by the lower amount of P in the column effluent, the sharp breakthrough curve showing a short saturation zone, and the higher sorption capacity. We therefore expect it to have a higher rate of P capture in solutions with competing constituents like the oxidized biomass. However, 0.1 N KOH did not efficiently recover the sorbed P. While the iron nanoparticles lead to higher sorption capacity than SBAX, they apparently made it more difficult to desorb the P. Poor recovery might indicate that at least part of the sorbed P was irreversibly adsorbed by the impregnated iron (hydr)oxide nanoparticles instead of sorbed entirely by anion exchange. Our result differs from previous studies that showed that 80-90% of the P could be released by elution from the HAX resin (Martin et al. 2009, Sengupta 2013) using 0.5-1.0 N NaOH plus 0.4 N NaCl. Differences with these previous studies include different influent matrices, not using combined NaCl and NaOH elutes or in as strong doses, and lower resin contact time. We avoided stronger eluent doses so the recaptured P would not be in such a high saline or high pH matrix that it would be unsuitable for

subsequent microbial growth. Since elution of the SBAX resin with 0.1 N NaCl showed the best recovery, we focused our subsequent ion-exchange work on it.

In order to improve performance with the SBAX resin, we varied column operation parameters to improve the P capture and release. For P capture, a steep breakthrough curve is desired so that all of the P is captured until the inception of breakthrough, at which time the column is stopped and regenerated. The SBAX breakthrough curve could be made steeper by lowering the hydraulic loading rate. Figure 3.4 shows results for a SBAX column receiving 100 mgP/L influent in DI water with an EBCT of 20 min (instead of 2 min) and a lower hydraulic loading rate of 3 BV/hr (instead of 30 BV/hr). Consequently, the resin captured all ortho-PO_4^{3-} for 200 BV before exhibiting a steep and desirable breakthrough curve. This gave a sorption capacity of 35.6 mgP/g resin. For P regeneration, slower elution (2 BV/hr) gave 99% recovery of the loaded P within 4 BVs. This allowed us to achieve an 80-fold increase in P concentration in the regenerant. Additional tests (data not shown) indicated greater ortho-PO_4^{3-} exchange capacity at pH 5 instead of 8. This effort aimed to show that each step in this proof-of-concept P-recovery sequence could be optimized to obtain desired performance outcomes.

3.4. Recovery of Ortho-PO_4^{3-} by Resins from Oxidized Biomass

We pumped oxidized primary residual through the ion exchange columns with enough resin so the influent did not exceed 20 bed volumes to ensure complete capture of the P. The HAX column effluent contained 1.7±0.3 mg of P out of the 72±0.9 mgP influent, indicating 98% P capture on the resin. After elution, 16.7±0.0 mg P was in the

100 mL elute. Of this, 14.9±0.1 mg was ortho-PO_4^{3-}. The pH of the pooled elute was 12.4±0.5. Overall, the HAX resin recovered 23%±0.2% of the influent P to the regeneration solution.

The SBAX column effluent contained 20.9±7.6 mg of P out of 108±7.6 mgP influent, indicating 81% of the P sorbed to the resin. After elution, 54.4±8.9 mg of P was in the 100 mL elute. Of this, 53.0±8.2 mg was ortho-PO_4^{3-}. The pH of the pooled elute was 6.6±0.1. Overall, the SBAX resin recovered 50%±5% of the influent P to the regeneration solution.

Both resins were only able to recover about half as much P when loaded from oxidized biomass as opposed to when loaded from DI water: HAX went from 51% to 23%, and SBAX went from 119% to 50%. Previous studies have also observed lower recovery from complex solutions like sludge liquor than from synthetic solutions (Bottini and Rizzo 2012). In addition to ortho-PO_4^{3-}, the solutions from the oxidized biomass also contained residual organic matter (after oxidation 15 mg P out of 90 mg P was still organic-bound) and other anions (bicarbonate, carbonate, sulfate, and nitrate) that were probably also exchanged by the resins. Additionally, the influent pH for DI tests was 5, but for influent oxidized biomass it was over 6. Having the pH approach the second deprotonation for ortho-PO_4^{3-} ($pK_{a,2}$ = 7.2) during loading shifted a small fraction of its speciation away from the single charge $H_2PO_4^-$ to the double charged HPO_4^{-2}. This may have reduced ortho-PO_4^{3-} adsorption capacity because each HPO_4^{-2} takes up two anion-exchange sites. This effect would be even stronger during regeneration due to the higher pH (12 for the HAX) of the elute when almost all of the ortho-PO_4^{3-} would be present as HPO_4^{-2}. In the case of the HAX resin, this competition for anion exchange sites may

have forced more ortho-PO_4^{3-} to be sorbed to the iron (hydr)oxide nanoparticles which could form inner sphere complexes with stronger bonding and less elution.

3.5. P Recovery and Reuse

Figure 3.5 summarizes results for each process step in the overall recovery process using the SBAX resin. The lipid extraction, cellular oxidation, and nutrient isolation steps were, respectively, able to recover 93%, 106%, and 50% (using SBAX) of the starting P. The overall process recovered 54% of the starting intracellular P into a pure and concentrated nutrient solution. This yield is similar to other systems designed for complete P recovery (Blocher et al. 2012) and shows that nutrient reuse in the context of microalgae biofuel production is viable.

The recovered solution had an ortho-PO_4^{3-} concentration of 10.6 mgP/L, compared to 5.4 mgP/L required in standard BG-11. We also measured 0.95 mg NO_3^--N/L and 1.5 mg SO_4^{2-}-S/L, compared to 247 and 9.8 mg/L required for BG-11, respectively, demonstrating the selectivity of the resin for P.

The P solution recovered from the SBAX supported cyanobacteria growth. The optical density increased from 0.12 initially to 0.55 after one day and to 1.11 after one week. This correlates to specific growth rates of 1.4 day^{-1} over one day and 0.7 day^{-1} over one week. For comparison, the optical density of the same cell culture grown in a BG-11 solution without any P went from 0.12 initially to 0.16 after one day and 0.10 after one week, corresponding to specific growth rates of 0.26 day^{-1} after one day and -0.06 day^{-1} after one week. The nearly ten-fold increase in cell density over one week in the solution containing recovered P confirms that the recovered P was available for

cyanobacteria uptake. It also demonstrates that we did not co-recover any substances that would inhibit reuse, such as harmful heavy metals or residual oxidant. These rates are comparable to growth rates previously observed for *Synechocystis* using BG-11 (Kim et al. 2010) albeit in a different reactor configuration.

We recommend future work improving P release methods that can co-recover other valuable products produced by cyanobacteria, like other nutrients, proteins, or ethanol (Wijffels et al. 2013). We further recommend improving P capture efficiency, reducing the overall cost, energy, and chemical footprint of the process, and demonstrating recovery on full-scale. Other future work could compare the effectiveness of growing microalgae on recovered P compared to other sources of P with complete controls.

4. CONCLUSIONS

Efficient P recycling in microbial biofuel production will be essential to preventing competition between food and energy systems. This work demonstrates:

- After lipid processing, over 90% of the P remained in the residuals. Most cellular P is in nucleic acids, with very little in phospholipids.
- Advanced oxidation transformed over 80% of that organic P into useful and recoverable ortho-PO_4^{3-}.
- While HAX resin showed higher affinity for ortho-PO_4^{3-}, the SBAX resin released the ortho-PO_4^{3-} more completely.
- Both resins recovered less P from oxidized biomass than from P spiked DI water, likely due to interference with residual organics or competing oxyanions.

Acknowledgements

A Dean's Fellowship from the Ira A. Fulton Schools of Engineering at Arizona State University provided partial funding for this study, as did the Central Arizona Phoenix Long Term Ecological Research (CAP LTER) project from the National Science Foundation (BCS-1026865). Thank you to Jie Sheng who provided training on lipid extraction and biofuel processing. Thank you to Chao Zhou and Levi Straka for culturing the cyanobacteria.

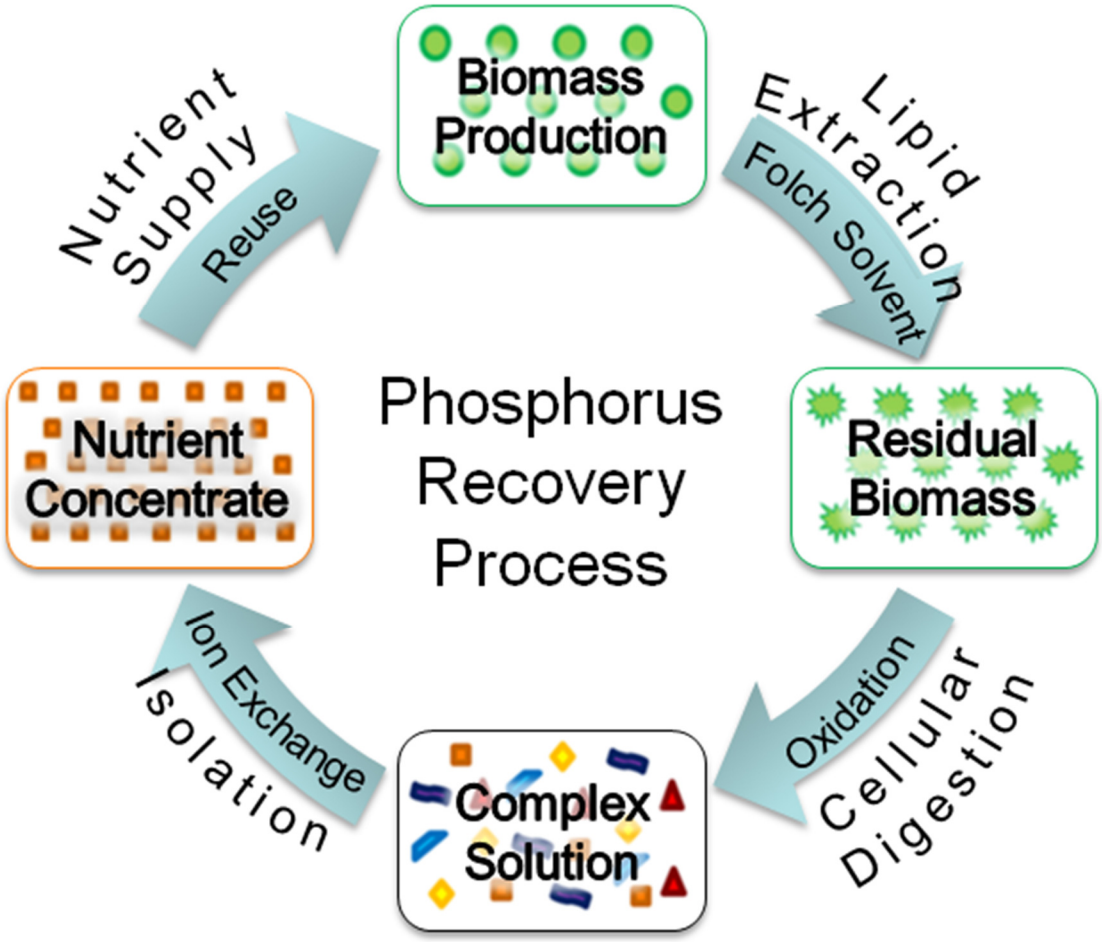

Figure 3.0. Graphical Abstract

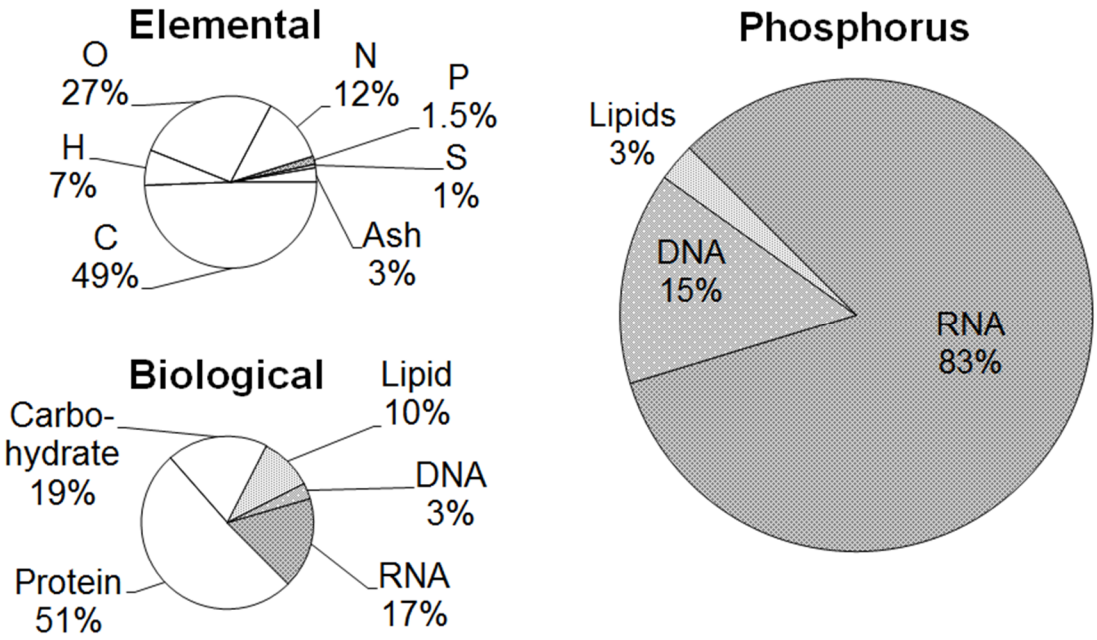

Figure 3.1. The estimated location of P within Synechocystis sp. PCC 6803 shown on the right determined by the elemental (Kim et al. 2010) and biological (Shastri and Morgan 2005) composition shown on the left. All numbers given are percent by weight of the total biomass (left) or total P in the biomass (right). A majority of cellular P is in RNA, and only small amounts are in lipids. Thus, almost all P is in the primary residuals after lipid extraction, not in the lipid extract.

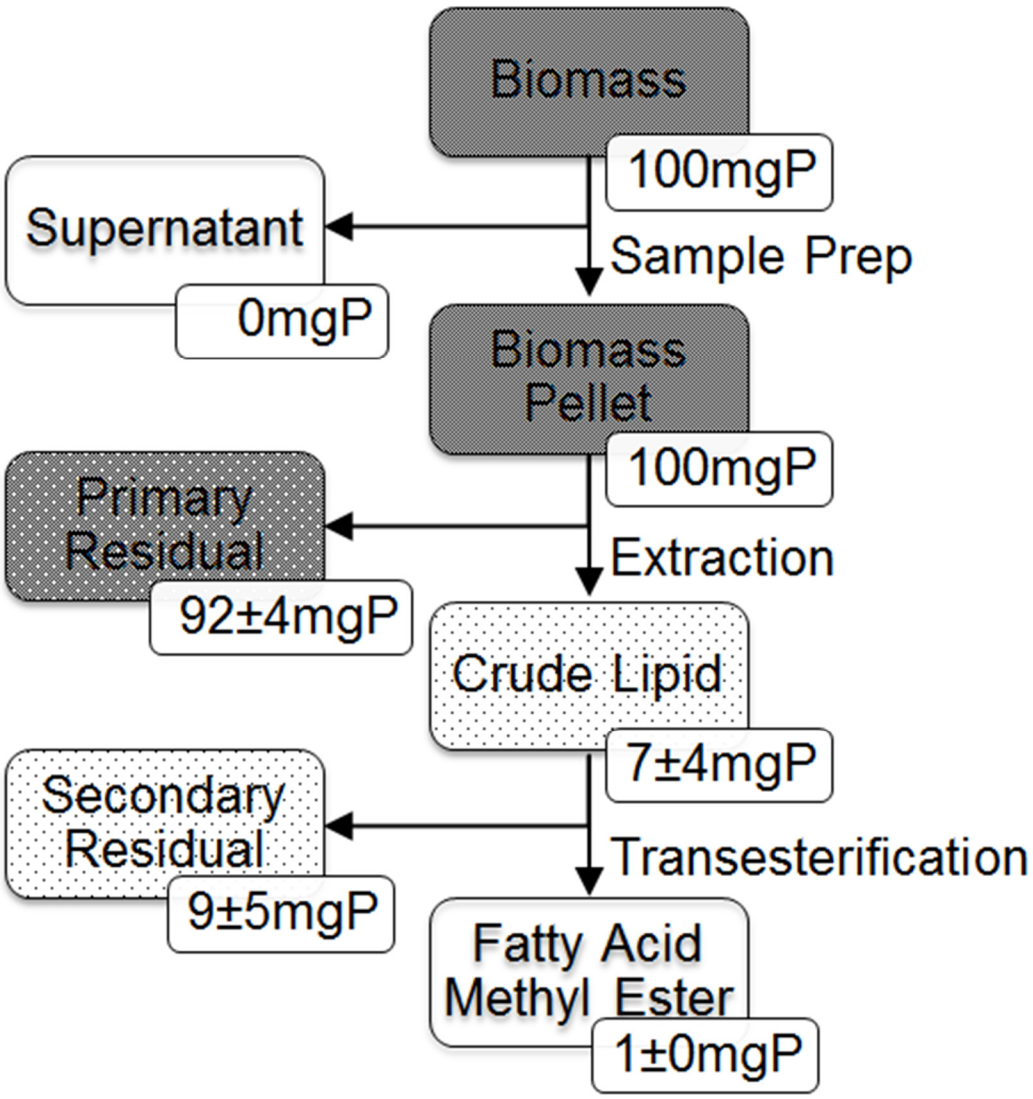

Figure 3.2. The fate of 100 mg of starting P through the lipid extraction process. Most of the P remained with the biomass in the primary residual, although some was associated with the crude lipid remains in the secondary residual. The FAME only contained about 1% of the starting P.

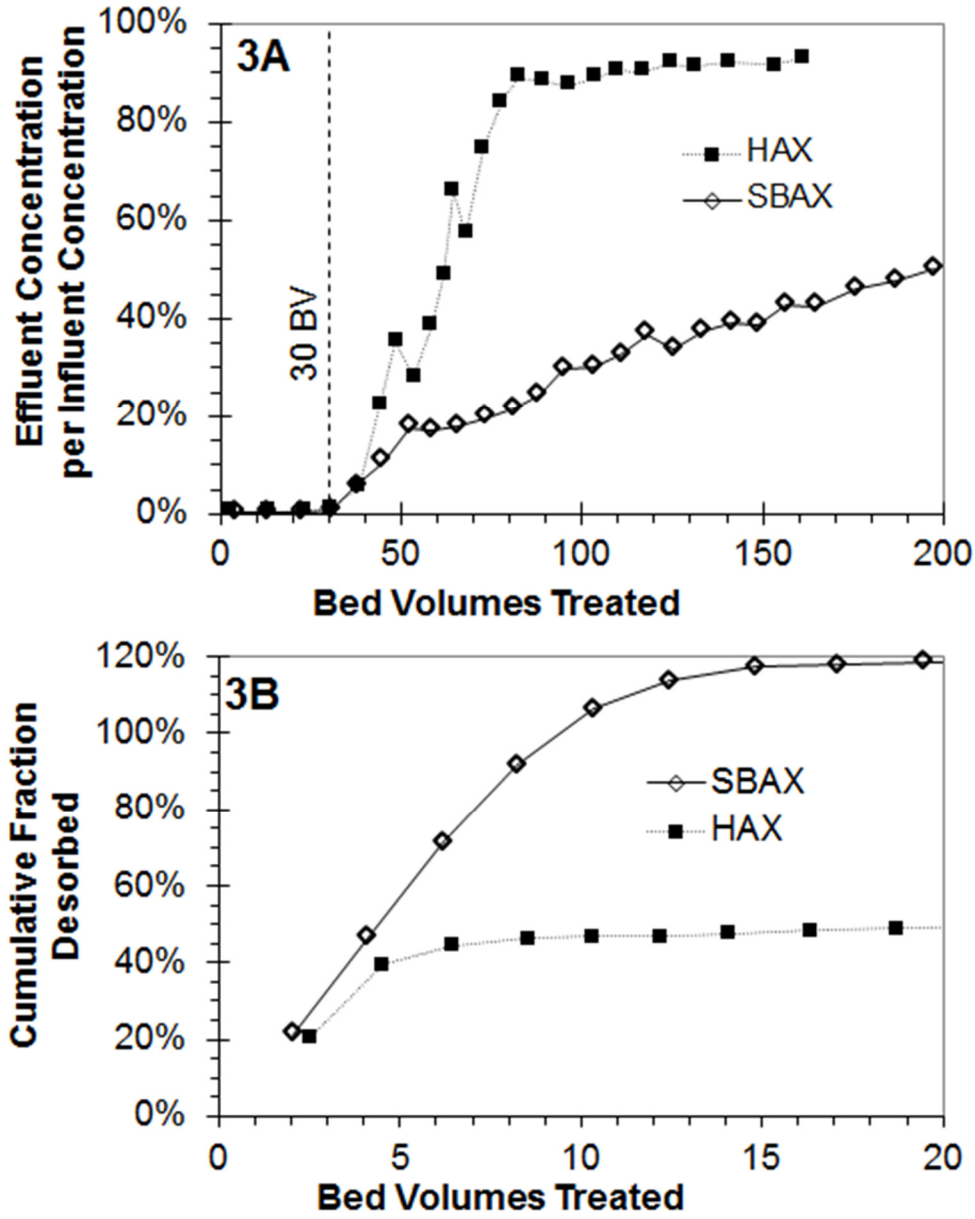

Figure 3.3. Performance of an iron hydr(oxide) impregnated anion exchange (HAX) resin (squares) and a strong-base anion exchange (SBAX) resin (diamonds) for recovering phosphate from DI water. (A) Uptake of phosphate by fresh resin in column test. Uses hydraulic loading rate of 30 BV/hr, an initial P concentration of 80 mgP/L, and influent pH 5. (B) Desorption of phosphate from resin by 0.1 N KOH for HAX or 0.1 N NaCl for SBAX with hydraulic loading rate of 6 BV/hr, normalized to mass of P sorbed. The HAX resin shows higher affinity for P during sorption, but the SBAX releases more P upon elution.

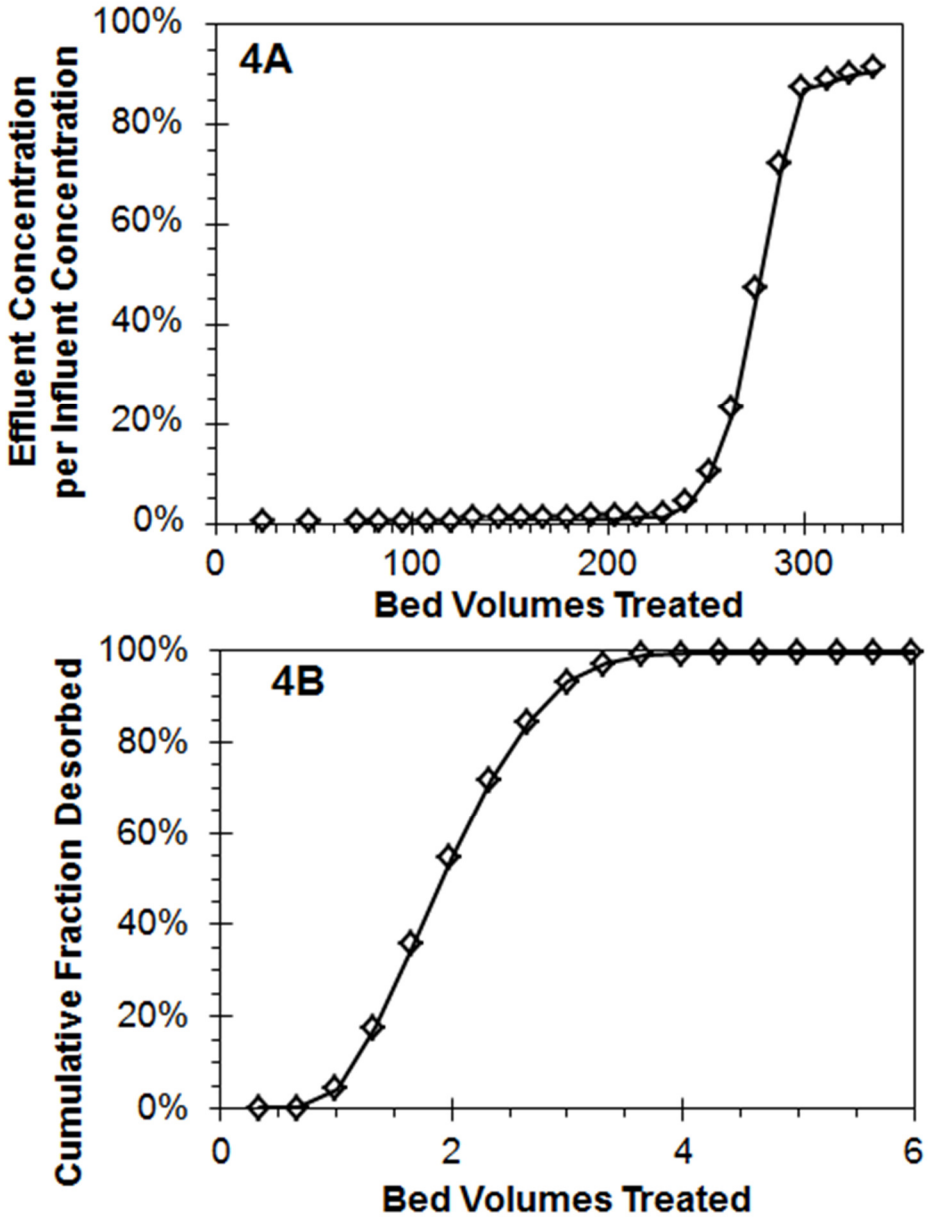

Figure 3.4. Enhanced P recovery from DI water on SBAX resin by improving operating conditions. (A) Uptake of phosphate by fresh resin in column test. Uses hydraulic loading rate of 3 BV/hr, an initial P concentration of 100 mgP/L, and influent pH 8. (B) Desorption of phosphate from resin by 1 N NaCl at a hydraulic loading rate of 2 BV/hr, normalized to mass P sorbed. The steep breakthrough after a long bed run is optimal for P recovery, and subsequent elution in few bed volumes gives an 80-fold increase in P concentration.

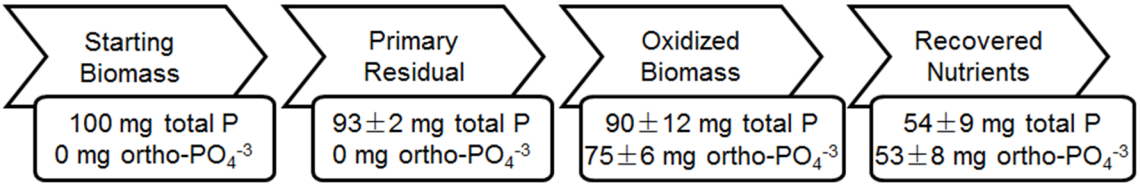

Figure 3.5. Process step yields of total P and ortho-PO_4^{3-} for 100 mg starting P through the P-recovery process using advanced oxidation and SBAX. Nearly all cellular P was found in the primary residual after lipid extraction. Advanced oxidation transformed a majority of the P to recoverable and beneficial ortho-PO_4^{3-}. SBAX resin could then sorb and elute a concentrated nutrient solution. The overall tested P-recovery process could capture more than 50% of the starting P in a beneficial form.

CHAPTER 4

NANO-ENABLED SORBENTS OUTPERFORM TRADITIONAL SORBENTS FOR SIMULTANEOUS HEXAVALENT CHROMIUM AND ARSENIC REMOVAL

ABSTRACT

This work demonstrated nanotechnology can reduce multiple contaminants of health concern, resulting in groundwater treated to drinking water standards. Many municipal and private well are treated to meet arsenic (As(V)) regulations, and new regulations for hexavalent chromium (Cr(VI)) are soon possible. Rather than adding costly capital infrastructure, we explored sorbents' ability to remove both oxo-anions simultaneously. We compared removal efficiency of traditional metal (hydr)oxide sorbents and weak base anion exchange (WBAX) resins against nano-enabled sorbents with iron or titanium nanoparticles embedded inside the porous structure of an anion exchange resin. To our knowledge, this is the first use of metallic nanoparticles embedded in WBAX for simultaneous contaminant treatment. In laboratory batch and column tests, metal (hydr)oxide sorbents demonstrated high affinity for As(V) but exhibited low capacity to remove Cr(VI). WBAX resins had some ability to sorb both Cr(VI) and As(V), but competing anions lowered their sorption capacity. The nano-enabled sorbents demonstrated high ability to remove Cr(VI) and As(V) simultaneously despite competition and were able to remove both pollutants for twice as long in column mode as the traditional sorbents. To quantitatively rank sorbents' ability to remove multiple pollutants, we developed a Simultaneous Removal Capacity scoring tool.

1. INTRODUCTION

Recent advancements in nanotechnology have enabled tremendous opportunities for environmental protection and pollution mitigation. Applications employing nanotechnology toward providing clean drinking water include sorption, disinfection, and photocatalytic reduction of pollutants that benefit from high surface area to mass ratio (Qu et al. 2013). The small size of nanoparticles allow them to be embedded inside of the porous structure of other materials, such as nano-sized zero-valent iron in polymers (Du et al. 2013), nano-scale metal (hydr)oxides inside of biochar (Hu et al. 2015), chitosan (Yamani et al. 2012), or activated carbon (Sandoval et al. 2011). The porous and composite nature of such hybrid sorbents may provide a dual functionality, which has a useful application in groundwater treatment.

Groundwater serves as the primary water source for 95% of drinking water systems in the United States (US), over 60% of which provide no treatment beyond disinfection (Impellitteri et al. 2007). Groundwater often contains mixtures of inorganic pollutants including chromium, arsenic, nitrate, and fluoride. Anion exchange resins embedded with metallic nanoparticles may be able to simultaneously treat multiple inorganic pollutants, as has been demonstrated for arsenic and nitrate (Elton et al. 2013) as well as arsenic and perchlorate (Hristovski et al. 2008b). This study explored using these hybrid anion exchange (HAX) sorbents for simultaneous treatment of chromium (Cr(VI)) and arsenate (As(V)), which co-occur in oxidized groundwaters throughout the southwest US and elsewhere.

Removing chromium from drinking water is becoming vital. Chromium in groundwater is primarily found in hexavalent form as a divalent anion (Schweitzer and

Pesterfield 2010) at concentrations of up to 50 µg/L (Frey et al. 2004). It is part of the Unregulated Contaminant Monitoring Rule 3 (Federal Register 2012) and is undergoing a Human Health and Carcinogenicity Risk Assessment (USEPA 2010a). The US Environmental Protection Agency (USEPA) regulates total chromium in drinking water at 100 µg/L, and California recently set a 10 µg/L maximum contaminant level (MCL) for Cr(VI) with only 11 weeks between regulatory notification and start of enforcement (CCR 2014). Compliance costs in one California system are expected to increase monthly water fees by $30 to $50 per household (CVWD 2014).

Arsenic is a known human carcinogen in drinking water and underwent a similar review process in 2006 that lowered its federal MCL from 50 µg/L to 10 µg/L (USEPA 2010b). However, many systems are still non-compliant for arsenic; 67% of the non-compliant systems serve fewer than 500 people (McGavisk et al. 2013), indicating a disproportionate risk to customers served by small systems. Arsenic exists in a pentavalent oxidation state within a divalent anion in oxidized groundwater (Schweitzer and Pesterfield 2010) and is easily oxidized from As(III) to As(V) by free chlorine.

As occurs in more than 27% of community groundwater sources nationally, and 5% exceed 10 µg/L (USEPA 2000). Cr(VI) occurs in more than 31% of community groundwater sources nationally, and 4% exceed 10 µg/L (USEPA 2015b). Because Cr(VI) and As(V) are common groundwater pollutants, co-occurrence is possible. A national co-occurrence study found that groundwater containing total or hexavalent chromium was just as likely as any other groundwater to contain arsenic. Of 29 sampled groundwater sites with Cr(VI) above 5 µg/L, the mean and maximum levels of As(V) were 16.7 and 60 µg/L, respectively (Brandhuber et al. 2004b).

Leading treatment technologies for Cr(VI) include strong base anion exchange (SBAX) or weak base anion exchange (WBAX) resins and reduction to trivalent chromium followed by coagulation and filtration (Brandhuber et al. 2004b, McGuire et al. 2007). As(V) treatment technologies are well documented and include sorption to metal (hydr)oxide sorbents (MO), anion exchange, or aluminum and ferric hydroxide precipitates (Lin and Wu 2001, Mohan and Pittman 2007, Westerhoff et al. 2005). Treatment of each individual pollutant has been studied, but it remains ill-defined if any of these technologies can simultaneously treat for both As(V) and Cr(VI). This study focused on sorbents because they are common treatment techniques for both pollutants, can be delivered in a single easy to operate cartridge, and may be the cheapest treatment option if disposal is available (Najm 2013). Simultaneous treatment using these traditional sorbents was compared to the nano-enabled sorbents.

There is a need to compare sorbents' ability to remove multiple pollutants. Sorbent removal capacity is often expressed in terms of equilibrium sorption capacity (q), but this quantity only communicates the capacity for one pollutant. Comparative capacities for multiple pollutants are often expressed by a selectivity coefficient or separation factor (α); however, this only communicates relative preference and not absolute capacity. Therefore this study proposed a new analysis tool that includes both absolute and relative capacity to be used to quantify sorbents having the highest ability to treat multiple pollutants.

The goal of this study was to compare ability of currently available sorbents to nano-enabled hybrid sorbents to remove Cr(VI) and As(V) from drinking water. Performance was initially based on equilibrium batch testing. The effect of co-occurring

constituents was explored by comparing removal capacity in a simple lab grade water to a challenging groundwater matrix. A technique for quantitatively comparing sorbents for simultaneous removal was developed, and the best performing sorbents in equilibrium tests were evaluated in column tests.

2. MATERIALS & METHODS

2.1. Selection of Traditional and Nano-Enabled Sorbents. Seven traditional sorbents and three nano-enabled sorbents were included in this study as described in Table 4.1. The traditional sorbents included four commercially available MO sorbents that are widely used for As(V) treatment and three commercially available WBAX resins that are widely used for Cr(VI) treatment.

	Designation	Manufacturer	Commercial Name	Description	Form	Observed Water Content
Traditional Sorbents	MO1	Adedge	Bayoxide E33	Iron (hydr)oxide	Pellet	4.7%
	MO2	Dow	Adsorbsia GTO	Titanium (hydr)oxide	Flake	3.5%
	MO3	Siemens	GFH	Iron (hydr)oxide	Flake	37%
	MO4	Associated Materials Processing	AMP35	Iron (hydr)oxide	Powder	6.4%
	WBAX1	ResinTech	SIR700	Epoxy polyamine weak base anion exchange	Spherical	37%
	WBAX2	Purolite	S106	Epoxy polyamine weak base anion exchange	Spherical	61%
	WBAX3	Dow	Amberlite PWA7	Polycondensate weak base anion exchange	Granules	63%
Nano-Enabled Sorbents	HAX1	Layne Christensen	LayneRT	Iron (hydr)oxide nanoparticles inside strong base anion exchange	Spherical	62%
	HAX2	Lab synthesized	-	Iron (hydr)oxide nanoparticles inside weak base anion exchange	Spherical	72%
	HAX3	Lab synthesized	-	Titanium (hydr)oxide nanoparticles inside weak base anion exchange	Granules	81%

Table 4.1. Description of sorbents included in this study for evaluation of simultaneous Cr(VI) and As(V) removal capacity.

The three nano-enabled sorbents include a commercially available sorbent marketed for As(V) removal that is reported to have iron (hydr)oxide nanoparticles embedded inside a SBAX resin (HAX1). Two additional nano-enabled hybrid sorbents were synthesized for this study using protocols previously developed for SBAX and applied to chromate-selective WBAX. At the time of the study design, literature review showed that this study was the first to embed MO nanoparticles in WBAX for simultaneous treatment of Cr(VI) and As(V). Adding nanoparticles to another sorbent was intended to create a sorbent with dual functionality of As(V) and Cr(VI) removal capacity. HAX2 has iron (hydr)oxide nanoparticles precipitated in-situ within WBAX1 (Hristovski et al. 2008b). Briefly, WBAX1 was soaked in a 10% $FeCl_3$ solution, then the nanoparticles were precipitated in a 1N NaOH solution, and finally the anion exchange sites were converted to the Cl^- form using 5% NaCl. HAX3 has titanium dioxide nanoparticles precipitated in-situ within WBAX3 (Elton et al. 2013). Briefly, the WBAX3 was soaked in a 10% $TiOSO_4$ solution and decanted, then the nanoparticles were precipitated by oven hydrolysis at 80°C for 24 hours.

Besides those synthesized for this study, all sorbents were used as received, and masses reported were not adjusted for water content. If dry weight had been used in this analysis, removal capacities (mass of pollutant removed per mass of sorbent) of sorbents with high water content would increase more drastically compared to those with low water content.

2.2. Laboratory Pseudo-Equilibrium and Packed Bed Testing. Laboratory experiments were carried out in one of three water matrices. First, deionized water (DI) was fortified with 0.1 mM HCO_3^- for pH buffering capacity. Second, simulated

groundwater (SG) (NSFI/AN 2007) was prepared including 20 mg/L SiO_2, 180 mg/L HCO_3^-, 50 mg/L SO_4^{2-}, 8.8 mg/L NO_3^-, 1.0 mg/L F^-, 0.12 mg/L PO_4^{3-}, and 71 mg/L Cl^-. Third, a real groundwater (GW) from a southern California utility that operates primarily on groundwater was included to verify performance. The GW contained 15 mg/L Si, 2 mg/L NO_3^-, 24 mg/L SO_4^{2-}, 200 mg/L total dissolved solids, and 130 mg/L HCO_3^-. Experiments in each matrix were conducted at pH 7.5–8.5 with a mixture of equal molar concentrations of Cr(VI) and As(V). Sorbent performance in real groundwater was expected to fall somewhere between that demonstrated in DI and in SG.

Initial screening of all sorbents was performed by pseudo-equilibrium batch testing. This was completed by spiking 50 mL of DI, SG, or GW with 0.2 mM, 0.04 mM, or 0.01 mM Cr(VI) and As(V). Samples were then dosed with between 375 and 1,500 mg/L of sorbent. Samples were agitated on a shake table for 6 days before being filtered with a 0.45 µm nylon membrane, preserved with 1% nitric acid and refrigeration, and analyzed within 14 days. Kinetic sampling showed no change in aqueous concentration between four hours and one day, inferring that equilibrium should well be reached within six days. Batch data were fit with Fruendlich isotherms (Equation 1),

$$q_e = K * {C_e}^{1/n} \quad (1)$$

where K ((mmol/g)(L/mmol)$^{1/n}$) and 1/n (dimensionless) are fitted parameters based on best-fit lines through experimental data, C_e (mM) is the equilibrium pollutant concentration, and q_e (mmol/g) is sorption capacity.

Two sets of continuous flow column tests with select sorbents were conducted representing simple and challenging conditions. First, a 1 cm inner diameter glass column was packed with glass beads, glass wool, and 6 g of sorbent. Influent DI water was

spiked to 150 µM pollutant (8 mg/L Cr(VI) and 12 mg/L As(V)) at pH 7.9. It was pumped through the column at 4.3 mL/min, giving an empty bed contact time (EBCT) of 2 minutes and hydraulic loading rate of 3.3 m/hr. High pollutant concentration and simple background matrix make this a favorable condition for sorbent performance. In the second condition, a 2.5 cm inner diameter glass column with 15 g of sorbent was used. Influent SG was spiked with 2 µM pollutant (100 µg/L Cr(VI) and 140 µg/L As(V)) at a pH of 7.7. It was pumped through the column at a rate of 45 mL/min, giving an EBCT of 30 s and hydraulic loading rate of 5.5 m/hr. A complex background matrix and short EBCT make this condition more challenging for sorbent performance. In both cases, effluent samples were taken, preserved with 1% nitric acid and refrigeration, and analyzed within 14 days.

2.3 Ranking Simultaneous Removal. A new method to quantify sorbents with the highest capacity to treat multiple pollutants was developed and shown in Equation 2.

$$SRC = (Combined\ Capacity) * (Weighting\ Factor) \quad (2)$$

The Simultaneous Removal Capacity (SRC) is a quantitative tool used to assess and rank the capacity of sorbents to simultaneous remove multiple contaminants under the same experimental conditions. It has units equivalent to those used to express the removal capacity and a high score indicates high performance.

The first term (Combined Capacity) is an average of the removal capacities for the individual pollutants as calculated in Equation 3, where q_1 and q_2 are the sorbent removal capacities for each pollutant.

$$Combined\ Capacity = \left(\sqrt{{q_1}^2 + {q_2}^2}\right) \quad (3)$$

The mathematical form of Combined Capacity is equivalent to the Pythagorean Theorem and represents a 'distance' from zero capacity. This term assigns higher scores to sorbents with greater pollutant removal capacity.

The second term is a weighting factor that is a function of removal capacity ratio for two pollutants. This term assigns higher scores to sorbents with similar removal capacity for both pollutants over sorbents with preferential removal capacity. It ranges from 1 to 0, giving 1 to sorbents with equal capacity for both pollutants and 0 to sorbents with zero capacity for either pollutant. This is shown in Equation 4. Its mathematical form was selected subject to the described constraints without empirical or mechanistic basis.

$$Weighting\ Factor = \left(\sin\left(2 * \tan^{-1}\frac{q_1}{q_2}\right)\right) \tag{4}$$

For example, the weighting factor is 0.8 for a sorbent with two times the capacity for one pollutant over the other. It is 0.2 for a sorbent with ten times capacity for one over the other. The value of this weighting factor as a function of removal capacity ratio for each pollutant is illustrated in Figure 4.1.

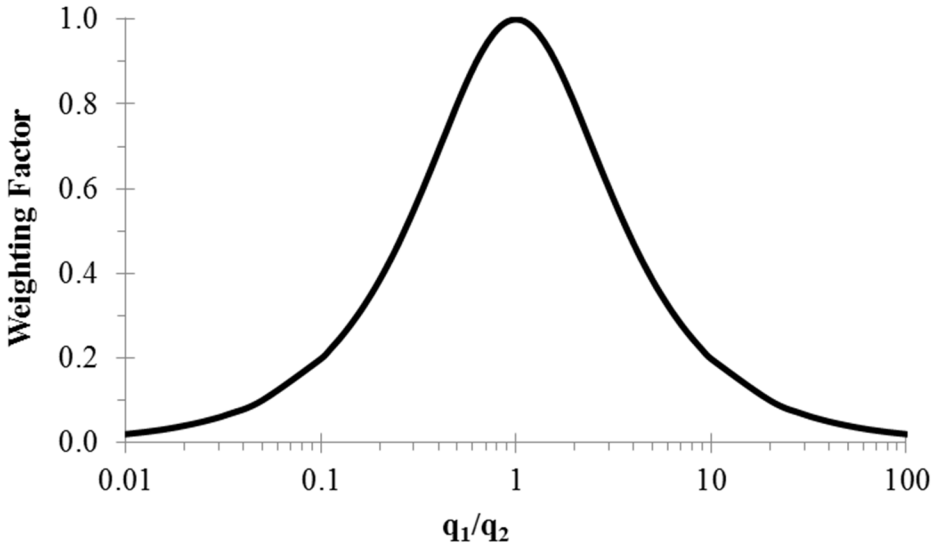

Figure 4.1. Distribution of weighting factor for computing SRC. The factor gives full score to sorbents that remove both pollutants equally and penalizes the score for sorbents that preferentially remove only one pollutant.

Overall, sorbents with high capacity for one pollutant and low capacity for the other, or sorbents with an equal but low capacity for both pollutants, will result in a low SRC. Only sorbents with a high capacity for both pollutants will result in a high SRC.

2.4. Contaminant Analysis. Total chromium and total arsenic were analyzed using inductively coupled plasma optical emission spectroscopy (Themo iCAP6300) with a quantification limit of 20 µg/L. Cr(VI) from pilot testing was analyzed using ion chromatography (Dionex ICS) with post column derivitization (USEPA 2011). Nitrate from pilot testing was analyzed using the dimethylphenol method for spectrophotometer (HACH DR5000).

3. RESULTS & DISCUSSION

3.1. Comparing Sorbents' As(V) and Cr(VI) Removal Capacity. The goal of developing sorption isotherms from batch reactor data was to screen sorbents, select sorbents for column testing, and rank their ability to simultaneously remove both pollutants. Figure 4.2 illustrates typical results with fitted isotherms for three sorbents (MO1, WBAX1, and HAX1) to compare performance of traditional sorbents to a nano-enabled sorbent. Figure 4.2 also shows results for each sorbent in DI and SG waters to represent best-case and worst-case scenarios. Table 4.2 reports isotherm parameters for all tested sorbents, pollutants, and water matrices.

The MO sorbents all demonstrated a greater capacity for As(V) than for Cr(VI) in DI, SG, and GW. Low 1/n values (0.21–0.29) were determined for As(V) in MO1, MO2, and MO3, indicating favorable energetics and high removal ability at low concentrations. MO4 demonstrated the highest K value for As(V), but surface area may have contributed

to this since it was the only powdered sorbent. Very low K values (0.02–0.24 $(mmol/g)(L/mmol)^{1/n}$) were observed for Cr(VI) in all MOs, indicating almost negligible Cr(VI) removal at all concentrations. Unexpectedly, the removal capacity for As(V) increased for all MO sorbents in SG matrix over the DI water matrix. This demonstrates affinity for As(V) despite presence of competing constituents. This is likely because As(V) sorption is typically diffusion limited (Westerhoff et al. 2005), and the higher ionic strength of the SG compressed the stagnant double layer. The Cr(VI) removal capacity decreased in SG compared with DI. For example, MO2 in SG showed no statistically significant difference in Cr(VI) levels from raw water to treated water.

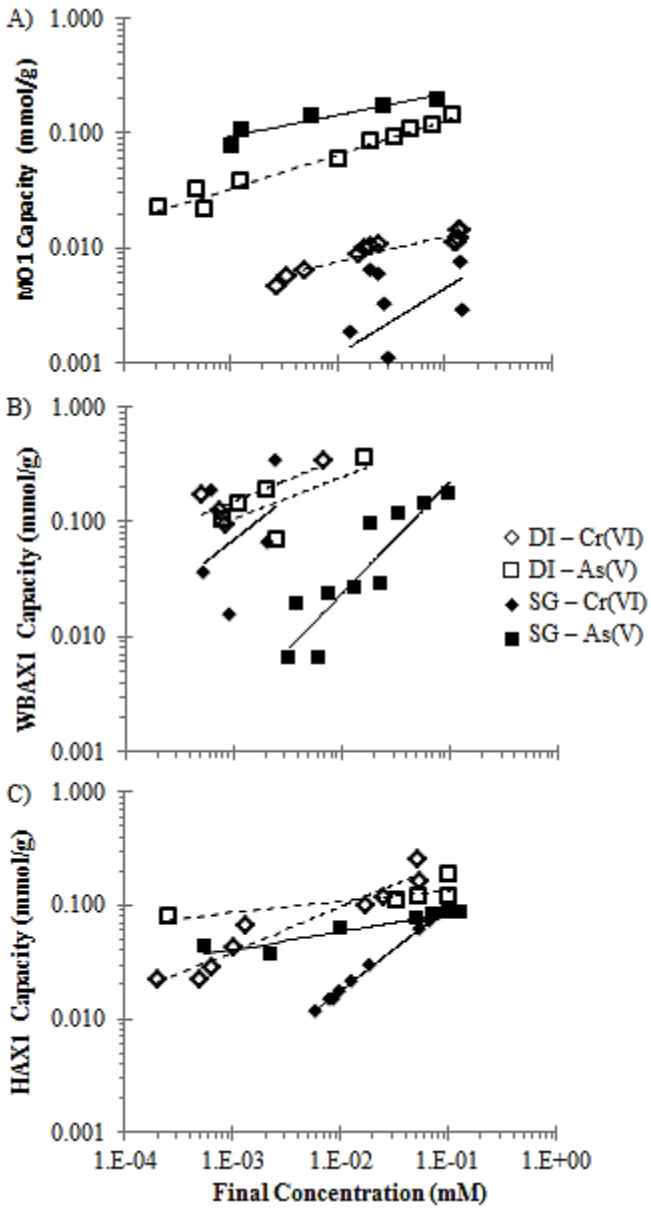

Figure 4.2. Equilibrium isotherms for arsenic (As(V), square symbols) and chromium (Cr(VI), diamond symbols) in buffered deionized water (DI, open symbols) or simulated groundwater (SG, filled symbols) for sorbents A) MO1, B) WBAX1, and C) HAX1. Initial pollutant concentration ranged from 0.01–0.2 mM, and final pH was 7.5–8.5.

Sorbent	Pollutant	Deionized Water			Simulated Groundwater			Real Ground Water		
		K	1/n	R^2	K	1/n	R^2	K	1/n	R^2
MO1	Cr(VI)	0.021	0.218	0.863	0.017	0.574	<0.5	0	0	0
	As(V)	0.250	0.293	0.969	0.341	0.188	0.909	0.216	0.196	0.910
MO2	Cr(VI)	0.031	0.511	0.907	0	0	0			
	As(V)	0.501	0.214	0.969	0.558	0.265	0.966			
MO3	Cr(VI)	0.072	0.359	0.991	0.013	0.327	<0.5			
	As(V)	0.149	0.224	0.874	0.405	0.320	0.948			
MO4	Cr(VI)	0.245	0.510	0.867	0.315	0.647	0.853			
	As(V)	235	0.827	0.671	1.38	0.335	<0.5			
WBAX1	Cr(VI)	2.06	0.380	0.652	1.00	0.356	<0.5	6.38	0.574	0.526
	As(V)	2.40	0.475	0.661	2.07	0.974	0.819	0.833	0.442	0.953
WBAX2	Cr(VI)	1.80	0.576	0.941	2.27	1.06	0.993			
	As(V)	0.320	0.487	0.904	0.165	0.937	0.979			
WBAX3	Cr(VI)	1.39	0.461	<0.5	1.63	0.658	0.795			
	As(V)	0.721	0.751	0.730	0.739	1.36	0.984			
HAX1	Cr(VI)	0.594	0.394	0.927	0.526	0.738	0.998	0.568	0.598	0.999
	As(V)	0.168	0.096	0.610	0.120	0.157	0.895	0.123	0.153	0.992
HAX2	Cr(VI)	1.64	1.31	0.875	0.836	0.879	0.963			
	As(V)	0.182	0.788	0.778	0.123	0.536	0.858			
HAX3	Cr(VI)				0.233	0.347	0.696			
	As(V)				0.039	0.185	<0.5			

Table 4.2. Fruendlich isotherm parameters. Equilibrium tests were performed for seven traditional sorbents (MO and WBAX) and three nano-enabled hybrid sorbents (HAX) in buffered deionized water, simulated groundwater, and a real groundwater from southern California. Each matrix was spiked with an initial equimolar concentration of 0.01–0.2 mM chromium (Cr(VI)) and arsenic (As(V)). The Fruendlich isotherm fitting parameters 1/n and K (in $(mmol/g)(L/mmol)^{1/n}$) are shown. Blank values were not tested. Zero values indicate no observable removal.

The WBAX resins all demonstrated a higher capacity for Cr(VI) than for As(V) in all water matrices (i.e., the Cr(VI) capacity calculated from Equation 1 was higher based on the observed K and 1/n values in the concentration range of interest). Generally, WBAX had lower K values for As(V) than those for Cr(VI) but did show some ability to remove both pollutants. The 1/n values (0.35–1.1) for Cr(VI) were higher for the WBAX resins than those observed in the MOs. The 1/n values (0.48–1.4) for As(V) were slightly higher than Cr(VI) indicating less favorable binding energetics and lower removal capacity at lower concentrations. Removal capacities for both Cr(VI) and As(V) decreased in SG compared to DI water matrices, indicating other ions (sulfate, nitrate, or carbonate, e.g.) compete for ion exchange binding sites despite affinity for Cr(VI).

The hybrid sorbents show preliminary promise for simultaneous removal of both pollutants. The low 1/n values (0.10–0.54) for As(V) show favorable sorption, similar to the MO behavior for As(V). The 1/n values (0.35–1.3) for HAX removal of Cr(VI) are very close to those for WBAX. The removal capacity for hybrid sorbents remains similar to WBAX for Cr(VI) and similar to MO for As(V). This perhaps indicates that the removal mechanism includes both anion exchange and sorption to the nanoparticles.

Scatter in isotherm data is expected for sorbents that have very little capacity for a pollutant, as demonstrated by MO1 for Cr(VI) in SG (Figure 4.2A, $R^2 < 0.5$). This is an artifact of log scale exaggerating small differences at low capacities (e.g., below 0.01 mmol/g), even if due only to normal analytical variability and not true pollutant removal. The observed scatter reinforces the conclusion of poor sorbent performance for that pollutant under those conditions. Scatter in data is also observed at low final pollutant concentrations that approach the method quantification limit of 0.15 µM, as demonstrated

by WBAX1 for Cr(VI) in DI (Figure 4.2B, $R^2 = 0.65$). Although data are scattered, nearly all pollutant was removed, therefore reinforcing the strong sorbent performance for that pollutant under those conditions.

Table 4.3 shows the SRCs and quantitatively compares the sorbents' ability to remove both pollutants. HAX3 had the highest ability to treat both contaminants (SRC = 23 µmol/g) followed by MO4 and HAX1 (SRC = 11 µmol/g). HAX3 does not have the highest absolute removal capacity for either pollutant, but scored the highest SRC because it had capacity for both pollutants and a similar capacity for both. WBAX1 had the highest capacity for Cr(VI) but received only a moderate SRC of 10 µmol/g because it has only a small capacity for As(V). This is also true for MO2, which had the highest As(V) capacity but very little for Cr(VI) and scored 3 µmol/g. WBAX3, MO1, and WBAX2 had the lowest SRC (less than 1 µmol/g) due to low absolute removal capacities and different capacities for the two pollutants.

	$q_{Cr(VI)}$ (µmol/g)	$q_{As(V)}$ (µmol/g)	SRC (µmol/g)
HAX3	27.0	12.4	22.5
MO4	5.7	172.1	11.3
HAX1	5.4	45.2	10.6
WBAX1	109.4	4.9	9.7
HAX2	3.5	4.4	5.5
MO3	1.7	55.4	3.4
MO2	1.4	107.5	2.8
WBAX2	3.1	0.5	1.0
MO1	0.5	106.0	1.0
WBAX3	27.3	0.2	0.3

Table 4.3. Sorbents ranking based on SRC from sorption capacity (q) for C_e=2µM. The Simultaneous Removal Capacity (SRC) quantitatively compares the simultaneous removal of two pollutants with a high score indicating a high capacity for both pollutants.

Figure 4.3 shows calculated removal capacity of each sorbent for Cr(VI) plotted against that for As(V). This was done using the isotherm parameters in SG at equilibrium concentration (C_e) of 2µM (100 µg/L Cr(VI) and 144 µg/L As(V)) using Equation 1. Sorbents plotted along the diagonal dashed line have equimolar capacity for removing both pollutants with those closest to the origin having little capacity to remove either pollutant in the conditions tested and those in the top right having high capacity for both pollutants. Sorbents in the top left have high capacity for As(V) with little capacity for Cr(VI), and visa-versa for the bottom right corner.

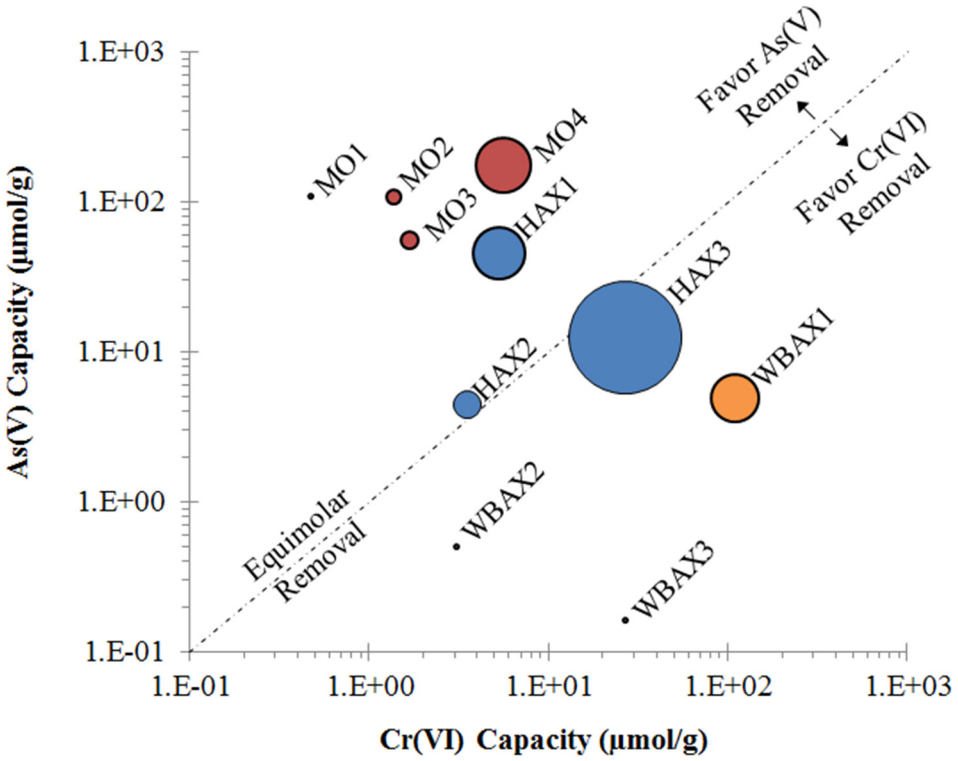

Figure 4.3. Sorbent equilibrium removal capacity. The equilibrium capacity for each sorbent and each pollutant is calculated from observed isotherm fitting parameters in SG at an equilibrium pollutant concentration of 2µM. Dashed line indicates equimolar capacity for both pollutants. Symbol size is proportional to SRC. Sorbents above the line demonstrate high arsenic capacity but little chromium capacity and the opposite for sorbents below the line. Sorbents closest to the line demonstrate high simultaneous pollutant removal capacity.

Figure 4.3 illustrates that MO sorbents preferentially remove As(V) while WBAX resins preferentially sorb Cr(VI). MO4 demonstrates the highest As(V) removal capacity, and WBAX1 demonstrates the highest Cr(VI) removal capacity. The three nano-enabled HAX sorbents are the closest to the equimolar line, demonstrating the capacity to remove similar amounts of both oxo-anions. This suggests they employ different and non-competing sorption mechanisms.

These examples illustrate how the SRC can be used to rank sorbents' ability to remove multiple contaminants taking into account both absolute removal capacity as well as affinity for both pollutants. Visualizing the results in Figure 4.3 clarifies the purpose of the two terms in the SRC calculation (Equation 2). The first term is an average of the removal capacities for the individual pollutants calculated as a distance from the origin in Figure 4.3. The second term is a weighting that can be visualized as proximity to the 1:1 line in Figure 4.3.

3.2. Lab Column Testing of Sorbents with High SRC. The goal of packed bed tests was to validate batch testing results, screen simultaneous removal potential, and evaluate potential to run in more lengthy pilot tests.

Figure 4.4 shows the first set of column testing results for HAX1. HAX1 was used in lieu of HAX3 since larger volumes of sorbent were available. The test conditions (high pollutant concentration, simple matrix, long EBCT) represent a best-case scenario to verify simultaneous removal by nano-enabled sorbents. Complete removal of both pollutants occurred during the first 350 BV, verifying the simultaneous removal potential. At 725 BV, the column had removed 474 µmol of Cr(VI) and 368 µmol of As(V), as calculated from the area above the respective breakthrough curves. This is equivalent to a

removal capacity of 155 µmol/g for Cr(VI) and 120 µmol/g for As(V). The As(V) broke through first even though equilibrium testing predicted a higher capacity for As(V). This was observed previously for other sorbates (Sandoval et al. 2011) and demonstrates mass transport plays an important role in sorbent performance. Sorbent removal capacity can therefore be controlled by proper selection of contact time to avoid preferential sorption of solutes with higher diffusivity (liquid diffusivity of $H_2AsO_4^-$ is $0.905*10^{-5}$ cm^2/s, and of CrO_4^{2-} is $1.132*10^{-5}$ cm^2/s (Haynes et al. 2015-2016)).

These HAX1 column test results demonstrated that simultaneous removal is possible as this nano-enabled sorbent demonstrated high capacity to remove both pollutants. Based on the pH and equimolar concentrations, both pollutants are expected to exist in aqueous solution as divalent oxyanions in equal numbers. On a sorbent with equal affinity for both sorbates the pollutants would occupy the same number of ion exchange sites and would break through simultaneously. However, the dissimilar breakthrough curves indicate different sorbate affinities, mass transport, or sorption mechanisms (ion exchange and sorption to iron nanoparticles) were in effect.

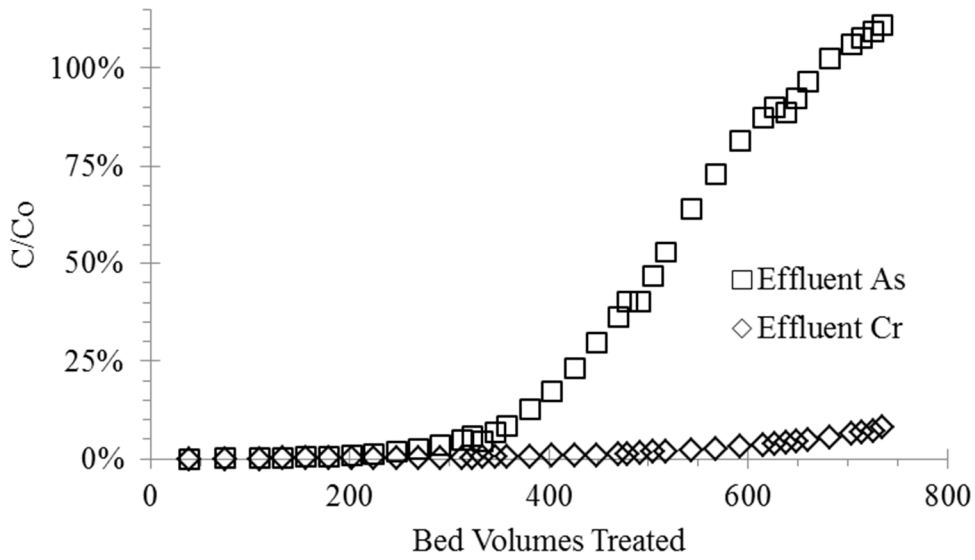

Figure 4.4. Pollutant breakthrough curves for As(V) and Cr(VI) by iron nanoparticle embedded HAX1 in packed bed column test in buffered deionized water (DI) water matrix at pH 7.9 with 2 min EBCT and influent pollutant concentrations of 150 mM (8 mg/L Cr(VI) and 12 mg/L As(V)).

Figure 4.5 shows dynamic column testing results for MO1, WBAX1, and iron nanoparticle embedded HAX1 under more challenging conditions (lower pollutant concentration, more complex matrix, and shorter EBCT). These sorbents were selected due to their high SRC in batch mode. MO1 was used in lieu of other MO sorbents despite a lower SRC because pelletized sorbents are easier to work with in packed bed columns. This short contact time demonstrates sorbent preference for one or both pollutants and confirms the SRC is an indicator for column performance.

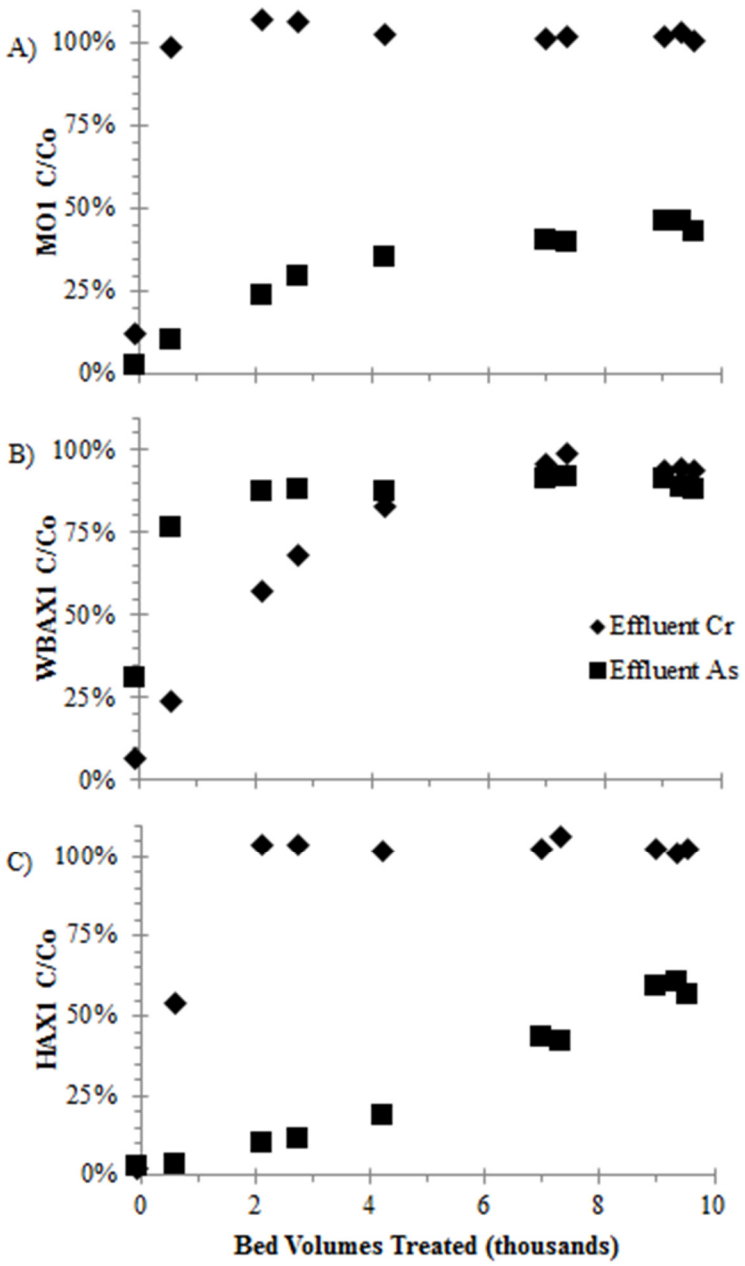

Figure 4.5. Pollutant breakthrough curves for sorbents in fixed bed. A) MO1, B) WBAX1, and C) iron nanoparticle embedded HAX1 were tested in simulated groundwater (SG) at pH 7.7 and 30 sec EBCT and an initial pollutant concentration of 2 µM (100 µg/L Cr(VI) and 140 µg/L As(V)).

HAX1 and WBAX1 were able to remove some of both pollutants through 2000 bed volumes (BV), while Cr(VI) broke through for MO1 almost immediately. MO1 and HAX1 both demonstrated a slow lagging removal of As(V). HAX1 and WBAX1 both had a sharply shaped breakthroughs for Cr(VI), with HAX1 reaching exhaustion around 2,000 BV and WBAX1 reaching exhaustion around 6,000 BV. Therefore, the nano-enabled sorbent did not have the same affinity for Cr(VI) and its removal capacity was limited by competition with other constituents. The apparent loss in capacity from HAX1 to WBAX1 is because the parent resin for HAX1 is a nitrate selective SBAX, which is much more sensitive to influent nitrate and sulfate compared to the chromium selective WBAX. However the fact that the HAX1 breakthrough curve for As(V) was similar to that of MO1 for As(V), and its curve for Cr(VI) was similar shape to that of WBAX1 for Cr(VI) demonstrates that separate and non-competing adsorption mechanisms are present. We hypothesized that the hybrid nano-enabled sorbent continued to remove Cr(VI) by anion exchange, and removed As(V) by sorption to the metal nanoparticles. This verfies the potential for nano-enabled hybrid sorbents to remove both pollutants simultaneously.

WBAX1 had a removal capacity of 6.2 µmol/g for Cr(VI) and 3.8 µmol/g for As(V) calculated from the area above the curve normalized to sorbent mass. HAX1 had a removal capacity of 1.6 µmol/g for Cr(VI) and 20 µmol/g for As(V). MO1 had a removal capacity of 0.23 µmol/g for Cr(VI) and 18 µmol/g for As(V). These column capacities are all smaller (6%–78%) than those observed in batch equilibrium testing, but are consistent with the preferences shown between the two pollutants. Inserting the column capacities into Equation 2 gives an SRC of 6.5 µmol/g for WBAX1, 3.2 µmol/g for

HAX1, and 0.46 µmol/g for MO1. While HAX1 SRC ranked slightly higher than WBAX1 in batch tests, the WBAX1 ranked higher in this column test that had lower pollutant concentration.

This change in rank demonstrates the necessity to perform column testing to determine sorbent performance. However, batch testing is a valid way to screen through many sorbents given the decreased time, monitoring, and sorbent mass often required to perform it compared to column testing. Using the SRC is a quantitative and justifiable way to screen which sorbents to advance to column testing, understanding it does not predict column performance. Furthermore, these column results demonstrate that though nano-enabled sorbents have great potential to remove multiple pollutants simultaneously, perhaps more development is called for to outperform traditional sorbents in challenging conditions.

Next it was briefly explored if the iron (hydr)oxide nanoparticles in the hybrid sorbents could leach into the finished water, thereby posing possible health risks. Effluent samples from the HAX1 packed bed column test were analyzed for total Fe using ICP-OES. All samples were below detection limit (20 µg/L). This suggested that high iron leaching did not occur in the conditions described over this operation period.

4. CONCLUSIONS

Traditional MO and WBAX sorbents have more favorable binding energy and higher removal capacity for one pollutant with little capacity to treat another pollutant for an extended duration.

Metal nanoparticle embedded ion exchange media showed potential for simultaneous removal, especially at elevated pollutant concentrations. These hybrid sorbents demonstrated a higher total pollutant removal capacity than traditional sorbents even though they had lower capacity for each individual pollutant. Breakthrough curves of these nano-enabled sorbents suggest Cr(VI) removal capacity similar to WBAX and As(V) removal capacity similar to MO. This indicates multiple removal mechanisms are present and that they do not interfere with each other. This is likely Cr(VI) removal by anion exchange and As(V) removal by metal nanoparticle sorption.

However, because some ability to remove both pollutants was lost in challenging column conditions, further development of nano-enabled sorbents is still required. Their potential for high removal capacity of multiple pollutants indicates that they should continue to be developed and may eventually outperform traditional sorbents in even the most challenging water matrix conditions.

Because As(V) sorption is typically diffusion limited, providing circumstances that compress the stagnant double layer (for example, a higher ionic strength matrix) may increase As(V) removal. However, the competition from other ions will reduce Cr(VI) removal.

When treating both Cr(VI) and As(V) by packed bed treatment, adequate contact time must be selected such that both pollutants have access to binding sites. Because As(V) has a lower diffusivity than Cr(VI), inadequate time will favor Cr(VI) removal.

The proposed SRC equation can be used as a tool to quantitatively rank the ability of various sorbents to co-treat mixtures of pollutants, taking into account both removal capacity and pollutant affinity. Because performance in batch and column mode may

differ, it quantitatively screens many sorbents to select the highest performing to advance to more time-intensive testing.

5. ACKNOWLEDGEMENTS

Funding for this study was provided by the US Environmental Protection Agency under EPA-G2011-STAR-G1 and EPA-F2013-STAR-E1 Graduate Fellowship for Environmental Studies. Thank you to Zaid Chowdhury, Jacqueline Rhoades, Chelsea Francis, Steve Bigley, and Joe Morales for providing groundwater.

CHAPTER 5

SYNTHESIS OF IRON HYDROXIDE OR TITANIUM DIOXIDE NANOPARTICLES IN WEAK BASE ANION EXCHANGE RESINS FOR THE SIMULTANEOUS REMOVAL OF HEXAVALENT CHROMIUM AND ARSENIC

ABSTRACT

Nano-composite sorbents have metal nanoparticles inside the porous structure of larger sorbents, giving a dual functionality to remove multiple pollutants from drinking water. Previous studies have developed synthesis processes using a single metal with strong base anion exchange, sand, or activated carbon. This is among the first papers to tailor the nano-composite synthesis procedure for weak base anion exchange, which has superior selectivity for some oxo-anions like hexavalent chromium. We demonstrate that selection of variables during the synthesis process influences subsequent characteristics and sorption capacity of the final sorbent, and require consideration of the unique properties of weak base anion exchange resin. This is among the first papers to directly synthesize and compare iron and titanium nanoparticles on the same parent resin, either of which add arsenic removal capacity to the sorbent. We explore a concentration of metal precursor solution that leads to sorbent with high pollutant removal performance, and find that excessive metal content is detrimental to sorbent pore size distribution and pollutant removal performance. We find that an acid rinse is required to re-functionalize tertiary amine functional groups on the weak base anion exchange resin after exposure to a basic solution during creation of iron nanoparticles. We find that oven heating time during titanium nano-composite synthesis may be significantly reduced from that

proposed by previous studies without severe impacts to characteristics or pollutant removal capacity.

1. INTRODUCTION

Metallic nanoparticles made of sorptive material have high capacity for pollutant removal from water due to high surface area, but dispersed nanoparticle slurries are energy intensive to remove from water after use (Dutta et al. 2004). Instead, the nanoparticles can be enmeshed in porous scaffolding structures such as sand (Yamani et al. 2012), non-polar resin (Balaji and Matsunaga 2002), ion exchange (Cumbal and Sengupta 2005), or activated carbon (Guan et al. 2012). The macrostructure provides structural support for use in packed beds while limiting diffusive transport concerns, reduces risk of entering finished waters, and provides favorable sorption conditions by increasing intra-porous pollutant concentration through Donnan equilibrium mechanisms (Cumbal and Sengupta 2005, Sarkar et al. 2012, Shahadat et al. 2015, Zhao et al. 2011). These nano-composite sorbents are of particular interest in drinking water treatment when both the parent media and the nanoparticles actively provide pollutant removal capacity, allowing removal of multiple pollutants by a single process (Elton et al. 2013, Hristovski et al. 2008b, Mak et al. 2011b, Sandoval et al. 2011).

Here we synthesized and tested nano-composite sorbents with weak base anion exchange (WBAX) parent material, which has unique chemistry and high selectivity for oxo-anions such as hexavalent chromium (Cr(VI)). Most studies use strong base anion exchange (SBAX), granular activated carbon (GAC), sand, or non-ionic porous polymer, but very few study WBAX which have affinity for a different set of pollutants. We

further compared embedding iron and titanium nanoparticles, both of which have high affinity for pentavalent arsenic (As(V)). Most nano-composite sorbents are synthesized using iron nanoparticles. Rarely do they directly compare synthesis or performance of two different nanomaterials.

In this study, the in-situ synthesis of iron or titanium nanoparticles was tailored for weak base anion exchange resins, the nano-composite sorbent was characterized, and the simultaneous removal of Cr(VI) and As(V) was tested. Three different WBAX resins with unique characteristics that are commonly used for treatment of groundwater pollutants were tested and embedded with either iron or titanium nanoparticles. The metal precursor concentration was varied, which influences the nanoparticle formation, characteristics of the final sorbent, and pollutant removal performance.

Remarkably few studies explore in-situ synthesis of metal nanoparticles inside of WBAX resins. Those that do apply a synthesis method developed for GAC or SBAX macrostructures without tailoring it to WBAX (Vatutsina et al. 2007). WBAX differs chemically from SBAX because it has a tertiary amine functional group instead of quaternary amine. WBAX typically has a smaller average pore size distribution, and high selectivity for a different set of pollutants. It is a preferred treatment method for Cr(VI) due to its selectivity for the chromate molecule in low concentrations and very long run life in column operation (Najm et al. 2014). It is typically considered a single use media for disposal after exhaustion as opposed to being regenerated (McGuire et al. 2007). The high capacity and single use of a WBAX nano-composite sorbent is thus more robust than one with SBAX which would require frequent regeneration with high solutions of mixed regenerant (Chaudhary and Farrell 2015).

An application of this WBAX-metal nano-composite sorbent is simultaneous removal of Cr(VI) and As(V) from groundwater. Cr(VI) removal from drinking water may become increasingly important in the next few years. It is currently under enhanced monitoring and toxicology review by the United States Environmental Protection Agency (USEPA 2010a, 2015b) for possible new federal regulation. California recently enacted regulation treating it as a possible ingested human carcinogen, with an enforceable maximum contaminant level (MCL) of 10 parts per billion (CCR 2014). One of the leading treatment technologies is anion exchange (Blute et al. 2012, Malaviya and Singh 2011). Arsenic went through a similar regulation process when its MCL was lowered to 10 parts per billion in 2006. It has a variety of human ailments including cancer of the bladder, lungs, and skin (USEPA 2010b). Targeted treatment processes including adsorption to zero valent iron and metal hydroxide sorbents have been widely investigated (Bang et al. 2011, Speitel Jr. et al. 2010, Westerhoff et al. 2005). These two inorganic contaminants were the focus of this study due to current regulatory relevance, common occurrence in groundwater, and similar divalent oxygenated anionic state in pH ranges relevant to drinking water.

During synthesis of the nano-composite sorbent, a high metal content provides a higher concentration gradient to drive the metal deeper into the parent resin pores, and provides a higher mass of metal available for precipitation (Guan et al. 2012, Hristovski et al. 2008b). However, excess metal content can block ion exchange sites through surface coating or pore clogging, thus reducing both surface area and removal capacity (Balaji and Matsunaga 2002). Few studies vary the precursor concentration to explore this tradeoff. By identifying the metal precursor concentration that balances metal

available without clogging pores, this study aims to improve the nano-composite sorbent pollutant removal capacity.

The nano-composite resins are characterized for surface area and pore size distribution, metal content, and metal hydroxide form. We developed a new surface area analysis sample preparation method, which is traditionally very difficult due to the low melting point of polymeric resins. The performance of the various synthesized nano-composite sorbents was explored by equilibrium isotherms conducted at ratios of contaminants, foulants, and sorbents relevant to drinking water.

Through performing this synthesis and characterization, this study aimed to determine if the nano-composite synthesis indeed augmented removal capacity for a second pollutant or diminished the original target pollutant removal capacity. This evaluated if simultaneous removal is additive or must be competitive, if pollutants targeted by weak base anion exchange resins can be included in simultaneous treatment, if the weak base anion exchange resins can withstand the synthesis protocol, and how the synthesis protocol must be adapted.

2. METHODOLOGY

2.1 Nano-composite Sorbent Synthesis.

Nano-composite sorbents are synthesized by precipitating titanium or iron nanoparticles in-situ within the porous structure of WBAX resin. Previous methods for embedding titanium (Elton et al. 2013) and iron (Hristovski et al. 2008b) have been developed for SBAX resins. Briefly, this involves soaking the parent resin in a high concentration metal precursor solution, then precipitating the metal with strong base or

oven heating. Here, we adapt the process for WBAX by varying the parent resin, the embedding metal (ie. Ti or Fe), the metal precursor concentration, oven hydrolysis time, and post treatment method. All resins were stored in deionized water until use and characterization.

Three WBAX resins are used for this study. They each have unique structure, composition, and pore size distribution, as well as each being leading commercially available products for Cr(VI) removal. Each has tertiary amine functional groups. The first resin was denoted as WBAX1 (Dow Amberlite PWA7). It is a cross-linked phenol-formaldehyde polycondensate matrix with a microporous structure. It is angular, 0.3 to 1.2 mm in diameter, and orange, cream, or grey color. It can be seen in the inset of Figure 5.1A. WBAX2 (ResinTech SIR700) is yellow, spherical granules made of microporous polyamine epoxy. WBAX3 (Purolite S106) is a translucent epoxy polyamine with a spherical shape and gel type pore structure. Additionally, one SBAX (ResinTech SIR100) with quaternary amine functional groups is also included for comparison to previous studies.

Fe-WBAX was synthesized by first, making metal precursor solution by dissolving $FeCl_3$ in methanol. To explore the effect of metal precursor the concentration of $FeCl_3$ in methanol was 0%, 2%, 10%, or 20% (mass per mass). Second, 25 mL of parent WBAX resin was soaked in 100 mL precursor solution for 1 hour then the precursor was decanted. Herein the nano-composite sorbent synthesized with 10% precursor solution is called FeWBAX-10%. Third, 75 mL of 7.5% NaOH was added and shaken for 1 hour to precipitate iron (hydr)oxide nanoparticles. Forth, the base was decanted and the sorbent was rinsed with 1 L of deionized water in 100 milliliter aliquots.

Fifth, the entire process was repeated for a second cycle. Last, the sorbent was soaked in 5% solution of NaCl for 1 day, then rinsed with an additional 1 liter of deionized water. In situ precipitation of the iron hydroxide nanoparticles follows Equation 1:

$$FeCl_3 + 3NaOH \rightarrow FeOOH_{(s)} + H_2O + 3Na^+ + 3Cl^- \quad (1)$$

Ti-WBAX was synthesized by first, making metal precursor solution of $TiOSO_4$ dissolved in deionized water warmed to 80°C with continuous mixing. The concentration of $TiOSO_4$ in this solution was 10%, 50%, or 100%. Second, 5 mL of parent WBAX resin was soaked in 10 mL of metal precursor solution for 5 minutes then the precursor was decanted. Third, the soaked WBAX was heated in an oven at 80°C to hydrolyze the metal to amorphous TiO_2 nanoparticles. Previous synthesis protocol uses 24 hours of heating time, but does not explore if this time can be reduced. Here, the oven heating time was 4, 8, 16, or 24 hours. The TiWBAX synthesized with 24 hours of oven heating time is denoted as TiWBAX-24hr. Last, the resin was cooled and rinsed with 500 mL of deionized water, soaked in a 5% solution of NaCl for 1 day, then rinsed with an additional 500 mL of deionized water. Hydrolysis of titanium dioxide nanoparticles follows Equation 2:

$$\mathrm{TiOSO_4 + H_2O \rightarrow TiO_{2(s)} + SO_4^{2-} + 2H^+} \quad (2)$$

An optional post-treatment step was explored for the nano-composite sorbents to re-functionalize the tertiary amine functional groups of the WBAX. Ten mL of FeWBAX or TiWBAX was soaked in 25 mL of a 5% sulfuric acid solution for 10 minutes. The acid was decanted and the sorbent was rinsed with 1 liter of deionized water in 50 mL aliquots. Herein, samples that underwent this acid wash post-treatment are denoted FeWBAX-acid or TiWBAX-acid.

2.2 Nano-composite Sorbent Characterization.

We developed a new sample preparation method for pore size distribution and surface area analysis. Analytical systems require samples with very low water content, but polymeric resins often have very high water content. Neither the parent resins nor the nano-composite resins can be dried by oven heating because the polymeric structure would melt and collapse the pore structure. To overcome this, we soaked samples in methanol for 1 day to displace the water. We then allowed the methanol to volatilize by placing the sample in a vacuum desiccator for 1 day. We could then analyze pore size distribution and Brunauer, Emmett and Teller (BET) surface area (TriStar II 3020).

Water content of the nano-composite sorbents was quantified by soaking samples in nanopure water for 1 day, decanting, then measuring mass to determine wet weight. Samples were then dried at 105°C for 1 day, and mass was measured to determine dry weight. Water content was calculated as the difference between wet weight and dry weight normalized to wet weight.

Iron content of the Fe-WBAX was determined by acid digestion. A 50 milligram sample of dried sorbent was placed in 9 mL of nitric acid plus 1 mL of hydrochloric acid in a covered but uncapped vessel (MARS XPRESS) and allowed to pre-digest for 1 day. The vessel was then capped and heated in a microwave (CEM MARS) with carousel at 1600 watts by ramping temperature to 175°C for 15 minutes then holding at 175°C for 10 minutes. The sample was volumized using nanopure water, then analyzed for total iron using ICPOES. Iron content was calculated as the mass of iron normalized to sorbent dry weight.

Titanium content of the Ti-WBAX was determined gravimetrically. Dry samples were heated in a furnace at 550°C for 6 hours, allowed to cool in a desiccator, then mass was measured. Remaining ash was assumed to be TiO_2 comprised of 59.9% Ti. Metal content was calculated as the titanium mass normalized to sorbent dry weight. Titanium content was not determined by acid digestion due to insolubility in nitric acid. Split samples determining iron content of sorbents gravimetrically (assuming the remaining ash is FeO(OH) comprised of 62.9% Fe) and by acid digestion were performed to verify comparability of the results. This is seen in the Supplemental Information Table 5.1. A FeWBAX sample had only 6% relative error, indicating good correlation between the two metal content determination methods.

Imaging of the nano-composite sorbents was completed by first, allowing a small sample to air dry for 1 day. Second, it was fixed in conductive silver epoxy to avoid static charging of the ion exchange resin during imaging. This slurry was sandwiched between two small silicon wafers for structural support. Third, after the epoxy set, the sample was cut with a diamond blade to expose the inner surface of the nano-composite sorbent. The sample was not gold sputtered to avoid misinterpreting gold colloids as synthesized iron or titanium nanoparticles. Elemental mapping was performed by energy dispersive x-ray spectroscopy (EDX) and focused ion beam (FIB), and imaging by scanning electron microscope (SEM) (Nova 200 NanoLab UHR FEG-SEM/FIB).

2.3 Nano-composite Sorbent Performance Testing.

Equilibrium isotherms were performed in 500 mL amber bottles filled with synthetic groundwater spiked to 2 µM of both Cr(VI) and As(V) (100 µg/L Cr(VI) and

140 µg/L As(V)). Synthetic groundwater was prepared as described (NSFI/AN 2007) including 20 mg/L SiO_2, 180 mg/L HCO_3^-, 50 mg/L SO_4^{2-}, 2.0 mg/L NO_3^--N, 1.0 mg/L F^{1-}, 0.04 mg/L PO_4^{3-}-P, and 71 mg/L Cl^{1-}. This challenging water matrix was used so that performance in most real groundwaters would exceed results shown here. Previous work has compared sorbent performance in deionized water and this synthetic groundwater (Chapter 4). At least five bottles were dosed for each sorbent with 45 to 450 mg/L sorbent (all sorbent weights given as dry weight). The bottles were shaken and allowed to equilibrate for 7 days. Total Cr and total As were analyzed by inductively coupled plasma optical emission spectroscopy (ICPOES, Thermo iCAP6300). Other anions were analyzed by ion chromatography (Dionex ICS 2000). Isotherm data was analyzed by the Fruendlich isotherm model ($q_e = K * C_e^{1/n}$) with best-fit lines through experimental data for the equilibrium oxyanion concentration, C_e, and sorption capacity, q_e.

3. RESULTS & DISCUSSION

3.1 Physical & Chemical Characterization of Nano-Composite Sorbents

All nano-composite synthesis methods yielded sorbents with solidified metal attached to the anion exchange resins. None visually demonstrated any obvious changes to angularity or granular size distribution from the parent resin. Titanium dioxide infused resins took on a white color with opacity that increased proportionally to metal precursor concentration. Iron hydroxide infused resins took on a black opaque color for all synthesis methods. Representative photographs of two nano-composite resins are included inset in Figure 5.1.

3.1.1 Imaging of Nano-Composite Sorbents. EDX imaging of cross sections of the synthesized sorbents located the precipitated metal. In all cases the Ti was dispersed across the exposed TiWBAX face, as also Fe across FeWBAX. This is consistent with previous findings (Hristovski et al. 2008b). Figure 5.1A shows a photograph of raw WBAX2 to demonstrate the status of the analyzed sorbents. The dark surrounding area is the silver epoxy and the light angular shape is the exposed internal face of the sliced WBAX. There is a small gap between the resin and the silver epoxy that we attribute to slight melting and shrinking of the resin resulting from frictional heat during sawing. Figure 5.1B shows the EDX mapping of Ti in the TiWBAX2-100%. The Ti appears to be distributed throughout the sorbent and not only coated to exterior surfaces. The slight concentration increase around the bottom edges is attributed to the slight sorbent melting and contraction. Figure 5.1C shows the EDX mapping of Fe in FeWBAX2-10%, which also appears to be distributed across the sorbent depth. These images are typical of the other TiWBAX and FeWBAX sorbents synthesized under different conditions.

Figure 5.2 includes SEM images of titanium dioxide-infused WBAX synthesized with varying metal precursor concentrations and the parent WBAX for comparison. The WBAX1 demonstrates a rough inner surface with many nodular protrusions. The TiWBAX1-10% and TiWBAX1-50% demonstrate a similar morphology, but have an even higher number of these small protrusions contributing to an even rougher surface. The synthesized metal hydroxide may be present as additional protuberances and/or as a nano-thick coating. Either adds surface area and functionality to the sorbent. The TiWBAX1-100% is visually dissimilar than the other three resins. The surface is smoothed over and wavy without any of the high surface area projections characteristic

of the other three sorbents. The resin surface appears to be coated by the precipitated metal, which could block access to the anion exchange functional sites and much of the porous structure having a negative effect on surface area.

3.1.2 Metal Content and Water Content of Synthesized Sorbents. Table 5.1 displays the metal content of the synthesized nano-composite sorbents, and SI Table 5.2 displays the water content. All tested parent sorbents had nearly zero metal content and a sharp increase after the nano-composite synthesis process. This confirms that metal found in the synthesized nano-composite sorbents was from the synthesis process and not native to the parent resin. The small amounts of titanium reported in the parent resins are likely due to incombustible ash in the resin rather than actual titanium, putting bounds of the magnitude of analytical error associated with the metal content analysis method (average of 0.3%, always less than 0.8%).

The iron nano-composite sorbents had higher metal content than the titanium nano-composite sorbents. For any of the parent sorbents, the FeWBAX-10% had nearly double the iron content (2% – 20% Fe) compared to the corresponding TiWBAX-10% (0.4% - 8% Ti). The atomic mass of Fe is only 16% higher than Ti and cannot fully account for that difference, indicating that Fe atoms are more abundant in the FeWBAX-10% compared to the Ti in the TiWBAX-10%. This could be because the Fe synthesis method calls for repeating the metal precursor soak – precipitation step, whereas the Ti synthesis method only exposes the parent sorbent to the metal precursor a single time.

Of the three tested WBAX resins, the highest metal uptake was in WBAX1 (8% – 23%), and the lowest was WBAX3 (1% – 8%). This appears to be related to pore size distribution as the gel-type (WBAX3) would require a much higher concentration

gradient to drive metal precursor into the tight pores. The macroporous structure of WBAX1 would lower the required energy to allow the cationic metal precursor past the cationic surface functional groups of the anion exchange resin, allowing deeper penetration and higher uptake.

In all cases, increasing the metal precursor concentration resulted in an increase in final metal content. Here, the titanium content of TiWBAX sorbents rose by a factor of nearly three or more by increasing the precursor concentration from 10% to 100%. For example, TiWBAX1 rose from 7.9% to 23%, while the water content correspondingly decreased from 81% to 67%. The iron content of FeWBAX sorbents rose by a factor of 2 or more by increasing the metal precursor concentration from 2% to 20%. For example the metal content of FeWBAX2 rose from 1.1% to 2.6%, while the water content correspondingly changed from 71% to 75%.

The acid post rinse reduced metal content slightly. Iron content of FeWBAX-10% reduced from 20% to 17%, and the titanium content of TiWBAX-10% reduced from 15% to 12%. Both resins demonstrated a 3% loss in metal content due to the acid rinse, presumable due to metal solubility in acid that caused slight dissolution of the nanoparticles and/or some detachment.

The hydrolysis time did not produce a consistent effect on resulting titanium or water content of TiWBAX. The metal content of TiWBAX1-10% given 24, 16, 8, or 4 hours of hydrolysis time was 9.0%, 7.0%, 7.5%, and 8.1% respectively. The water content was 66%, 66%, 73%, and 75%, respectively. No clear correlation is observed, concluding that hydrolysis time is not a critical variable in controlling final titanium content.

Generally, the tested resins exhibited a decrease in water content after nano-composite synthesis. For example, the water content decreased from 78% in WBAX1 to 70% in FeWBAX1-10% and 74% in TiWBAX1-10%. This is expected since metal nanoparticles have little entrained water, and the highly saturated polymer resin now comprises a smaller portion of the overall sorbent. Interestingly, the decrease in water content seems to be directly proportional to the increase in metal content. A loose correlation of approximately 2% increase in metal content resulted in a 1% drop in water content as shown in SI Figure 5.1.

The synthesis procedure was carried out on SBAX to compare results to previous studies. Here the titanium content of TiSBAX-100% was 9.6%, which compared well to the previously reported (Elton et al. 2013) titanium content of 9.8%. Here, the iron content of FeSBAX-10% was 19%, which compared well to the previous study (Hristovski et al. 2008b) which resulted in iron content of 16-24% for various parent SBAX resins. The good correlation with previous results validates the nano-composite synthesis procedure conducted in this study.

3.1.3 Surface area and pore size distribution. Pore size distribution and surface area analysis requires samples be dry in order to create a vacuum. This is very difficult for polymeric resins with high water content, especially since heating to evaporate the water would melt the resin structure and result in artificially low surface area. The new sample preparation method proposed here uses methanol to displace the water, then a vacuum desiccator to volatilize the methanol at a low temperature. It sufficiently dried WBAX1, WBAX2, and SBAX samples to allow for successful pore size and surface area

analysis, which was otherwise not possible. WBAX3 samples were still not dry enough to analyze, possibly owing to the tight gel-type structure and high initial water content.

The BET surface area rose from 28.2 m^2/g for WBAX1 to 84.3 m^2/g, 84.7 m^2/g, and 90.2 m^2/g for TiWBAX made with 10%, 50%, and 100% precursor concentration, respectively. The addition of the titanium nanoparticles tripled the total surface area for any of the synthesis conditions over the parent resin. Figure 5.3 shows the correlated pore size distributions. The TiWBAX1-10% and TiWBAX1-50% maintained extremely similar pore size distributions to each other and followed the same trend as the raw resin, with all three peaking around 60 Å. The TiWBAX1-100% solution did exhibit a slight additional increase in total surface area, but had a very different pore size distribution. Most all of the pore surface area was available as micropores less than 40 Å in diameter with significantly less surface area available in pores between 100 Å and 1,000 Å in diameter compared to the other nano-composite sorbents. The high metal precursor concentration seems to result in a nano-composite sorbent with excess metal content that clogged pores.

The hydrolysis time produced an unclear effect on the BET surface area of TiWBAX1-10%. Given 24, 16, 8, or 4 hours of heating time, the final sorbents had 60.6, 53.2, 56.3, and 83.4 m^2/g surface area, respectively. If anything, it appears that excess precipitation and heating reduced the total surface area, showing preference to shorter hydrolysis time. Future work will more clearly identify the relationship between hydrolysis time and nanoparticle morphology

The BET surface area rose to 104.3 m^2/g and 177.6 m^2/g for FeWBAX1-10% and FeWBAX1-10%-acid, respectively. The Fe nano-composite sorbents had higher surface

area compared to the Ti nano-composite sorbents. This is consistent with having higher metal content also. The increase in surface area due to the acid post treatment, despite a slight drop in metal content, likely indicates that pores were created within the iron hydroxide nanoparticles themselves.

Combined with metal content data, the surface area data offers a glimpse at the morphology of the synthesized nanoparticles. For Ti sorbents, the three metal precursor concentrations produced sorbents with nearly identical total surface areas, but with a two or three-fold difference in metal content. In order for TiWBAX1-100% to have had the same surface area with three times as much incorporated metal as the TiWBAX1-10%, the metal nanoparticles must have been larger on average. Assuming nanoparticles were solid TiO_2 spheres with a density of 4.2 g/cm^3, the average radius of the nanoparticles in TiWBAX1-100% is 4.5 nm, and in TiWBAX1-10% is 1.7 nm.

Similarly for the Fe sorbents, the FeWBAX1-10% had a smaller surface area with higher metal content compared to FeWBAX1-10%-Acid, indicating the synthesized nanoparticles must be larger on average. Assuming nanoparticles are solid FeOOH spheres with a density of 3.8 g/cm^3, the average radius of the nanoparticles is 1.5 nm with the acid post treatment and 3.3 nm without. The alternate interpretation of the data is that the acid post treatment did not change the size of the nanoparticles, but opened pores within the iron nanoparticles.

3.2 Simultaneous Pollutant Removal Ability

Psuedo-equilibrium batch tests conducted in simulated groundwater spiked with 2 μM Cr(VI) and As(V) demonstrated that all synthesized sorbents were able to remove

one or both of the pollutants. Comprehensive results of all tests including Fruendlich isotherm parameters and pollutant removal capacities are included in SI Table 5.3. Informative cases will be further discussed here.

Figure 5.4 shows pollutant removal found by preliminary single point equilibrium tests for each of the parent sorbents and Ti and Fe nano-composite sorbents synthesized with 10% precursor concentration. As expected, each of the three parent WBAX resins showed higher Cr(VI) than As(V) removal. For each sorbent, the Fe nano-composite lost Cr(VI) removal but added As(V) removal. The Ti nano-composite gained both Cr(VI) and As(V) removal and maintained preference for Cr(VI). Of the three parent sorbents, nano-composites synthesized using WBAX1 demonstrated the highest pollutant removal, so the remaining results focus on WBAX1.

3.2.1 Acid Post Treatment. Figure 5.5 shows the equilibrium isotherms for WBAX1, FeWBAX1-10%, and FeWBAX-10%-acid. The WBAX1 exhibited the highest capacity to remove Cr(VI). This is demonstrated by a 1/n value <1 (a flat line on the graph) which indicates favorable binding energy, as well as a high K value (high on the graph) which indicates high capacity for pollutant removal at the thermodynamic state characterized by the 1/n value. However WBAX1 exhibited the lowest capacity to remove As(V) with final pollutant concentrations nearly equivalent to the initial concentration. This shows the parent resin has a very high capacity for Cr(VI), but is unable to remove As(V).

In order to simultaneously remove both Cr(VI) and As(V), the FeWBAX needs an acid post rinse after synthesis. After embedding with Fe nanoparticles using only the previously published process developed for SBAX (i.e. FeWBAX1-10%), some As(V)

removal capacity is added. However, most of Cr(VI) removal capacity was lost, dropping below even the As(V) removal capacity. The isotherm line became much steeper indicating unfavorable sorption. However, with an acid rinse during the final synthesis step (i.e. FeWBAX1-10%-Acid), both the Cr(VI) and As(V) removal capacity were significantly increased in subsequent batch sorption testing. The Cr(VI) removal capacity was restored nearly to the same level as the parent resin with the same flat isotherm line, and the As(V) removal capacity was nearly equivalent.

In contrast, the effect of the acid post rinse was not observed in the TiWBAX. As seen in SI Table 5.3, both the TiWBAX1-10% and TiWBAX1-10%-Acid demonstrated high capacity to remove both Cr(VI) and As(V) similar to that of FeWBAX1-10%-acid without the significant loss in capacity seen in FeWBAX1-10%. The TiWBAX does not demonstrate a need for the acid post rinse after synthesis.

We attribute the loss of Cr(VI) and As(V) removal capacity in the FeWBAX without the acid post rinse to a change in the ion exchange functional group during exposure to sodium hydroxide during the precipitation step. WBAX has a tertiary amine functional group which is uncharged at high pH. The nitrogen only takes on a positive charge if its electron pair becomes associated with a proton. That is why WBAX resins report optimal performance below pH 6.5 (McGuire et al. 2007), and why they are classified as being only weakly basic. During nano-composite synthesis, the Fe is precipitated in-situ by soaking in a strong base solution. Besides just precipitating the iron nanoparticles, the hydroxide also reacts with the anion exchange functional groups. It strips them of the associated protons and renders the nitrogen atoms uncharged, drastically reducing the ion exchange capacity. Therefore, an acid post-rinse is then

required in order to restore the ion exchange capacity of the tertiary amines. The acid provides a high proton concentration to replace those lost during hydroxide soaking and reactivates the ion exchange functional groups. This is illustrated in Figure 5.6. In comparison, TiWBAX does not require the acid post-rinse because the synthesis procedure does not include a hydroxide soak (instead precipitating the metal nanoparticles via high temperatures). Thus the acid post rinse has little effect on the TiWBAX, but is required for the FeWBAX.

The null hypothesis to this interpretation was that the acid post rinse left localized low pH areas, where both Cr(VI) and As(V) would be present as monovalent anions instead of divalent anions and therefore take fewer sorption sites and increase the sorbent capacity. This was disproved by performing the synthesis process with no metal in the precursor solution to demonstrate removal capacity was not just a pH effect but actual sorption to the metal nanoparticles and anion exchange. The results are included in SI Table 5.3. The FeWBAX-0% showed almost no capacity to remove either Cr(VI) or As(V). This is because the hydroxide rinse removed the anion exchange capacity and did not have any metal nanoparticles. The FeWBAX-0%-Acid successfully restored the anion exchange capacity for Cr(VI) removal, but without the metal nanoparticles still exhibited no As(V) removal capacity.

These results demonstrate that As(V) removal by FeWBAX is due to the presence of the iron hydroxide nanoparticles, and is not due to any other artifacts from the impregnation process itself or pH effects from the acid post-treatment. They further confirm that the acid post-treatment is required to restore the ability to remove Cr(VI) after the iron impregnation process, independently of the actual presence of any metal.

Pollutant removal capacity of the titanium infused WBAX is largely unaffected by the acid post-rinse, and may not merit the small loss in metal content.

3.2.2 Metal Precursor Concentration. Figure 5.7 shows the equilibrium isotherms of WBAX1, TiWBAX1-10%, TiWBAX1-50%, and TiWBAX-100%, all with 24 hour hydrolysis time. The WBAX1 data is repeated from Figure 5.5 for comparison. WBAX1 demonstrated high removal of Cr(VI) and insignificant removal of As(V). TiWBAX1-10% and TiWBAX1-50% both demonstrated favorable binding energy for both Cr(VI) and As(V) with capacity almost as high as WBAX1 for Cr(VI). TiWBAX-100% demonstrated only mediocre removal of both Cr(VI) and As(V).

Figure 5.7 demonstrates that the parent resin had a very high capacity for Cr, but was unable to remove As(V). After embedding with Ti nanoparticles via the previously published process developed for SBAX (100% precursor solution), some As(V) removal capacity was added. However, significant amounts of Cr(VI) removal capacity was lost. Sorbent synthesized with 10% or 50% solution lost only a very small amount of ability to remove Cr(VI), but added an almost equimolar ability to remove As(V). Between the two, TiWBAX-10% was slightly higher for Cr, but TiWBAX-50% was slightly higher for As(V).

3.2.3 Hydrolysis Time. Figure 5.8 shows the pollutant removal capacity at 2µM pollutant concentration of Ti sorbents synthesized with various oven heating times. The Cr(VI) removal capacity ranged from 16.5 to 26.2 µmol/g and the As(V) capacity from 7.4 to 19.7 µmol/g. Overall, very little difference in pollutant removal capacity, metal content, or surface area is observed by reducing the heating time from 24 hours to 16, 8, or 4 hours. While some statistically significant differences are evident sample to sample,

further testing would be required to clarify these trends. Separately, a slight increase in removal capacity by performing the acid post-treatment from TiWBAX1-10%-24hr to TiWBAX1-10%-24hr-acid is observed, but it is not as significant of an increase as that seen between FeWBAX1-10% and FeWBAX1-10%-acid.

3.3 Impacts of Synthesis Conditions on Simultaneous Removal Ability

The acid post rinse was the most significant variable during synthesis of FeWBAX sorbent in terms of characteristics and pollutant removal capacity. This resulted in loss of some iron content, but was small compared to the large gains in pollutant removal capacity. Comparatively for the TiWBAX, the acid post rinse resulted in only marginal gains on pollutant removal capacity. Therefore it may not be worth the associated loss of titanium content.

The metal precursor concentration was the most significant variable during synthesis of TiWBAX in terms of sorbent characteristics and pollutant removal capacity. While previous studies have concluded that higher metal content is favorable (Hristovski et al. 2008b), this study demonstrated there can be too much of a good thing. The TiWAX1-100% had lower pollutant removal capacity than TiWBAX1-50% or TiWBAX1-10% (Figure 5.7). This shows that strictly increasing surface area is not sufficient because TiWBAX-100% had the highest surface area (Figure 5.3), and that a proper pore size distribution with surface that is accessible to pollutants and useful to sorption is required. SEM imaging (Figure 5.2) further supports that the loss in removal capacity is due to excess metal precipitation clogging pores and covering ion exchange sites. Figure 5.9 shows this effect by normalizing pollutant removal capacity to metal

content. The figure demonstrates that TiWBAX1-100% showed little ability to remove pollutants with very high metal content. TiWBAX1-50% had a high pollutant removal capacity, but with a high metal content. TiWBAX1-10% solution had similarly high pollutant removal capacity with lower metal content. This suggests that the additional metal content beyond that provided by the 10% precursor solution did not add any additional functionality to the sorbent. TiWBAX-10% achieves nearly identical pollutant removal capacity and pore size distribution as TiWBAX1-50% using five times less titanium during synthesis and only half as much final titanium content.

4. CONCLUSIONS

Nano-composite sorbents with sorptive metal nanoparticles synthesized in-situ inside of porous sorptive material can be used to simultaneously remove multiple pollutants from drinking water. Nano-composite synthesis procedures cannot be blindly applied to any parent sorbent or any embedding metal. Unique properties of WBAX require adaptation in the synthesis process compared to other sorbents, and even Fe and Ti nanoparticles should be synthesized differently. Selection of synthesis variables such as metal precursor concentration can influence nano-composite characteristics and subsequent capacity to remove both Cr(VI) and As(V). The highest pollutant removal capacity demonstrated for an iron infused sorbent was FeWBAX1-10%-acid, and for a titanium infused sorbent was TiWBAX1-10%. This work has shown:

- Nano-composite synthesis methods developed for GAC or SBAX cannot blindly be applied to WBAX. Synthesis methods should be optimized for compatibility with its unique functional groups and chemistry.

- Infusion of Fe or Ti nanostructures does not significantly decrease the parent resin capacity for Cr(VI) removal, but does significantly increase the capacity for As(V) removal. TiWBAX has higher capacity for simultaneous removal of Cr(VI) and As(V) than FeWBAX, which is still higher than the other existing sorbents.
- Acid post-treatment is required to restore ion exchange capacity of tertiary amine functional groups on FeWBAX after exposure to high pH during nanoparticle precipitation.
- Lower precursor concentrations result in smaller size nanoparticles in FeWBAX and TiWBAX. Excessively high precursor concentrations result in higher metal contents but block pores and coat binding sites, resulting in lower treatment capacity.
- Oven hydrolysis time in titanium synthesis can be reduced without significant loss in metal content or pollutant removal capacity.
- Metal nanoparticles are dispersed throughout the resin, not coated on the exterior.
- Increasing total surface area is not directly related to increasing pollutant removal performance, but creating a pore size distribution that is accessible and useful for pollutant sorption.

5. ACKNOWLEDGEMENTS

The United States Environmental Protection Agency provided funding for this study under Star Grant EPA-G2011-STAR-G1 and Graduate Environmental Fellowship EPA-F2013-STAR-E1. Thank you to Ken Mossman and Jason Ng at the Leroy Eyring

Center for Solid State Science for the FIB/SEM imaging. Thank you to Marisa Masles and the Goldwater Environmental Laboratory for the ICPOES analysis.

Sample	Fe Content		Relative Error
	Gravimetric	Acid Digest	
FeWBAX1-10%	19.3%	19.9%	3.1%
FeWBAX1-10%-Acid	5.2%	4.9%	5.8%
FeWBAX2-10%	2.7%	2.6%	3.7%
FeWBAX3-10%	3.3%	1.9%	42.4%
FeSBAX-10%	7.2%	18.7%	160%
Bayoxide E33	55.9%	59.4%	6.3%

SI Table 5.1. Comparison of metal content determination methods. Fe content of FeWBAX was determined by acid digestion, but Ti content of TiWBAX was determined gravimetrically (due to insolubility in nitric acid). To verify the ability to compare results from the two methods, the Fe content of split samples was determined both ways.

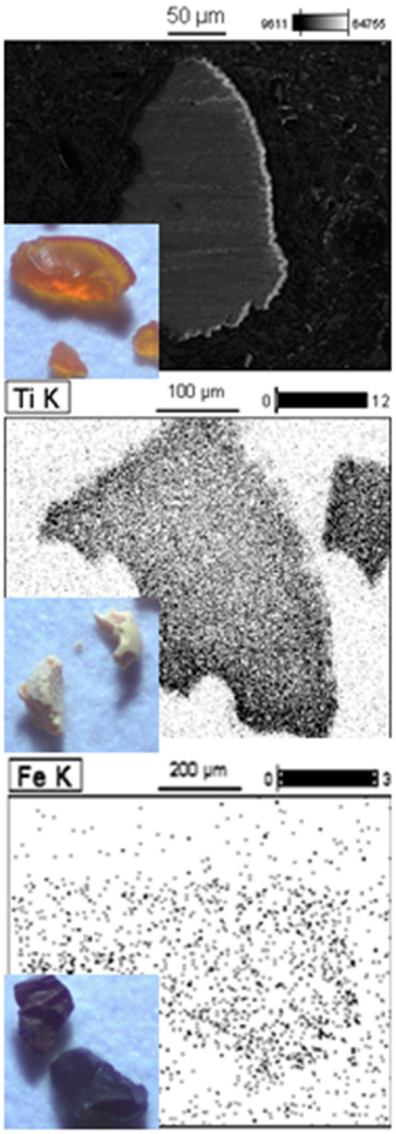

Figure 5.1. Images of the synthesized sorbents. A) is the parent WBAX magnified in the silver epoxy. B) is an EDX image showing the location of Ti in the TiWBAX-100%Ti. C) is an EDX image showing the location of Fe in the FeWBAX-10%. Inset light microscopy photographs are WBAX, TiWBAX-100%Ti, and FeWBAX-10% at 60x magnification respectively.

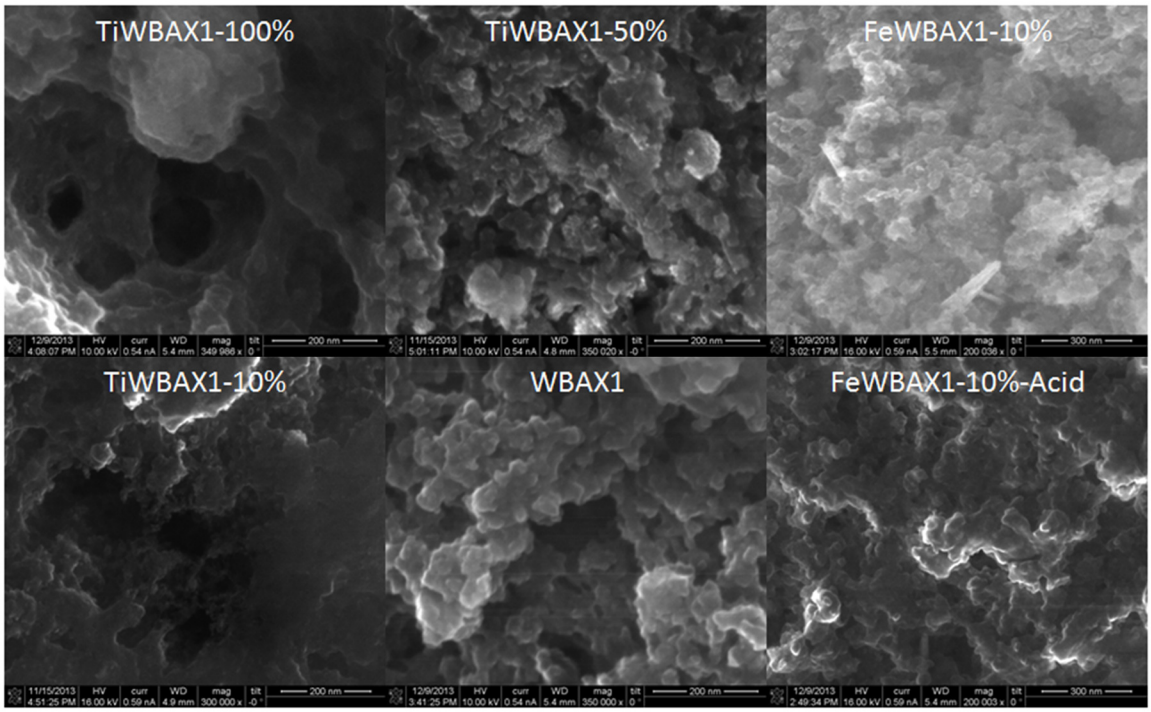

Figure 5.2. SEM images of TiWBAX1 synthesized with various metal precursor concentrations and the parent WBAX1 resin at 350,000x magnification, and FeWBAX1 with or without acid post-treatment at 200,000x magnification.

	Fe							Ti			
Parent Sorbent	Parent	0%	0%-Acid	2%	10%	10%-Acid	20%	Parent	10%	50%	100%
WBAX1	<0.1%	0.3%	0.1%		20%	17%		0.8%	7.9%	18%	23%
WBAX2	<0.1%	0.3%	0.2%	1.1%	2.6%	1.4%	2.6%	0.2%	0.4%	3.4%	7.7%
WBAX3	<0.1%	0.3%	0.3%		1.9%	1.2%		0.2%	1.1%	3.0%	7.6%
SBAX	<0.1%				19%	15%		0.1%	3.7%	9.7%	9.6%

Table 5.1. Metal Content of Synthesized Sorbents. The Fe or Ti compositional percentage of dry nano-composite sorbents synthesized with one of four parent resins and different metal precursor concentrations.

		Fe						Ti		
Parent Sorbent	Parent	0%	0%-Acid	2%	10%	10%-Acid	20%	10%	50%	100%
WBAX1	80%	75%	78%		70%	74%		81%	74%	67%
WBAX2	70%	74%	71%	71%	72%	77%	75%	72%	68%	64%
WBAX3	77%	75%	69%		76%	75%		74%	67%	61%
SBAX	70%				60%	63%		68%	64%	63%

SI Table 5.2. Water Content of Synthesized Sorbents. The water compositional percentage of saturated nano-composite sorbents synthesized with one of four parent resins and different metal precursor concentrations.

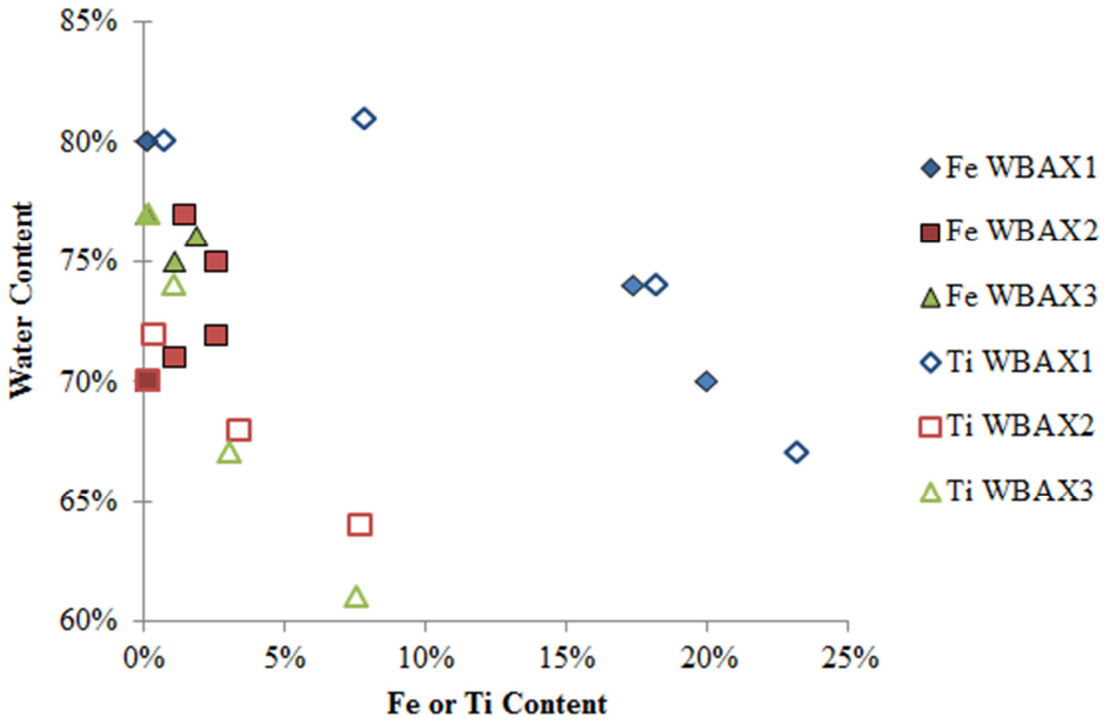

SI Figure 5.1. Water content as a function of metal content for synthesized hybrid sorbents. Diamond symbols indicate sorbents based on WBAX1, square symbols indicate sorbents based on WBAX2, and triangle indicate sorbents based on WBAX3. Filled symbols indicate iron content as Fe, and empty symbols indicate titanium content as Ti. Increasing metal content correlates with decreased water content for the titanium embedded sorbents and iron embedded WBAX1.

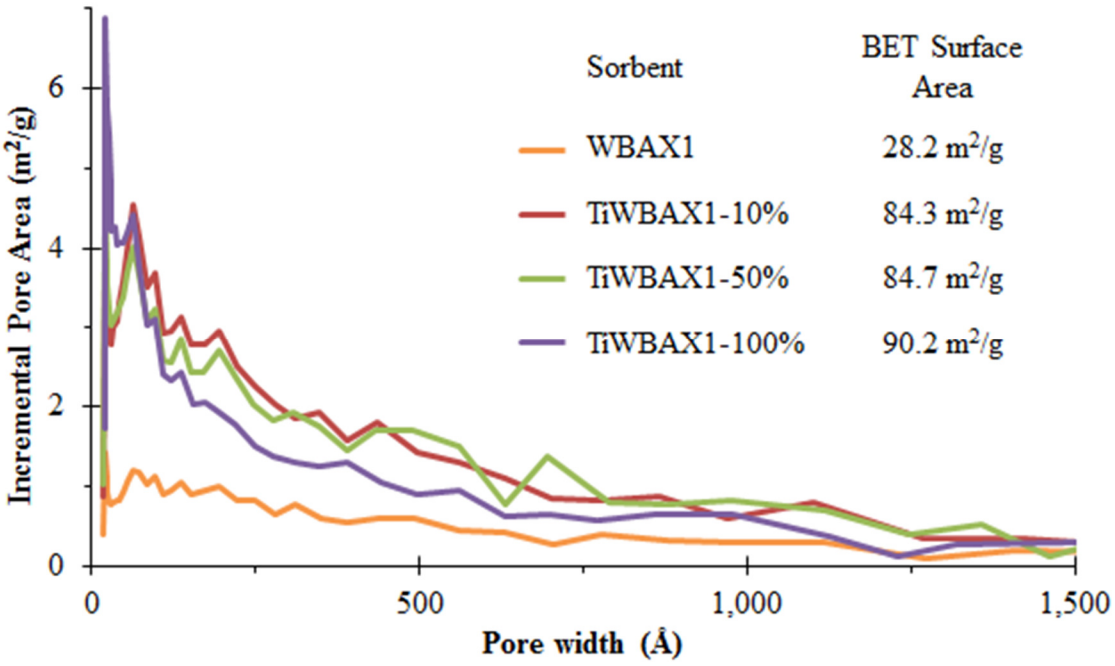

Figure 5.3. Pore size distribution and total surface area of titanium nano-composite WBAX using various precursor concentrations.

			Cr Isotherm Parameters			As Isotherm Parameters			Calculated Capacity			
Primary Variable	Sorbent Name	Data Set	K	1/n	r^2	K	1/n	r^2	Ce (µM)	qCr (µmol/g)	qAs (µmol/g)	SRC
Basis of Comparison	WBAX1	Isotherm	28.52	0.44	0.91	0.00	0.00	0.00	2.0	38.6	0.0	0.0
	WBAX1	Single Point							2.0	0.3	0.0	0.1
	WBAX2	Isotherm	5.65	0.20	0.25	0.76	0.78	0.76	2.0	6.5	1.3	2.6
	WBAX2	Single Point							2.0	0.2	0.1	0.1
	WBAX3	Single Point							2.0	0.1	0.1	0.1
	SBAX	Single Point							2.0	0.2	0.1	0.1
Ti Precursor	TiWBAX1-100%-24Hr	Isotherm	3.97	0.34	0.49	3.12	-0.03	0.02	2.0	5.0	3.1	5.2
	TiWBAX1-50%-24Hr	Isotherm	16.88	0.35	0.91	13.75	0.37	0.95	2.0	21.6	17.7	27.4
	TiWBAX1-10%-24Hr	Isotherm	21.23	0.35	0.70	10.82	0.18	0.42	2.0	27.0	12.3	22.4
Hydrolysis Tim	TiWBAX1-10%-4Hr	Isotherm	16.92	0.34	0.98	13.09	0.42	0.97	2.0	21.4	17.5	27.1
	TiWBAX1-10%-8Hr	Isotherm	19.70	0.43	0.70	13.96	0.49	0.64	2.0	26.6	19.7	31.6
	TiWBAX1-10%-16Hr	Isotherm	10.59	0.64	0.89	6.08	0.27	0.93	2.0	16.5	7.4	13.4
	TiWBAX1-10%-24Hr-Acid	Isotherm	15.56	0.43	0.96	10.21	0.57	0.89	2.0	20.9	15.1	24.5
	TiWBAX1-10%-24Hr	Isotherm	10.00	0.85	0.84	6.53	0.63	0.70	2.0	18.1	10.1	17.7
Acid Post Treat	FeWBAX1-10%	Isotherm	1.50	1.70	0.93	9.40	1.13	0.77	2.0	4.9	20.5	9.5
	FeWBAX1-10%-Acid	Isotherm	9.68	0.33	0.79	11.90	0.35	0.98	2.0	12.1	15.1	18.9
Fe Precursor Concentration	FeWBAX1-0%	Single Point							2.0	3.7	0.2	0.4
	FeWBAX2-0%	Single Point							2.0	1.6	0.4	0.7
	FeWBAX3-0%	Single Point							2.0	2.3	0.7	1.4
	FeWBAX1-0%-Acid	Single Point							2.0	11.5	0.4	0.7
	FeWBAX2-0%-Acid	Single Point							2.0	7.6	1.7	3.3
	FeWBAX3-0%-Acid	Single Point							2.0	6.8	1.0	1.9
	FeWBAX2-2%	Isotherm	0.09	7.78	0.88	0.00	0.00	0.00	2.0	18.9	0.0	0.0
	FeWBAX2-10%	Isotherm	0.16	6.45	0.83	1.07	1.85	0.52	2.0	13.6	3.9	7.4
	FeWBAX2-20%	Isotherm	0.30	4.69	0.97	0.80	2.86	0.87	2.0	7.7	5.8	9.2
Parent Sorbent	FeWBAX1-10%	Single Point							2.0	0.1	0.1	0.1
	FeWBAX2-10%	Single Point							2.0	0.1	0.1	0.1
	FeWBAX3-10%	Single Point							2.0	0.1	0.1	0.2
	FeSBAX-10%	Single Point							2.0	0.1	0.2	0.2
	FeWBAX1-10%-Acid	Single Point							2.0	0.2	0.2	0.3
	FeWBAX2-10%-Acid	Single Point							2.0	0.2	0.2	0.3
	FeWBAX3-10%-Acid	Single Point							2.0	0.2	0.2	0.3
	FeSBAX-10%-Acid	Single Point							2.0	0.2	0.3	0.3

SI Table 5.3. Equilibrium batch test results. For Cr(VI) and As(V) removal capacity for all nano-composite synthesized sorbents is shown based on a single point or a full isotherm. For full isotherms, the observed Fruendlich isotherm parameters (K in $(\mu mol/g)(L/\mu mol)^{1/n}$ and 1/n) are shown. The Simultaneous Removal Capacity (SRC) is a weighted average of the two removal capacities as previously described (Chapter 4). Blank values were not measured. Zero values indicate no observable removal. Sorbents with multiple entries indicate multiple batches of sorbent were synthesized.

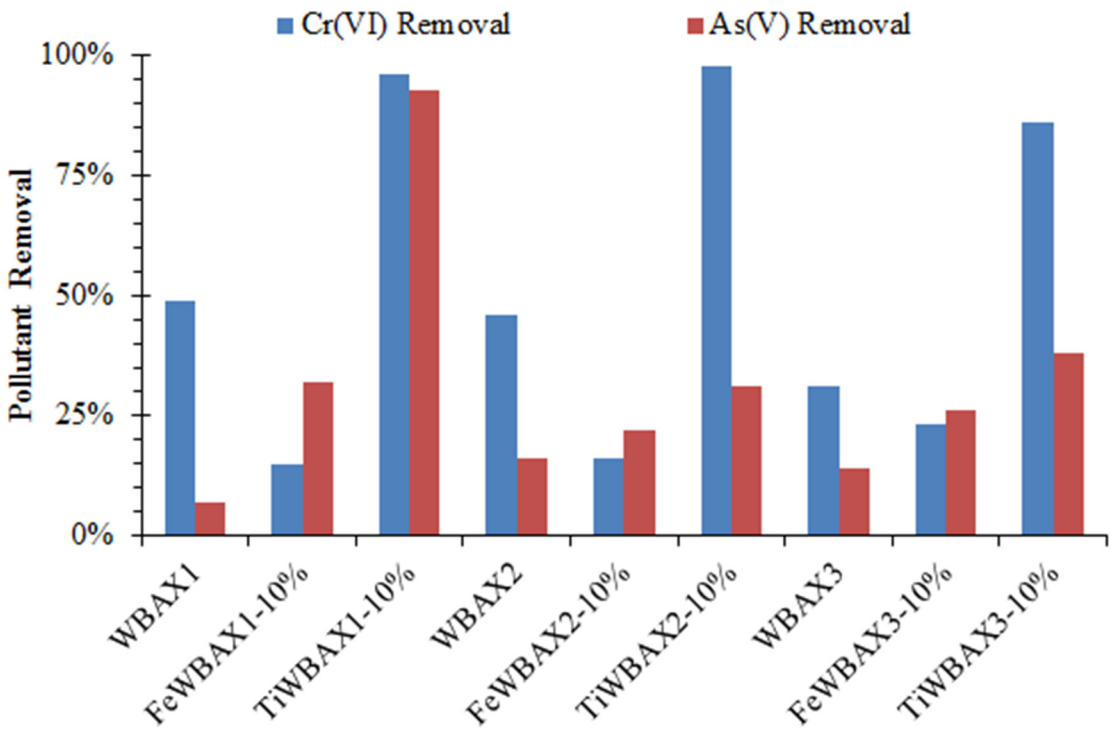

Figure 5.4. Pollutant removal by three WBAX parent sorbents and Ti or Fe nano-composite sorbents.

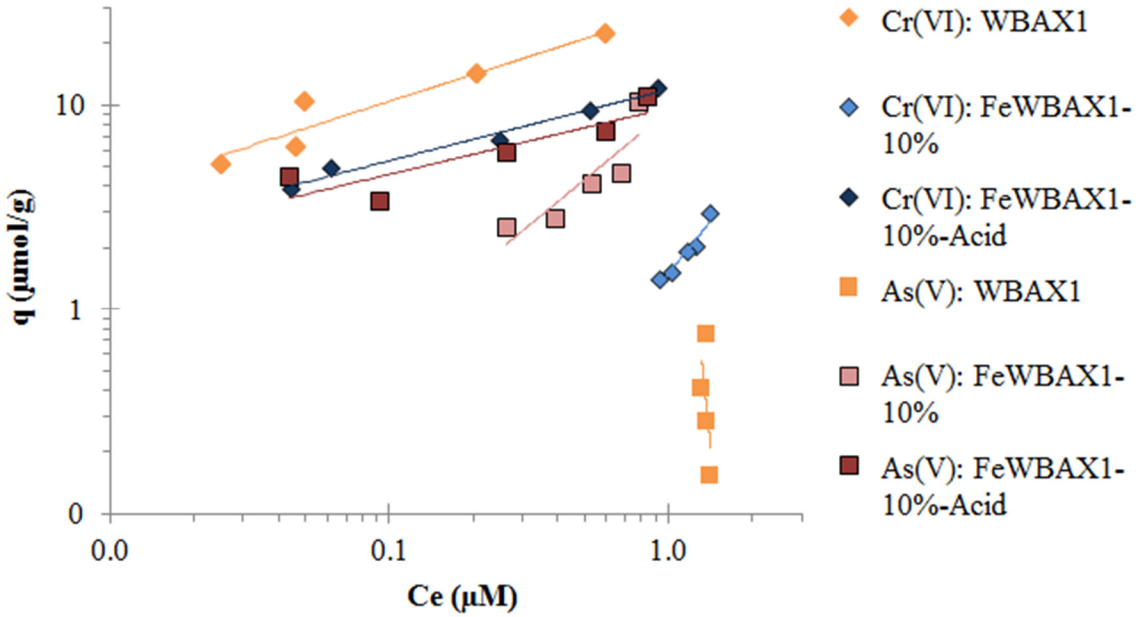

Figure 5.5. Equilibrium isotherm for three sorbents; WBAX1, WBAX1 with embedded iron nanoparticles, and WBAX1 with embedded iron nanoparticles plus an acid post-rinse. Performed in a simulated groundwater matrix with Cr(VI) and As(V) spiked at 2 µM.

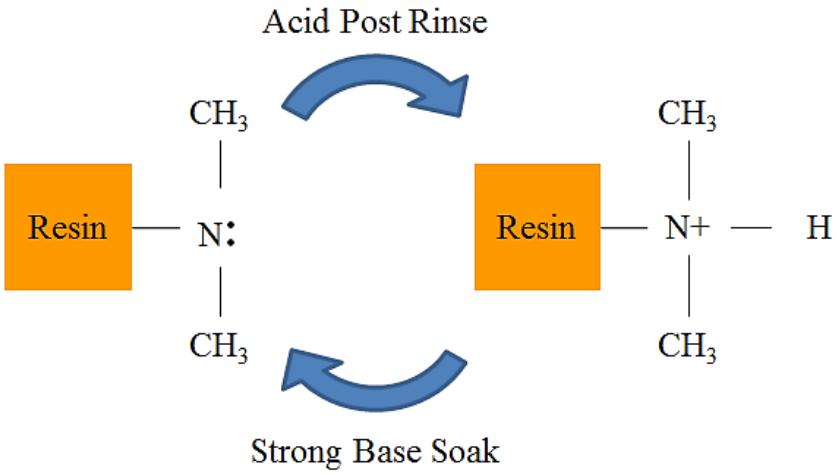

Figure 5.6. Tertiary amine functional group on the surface of weak base anion exchange resin requires a proton to carry a charge. The exposure to strong base during synthesis of iron nanoparticles strips the proton and must be counteracted by an acid post rinse.

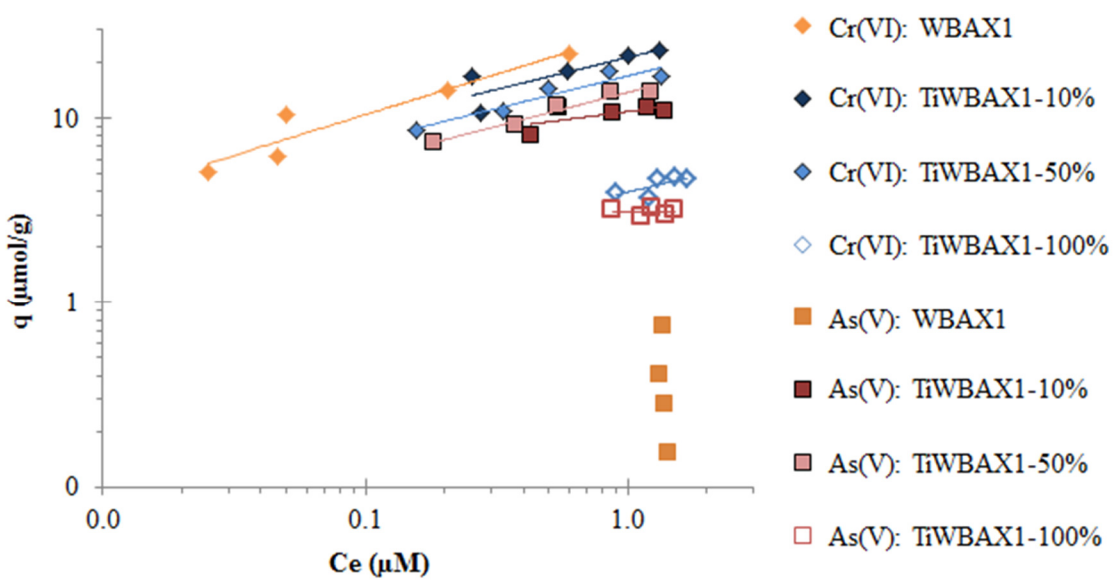

Figure 5.7. Equilibrium isotherm for titanium nanoparticle embedded WBAX synthesized using various precursor concentrations. Performed in a simulated groundwater matrix with Cr(VI) and As(V) spiked at 2 µM.

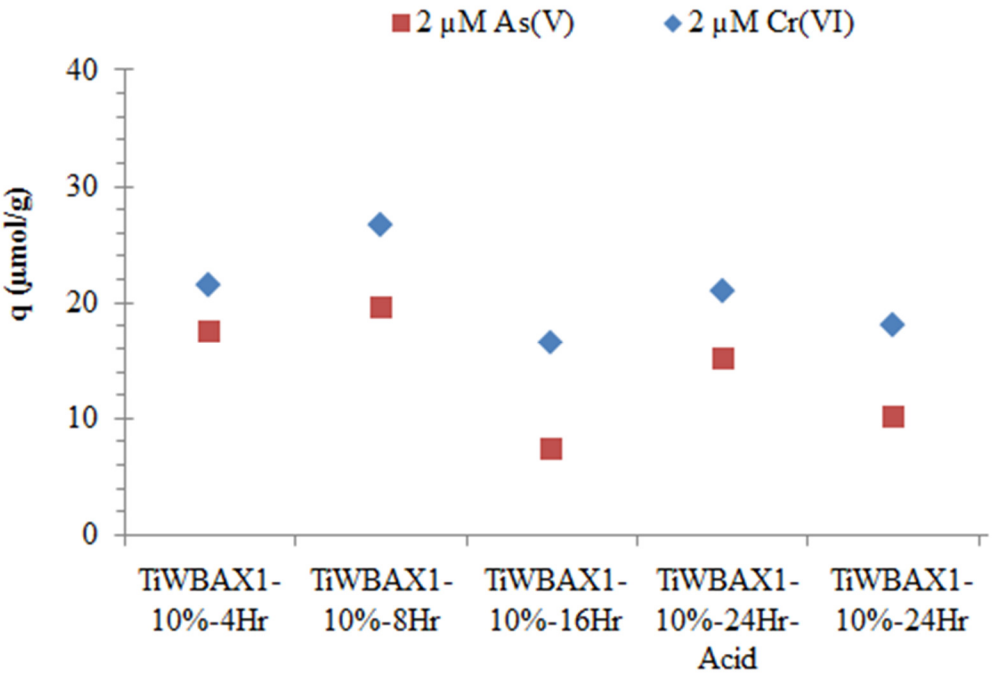

Figure 5.8. Pollutant removal capacity of five titanium nanoparticle embedded WBAX sorbents using 10% precursor solutions and various oven hydrolysis times.

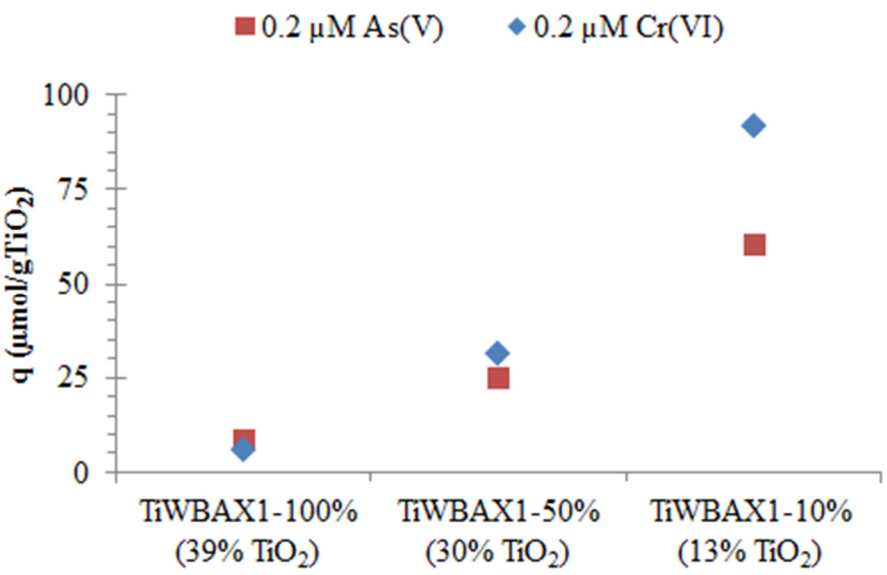

Figure 5.9. Equilibrium pollutant removal capacity normalized to metal content for Ti nano-composite sorbents synthesized with three different metal precursor concentrations. Removal capacity at 0.2 µM pollutants calculated by Fruendlich isotherm parameters observed in simulated groundwater batch experiments.

CHAPTER 6

REDUCING SUSTAINABILITY IMPACTS OF METAL NANOPARTICLE EMBEDDED ANION EXCHANGE RESINS USING ANTICIPATORY LIFE CYCLE ASSESSMENT

ABSTRACT

Nano-composite sorbents are an emerging technology for drinking water treatment of multiple pollutants. This novel technology can be developed in a proactively sustainable way when informed by anticipatory life cycle assessment. This allows comparison of synthesis methods and treatment options, identifies critical steps in their creation and use, and directs reduction of the environmental and human health impacts such that it becomes favorable compared to the existing technology. Here we use anticipatory life cycle assessment for nano-composite sorbents that have iron or titanium nanoparticles created in-situ within the porous structure of a weak base anion exchange resin (Fe-WBAX and Ti-WBAX). These provide targeted removal of hexavalent chromium and arsenic for drinking water. They are compared to the existing technology of using two different materials (anion exchange and granular ferric hydroxide) in a mixed bed (MB).

The Ti-WBAX had the lowest environmental and human health impacts compared to Fe-WBAX and MB for nine TRACI categories. The Fe-WBAX had the highest. The synthesis phase contributes 50% – 100% of the total impacts for each category for each sorbent. The greatest opportunity to improve the Fe-WBAX synthesis was increasing the sorbent pollutant removal capacity through chemical re-

functionalization of ion exchange groups to require less sorbent for treating the functional unit. This reduced impacts by 26% – 42%, making it favorable or equal with MB for six of nine categories. The greatest opportunity to improve Ti-WBAX is in reducing oven heating time for nanoparticle hydrolysis. Reducing heating time from 24 to 4 hours had only a small loss in sorbent capacity but reduced impacts by 3% – 31%. Future development of synthesis methods for nanocomposite sorbents should focus on optimizing sorbent capacity, decreasing heating energy demand, and efficiently reusing metal precursors and solvents. This study shows that benefits of treating drinking water do involve other environmental and human health tradeoffs, and that impacts associated with treatment are on the same order of magnitude as distribution pressurization.

1. INTRODUCTION

Development of nanotechnology has led to many exciting applications for treating water to drinking standards. Nanoparticles have high surface area to mass ratio providing unique sorption, disinfection, and photocatalytic pollutant reduction abilities (Qu et al. 2013), but on their own are difficult to remove from finished water after dosing. Composite sorbents have nanoparticles embedded in the porous structure of another sorbent (Du et al. 2013, Hu et al. 2015, Yamani et al. 2012). The parent sorbent provides mechanical strength for use in packed beds, attachment so nanoparticles are not lost into the bulk solution, and a beneficial elevated concentration gradient within the pores due to Donnan exclusion(Cumbal and Sengupta 2005, Zhao et al. 2011). These nano-composite sorbents can exhibit high removal capacity for multiple pollutants (Elton et al. 2013, Hristovski et al. 2008a, Sandoval et al. 2011, Sarkar et al. 2012). Continued technological progress of novel applications and abilities for nanocomposite sorbents is expected.

Emerging technologies should be developed with an eye toward sustainably instead of relying upon costly mitigation after widespread adoption. Life cycle assessment (LCA) provides a framework to anticipate proactively the environmental and human health impacts of a technology as it is developed. Currently, the most common use of LCA in studying water is to quantify embedded energy in water supply and transportation (Plappally and Lienhard 2012, Stokes and Horvath 2006, 2011). It has been used with other emerging technologies to set performance metrics, such as hybrid cars (Hawkins et al. 2012), high speed rail(Chester and Horvath 2010), and photovoltaic energy (Wender et al. 2014). Anticipatory LCA of an emerging technology is challenging because of an inherent lack of data regarding technology improvements and production

scale-up, and one way to address the challenge is through use of prospective structured scenarios(Wender et al. 2014). One other study has used LCA to set performance metrics for an emerging water treatment technology (Choe et al. 2015). This approach allows sustainability performance to be a design constraint instead of an afterthought.

The goal of this paper was to inform sustainable development of nano-composite sorbents using anticipatory LCA. Critical processes in the environmental performance involved with the deployment of this emerging technology were identified. Multiple nanocomposite sorbents were compared from an environmental performance perspective, and technology development scenarios were explored to identify what is required to outperform traditional sorbents. It demonstrated how anticipatory LCA can be used to improve product design and development. The present study is unique because it informs selection between treatment options, and because it studies nanocomposite sorbents.

This paper will focus on two nano-composite sorbents composed of metal oxide nanoparticles inside anion exchange resin. The nanoparticles are created in-situ made of either iron (Fe) hydroxide or titanium (Ti) dioxide. These are selected for comparison because Ti nanoparticles are hydrolyzed using heat and Fe nanoparticles are precipitated chemically. Previous studies have established synthesis protocols for Fe embedded (Hristovski et al. 2008a) or Ti embedded (Elton et al. 2013) anion exchange resins. In Chapter 5, these synthesis procedures were applied to weak base anion exchange resins (Fe-WBAX and Ti-WBAX). This study will provide critical information to inform technology development, quantify environmental impacts of their use, and determine which of the two resins is superior in terms of environmental performance.

The Ti and Fe nano-composite sorbents made with WBAX are useful to provide simultaneous treatment of chromium (Cr) and arsenic (As). These are prevalent groundwater pollutants that are challenging to remove at low concentrations. Cr is an oxidized metal for which California recently enacted an maximum contaminant level (MCL) of 10 $\mu g\ L^{-1}$. One of the leading treatment technologies is anion exchange(Brandhuber et al. 2004a). The national MCL for arsenic (As) was lowered to 10 $\mu g\ L^{-1}$ in 2006 due to a variety of human ailments including cancer of the bladder, lungs, and skin. The leading treatment processes is adsorption to iron oxides(Speital et al. 2010). Combining metal oxide and anion exchange into a single composite sorbent provides targeted removal capacity for both pollutants of interest.

The evaluation of these new hybrid resins were compared to the environmental impacts of using the existing technology. Standard practice would otherwise be to use two separate sorbents, one specialized to remove one pollutant and the other sorbent specialized for the other pollutant. These two sorbents used together could be configured either in two separate packed bed reactors that the water passes through in series, or mixed together into a single larger reactor. This treatment option is referred to as Mixed Bed (MB). The assumed specialized sorbents anion exchange (WBAX) for Cr removal, and a metal oxide (MO) sorbent for As removal.

2. METHODOLOGY

The environmental impacts of two metal oxide infused weak base anion exchange resins were assessed via comparative, attributional life cycle assessment (LCA). Two scenarios were included for each sorbent; an existing protocol scenario using established

protocols meant to inform how the synthesis procedure can be improved, and an improved technology scenario demonstrating the hybrid sorbents can outperform existing technology. The existing technology of using two separate specialized sorbents in a mixed bed was analyzed for a comparative benchmark. Impacts of pressurizing the system were also analyzed for anchoring and comparison to previous studies.

First, a functional unit was defined to compare the treatment options. Next, the system boundary was defined, which enabled the life cycle inventory to be compiled. This inventory is a list of all material and energy inputs into and out of the system boundary. The quantities of these inputs were scaled according to the functional unit. Finally, the environmental impacts associated with the line items from the inventory were assessed. This was done using impact factors that convert mass of an inventory item into midpoint environmental impact equivalents that, in turn, may be summed to give total impact associated with each product. This approach enabled comparison of the two sorbents from an environmental standpoint, as well as identifying phases of the sorbent life cycle with the largest potential for environmental improvement.

2.1 Functional Unit

The functional unit for this study was 20 million gallons (MG) of drinking water treated to an acceptable level. This represented the annual average domestic water use of 500 people (110 gallons $capita^{-1}$ day^{-1}). An acceptable level of use characteristics such as fines lost, chemical stability, and resin durability was assumed to be met by every treatment option.

In order to fairly compare disparate pollutant removal capacities between the three treatment options it was requisite to define a raw water quality and treated water quality goal. This study assumed a raw water quality of 20 µg Cr L^{-1} and 20 µg As L^{-1}. These levels were sufficiently high that treatment would be required beyond blending with uncontaminated wells. The assumed water treatment quality goal was 8 µg Cr L^{-1} and 8 µg As L^{-1}, which provided a margin of safety beyond the federal mandated 10 µg As L^{-1} maximum and California state mandated 10 µg Cr L^{-1}. It was therefore equivalent to think of the functional unit as a mass of sorbent required to remove 12 µg Cr L^{-1} and 12 µg As L^{-1} from 20 MG of water. The mass of sorbent included in the inventory was therefore the mass required to treat a volume of water defined by the functional unit keeping both pollutants below the defined limit. A low capacity to remove either pollutant would result in an increased mass of resin considered.

The capacity of each sorbent to remove each pollutant for the existing protocol and improved protocol scenarios was determined in Chapter 5. Following the original synthesis procedures, the Fe-WBAX has an estimated removal capacity of 490 µg Cr g^{-1} and 172 µg As g^{-1} at the pollutant concentration of interest. Therefore treating the functional unit worth of water would require 1,800 kg of sorbent if determined by Cr capacity or 5,300 kg if determined by As capacity. The larger was selected since it would be unacceptable to keep using the resin after As capacity was exhausted even if it was still removing Cr. The improved synthesis method for FeWBAX yielded a sorbent with 300 µg Cr g^{-1} and 510 µg As g^{-1} removal capacity. It was therefore limited by Cr capacity and requires 3,040 kg of sorbent to treat the functional unit worth of water. The original Ti-WBAX had 630 µg Cr g^{-1} and 600 µg As g^{-1} removal capacity requiring 1,500 kg

sorbent. The improved TiWBAX had 510 µg Cr g^{-1} and 500 µg As g^{-1}, requiring 1,800 kg sorbent. The WBAX had a Cr capacity of 310 µg Cr g^{-1} requiring 2,900 kg of sorbent to treat the functional unit. Another study found the MO had an As capacity of 280 µg g^{-1} ((Westerhoff et al. 2005)) requiring 3,200 kg to treat the functional unit. The MB option includes both the 2,900 kg of WBAX and the 3,200 kg of MO.

2.2 System Boundary

This LCA was unique because it follows the life cycle of the treatment product itself instead of the water. The evaluated system boundary had three principle phases: 1) Synthesis, 2) Use, and 3) Disposal. Figure 6.1 depicts the system boundary.

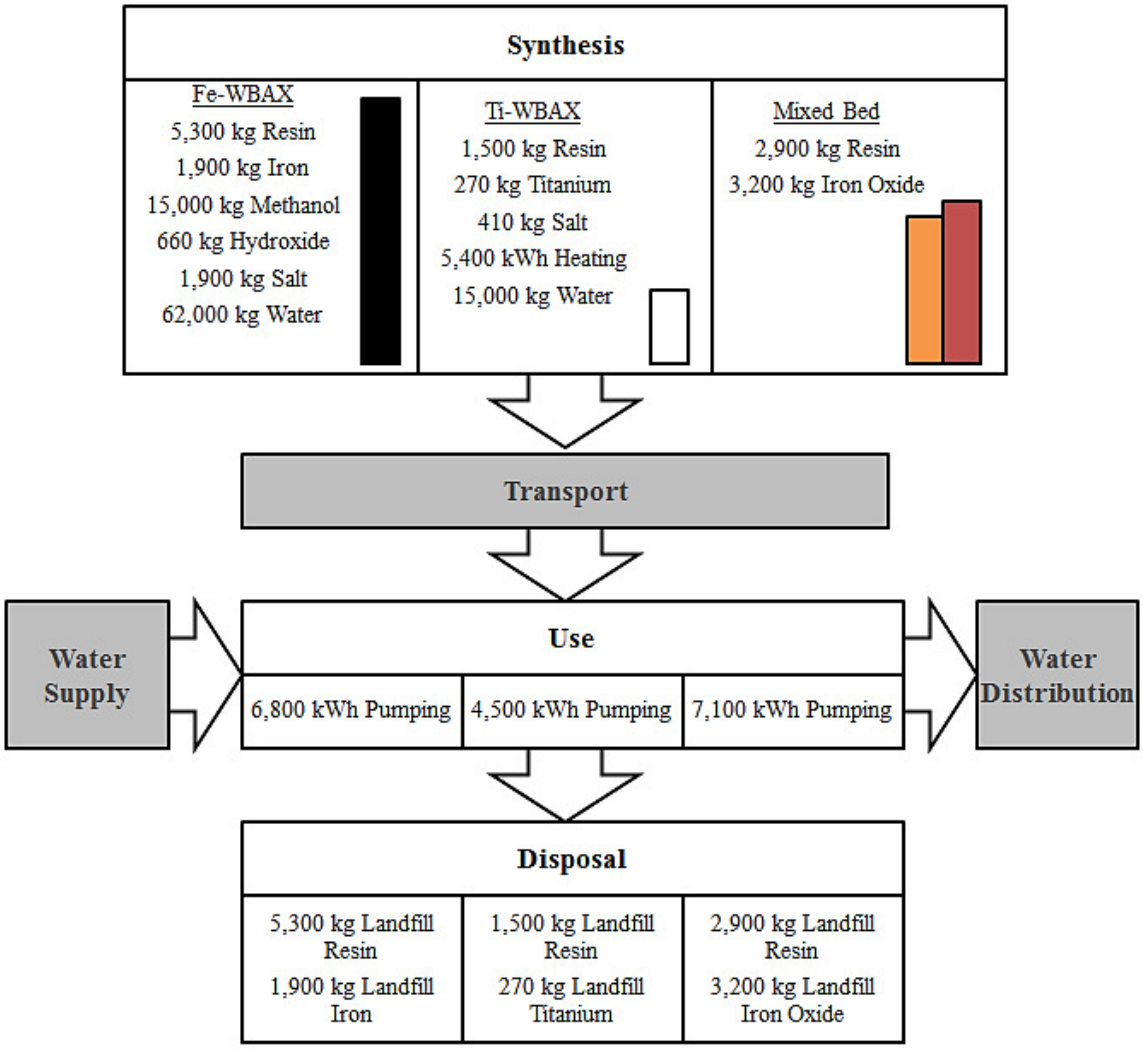

Figure 6.1. The system boundary includes the synthesis of the water treatment material by the original synthesis method, the energy required to overcome headloss during use, and landfill disposal after exhaustion. It excludes (greyed boxes) any impacts from material transport and water transport before or after treatment, as these are highly sensitive to assumptions on system location and not dependent on the treatment method itself.

2.2.1 Synthesis Phase. The methods for synthesis of the hybrid resins have been previously described (Elton et al. 2013, Hristovski et al. 2008a), and proposed modifications are described in Chapter 5. They each required inputs of the parent ion exchange resin, a precursor solution consisting of a high concentration of aqueous metal, and some post treatment chemicals. The Fe-WBAX used chemicals like methanol and sodium hydroxide to precipitate the metals, whereas the Ti-WBAX used heat-induced hydrolysis that expends electricity.

The original synthesis procedure for Fe-WBAX used hydroxide and has no acid post-rinse to restore the ion exchange capacity of the WBAX, resulting in a sorbent with little pollutant removal ability. The improved synthesis procedure included an acid post rinse to increase sorbent capacity. This added environmental impacts from the acid, but greatly reduced the mass of sorbent needed to treat the functional unit and is a net benefit. The original synthesis procedure for Ti-WBAX called for 24 hours of oven heating to hydrolyze the Ti nanoparticles. The improved synthesis scenario used 4 hours of oven heating with only little drop in pollutant removal ability.

The Ti-WBAX was heated in a Cole Palmer StableTemp 374B laboratory oven and electricity demand measured using a DFE Kill-a-Watts EZ power monitor. Set at 80°C, the oven consistently used 165 watts over a 72 hr monitoring period. This is noted to be much lower than the manufacturer power rating of 800 watts. Heating for 24 hours therefore demanded 4.0 kW hr for each liter of resin. It is recognized that large scale production would likely utilize more efficient oven packing and further reduce the energy demanded.

2.2.2 Use Phase. The principle inventory of the use phase was the energy required to pump water through the resin. This was computed using headloss per bed depth of 5.2 ft ft^{-1} as reported from the parent resin product specification sheets (Rohm & Haas 2008). The headloss through the nano-composite sorbents was assumed to be the same as the parent resin, which was reasonable since the embedded nanoparticles do not add exterior surface friction. Only intraparticle mass transport would be affected, which is not related to advective mass transport. The main source of difference for energy required by the treatment options stemmed from different masses of sorbent required, such that higher mass of sorbent required more energy to pump through.

Results from the treatment option analysis were anchored to the amount of energy required to pressurize the water distribution system at the treatment vessel. Energy for pumping from the source or after treatment were not considered as these would be highly dependent on system location and not the choice of treatment material.

The bulk weight of moist resin is 1.1 kg per liter (Rohm & Haas 2008), which was used to convert the required mass of resin calculated in Section 2.1 to a volume. The contact vessel containing the sorbent was assumed to be cylindrical with an aspect ratio of 3. It was more reasonable to assume a constant aspect ratio than constant diameter to stay within typical design parameters since a larger volume of resin would likely be used in a larger diameter vessel to avoid an overly tall vessel. The original Fe-WBAX vessel was therefore estimated to be 4.2 feet in diameter and 12 feet tall. The original Ti-WBAX vessel was 2.7 feet in diameter and 8.2 feet tall. The MB vessel was 4.4 feet in diameter and 13 feet tall.

Pump power demand was estimated with the vessel dimensions according to Equation 2.

$$P=Q\,\rho\,g\,H\,\eta^{-1} \quad (2)$$

where P was pump power in kW, Q was water flow rate in gallons min^{-1}, ρ was water density in lb ft^{-3}, *g* was gravitational acceleration in ft s^{-2}, H was headloss through the resin in ft, and η is pump efficiency. The flow rate defined in Section 2.1 was 20 MG per year, equivalent to 38 gallons min^{-1}. Water density was 62.4 lb ft^{-3}, and gravity was 32.2 ft s^{-2}. Headloss in the resin bed at a loading rate of 10 gal min^{-1} ft^{-2} is 2.25 psi per foot of bed depth (Rohm & Haas 2008), equivalent to 5.19 feet of head per foot of bed depth. Pump efficiency was assumed to be 60%. Using the separate bed depths of the three treatment options yielded required pump power for Fe-WBAX as 0.77 kW, 0.51 kW for Ti-WBAX, and 0.81 for MB. These were equivalent to 6,800 kW hr for Fe-WBAX, 4,500 kW hr for Ti-WBAX, and 7,100 for MB over the course of one year.

2.2.3 Disposal Phase. It is not currently understood how to regenerate WBAX used for Cr(VI) treatment (McGuire et al. 2007), so the sorbents were assumed to be single use. As soon as the bed exceeded its removal capacity for either pollutant, it was considered exhausted and replaced. The spent sorbents, comprised of the WBAX resin and the metal, were landfilled. This study assumed disposal to a sanitary class III landfill, and future work will determine if the potential hazardous waste classification would require specialized disposal accommodations which cause alternate environmental impacts.

2.2.4 Exclusions from System Boundary. The system boundary excluded a few notable items from the life cycle inventory. The inventory did not include materials of the

treatment plant itself such as piping, valves, and contactor vessels. These materials would be required for physical operation of the water treatment technology, but were only loosely attributable to the choice of sorbent itself. Previous studies have indicated environmental impacts from treatment plant construction range between negligible (Raluy et al. 2005) to 4 – 9% (Stokes and Horvath 2006).

No pH control chemicals were included because the sorption capacities for each sorbent were reported for ambient pH. Each of the treatment options would perform better at depressed pH, but the relative benefit was assumed the same for each option and therefore excluded from this comparison.

Transportation of the resin was excluded across the life cycle, including moving the parent resin to the place of manufacture, transporting the hybrid resin to the water treatment site, and hauling exhausted resin away from the site. This is because impacts would vary widely based on an arbitrary assumption for treatment location, and they would not vary greatly between scenarios. Prior studies found that material delivery for a water treatment facility contributed less than 0.6% of total emissions (Stokes and Horvath 2006) and less than 2% of total global warming equivalents (Stokes and Horvath 2011).

Impacts associated with the water supply are excluded. Items such as well pumping, source water depletion, and distribution pumping are excluded. This LCA focused on differentiating treatment strategies, and impacts from those items would not vary.

2.3 Environmental Impacts

Environmental impacts were estimated by multiplying the life cycle inventory items with their respective impact factors. Impact factors were from the EcoInvent database version 2.2 (SCLCI 2010). Impact factors estimate the total environmental impacts that a single inventory item has normalized to a unit (e.g. mass) in terms of equivalent risk. It was important to match each inventory line item identified in the system boundary to a representative impact factor.

An impact factor for a general anion exchange resin was used (Anion Exchange Resin – Synthesis). It represents a strong base anion exchange resin made of polystyrene, functionalized with chloromethyl methyl ether and trimethylamine, and 50% moisture content. The three treatment options being studied used a weak base anion exchange resin made of phenol-formaldehyde polycondensate, had undergone an unknown functionalization, and had 60% moisture content (Rohm & Haas 2008). Though not exact matches, it was deemed appropriately representative for an impact factor since they are both organic polymer structures with some form of functionalization and high moisture content.

The chemical inventory items correlated closely with impact factors. Sulfuric acid, ferric chloride, sodium hydroxide, methanol, and sodium chloride each had impact factors with matching CAS numbers and descriptions. The titanium oxysulfate precursor was matched with the impact factor for titanium dioxide via sulfate production process. Electricity impact factors were a supply mix, medium voltage, at grid, with average United States production data.

The impact assessment categories to be evaluated were defined by TRACI (USEPA 2014). This system is of interest as it was developed in the United States and covers a range of environmental and human health midpoint impacts. Some of the impact categories were non-cancer toxicity, ocean acidification, and global warming potential.

2.4 Data Uncertainty Analysis

Due to a lack of published statistical analysis in the Ecoinvent database, data uncertainty is estimated using the approach outlined in the Ecoinvent manual (Frischknecht et al. 2007). First, six sets of data were qualitatively evaluated in a pedigree matrix shown in Table 6.1. Anion exchange resin, methanol, and electricity were each evaluated for inventory and for impact factors because these items contribute a majority of final impacts. These scores were converted to uncertainty factors and combined to produce a squared geometric standard deviation for each data set. This statistical information was applied to produce a lognormal distribution for each of the three inventory items and three impact factors. Monte Carlo analysis (1,000 simulations) was performed (Lumina Analytica v4.6) with the probabilistic information, with the other contributions remaining deterministic, to estimate the total magnitude of the data uncertainty.

Indicator score	Resin Inventory	Methanol Inventory	Electricity Inventory	Resin Impact Factors	Methanol Impact Factors	Electricity Impact Factors	Comments
Reliability	1	1	1	3	3	3	Inventory data measured, but impact assessment data comes from database with built in assumptions.
Completeness	5	5	5	2	2	2	Inventory data collected from a single site over small period, with unexplored variations. Impact assessment data is largely national averages studied for more than one year.
Temporal correlation	1	1	1	4	4	3	Inventory data is from recently developed methods. Impact assessment data is from the 2010 database, but were actually collected between 1994-2004.
Geographical correlation	2	2	2	3	3	2	Inventory data is from locally developed methods. Impact assessment data is largely European averages, except for electricity which is US average.
Further technological correlation	1	1	1	4	3	3	Though the methanol production process has not drastically changed, adoption of underground natural gas mining has likely changed acquisition of raw material for it. This resin is for a type 1 strong base anion exchange resin of polystyrene and divinylbenzene crosslinking which is a common method, but other widely varied technologies exist. Electricity generation technology has not drastically changed.
Sample Size	4	4	4	5	3	3	Inventory data repeated few times in laboratory setting. Impact assessment data for methanol and electricity collected from nation wide reports.
Basic Uncertainty Factor	1.05	1.05	1.05	3	3	3	Inventory uses process emissions for demand of electricity or products. Impact assessment data uses process emissions to air for polyromantic hydrocarbons as controlling
Squared Geometric Standard Deviation	1.24	1.24	1.24	3.33	3.11	3.07	

Table 6.1. Data Quality Assessment. The inventory and impact assessment factor quality for the three highest contributing items were analyzed. A score of 1 represents the data used has high reliability, and 5 represents low reliability. These are converted to uncertainty factors and combined to produce a squared geometric standard deviation.

3. RESULTS AND DISCUSSION

3.1 Life Cycle Inventory

The life cycle inventory was first compiled for each treatment option, and scaled to the mass of sorbent required to treat the functional unit (20 million gallons treated water). Figure 6.1 shows the items included in this inventory for the original synthesis methods. The original iron nanoparticle-infused anion exchange resin (Fe-WBAX) had a limiting pollutant capacity of 170 µg As g^{-1}, requiring 5,300 kg of resin to treat the functional unit. The synthesis phase of this resin included high chemical usage. The energy required during use phase equaled the headloss through a packed bed of the required mass of resin. This totaled 65 feet of headloss to deliver the functional unit requiring 6,800 kW hr to overcome over one year. Disposal after single use was to a landfill. The improved FeWBAX required only 3,000 kg of resin and 5,600 kW hr pumping energy.

The original titanium infused-anion exchange resin (Ti-WBAX) had a limiting pollutant capacity of 600 µg As g^{-1}, requiring 1,500 kg of resin to treat the functional unit. The synthesis phase of the resin required energy to heat an oven for hydrolysis. Heat required for the oven to reach 80°C for 1 hour was measured as 165 W, resulting in 5,400 kW hr demand for a scaled-size oven to heat for 24 hours. Pumping during use phase had to overcome 43 feet of headloss, requiring 4,500 kW hr of pump energy. Disposal after single use was to a landfill. Improved TiWBAX used only 4 hours of oven heating. The required mass of resin increases slightly to 1,800 kg sorbent, but the heating energy drops to 1,090 kW hr.

For the mixed bed treatment option, the parent WBAX resin had a removal capacity of 310 µg Cr g^{-1} requiring 2,900 kg of resin to remove just the Cr from the functional unit. In addition, the metal oxide had 280 µg As g^{-1} sorbent of arsenic removal capacity, requiring 3,200 kg sorbent to treat the arsenic. These two sorbents together created 68 feet of headloss, requiring 7,100 kW hr of pump energy to overcome. Disposal after single use was to a landfill.

The results of the three treatment options are anchored against the impact of pressurizing the system to a baseline pressure that is independent of the treatment option used. The pressure provided was 80 lb in^{-2} at the effluent of the treatment vessel, ignoring any friction losses that would subsequently occur in distribution piping. This required 19,000 kW hr of pump energy.

3.2 Life Cycle Impact Assessment

TRACI midpoint environmental impacts associated with all life cycle inventory items were estimated by use of impact factors obtained from EcoInvent v2.2 (SCLCI 2010). The impacts of all life cycle phases for each sorbent in each impact category are shown in Figure 6.2. These impacts were normalized to the sorbent option with the highest impact for ease of comparison.

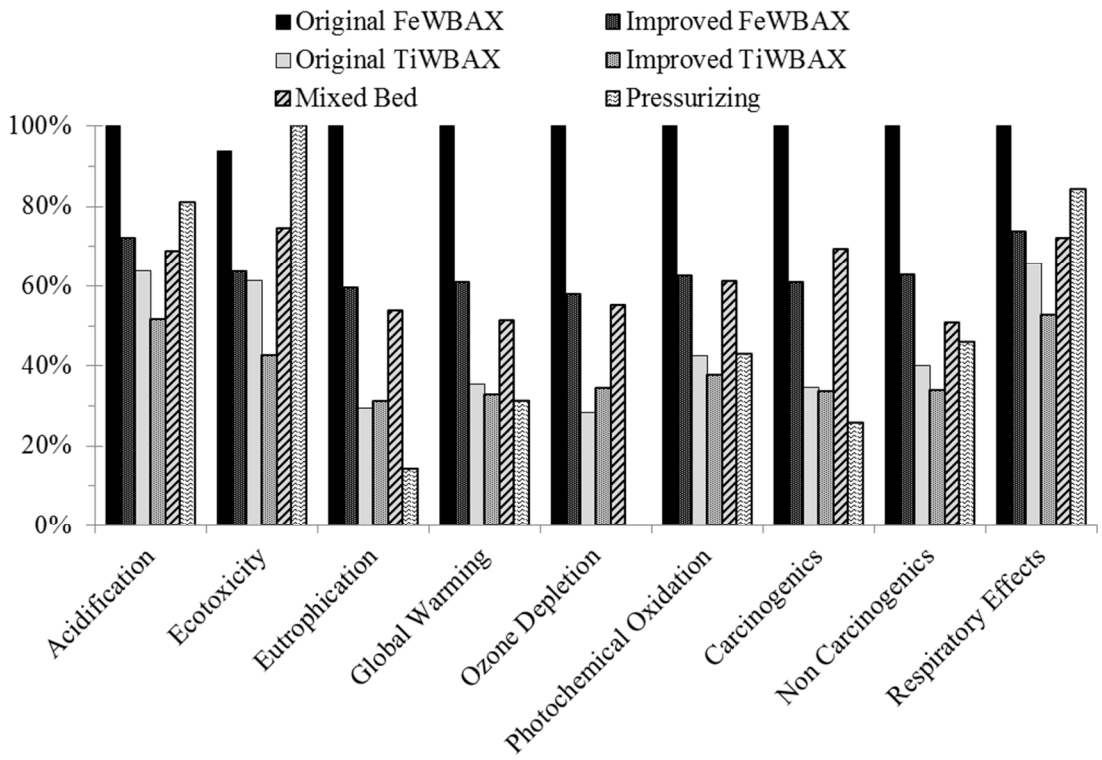

Figure 6.2. Total impacts of each treatment option anchored to pressurizing the treatment vessel and normalized to the option with the highest impact.

Original Fe-WBAX had the highest impacts of the treatment options for all impact categories. Its environmental impacts were 6,500 moles H^+-equivalents for ocean acidification potential, 9,000 kg 2,4 dioxane-equivalents for ecotoxicity, 13 kg N-equivalents for eutrophication potential, 47,600 kg CO_2-equivalents for climate change potential, 0.9 kg CFC-equivalents for ozone depletion potential, and 66 kg NO_x-equivalents for photochemical oxidation (smog) potential. Its human health impacts were 89 kg benzene-equivalents for human carcinogenicity potential, 137,000 kg toluene-equivalents for human non-carcinogenic toxicity potential, and 25 kg $PM_{2.5}$-equivalents for human respiratory effect potential.

The improved Fe-WBAX synthesis scenario with increased sorption capacity reduced impacts by 26% – 42% compared to the original scenario. These improvements made the impacts of Fe-WBAX lower than MB for ecotoxicity potential and human carcinogenicity potential, about equal (within 5%) with MB for four categories, and remained 10 – 24% higher than MB for the other three categories. These drastic reductions in impacts demonstrate the improved synthesis process was successful.

The impacts from the original Ti-WBAX ranged from 29% – 66% of those for the original Fe-WBAX. Both the original and improved Ti-WBAX scenarios had lower impacts than both Fe-WBAX scenarios and the MB for all impact categories. The improved Ti-WBAX reduced total impacts by 3% – 31% compared to the original scenario, except for eutrophication potential that increased by 5% and ozone depletion potential that increased by 20%. This demonstrates nanocomposite sorbents can outperform traditional treatment methods, and that titanium dioxide nano-sorbents may be preferable to those of iron hydroxide.

Impacts from pressurizing ranged from 14% – 100% of the highest, except for ozone depletion potential for which it was negligible. Besides that category, the pressurizing results were on the same order of magnitude as the five treatment options. This means that the treatment stage is a non-insignificant contributor to the total environmental impacts of the urban water cycle.

3.2.1 Phase Analysis. To understand the sources of the observed differences the results were next broken down by phase. Figure 6.3 shows the impacts of each treatment option divided by contribution from the synthesis, use, and disposal phases. For the original Fe-WBAX resin the synthesis phase contributed 57% - 100% of the total impacts for each impact category. The use phase contributed 0% - 37% to each category, and the disposal phase contributed 0% - 17%. For the Ti-WBAX resin the synthesis phase contributed 62% - 100% of the total impacts for each impact category. The use phase contributed 0% - 38%, and the disposal phase contributed 0% - 13% for each category. The two improved sorbent scenarios followed similar trends. For mixed beds, the synthesis phase contributed 50% - 100% of the total impacts for each category. The use phase contributed 0% - 50%, and the disposal phase contributed 0% - 15%. For pumping, all impacts occurred exclusively in the use phase by definition.

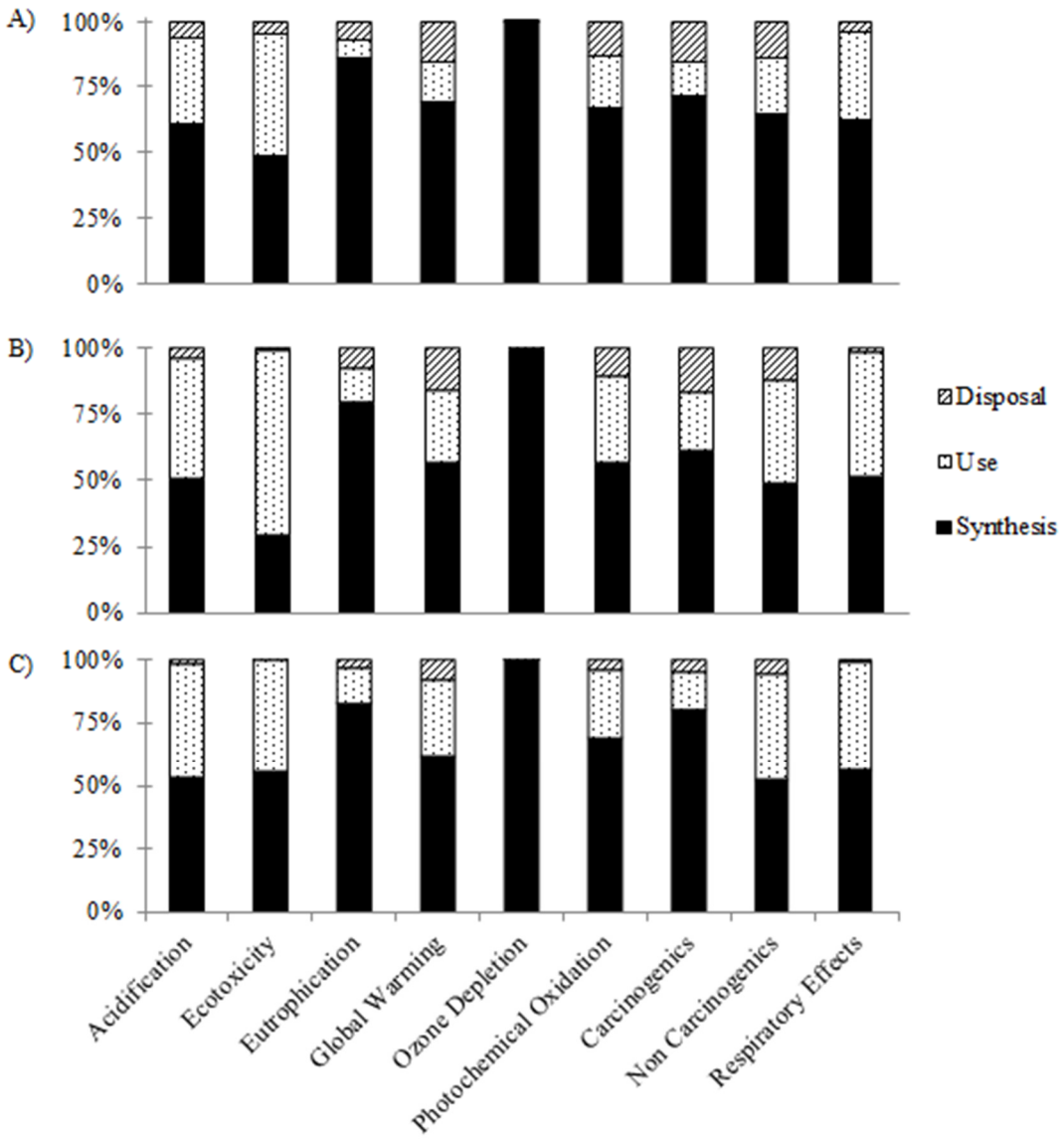

Figure 6.3. Relative contribution of each phase to total impacts for A) original Fe-WBAX, B) original Ti-WBAX, and C) Mixed Beds.

It is very evident that the synthesis phase was the main impact contributor for all life cycle phases and all treatment options. This was most evident in the case of ozone depletion, where over 99.9% of the calculated impact for any option happened during synthesis. This is due almost exclusively to the production of the parent anion exchange resin, which had an impact factor four orders of magnitude higher than that associated with any other inventory item. The production method for polymers often uses tetrafluoroethylene and chlorofluoromethane, which each have extremely high ozone depletion potential. This illustrated an interesting tradeoff in water treatment that uses polymer-based materials like ion exchange or coagulants. While the treatment was intended to lower human health risks from exposure to drinking water pollutants, it came at a high ozone depletion potential cost. Their use provided short-term human benefit to a localized population served by the water system, but contributed to a long-term regional environmental problem.

The other synthesis impacts associated with the Fe-WBAX resin synthesis were primarily from the cumulative impact of the chemicals used to precipitate the iron hydroxide nanoparticles. These chemicals included methanol and hydroxide, which are energy intensive to produce.

The synthesis impacts associated with the Ti-WBAX stemmed primarily from the energy required to heat the resin in an oven hydrolyzing the titanium dioxide nanoparticles. That is why large improvements in environmental performance were gained by reducing the heating time. These impacts were also sensitive to assumptions made about the oven utilization, i.e. the amount of resin heated per volume of oven. This is an area where both environmental performance and economic costs could be improved

if further efficiencies are found during commercialization and production scaling since the manufacturers can reduce electricity costs by filling the ovens to capacity.

Impacts associated with the Use Phase were the lowest for original Ti-WBAX compared to the Use Phase for other treatment options. They were 52% higher for the original Fe-WBAX and 60% higher for mixed bed. This was due to the larger mass of sorbent required for those options, and subsequently higher headloss that had to be overcome by pumping. Packed bed columns were assumed to maintain a 1:3 diameter to height aspect ratio. This means that even though more than three times as much volume of original Fe-WBAX resin was required to treat an equivalent volume of water as the original Ti-WBAX resin, the bed depth only increased by 52% with the rest of the volume compensated by increased column diameter. Different assumptions about bed configuration would alter the results, but the total impacts would still be relatively small compared to synthesis impacts.

Impacts associated with the disposal phase were very small for any of the treatment options. This analysis assumed disposal after single use to a landfill. It excluded any impacts associated with transporting the sorbent to the landfill. It also did not consider any impacts associated with special handling required for possible hazardous waste or radioactive waste classification. Previous study on WBAX suggests that spent sorbent would not be classified as toxic waste by Toxicity Characteristic Leaching Procedure (TCLP) or the Resource Conservation and Recovery Act (RCRA), but may be toxic waste as classified by Soluble Threshold Limit Concentration (STLC) and Total Threshold Limit Concentration (TTLC) (Najm et al. 2014). There are mixed results for if the spent sorbent would classify as Technologically Enhanced Naturally Occurring

Radioactive Material (TENORM) (McGuire et al. 2007, Najm et al. 2014), possibly dependent on how much uranium co-occurs in the source water. Either way, further exploration of this possibility was not considered because the disposal impacts relative to synthesis impacts were small, so the remaining focus turned to reducing impacts in the synthesis phase.

3.2.2 Hotspot Analysis. Next, further understanding of the impacts associated with the synthesis phase for the original sorbents was explored. Figure 6.4 compares the impacts for three midpoint indicators (global warming potential, human non-carcinogenic toxicity, and ocean acidification potential) delineated by each inventory item.

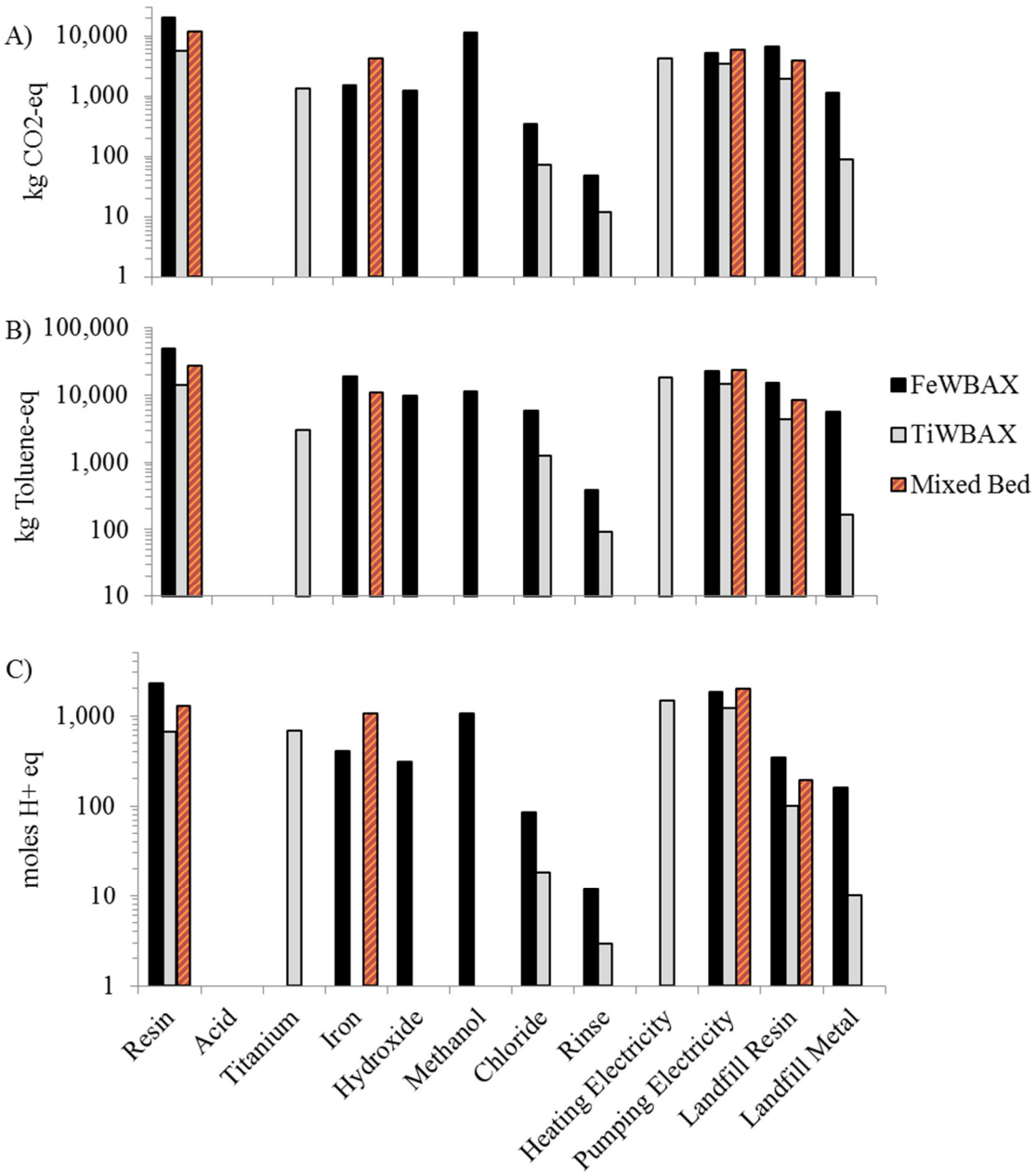

Figure 6.4. Hotspot analysis of original FeWBAX, original TiWBAX, and mixed bed showing impact contributions of individual inventory items to A) global warming potential, B) human non-carcinogenic toxicity potential, and C) ocean acidification potential.

The single inventory item making the largest contribution to impacts associated with original Fe-WBAX was from the parent anion exchange resin (20,100 kg CO_2-equivalents, 42% of the total in the case of climate change potential). This was pursuant to the high mass of resin required to treat an equivalent volume of water. The next highest impact was from methanol (11,200 kg CO_2-equivalents, 23% of the total in the case of climate change potential), which is an organic solvent and has high carbon footprint. The original Ti-WBAX used less parent anion exchange resin but still had significant impact associated with it (5,800 kg CO_2-equivalents, 34% of the total climate change potential). It also used less titanium precursor than the Fe-WBAX uses iron precursor, but the carbon footprint was nearly equivalent (1,400 and 1,500 kg CO_2-equivalents, respectively). Another primary synthesis impact associated with the Ti-WBAX was the electricity required for oven heating (4,200 kg CO_2-equivalents, 25% of the total climate change potential). The overall synthesis impact of TiWBAX was smaller than FeWBAX due to higher capacity for pollutant removal and not using methanol or other chemicals.

The acidification potential and human toxicity impacts associated with each sorbent broken down by inventory item showed similar overall trends as the global warming potential. The largest impacts were from the heating and pumping electricity and the parent anion exchange resin.

3.2.3 Proposed Impact Factors. So that future studies can simply use the results of this study, impact factors associated with the Fe-WBAX and Ti-WBAX are presented in Table 6.2. These were found by summing the total impacts for each category by phase and normalizing to 1 kg of resin. For consistency with data observed in the EcoInvent

database, the synthesis and disposal phases were presented separately with the use phase omitted.

	Acidification (moles H+ Eq)	Ecotoxicity (kg 2,4-D Eq)	Eutro-phication (kg N)	Global Warming (kg CO2 Eq)	Ozone Depletion (kg CFC-11 Eq)	Photo-chemical Oxidation (kg NOx Eq)	Carcin-ogenics (kg Benzene Eq)	Non-Carcinogenics (kg Toluene Eq)	Respiratory Effects (kg PM2.5 Eq)
Original FeWBAX Synthesis	7.89E-01	1.03E+00	2.15E-03	6.54E+00	1.73E-04	8.92E-03	1.26E-02	1.79E+01	3.10E-03
Original FeWBAX Disposal	9.58E-02	1.07E-01	1.82E-04	1.50E+00	1.09E-08	1.75E-03	2.76E-03	3.94E+00	2.61E-04
Improved FeWBAX Synthesis	9.38E-01	1.04E+00	2.16E-03	6.57E+00	1.73E-04	9.10E-03	1.28E-02	1.82E+01	3.79E-03
Improved FeWBAX Disposal	9.58E-02	1.07E-01	1.82E-04	1.50E+00	1.09E-08	1.75E-03	2.76E-03	3.94E+00	2.61E-04
Original TiWBAX Synthesis	1.88E+00	2.56E+00	2.08E-03	7.55E+00	1.72E-04	1.28E-02	1.42E-02	2.39E+01	7.55E-03
Original TiWBAX Disposal	7.25E-02	2.69E-02	1.63E-04	1.34E+00	7.69E-09	1.45E-03	2.72E-03	2.99E+00	1.42E-04
Improved TiWBAX Synthesis	1.06E+00	9.76E-01	1.79E-03	5.24E+00	1.72E-04	8.40E-03	1.06E-02	1.41E+01	4.27E-03
Improved TiWBAX Disposal	7.25E-02	2.69E-02	1.63E-04	1.34E+00	7.69E-09	1.45E-03	2.72E-03	2.99E+00	1.42E-04

Table 6.2. Proposed impact factors for 1 kg of Fe-WBAX and Ti-WBAX broken up by synthesis phase and disposal phase.

3.3 Reducing Environmental Impact of Hybrid Sorbents

A primary goal of this study was to proactively improve the synthesis method of hybrid sorbents by applying the LCA results to reduce the overall environmental impact. Energy associated with oven heating time to hydrolyze the titanium nanoparticles inside the TiWBAX was a very large contributor to environmental impacts that could be reduced. Previous synthesis protocol called for 24 hours of hydrolysis time(Elton et al. 2013). Here we compare pollutant removal performance of TiWBAX given 24 hours, 16 hours, 8 hours, and 4 hours of oven heating time. The remaining synthesis procedures were unchanged (same parent weak base anion exchange resin, 10% metal precursor concentration). Reducing the oven heating time to 4 hours reduces the climate change potential by 8%, human toxicity potential by 16%, and ocean acidification impact by 20%.

Figure 6.5 shows the pollutant removal performance of each of these sorbents. This was determined by methods used in Chapter 5. Briefly, 90 mg dry sorbent was placed in 500 mL of synthetic groundwater (NSFI/AN 2007) spiked with 2 µM hexavalent chromium and 2 µM pentavalent arsenic at pH 8. The pollutant removal percentage was the difference in pollutant concentration measured by inductively coupled plasma mass spectrometry (ICP-MS) before and after a 7 day equilibrium time.

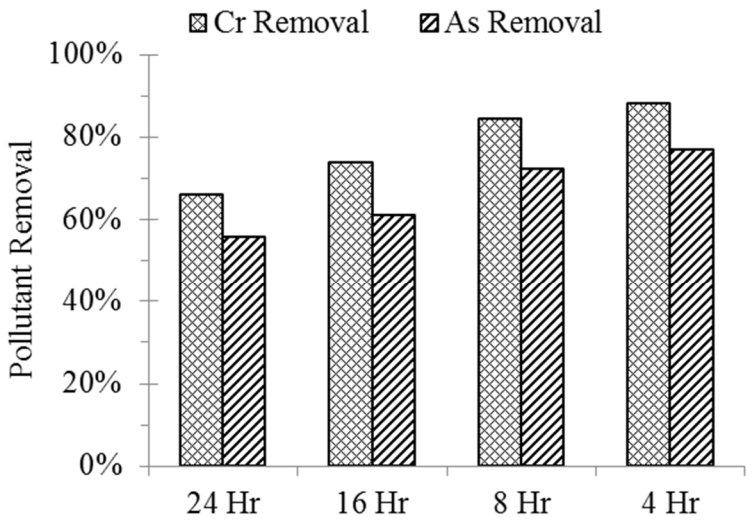

Figure 6.5. Effect of hydrolysis time on pollutant removal percentage of TiWBAX. Synthetic groundwater dosed with 180 g L^{-1} sorbent was spiked with 2 µM hexavalent chromium and 2 µM pentavalent arsenic at pH 8 and allowed to equilibrate for 7 days.

Decreasing the oven hydrolysis time from 24 hours to 4 hours increased chromium removal from 66% to 88%, and increased arsenic removal from 56% to 77%. It was observed that pollutant removal capacity was not significantly inhibited by reducing oven hydrolysis time to synthesize the TiWBAX. While it may have been possible that the reduced time increased removal performance, more detailed performance testing should be carried out to validate that claim. This did clearly show that the results of this study can be used to reduce environmental impacts without forfeiting water treatment performance efficiency. This corroborates reduced oven heating time as the improved scenario for TiWBAX in this study.

The original FeWBAX synthesis procedure calls for rinsing with hydroxide, which causes great loss in ion exchange capacity for the parent WBAX as further discussed in Chapter 5. This loss means more than three times additional sorbent was required for the original FeWBAX scenario and the greatest potential for improving the environmental performance was improving pollutant removal capacity to reduce the mass of sorbent required. The improved FeWBAX scenario included an acid-post rinse in the sorbent synthesis to counteract the effects of the hydroxide rinse and restore ion exchange capacity. This added some environmental impact associated with the production of acid, but greatly reduced the mass of sorbent required, providing a net reduction in climate change potential by 39%, human toxicity potential by 37%, and ocean acidification impact by 28%.

Other opportunities to further improve on the environmental performance of the hybrid sorbents included reducing the demand for metal as well as organic solvents. Efficient reuse of metal precursor solution would give large gains in sustainability

performance, and future development of hybrid sorbents should focus on reducing oven heating, increasing sorbent capacity, and reuse of precursor solution.

3.4 Data Quality Assessment

Data uncertainty stems from heavy reliance on the emission factors for TRACI impacts published in the EcoInvent database that unfortunately did not include any statistical analysis such as standard deviation. They were almost all assembled from sources in Europe, except for electricity generation (pumping, heating) were US data was available. All factors were used at plant, as desired, and did not include transportation to synthesis location or water treatment location. Good correlation between inventory items and described factors was generally found. For instance, specific chemicals with matching CAS numbers were identified in the database. One general anion exchange resin was used from the database, but synthesis procedures can vary widely and develop rapidly over time lending to low reliability. Titanium and iron ore impact factors also vary based on production process, and using a single data point has low reliability. The metal oxide sorbent used for water treatment in the mixed bed option is likely more highly processed than the metal oxide impact factor assumed by this study, and adding additional processing steps would serve to increase the environmental impacts associated with that treatment option.

A source of parameter uncertainty is the assumed pollutant removal capacity for each sorbent. Fruendlich isotherm parameters were used to calculate pollutant removal capacity at 0.4 μM from synthetic groundwater. However this capacity can vary greatly depending on the influent water quality and the way it is used. For example, removal

capacity for any sorbent is generally higher if usedion packed bed flow through column mode, which would presumably be the case here. However only the improved sorbents were tested in the more time consuming column mode, so for the sake of consistency between sorbents, equilibrium capacities were used. Using column mode capacities would likely have the effect of scaling impacts from all sorbents downward. Comparative trends between them would likely hold, while the absolute values of impacts would decrease.

The data uncertainty associated with this study was estimated using the above qualitative analysis and the quantitative method previously described to estimate a distribution for the inventory and impact assessment factor of the three items that most strongly impacted final results. The standard deviation of total global warming potential was found to range from 121% – 154% of the median value for the five sorbent options analyzed. The standard deviation of the total non-carcinogenic potential ranged from 94% – 143% of the median value for the five sorbent options. This range of variation is similar in scale for each treatment option, but is larger than the differences observed between them. This makes is hard to make recommendations between the options. Large uncertainty is inevitable with anticipatory LCA (Wender et al. 2014), but it does not interfere with other valuable findings like relative magnitude of the novel technologies compared to the existing, the hotspot analysis, and decreasing the overall impacts by using these results to improve the nanocomposite sorbent formulation.

4. CONCLUSIONS

This study demonstrates the value of using anticipatory life cycle assessment to improve a technology during its development. The analysis was able to proactively identify the largest contributors to environmental impacts associated with creating and using nanocomposite sorbents for groundwater treatment, and therefore inform improving their synthesis protocol. The improved Fe-WBAX had 26% – 42% lower impacts than the original, and the improved Ti-WBAX reduced most impacts by 3% – 31%. In the case of Fe-WBAX, the improvement brought the novel sorbent on-par with the existing technology in terms of environmental and human health impacts, whereas it was not a viable option under the original formulation.

Electricity use for oven heating during the synthesis of Ti-WBAX is one of the largest contributor to environmental impacts and one of the largest opportunities for reducing those impacts. Technology developers can help mitigate these impacts by focusing research efforts on reducing required hydrolysis time, and future commercial manufacturers can help mitigate these impacts through utilizing high efficiency ovens and verifying full use of oven capacity each time a batch is synthesized. The Fe-WBAX can be environmentally preferable to mixed beds when sorbent capacity is optimized to require less sorbent for treatment. This can be accomplished through adding sulfuric acid and sodium chloride post treatments to the synthesis process, which have small impacts compared to the parent anion exchange resin itself. Technology developers can mitigate impacts by optimizing tradeoffs between using chemical to maximize pollutant removal capacity and reducing the total mass of resin needed to treat a given volume of water.

Commercial manufacturers can help mitigate impacts through efficient reuse of metal precursor solutions and the associated solvents.

Second, this study demonstrates that using nanocomposite sorbents for simultaneous treatment of multiple pollutants is a valuable technological option compared to the existing approach of using mixed beds or beds in series. Environmental and human health impacts of the improved recipe Ti-WBAX nanocomposite sorbents are 48% – 74% of those of mixed beds. The traditional sorbents used in the mixed bed option have removal capacity for only one pollutant, and therefore require more mass with higher impacts to remove multiple contaminants. Even for the Fe-WBAX where impacts were similar to mixed beds (86% – 120%), a single process performing multiple tasks may require less capital equipment and be easier to operate. The ability to remove multiple pollutants will become more valuable to water treatment systems into the future as water supplies dwindle and require depending on lower quality sources, and as regulatory agencies enact tighter limits on increasing number of contaminants.

Lastly, this study calls attention to tradeoffs in making water related decisions. Water treatment is usually done in an effort to reduce human exposure to negative health effects. While lower exposure to contaminants such as Cr and As does reduce these risks, employing additional treatment technologies will add other environmental impacts. Tradeoffs between human health risks and environmental impacts should be understood in considering new water quality strategies beyond only performance efficacy and cost. By extension, water treatment is a non-negligible contributor to the total environmental footprint of the urban water cycle.

5. ACKNOWLEDGEMENTS

Funding for this study has been provided by the United States Environmental Protection Agency under EPA-F2013-STAR-E1 Graduate Fellowship for Environmental Studies, and the Dr. Ronald and Sharon Thomas Graduate Fellowship.

CHAPTER 7

EXPORTING CANCER AND OTHER HEALTH RISKS BY INSTALLING WELLHEAD DRINKING WATER TREATMENT

ABSTRACT

Water treatment reduces health risks to the population drinking the water, but also requires materials and energy, the production of which emits pollutants that increase health risks. This work explored the tradeoff between the human carcinogenic and non-carcinogenic health risks involved with water treatment by comparing dose-response curves to the indirect burden of providing that treatment using life cycle assessment. It studied a representative wellhead sorbent groundwater treatment system removing hexavalent chromium or pentavalent arsenic from 1,000 gal min^{-1} serving 3,200 people using both USEtox and EPA TRACI/IRIS methodologies. Reducing the concentration of pollutants in drinking water reduced the potential cancer cases by 0 – 37 and non-cancer disease cases by 0 – 64 cases. The embedded human carcinogenicity was 0.2 – 5.3 cases and non-carcinogenic toxicity was 0.2 – 14.3 cases (or 8 – 199 Mg benzene-eq and 18 – 1,510 Gg toluene-eq by EPA units) depending on treatment technology and degree of treatment. Impacts from treating Cr(VI) using strong base anion exchange were 1% – 8% of those from treating by weak base anion exchange. Acidification and neutralization contributed 90% – 99% of the impacts for treatment options that required pH control. In scenarios where benefit were higher than burdens, tradeoffs still existed because benefits are experienced by a local population but the burdens are born externally where the materials and energy are produced, thus exporting the health risks. In scenarios where the

burdens were clearly higher than the benefits achieved, cost considerations may still drive choosing a detrimental treatment level or technology.

1. INTRODUCTION

Drinking water treatment has saved untold numbers of lives and is a hallmark of improving quality of life in developed and developing countries. Drinking water filtration and chlorination have been hailed as the most important public health intervention of the 20th century (Cutler and Miller 2004), and continued treatment of major contaminants that pose acute or chronic health risks is essential. However as science is able to detect and treat increasing numbers of water constituents at increasingly low concentrations, it is possible that diminishing returns in improvement of human health could be approached, and tradeoffs with production should be considered. Similarly to any processed product, treating drinking water requires materials and energy. Production of these materials exposes workers to hazards and emits pollutants with deleterious health effects. While the population consuming the treated water directly enjoys the health benefits of reduced pollutants in drinking water, an external population bears the health burden of producing the treated water.

While regulatory negotiations over new drinking water standards include balancing opportunities for measurably reducing public health risks against economic costs, overlooked has been the consideration of life cycle human health or ecosystem risks now foreseeable through life cycle assessment thinking and approaches. Here we examined how recent and potential future regulation by the United States Environmental Protection Agency (USEPA) of two inorganic chemicals requires built infrastructure, materials, and operational and maintenance activities. While treatment reduces health risk to the population served by the drinking water, burden of providing that treatment potentially relocates indirect human carcinogenic and non-carcinogenic health effects.

Here we focused on human health tradeoffs of treating water to regulatory limits (i.e. reducing exposure) against exposures from industrial chemicals required to fabricate and operate the treatment system. Potential ecosystem effects undoubtedly also occur, but were not the focus here to maintain directly comparable types of impacts between benefits and burdens.

The advent of life cycle assessment (LCA) has brought frameworks to examine environmental and social tradeoffs. The focus of most LCAs concerning water has been the embedded energy used in water supply pumping. Previous findings show that providing water from surface water sources requires 0.1 – 1.5 kW hr m^{-3} (Arpke and Hutzler 2006, Crettaz et al. 1999, Stokes and Horvath 2011) depending on supply distance and treatment complexity. Groundwater sources often have less embedded energy, depending on well depth (Plappally and Lienhard 2012). In either case, energy demand is often dominated (56 – 94%) by on-site or distribution pumping (Plappally and Lienhard 2012, Racoviceanu et al. 2007, Stokes and Horvath 2006). However, water supply and pumping energy is needed regardless of water quality. Here we focus on treatment options that are determined by pollutant concentrations. Some studies have focused on energy required for individual treatment processes, finding that chlorination demands 0.000021 – 0.003 kW hr m^{-3} (Burton 1996, Kroschwitz 1995), and coagulants such as alum or polymers demand 0.4 – 0.7 kW hr m^{-3} (Kroschwitz 1995, Tripathi 2007). Even these studies do not assess impacts associated with that energy demand. One study has compares human health risk to environmental impacts associated with nanofiltration (Ribera et al. 2014). This study is unique because it directly compares the embedded

human health burden to the human health benefit provided by a number of treatment options.

1.1 Background on Pollutants of Concern. Pentavalent arsenic (As(V)) and hexavalent chromium (Cr(VI)) were selected as model pollutants due to recent regulatory concern, common occurrence in groundwater, and treatment viability with wellhead sorbent systems. Vast epidemiological evidence connects As(V) intake from drinking water to cancer of the skin, bladder, kidney, lung, liver, and prostate (USEPA 2010b). Non-cancer effects from chronic exposure include hyperpigmentation, keratosis, burning eyes, leg swelling, liver fibrosis, and lung disease (Choong et al. 2007). In the United States, 12% of groundwater sources contain greater than 20 $\mu g\ L^{-1}$ arsenic (USEPA 2010b). The USEPA reduced the As(V) regulation from 50 to 10 $\mu g\ L^{-1}$, requiring compliance by 2006. Many treatment systems were installed around that time, and this study hopes to enlighten the overall human health impacts it might have had. As(V) in this analysis served as a retrospective evaluation of prior regulations.

Cr(VI) regulation in drinking water is currently 100 $\mu g\ L^{-1}$, but is under scrutiny and may be revised in the near future. Its analysis in this study therefore informs possible future regulation to consider the health burdens embedded in treatment. It is a known human carcinogen through inhalation exposure (USEPA 1998a), but updated toxicological study from ingestion has observed neoplasms in the small intestines of mice and tumors in the oral cavities of rats exposed at high doses of Cr(VI) (USEPA 2010a). Non-cancer gastrointestinal effects from chronic oral exposure include ulcers, diarrhea, abdominal pain, and vomiting (USEPA 2010a). The national occurrence of Cr(VI) is also being investigated under the USEPA Unregulated Contaminant Monitoring Rule

(UCMR3). As of summer 2015 (monitoring will continue through 2016), 5% of groundwater systems exceed 10 µg L^{-1} (USEPA 2015b). Levels up to 53 µg L^{-1} have been observed (Frey et al. 2004).

The most common As(V) wellhead treatment technique is sorption to metal oxides (MO), including ferric oxide/hydroxide and activated alumina (Choong et al. 2007). These demonstrate a high sorption capacity ranging from 280 – 3,900 µg g^{-1} (Bang et al. 2011, Lipps et al. 2010, Speitel Jr. et al. 2010, Westerhoff et al. 2005) even at low contaminant levels. They do not require pretreatment, but sorption capacity is increased at depressed pH (Choong et al. 2007). Various treatment technologies are being piloted and constructed to meet low level Cr(VI) regulations. Weak base anion exchange (WBAX) has very high affinity and very high removal capacity, ranging from 5,300 – 5,600 µg g^{-1} (McGuire et al. 2007, Najm et al. 2014). Achieving high sorption capacity requires acidifying the influent water to pH 6 (Brandhuber et al. 2004b, McGuire et al. 2007, Najm et al. 2014). Acidification can be achieved by dosing with chemical acids or infusing carbon dioxide (Najm et al. 2014). Both MO and WBAX sorbents are generally single-use, requiring disposal after exhaustion. Strong Base Anion Exchange (SBAX) is another common Cr(VI) treatment option that does not require acidification but shows much lower affinity. Sorbent capacity ranges from 110 to 2,800 µg g^{-1} (Brandhuber et al. 2004b, McGuire et al. 2007, Najm et al. 2014), but is limited by nitrate and sulfate levels more than Cr(VI) levels. SBAX can be regenerated using strong salt solution for multiple reuses (Najm et al. 2014). Both As(V) and Cr(VI) can be treated by other technologies (such as coagulation, membrane filtration, or precipitation), but they are operationally

more difficult in a wellhead situation and more expensive for small systems where specialized operators and solid waste handling may be unavailable (Najm et al. 2014).

1.2 Study Area. As(V) regulations have heavily impacted small groundwater systems which prior only provided chlorine disinfection treatment (Impellitteri et al. 2007). Because As(V) and Cr(VI) often occur in groundwater, a representative groundwater system consisting of well head treatment producing 1,000 gal min^{-1} was selected for this study. This would be about the largest size system that would use wellhead treatment for a single pollutant. An example of such systems are wells utilized by the water district serving Palm Springs, California, USA. As(V) and Cr(VI) are common in groundwater there, wellhead treatment is a potentially viable option for a single inorganic pollutant, and California more rigidly regulates Cr(VI) at 10 μg L^{-1} (CCR 2014). The district includes 96 wells serving 320,000 people with 100 million gallons of water daily (CVWD 2014), indicating each well serves on average 3,200 people with 1,000 gal min^{-1}. Palm Springs is illustrational but results are not confined to that area, and are indeed intended to have national relevance.

1.3 Roadmap and Goal. The shifting human health impacts due to drinking water treatment were assessed in a three step process. First, life cycle assessment was used to estimate risks embedded in the production, use, and disposal of materials needed to treat drinking water. Second, benefits of treating drinking water were estimated using dose response curves. Third, the burdens and benefits were compared.

In order to make these comparisons, the entire process was carried out in two parallel methodologies; one, those developed by USEPA, and two, those developed by UNEP/SETAC USEtox. Both provided a valid and widely accepted set of consistent units

within which to describe human health impacts. Under USEPA, the embedded risks were described using TRACI (USEPA 2014) and dose-response curves were developed using information from IRIS (USEPA 2015a). Under USEtox (Hauschild et al. 2008, Rosenbaum et al. 2008), dose-response curves were developed using information from the Inorganic Database.

The goal is to explore human health tradeoffs of treating water to regulatory limits by 1) comparing the magnitude of health benefits against embedded burdens, 2) studying how these tradeoffs change with varying levels of treatment for a contaminant that has been regulated and another that may be in the near future, and 3) identifying what processes or practices may mitigate the risks.

2. METHODOLOGY

2.1 Life Cycle Assessment. The functional unit was 25 billion gallons (93 billion liters) of water treated to an acceptable quality over the period of 70 years. This was equivalent to the demand of 3,200 people each using 300 gallons per day, consistent with average single-well population and demand in Palm Springs (CVWD 2014). The total flow rate is 670 gallons per minute (1 million gallons per day). All withdrawn water was treated although human consumption averages only 2 liters per day.

The system boundary is depicted in Figure 7.1. It included materials and energy required for wellhead treatment to comply with As(V) or Cr(VI) regulation, including sorbent, energy to pump water through the packed bed, chemicals to adjust pH or regenerate the sorbent, energy to transport the sorbents and chemicals to the site, and storage tanks for the sorbents and chemicals. It excluded energy and infrastructure

associated with water supply or distribution, and chemicals required for disinfection, which are required independently of the Cr(VI) or As(V) treatment.

Influent concentration of either Cr(VI) or As(V) was assumed to be 20 μg L^{-1} unless stated otherwise. Other assumed influent water quality parameters were representative of groundwaters in southern California, including pH 8, 200 mg L^{-1} as $CaCO_3$ alkalinity, 5 mg L^{-1} nitrate-N, and 33 mg L^{-1} sulfate. The regulated effluent maximum contaminant level (MCL) was 10 μg L^{-1} unless stated otherwise, consistent with USEPA and WHO recommendations for As(V) in drinking water. The treatment goal was set as 80% of the regulatory level, or 8 μg L^{-1}. The treatment goal was met by treating portion of the total flow and bypassing portion such that the blended final quality met the treatment goal. Further details can be found in the Supplemental Information.

Three treatment scenarios were considered as summarized in Table 7.1. Scenario 1 treated Cr(VI) using WBAX, Scenario 2 treated Cr(VI) using SBAX, and Scenario 3 treated As(V) using a MO sorbent. Sub-scenarios were also considered with different methods of pH control. Scenario 1A acidified with hydrochloric acid (HCL) and neutralized with sodium hydroxide (NaOH), Scenario 1B acidified using sulfuric acid (H_2SO_4) and neutralized with lime ($Ca(OH)_2$), and scenario 1C acidified using carbon dioxide (CO_2) and neutralized by air stripping. These sub-scenarios are employed to mitigate scenario uncertainty because pH control chemicals are later found to be critical drivers of final results.

The foreground inventory (quantities of materials and energy directly required to produce the functional unit) for each of the three scenarios was developed using assumptions and methods detailed in the Supplemental Information. It includes sorbent

mass based on published pollutant capacity, oversea and overland transport of the sorbent, energy to overcome packed bed headloss, chemicals to reduce the pH to 6 before treatment and back up to 8 after treatment at doses consistent with assumed water quality, and overland transport of the pH control chemicals. Inventory development followed an approach developed for a Cr(VI) treatment cost estimate (Najm et al. 2014). Background inventory was provided by the EcoInvent database, and its data uncertainty was explored as described below.

2.1.1 Impact Assessment. Impact assessment converted inventory items into human health midpoints that could be added and compared. It used conversion factors of embedded human health impacts for common products and processes. These impact factors were taken from EcoInvent v2.2 (SCLCI 2010) and were matched to inventory items identified in this study. Impact factors converted to both EPA TRACI (USEPA 2014) (in units of benzene or toluene equivalents) and USEtox (Hauschild et al. 2008, Rosenbaum et al. 2008) (in units of cases). Discussion of matching impact factors available in EcoInvent to the identified inventory, as well as developing a few custom impact factors to explore inventory uncertainty, is included in the Supplemental Information.

2.1.2. Uncertainty and Sensitivity. Uncertainty in the LCA model includes data uncertainty and model uncertainty. Data uncertainty is associated with input parameters such as inventory (if the background energy and materials used to produce the primary inventory items adequately capture upstream processes) and impact assessment (if the point value impact factors are representative). These stem from temporal and geographical variations in processes, as well as technological advancements. Model

uncertainty includes variations in design constraints such as influent water quality, and limitations due to the calculation method that assume linear responses and rely on a published database in lieu of a directly observed facility.

In an effort to mitigate data and model uncertainty, extensive sensitivity analysis was carried out to explore which inputs and assumptions significantly influence final results and to what degree. Inventory sensitivity is explored by observing the change in final impacts due to varying the assumed influent water alkalinity, background nitrate and sulfate levels, sorbent capacities, influent pollutant concentrations, and treatment target. Impact assessment sensitivity is explored by observing the change in final total impacts by using different impact factors for the chemical storage tank, the anion exchange resin, and the size and emission levels of the overland delivery truck.

Uncertainty in the inventory and impact assessment was then mitigated through analyzing multiple scenarios for the inputs deemed to have the largest sensitivity. This was intended to give a range of variability in the life cycle assessment results. As pH control chemicals were later found to be the largest drivers of results, multiple pH control scenarios were analyzed.

Another way to mitigate inventory data uncertainty is to perform data distribution analysis by qualitatively assessing the reliability of the data and using empirical relationships to determine a distribution of data to use instead of relying on the published point values. This was not performed directly for this study, but was performed for a similar study (Chapter 6) that found impact factors could have a squared geometric standard deviation (GSD^2) of one to three. Final results could therefore vary by a factor

of 2 or 3 within a 95% confidence interval. Results of this study should be similarly interpreted.

2.2 Health Benefits of Treating Drinking Water. Dose-response relationships projected the human health benefit of lowering the drinking water pollutant concentration. This was done using both USEtox (Hauschild et al. 2008, Rosenbaum et al. 2008) and USEPA IRIS (USEPA 2015a) methodologies for ready comparison to the embedded human health burden estimated in the life cycle assessment results. Both of these calculated the estimated number of cases for cancer and non-cancer separately. For either methodology, the human health benefit from treating drinking water was calculated as the difference between the number of cancer or non-cancer cases expected at the influent concentration minus the number of cases expected at the MCL (not the treatment goal concentration).

2.2.1 Using USEtox. Human adult cancer and non-cancer cases associated with chronic ingestion of different concentrations of As(V) and Cr(VI) in drinking water were estimated under the USEtox methodology using the corresponding Human Health Effect Factor from the Inorganics Database 1.00 (Hauschild et al. 2008, Rosenbaum et al. 2008). The Effect Factor (in disease cases per kg lifetime intake) is used instead of the more typical Characterization Factor (in disease cases per kg emitted to the environment) because all of the pollutant in drinking water is being ingested. This is the same as setting the Intake Fraction to 100%. The cancer and non-cancer effect factors for As(V) are 0.52 and 39 cases kg^{-1} ingested respectively, and for Cr(VI) are 23 and 0.051 cases kg^{-1} ingested respectively (Hauschild et al. 2008, Rosenbaum et al. 2008). Uncertainty associated with human health factors for contaminants in freshwater have a GSD^2 of 215

(Rosenbaum et al. 2008). Another study found the GSD^2 for As(V) cancer response to be 3,025 and noncancer response to be 1,936, with the Cr(VI) cancer response to be 3,249 and noncancer response to be 15,876 (Huijbregts et al. 2005). This means response results can vary from one to two orders of magnitude above and below the calculated mean.

First, the lifetime mass of pollutant ingested per person was estimated by the product of the daily drinking water intake, the pollutant concentration, and the lifespan. Standard EPA assumptions (Hammer and Hammer Jr. 2011) of 2 L day^{-1} intake and 70 year $person^{-1}$ lifetime were applied to yield:

$$M_{ing} = 5.11 * 10^{-5} * C \quad (5)$$

where M_{ing} was the lifetime mass of pollutant ingested (kg $person^{-1}$), the factor was in (L kg $person^{-1}$ μg^{-1}), and C was the concentration of pollutant in drinking water in ($\mu g\ L^{-1}$).

The number of cancer or non-cancer disease cases was then estimated by:

$$DC = EF * M_{ing} * N_{pop} \quad (6)$$

where DC was the number of disease cases (cases), EF was the cancer or non-cancer effect factor (cases $kg_{ingested}^{-1}$), M_{ing} was the mass ingested (kg $person^{-1}$), and N_{pop} was the population (3,200 people).

2.2.2 Using IRIS. Human adult cancer cases associated with chronic ingestion of contaminants in drinking water were estimated using the drinking water unit risk published in units of cases L μg^{-1}. The cancer drinking water unit risk for As(V) is 0.00005 cases L μg^{-1} (USEPA 1998b), and for Cr(VI) is 0 (non-carcinogenic) (USEPA 1998a). Updated draft toxicological studies were released in 2010 that increased the estimated carcinogenicity for each of these contaminants, but have not yet been officially

adopted. The new, unofficial drinking water unit risk for As(V) is 0.00073 cases L μg^{-1} (USEPA 2010b) and for Cr(VI) is 0.000014 cases L μg^{-1} (USEPA 2010a). Analysis was carried out using both the official 1998 and the unofficial 2010 unit risk, while understanding that the 2010 estimates are more conservative. Both sets of data are reported to include uncertainty spanning at least an order of magnitude.

The number of cancer cases was estimated by:

$$DC = UR * C * N_{pop} \quad (7)$$

where DC was the number of disease cases (cases), UR was the unit risk (cases L μg^{-1}), C was the drinking water pollutant concentration ($\mu g\ L^{-1}$), and N_{pop} was the population (3,200 people).

IRIS does not publish dose-response information for human non-cancer cases. IRIS does publish a reference dose, which is the threshold dose below which no adverse toxic endpoint is expected, including a safety factor often an order of magnitude or more. It also publishes the No Observable Adverse Effect Level (NOAEL), which represents the highest experimental dose in previous studies for which no non-cancer effects were observed. The official As(V) reference dose and NOAEL are 0.003 mg kg^{-1} day^{-1} and 0.008 mg kg^{-1} day^{-1} respectively (USEPA 1998b). These values are the same in the updated draft toxicology report (USEPA 2010b). The official Cr(VI) reference dose and NOAEL are 0.003 mg kg^{-1} day^{-1} and 2.5 mg kg^{-1} day^{-1} respectively (USEPA 1998a). The updated draft values are 0.0009 mg kg^{-1} day^{-1} and 0.09 mg kg^{-1} day^{-1} respectively (USEPA 2010a), demonstrating higher toxicity and lower uncertainty factors.

In order to construct a dose-response relationship, the NOAEL was first converted to an Effective Dose-50 (ED50). The ED50 is the dose for which 50% of the exposed

population will demonstrate a non-cancer toxic effect. It was estimated by multiplying the published NOAEL by a factor of 9 (Hauschild et al. 2008, Rosenbaum et al. 2008). Next, the reference dose was converted to equivalent drinking water concentration using:

$$DWEL = 1000 * \frac{RfD * M_{body}}{DWI} \quad (7)$$

where DWEL is the drinking water equivalent level (μg L^{-1}), RfD was the reference dose (mg kg^{-1} day^{-1}), M_{body} was the body mass (70 kg)(Hammer and Hammer Jr. 2011), and DWI is the drinking water intake (2 L day^{-1}). The ED50 was also converted to a DWEL using the above equation but substituting ED50 for the RfD. Finally, a dose-response relationship was estimated as zero non-cancer cases between zero exposure up to the DWEL for the reference dose. It then linearly interpolates up to half of the population potentially being affected at the DWEL for ED50.

The calculated human health benefits by USEtox or by IRIS, as well as the LCA burdens, were interpreted as maximum potentials (i.e. worst case scenario). In each case, uncertainty in the underlying data spanned at least an order of magnitude (USEPA 2015a, Rosenbaum et al. 2008), and results were similarly interpreted.

3. RESULTS

Result depicting the shifting human health impacts due to drinking water treatment are presented by; first, estimation of human health risks embedded in drinking water treatment scenarios from life cycle assessment; second, assessment of the benefits of drinking treated water developed through dose response curves; and third, comparison of the burdens and benefits.

3.1 Human Health Burden Embedded in Treating Water. Table 7.2 shows a detailed inventory of items required to treat drinking water, the matched impact factors, and equivalent human health impacts summed for Scenario 1A. SI Tables 7.2 – 7.6 are similar tables for the other scenarios. Figure 7.2 shows the life cycle human health impacts embedded in treating water from 20 μg L^{-1} Cr(VI) or As(V) to 8 μg L^{-1} (80% of a 10 μg L^{-1} regulatory limit) for all scenarios.

Under TRACI methodology, human carcinogenicity ranged from 8 – 199 Mg benzene-eq depending on the treatment scenario (defined in Table 7.1), and non-cancer toxicity was 18 – 1,510 Gg toluene-eq. With USEtox methodology, carcinogenicity was 0.2 – 5.3 cases and non-cancer toxicity was 0.2 – 14.3 cases. In all treatment scenarios, treating Cr(VI) by SBAX had the lowest impacts in all categories. Treating Cr(VI) by WBAX with sulfuric acid and lime had the highest impacts in terms of TRACI carcinogencity, TRACI non-cancer toxicity, and USEtox. Treating As(V) by MO with hydrochloric acid and sodium hydroxide had the highest impacts for USEtox non-cancer toxicity.

Comparing results for treating Cr(VI), treatment by SBAX had significantly lower human health impacts than by WBAX. SBAX treatment impacts were only 1% – 8% of those from WBAX depending on pH control strategy. This is statistically significant compared to the expected uncertainty of a factor of 2 – 3 for the 95% confidence interval. If using WBAX and comparing pH control strategies, carbon dioxide with air stripping had the lowest human health impacts by a factor of 1 – 7. Sulfuric acid with lime had the highest TRACI carcinogenicity, USEtox carcinogenicity, and TRACI non-cancer toxicity potentials. Hydrochloric acid with sodium hydroxide had the highest USEtox non-

carcinogen toxicity potential. Comparing results for treating As(V), adding pH control to the MO sorbent system increased sorbent capacity by a factor of 1.5, but increased the human health impacts by a factor of 7.5 – 13 depending on category.

3.1.1 Critical Contributions to Impacts. Impacts associated with individual inventory items were analyzed to identify the largest contributors to the total impacts associated with each scenario. Inventory items were also grouped by treatment process (sorption, acidification, neutralization, regeneration, or headloss pumping) and illustrated by striping within each bar in Figure 7.2.

The production of pH control chemicals dominated human health impacts for scenarios that include it. Production of hydrochloric acid contributed 46% - 59% of the total impacts for scenario 1A, followed by sodium hydroxide with 35% - 53%. For scenario 1B, lime was responsible for 46 - 97% of the impacts and sulfuric acid was 3% - 50%. For scenario 1C, 56% - 73% of the impacts came from producing carbon dioxide. Electricity generation for neutralization by the blower and the repressurization pump then accounted for 21% - 38% of the impacts. For scenario 3A, acid production contributed 44% - 56% of the impacts and the production of caustic contributed 33% - 51%. The sorption process and headloss pumping each contributed less than 7% of the impacts in each of these scenarios.

For treating Cr(VI) by SBAX (scenario 2), energy production for pumping to overcome packed bed headloss contributed 39% to 61% of the total human health impact. Production of salt for regeneration contributed 34% - 53%, and the sorption process contributed 4% - 10%. When treating As(V) by MO without pH control (scenario 3B),

impacts from sorption comprised 73% - 93% of the total. Headloss pumping contributed the remaining 7% - 25%.

3.1.2 Model Sensitivity. Model sensitivity was explored by changing inputs and observing the final results to mitigate uncertainty by illustrating the range of variability in the results. Additionally it identified critical treatment choices, allowed results to be adapted for various water quality situations, and informed various future possible regulations. Sensitivity relationships are shown in SI Figure 7.1.

The model showed the greatest sensitivity to selection of pH control method, which is why sub-scenarios for each method were developed. When treating Cr(VI) by WBAX, acidification by sulfuric acid in lieu of hydrochloric acid reduced the final results by 30% – 40%, except for in USEtox carcinogenicity which increased by 3%. Acidification by carbon dioxide decreased overall results by 4% – 32%, except for TRACI carcinogenicity which increased by 19%. Neutralization by lime instead of sodium hydroxide increased results by 73% – 490%, except for USEtox non-cancer toxicity which was reduced by 38%. Neutralization by air stripping reduced results by 11% – 48%. The effect of changing pH control chemicals was not specifically explored in the As(V) removal by MO scenario since similar effects were expected as the changes observed in treating Cr(VI) by WBAX.

The assumed influent pollutant level highly affected the final human health impact results by changing the fraction of water to be treated. If the influent level was reduced to 15 $\mu g\ L^{-1}$, the results reduced by 19% – 22%. If reduced to 10 $\mu g\ L^{-1}$, the results were reduced by 59% – 66%. If the influent level was raised to 30 $\mu g\ L^{-1}$, the results increased by 18% – 25%.

The regulated effluent contaminant level (MCL) had strong influence on the results for all scenarios. A low MCL (requiring more treatment) of 5 $\mu g\ L^{-1}$ increased the impacts by 27% - 33%. A very low MCL of 1 $\mu g\ L^{-1}$ increased the impacts by 43% - 58%. A high MCL (requiring less treatment) of 15 $\mu g\ L^{-1}$ decreased the impacts by 27% - 33%. A very high MCL of 20 $\mu g\ L^{-1}$ decreased the impacts by 49% - 67%. The studied range of MCL from 1 to 20 $\mu g\ L^{-1}$ encompassed 27 to 6 USEtox total disease cases embedded in treating Cr(VI) by WBAX, 0.6 to 0.1 cases for treating Cr(VI) by SBAX, and 28 to 6 cases for treating As(V) by MO.

The other inputs with strong influence on results were the water alkalinity and the nitrate/sulfate levels. High influent levels could cause prohibitively high human health impacts. Other inputs had little effect on final results. The assumed sorbent capacity caused only small changes since its impacts were small compared to pH control chemicals. Similarly, the custom impact factor used for anion exchange resin had only a slight increase in this study, but could have a large impact in other studies where sorbent impacts drive results. The choice of truck size, truck engine emission standard, and chemical storage tank selection were each inconsequential to final results. Each of these observations is further developed in the SI.

3.2 Health Benefits of Reducing Pollutant Concentrations in Drinking Water. The purpose of developing dose response relationships was to estimate the human health benefit of changing the pollutant concentration in drinking water. Figure 7.3 shows potential cancer and non-cancer cases expected in the study population of 3,200 people using both EPA IRIS and USEtox methodology. For the IRIS data, results are displayed using both the 1998 official data and the updated 2010 draft data. Numeric descriptions

of each relationship are given in the SI, along with an equation and coefficients to calculate human health risk from drinking water containing Cr(VI) or As(V) for any size population. Calculated responses are mean values with 95% confidence intervals one to two orders of magnitude above and below.

Reducing As(V) concentration in drinking water from 20 $\mu g\ L^{-1}$ to 10 $\mu g\ L^{-1}$ changed the potential cancer cases in the exposed population from 47 to 23 cases by the 2010 IRIS relationship, a reduction of 24 cases. The number of potential non-cancer disease cases changed from 63 to zero. Using the 1998 IRIS relationship, the number of potential cancer cases reduced by 1 and the non-cancer toxicity cases reduced by 63. By USEtox methodology, the benefit was 1 cancer and 64 non-cancer cases.

The human health benefit of treating Cr(VI) from 20 $\mu g\ L^{-1}$ to 10 $\mu g\ L^{-1}$ was 1 cancer case and zero non-cancer cases by the 2010 IRIS relationship. By the 1998 IRIS relationship, zero cases were expected from these exposures and therefore zero were saved through treatment. However, USEtox relationships indicated that 37 cancer cases would be saved, with zero non-cancer cases expected at these exposures.

3.3 Comparing Benefits to Burdens. By reducing the contaminant level in drinking water, fewer disease cases occurred and thus increased the health benefit for the served population. However, greater level of treatment was also required so the embedded health burden also increased for the external population. Figure 7.4 shows this tradeoff for a range of possible Cr(VI) treatment levels, and Figure 7.5 shows the tradeoff for As(V), both using USEtox methodology. Corresponding figures using EPA methodology are found in SI Figures 7.2 and 7.3. These figures assumed 20 $\mu g\ L^{-1}$ pollutant in the influent, and increase the level of treatment (which is equivalent to

decreasing the regulatory level, i.e. the MCL) moving toward the right. In each case, results are shown for cancer effects and non-cancer effects separately, but both impacts would be incurred simultaneously. Health benefits were calculated by the difference in disease cases expected at the influent level and the MCL, while treatment burdens were the impacts required to treat from the influent level to 80% of the MCL to ensure compliance. All results are reported with 95% confidence spanning an order of magnitude above and below.

Figure 7.4 indicates that cancer benefit of treating Cr(VI) was an order of magnitude higher than cancer burden at nearly all MCL concentrations, but that non-cancer burden was an order of magnitude higher than non-cancer benefit at all MCLs. For example, with USEtox methodology treating Cr(VI) from 20 $\mu g\ L^{-1}$ to 10 $\mu g\ L^{-1}$ prevents 37 cancer cases and 0.1 non-cancer disease cases. However the impact of treatment from added facilities caused 3 – 5 cancer cases and 3 – 14 non-cancer disease cases if treating by WBAX depending on pH control method, or 0.2 cancer cases plus 0.2 non-cancer disease cases if treating by SBAX. SI Figure 7.2, using EPA methodology, shows treating Cr(VI) from 20 $\mu g\ L^{-1}$ to meet a 10 $\mu g\ L^{-1}$ MCL saved zero cases of cancer by the official 1998 IRIS data and 0.5 cases by the draft 2010 data, and zero non-cancer disease cases by either dataset. This came at an embedded life cycle health burden of 120 – 199 Mg benzene-eq and 226 – 1,510 Gg toluene-eq if treating by WBAX depending on pH control method, or 8.21 Mg benzene-eq and 17.9 Gg toluene-eq if treating by SBAX.

For As(V) treatment, Figure 7.5 shows cancer burden was higher than benefit if pH control was used under USEtox methodology. Without pH control, an MCL of 20 $\mu g\ L^{-1}$ would have a higher cancer burden than benefit, but the cancer benefit rose more

quickly relative to the burden such that a break-even point existed between 15 and 20 µg L^{-1} below which the benefit was higher than the burden. The non-cancer benefit was very large compared to the cancer benefit on a basis of number of cases and was higher than the non-cancer burden at nearly all concentrations. For example, treating As(V) from 20 µg L^{-1} to 10 µg L^{-1} avoided 1 cancer case and 63 non-cancer disease cases. This caused 3 cancer cases and 14 non-cancer disease cases if treating by MO with pH control, or 0.4 cancer cases with 1 non-cancer disease case if treating by MO without pH control. SI Figure 7.3 shows that cancer and non-cancer benefits had a more similar magnitude under EPA methodology. Treating As(V) from 20 µg L^{-1} down to meet a 10 µg L^{-1} MCL saved 2 cases of cancer by the official 1998 IRIS data and 23 cases by the draft 2010 data. It additionally saved 63 non-cancer disease cases by either dataset. This came at an embedded life cycle health burden of 126 Mg benzene-eq and 287 Gg toluene-eq if treating by MO with pH control or 16.5 Mg benzene-eq and 34.8 Gg toluene-eq if treating by MO without pH control.

4. DISCUSSION

Quantitatively comparing the benefits of a population consuming treated water to the health burdens embedded in providing that treatment can yield results where the benefits seemingly outweigh the burdens, or where the burdens outweigh the benefits. However the implications of tradeoffs involved in either scenario may be more far-reaching than a simple ratio.

4.1 Net Benefits Export Disease. Treating Cr(VI) benefits a greater number of cancer cases than the number of non-cancer cases the treatment causes under USEtox

(Figure 7.4). The benefit ratio (number of cancer or non-cancer cases saved over the number of cancer or non-cancer cases caused, with values over 1 indicating net benefit) ranges from 2 – 12 for WBAX and is 185 for SBAX. This superficially indicates that treatment is well warranted from an overall human health standpoint. However, consideration should also be given to the fact that the population benefiting is separate from the population being burdened.

The benefits of treating water are realized locally, i.e. directly by the population being served by the water treatment system (e.g. the residents of Palm Springs). The disease cases being saved would have been dispersed throughout a large population, more likely encompassing diverse socio-economic groups. Comparatively, the embedded burdens are borne by external parties in geographically separate locations. These health risks are given to workers at the material or energy production plants (e.g. acid or caustic production in Los Angeles or Houston) and nearby neighbors within influence of the plant emissions. These are more likely low-income low-skill laborers, resulting in concentrating disease among blue-collar laborers. Health care may be harder to find or pay for and lost work has a higher impact to this subpopulation. Installing treatment to meet regulations at any level therefore relocates cancer and non-cancer disease risk. It is transferred and concentrated from a large population with a disperse disease risk to a smaller sub-population with direct exposure now carrying a disproportionate share of health risk. This scenario presents an ethical dilemma for regulators deciding on drinking water regulations. On a national scale, the detriments involved with producing extra materials and energy for treatment must be weighed against the benefits gained by

treating water. Current regulation methodology considers cost of treatment but not the human health burden.

As(V) treatment by USEtox indicates a benefit ratio of 3 – 60 (Figure 7.5). However a significant shift in the type of potential disease is incurred through treatment. Reducing As(V) concentrations prevents many potential non-cancer cases, but the removal causes some cancer cases. The legislation regulating As(V) in 2006 may therefore have had the net effect of reducing the total number of disease cases, but came at the side effect of increasing the incidence of cancer. The number of cases itself says nothing of lethality, but it is likely that society values cancer and noncancer cases differently, perhaps to the point of preferring to prevent any occurrence of cancer even if it means incurring non-cancer disease by not treating water.

4.2 Cost Drives Incurring Net Burden. In some cases the burden of treatment clearly outweighs the benefit from a total human health perspective. It might seem clear that requiring treatment in this situation is not merited. However, cost and familiarity are two reasons this might be done anyway. For example, the embedded cancer in As(V) treatment using MO with pH control (Scenario 3A) is much higher than the health benefit using USEtox (Figure 7.5A) and the official EPA (SI Figure 7.3A). This indicates that avoiding pH control (Scenario 3B) is a far superior choice. However, the cost of media replacement is often responsible for more than 90% of the operational cost of an As(V) wellhead sorbent system (Lipps et al. 2010). Maximizing sorbent capacity to minimize replacement is considered a cost-savings maneuver. Therefore decision makers would be forced to choose between cost and overall health risk.

Tradeoffs between cost and overall health benefit is also seen in comparing Cr(VI) pH control scenarios. Using CO_2 with air stripping (Scenario 1C) nearly always had lower human health impact than using either type of acid or caustic (Figure 7.4, SI Figure 7.2). However, pH control using HCl with NaOH is cheaper than CO_2 with air stripping for systems smaller than 1000 gpm (Najm et al. 2014), not to mention the environmental impacts of the chemicals are three to seven times higher (Choe et al. 2015).

In another example, Cr(VI) treatment using EPA methodology appears to have very little benefit compared to the caused burden (SI Figure 7.2). A benefit ratio cannot be calculated since benefits and burdens are not expressed in the same units, but only 0 – 1 potential cases can be saved while incurring burdens on the order of Mg-benzene equivalents and Gg-toluene equivalents. This presents an ethical dilemma on a local scale. Local decision makers could see that benefits of higher water treatment are realized within the local area by neighbors, friends, and voting constituents. While the detriments incurred due to imposing treatment are real, they are exported to unknown factory workers located far away. It may be unlikely that the local populous would be willing to forgo treatment and therefore incur a few more disease cases locally in order to save a few more cases for faceless entities elsewhere in the world.

The Cr(VI) MCL is currently under review by the EPA, and this study informs considerations beyond only cost, occurrence, and direct toxicity. USEtox results suggest that low MCLs have high cancer benefit relative to cancer burden (Figure 7.4A), but also has high non-cancer disease burden with very little non-cancer disease benefit. Results from EPA data only prescribe treatment at any MCL if the 2010 draft cancer toxicology

report is adopted, as there is neither cancer nor any non-cancer benefit by the 1998 official data. Even with the updated data, the number of benefit cases is very small and requires incurring a great deal of embedded cancer and non-cancer risk.

4.3 Health Impacts of pH Control Chemicals. The production methods of pH control methods are briefly reviewed to explore where and how the embedded health risks may be occurring. HCl is co-produced by chlorinating dichloromethane or trichloroethylene. Air emissions are primarily from combustion of coal, but also from volatilized HCl, chlorine, and chlorinated organic compounds escaping the purification system (USEPA 1995). Sulfuric acid is produced by combusting elemental sulfur, catalytically oxidizing it, then absorbing it into acid. Air emissions are sulfur dioxide from all unconverted sulfur (USEPA 1995). Lime is a product of high temperature calcination of limestone. Air emissions are primarily particulate matter from crushing limestone, but include combustion gasses in the kiln such as carbon monoxide, carbon dioxide, sulfur dioxide, and nitrogen oxide (USEPA 1995). Water treatment using lime has a high average embedded energy of 0.42 kWh m^{-3} (Kroschwitz 1995).

Since most emissions associated with production of chemicals required for pH control in water treatment are airborne, the exposed parties are likely workers at the production facilities and downwind neighbors. Practices to mitigate human health risks embedded in water treatment therefore include reducing worker inhalation and improving plant air emission standards.

4.4 Comparison to Previous Studies. Some studies have found that treatment chemicals contribute only 6 – 10% of total impacts (Arpke and Hutzler 2006, Crettaz et al. 1999, Racoviceanu et al. 2007), and construction and disposal of treatment facilities

contributes 4 – 9% (Raluy et al. 2005, Stokes and Horvath 2006). However, another found energy used by material production for treatment chemicals to be as high as 37%. Manufacturing treatment chemicals is the largest part (73%) of that material production (Stokes and Horvath 2011). The treatment phase contributes 42% – 44% of water treatment impacts (Crettaz et al. 1999, Stokes and Horvath 2011). The corresponding supply phase contributes 21% – 38%.

4.5 Conclusions. Current drinking water contaminant regulations do not consider embedded life cycle health risks. Imposing regulatory limits will save some number of health cases, but will also cause a non-trivial level of health burden associated with increased production of materials and energy required for additional treatment to meet the regulation. The degree of this burden depends on treatment technology choices and level of required treatment. For example, water treatment technologies that do not depend on pH control are likely to have significantly less embedded human health burden than those that do.

Furthermore these detriments are likely not carried by the same populace that experiences the benefits since the materials and energy are not typically produced in the same location where the treated water is consumed. Installing treatment to meet regulations at any level therefore exports cancer and non-cancer disease risk. It is transferred from a large population with a disperse disease risk to a concentrated sub-population with direct exposure.

It may also shift the type of disease expressed between cancer and non-cancer. Evaluating prior legislation regulating As(V) in drinking water suggests implementing the rule may have had the net effect of reducing the total number of disease cases, but

came at the side effect of increasing the incidence of cancer cases. Potential new Cr(VI) regulation can only be justified if the draft 2010 toxicology report is adopted. Even then, imposing a low Cr(VI) MCL may have the effect of shifting toxicity expression from cancer to noncancer cases.

Unfortunately stakeholders may be incentivized to choose treatment options that produce a net health detriment. One reason could be due to cost-savings. For example, adding pH control would increase sorbent capacity and reduce replacement costs but increase embedded health risks. Another reason is familiarity. The exported risks transcend local geopolitical boundaries, but treatment decisions are made locally and would favor friends and neighbors over far away strangers. Therefore regional or national policies must be responsible to consider the life cycle burden along with the benefit. These policies may concern the allowable level of contaminant in drinking water, acceptable treatment strategies, workplace exposures in chemical production facilities, and airborne emission standards. Balancing all of these tradeoffs queries values such as who should bear the health risk, what type of disease should be incurred, and how much money one's health is worth.

5. ACKNOWLEGEMENTS

Funding for this study has been provided by the United States Environmental Protection Agency under EPA-F2013-STAR-E1 Graduate Fellowship for Environmental Studies, and the Dr. Ronald and Sharon Thomas Graduate Fellowship.

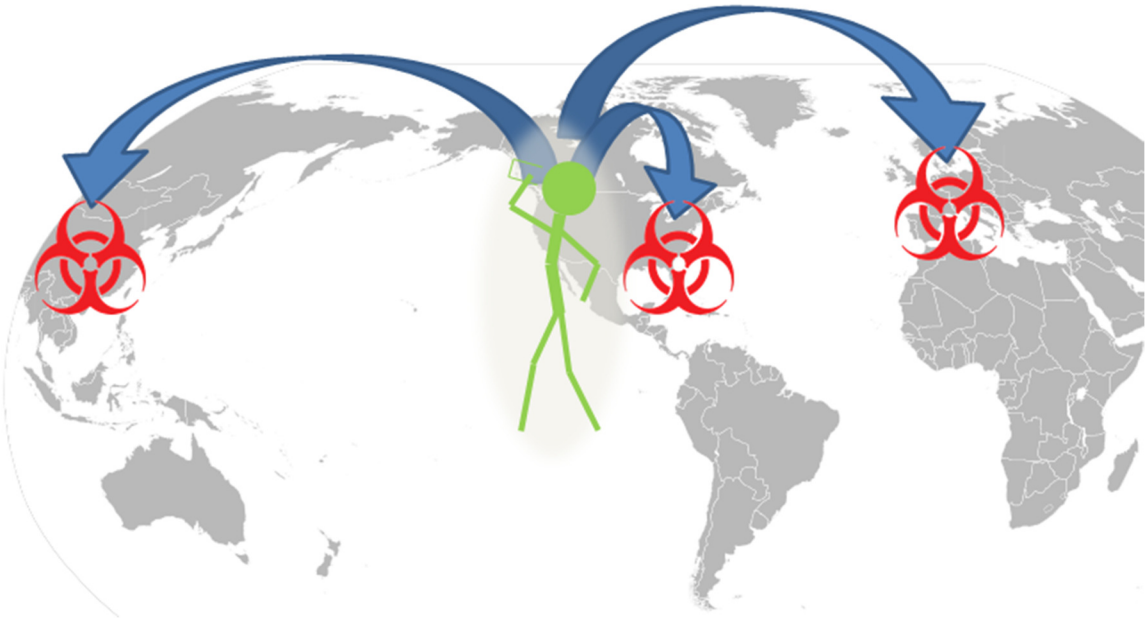

Figure 7.0. Graphical Abstract.

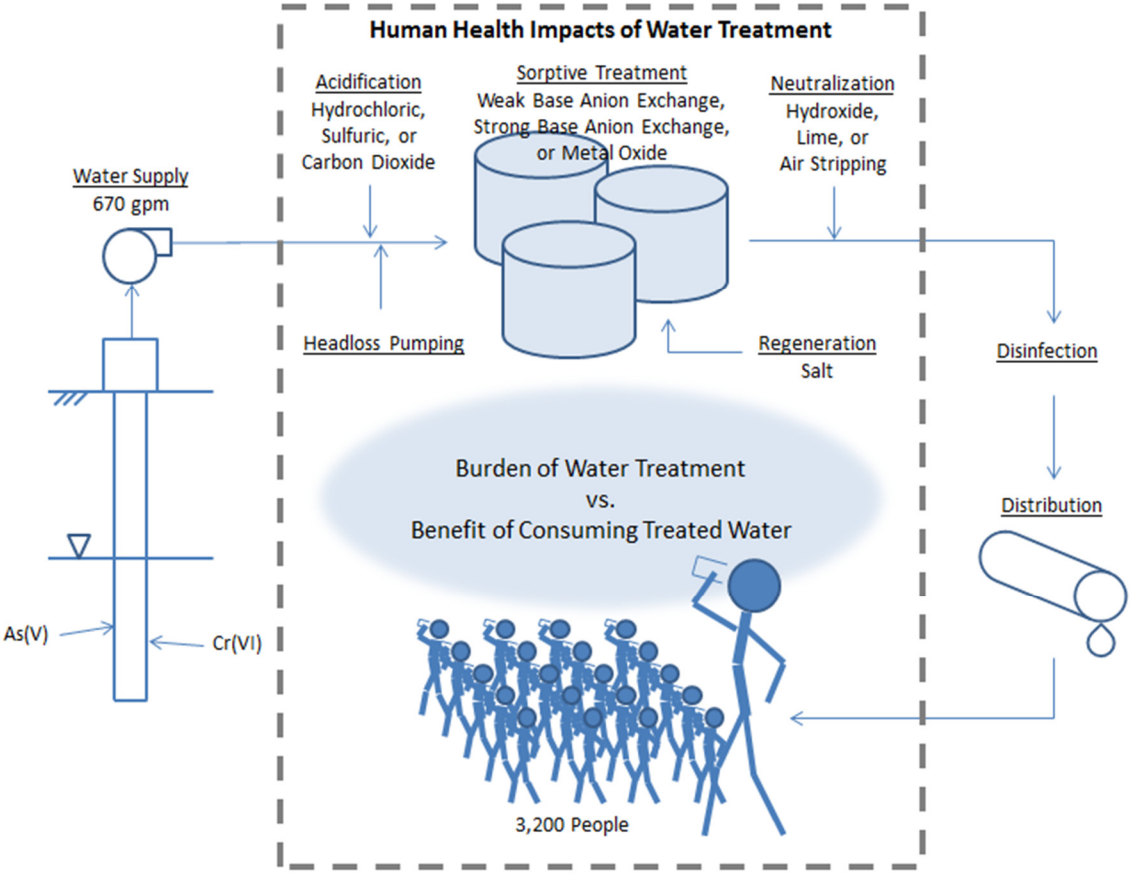

Figure 7.1. System Boundary Diagram.

Scenario	Pollutant	Sorbent	Regeneration	Acidification	Neutralization
1A	Cr(VI)	WBAX	-	HCl	NaOH
1B	Cr(VI)	WBAX	-	H_2SO_4	$Ca(OH)_2$
1C	Cr(VI)	WBAX	-	CO_2	Air Stripping
2	Cr(VI)	SBAX	NaCl	-	-
3A	As(V)	MO	-	HCL	NaOH
3B	As(V)	MO	-	-	-

Table 7.1. Scenario Definition.

Inventory				Impact Factor	TRACI Impacts		USEtox Impacts	
Process	Inventory Item Description	Quantity	Unit	Impact Factor Descripton	Cancer Potential (kg benzene-eq)	Non-Cancer Potential (kg toluene-eq)	Cancer Potential (cases)	Non-Cancer Potential (cases)
Sorbent	Total Sorbent Used	333,771	kg	anionic resin, at plant	2,773	3,082,543	0.0	0.1
	Naval Sorbent Delivery	4,292,786	t-km	transport, transoceanic freight ship	56	94,231	0.0	0.0
	Ground Sorbent Delivery	11,909	v-km	operation, lorry 3.5-7.5t, EURO3	1	11,997	0.0	0.0
	Sorbent Vessel	3	each	hot water tank 600l, at plant	23	39,603	0.0	0.0
	Disposal Sorbent	333,771	kg	disposal, anion exchange resin, 50% water, to municipal incineration	824	960,393	0.0	0.0
Acidification	Total HCl Usage	19,742,479	kg	hydrochloric acid, 30% in H2O, at plant	71,418	150,743,697	1.5	6.3
	Ground HCl Delivery	187,005	v-km	operation, lorry 3.5-7.5t, EURO3	14	188,389	0.0	0.0
	Total H2SO4 Usage	0	kg	sulphuric acid, liquid, at plant				
	Ground H2SO4 Delivery	0	v-km	operation, lorry 3.5-7.5t, EURO3				
	Total CO2 Usage	0	kg	carbon dioxide liquid, at plant				
	Ground CO2 Delivery	0	v-km	operation, lorry 3.5-7.5t, EURO3				
	Acid Storage Tanks	1	each	hot water tank 600l, at plant	8	13,201	0.0	0.0
Neutralization	Total NaOH Usage	12,901,026	kg	sodium hydroxide, 50% in H2O, production mix, at plant	42,131	109,564,541	1.3	7.2
	Ground NaOH Delivery	122,149	v-km	operation, lorry 3.5-7.5t, EURO3	9	123,053	0.0	0.0
	Total Ca(OH)2 Usage	0	kg	lime from lithium carbonate hydration				
	Ground Ca(OH)2 Delivery	0	v-km	operation, lorry 3.5-7.5t, EURO3				
	Air Stripping Electricity	0	kWh	electricity, medium voltage, at grid				
	Repressurize Electricity	0	kWh	electricity, medium voltage, at grid				
	Caustic Storage Tanks	1	each	hot water tank 600l, at plant	8	13,201	0.0	0.0
Regen-eration	Total Salt Usage	0	kg	sodium chloride, powder, at plant				
	Ground Salt Delivery	0	v-km	operation, lorry 3.5-7.5t, EURO3				
	Salt Storage Tanks	0	each	hot water tank 600l, at plant				
Headloss Pumping	Headloss Pump Energy	2,677,341	kWh	electricity, medium voltage, at grid	3,203	8,780,874	0.1	0.1
	Total				**120,467**	**273,615,724**	**3.0**	**13.7**

Table 7.2. Inventory and impacts for Scenario 1A (treating Cr(VI) by WBAX with HCl and NaOH).

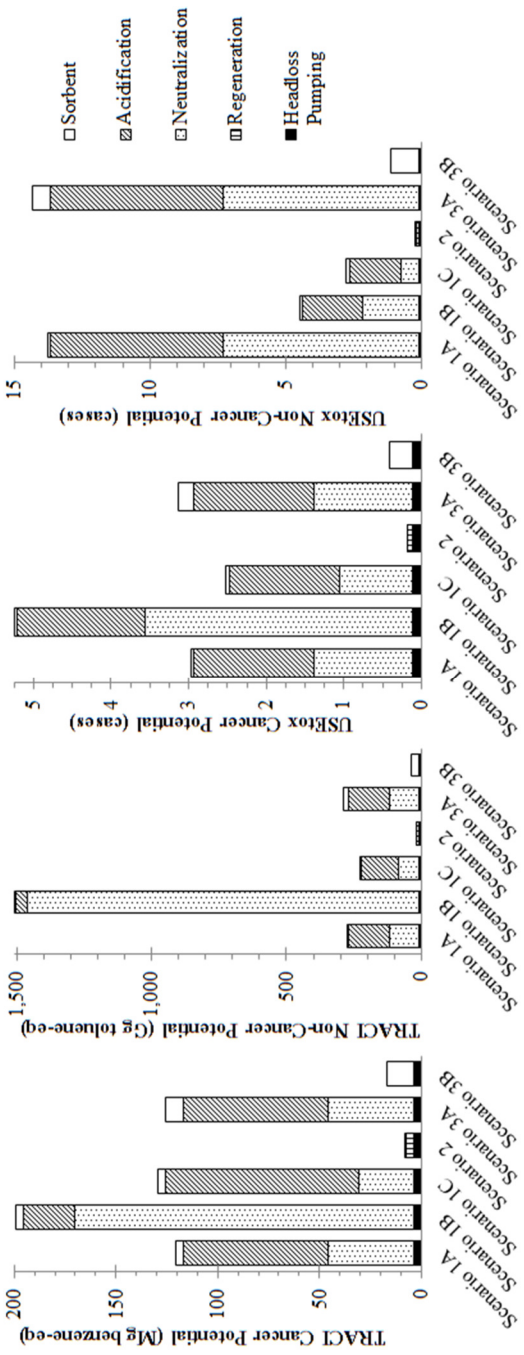

Figure 7.2. Life cycle human health impacts embedded in the water treatment system that treats water from 20 µg L^{-1} to 8 µg L^{-1} (80% of the 10 µg L^{-1} regulatory limit). The four graphs are the life cycle cancer and non-cancer potential for the EPA TRACI and USEtox methodologies. The six bars in each graph represent the six treatment scenarios defined in Table 7.1. The stripping within each bar represents the contribution of each process to total impact of each scenario.

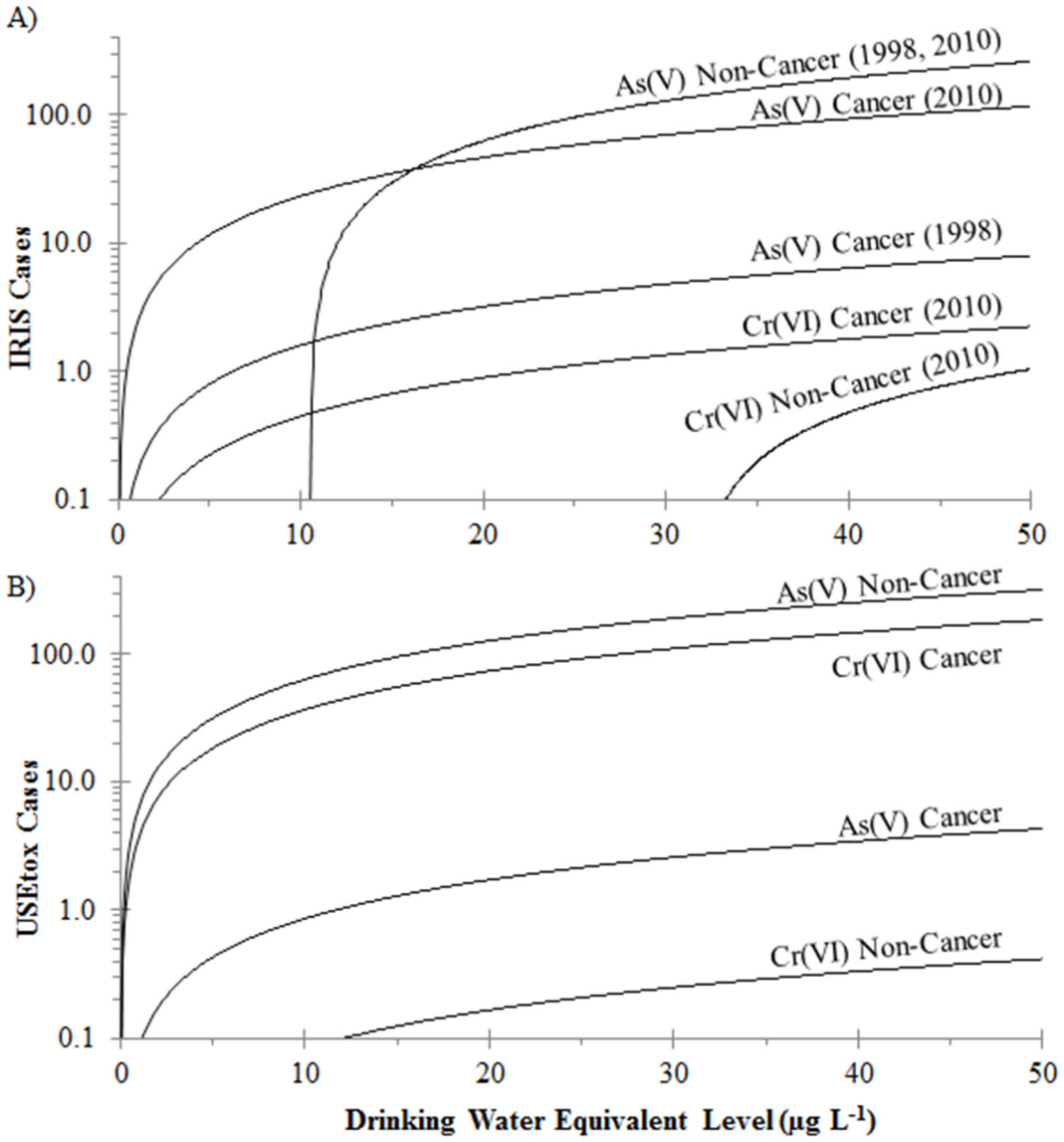

Figure 7.3. Dose-response relationships for oral ingestion of contaminated drinking water by 3,200 people calculated by A) EPA IRIS and B) USEtox data. Lines depict mean values, and 95% confidence intervals would be between one to two orders of magnitude above and below. All relationships are linear. IRIS carcinogenic responses and all USEtox responses begin at the origin, but IRIS non-carcinogenic responses have a threshold value (reference dose) below which no adverse effects are expected. Cr(VI) Cancer and Non-Cancer by 1998 IRIS data are zero in all depicted concentrations.

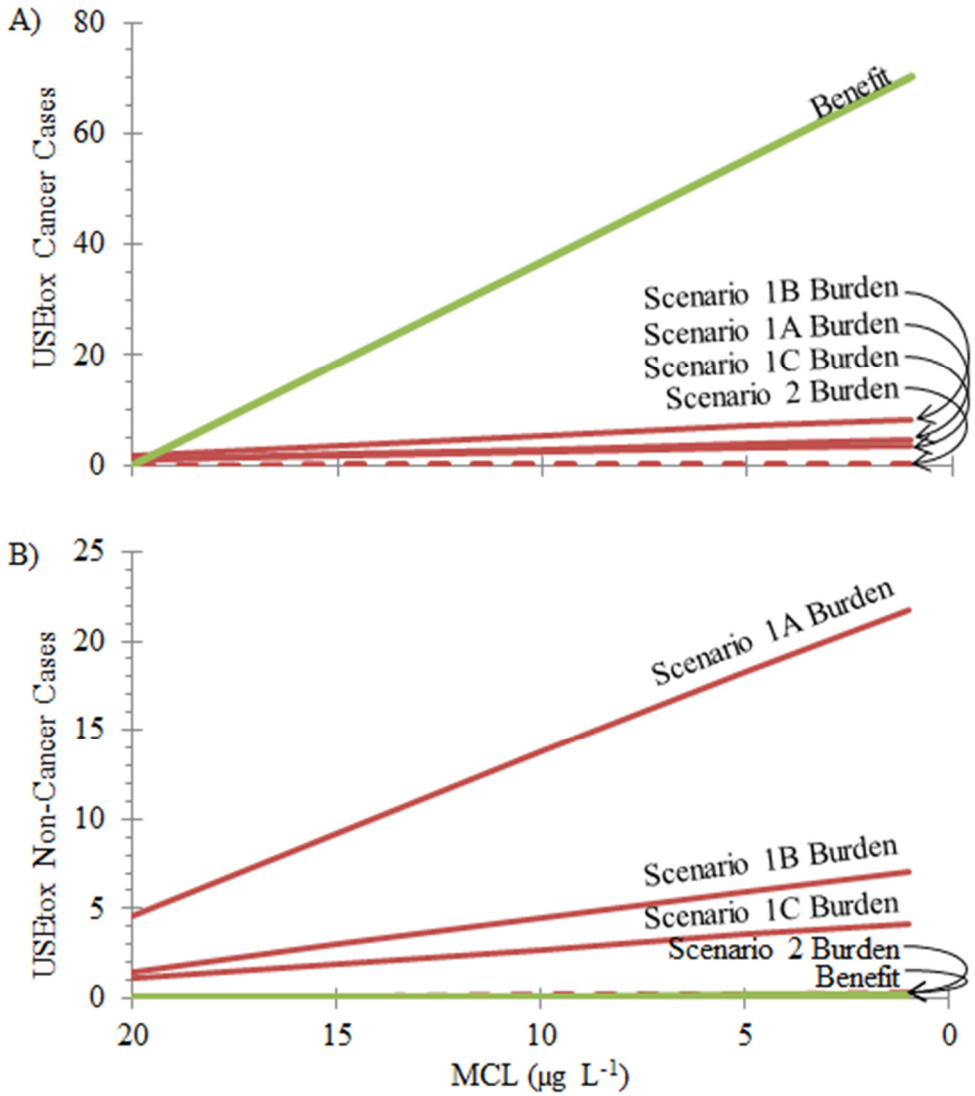

Figure 7.4. Tradeoffs of increasing treatment (i.e. reducing MCL) of Cr(VI) on A) cancer and B) non-cancer disease using USEtox methodology for a 3,200 person population with a 20 µg L^{-1} influent. Scenario 1A is treating by WBAX with HCL/NaOH, 1B is WBAX with $H_2SO_4/Na(OH)_2$, 1C is WBAX with CO_2/air stripping, 2 is SBAX. Scenario 2 in both figures and Treatment Benefit in the bottom figure are both nearly zero.

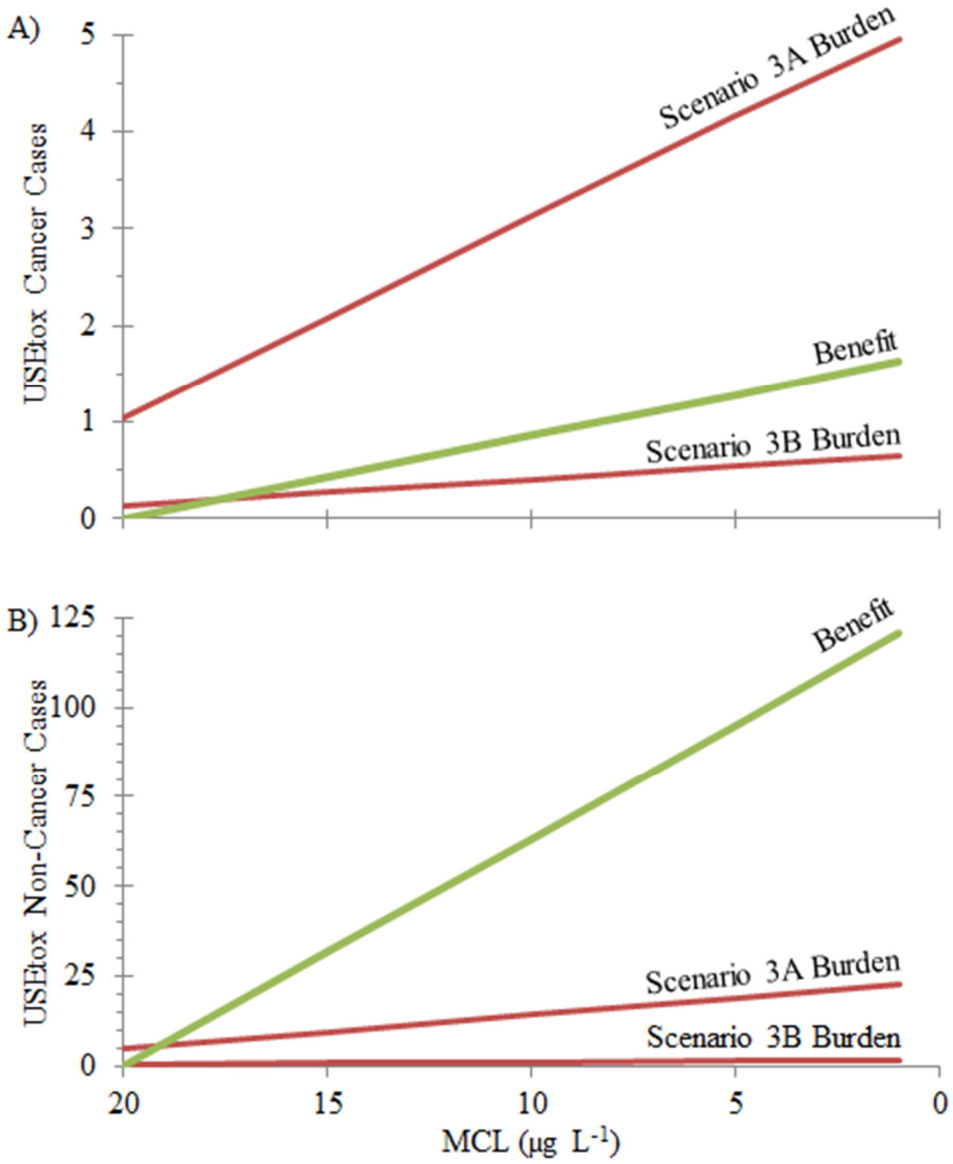

Figure 7.5. Tradeoffs of increasing treatment (i.e. reducing MCL) of As(V) on A) cancer and B) non-cancer disease using USEtox methodology for a 3,200 person population with a 20 µg L^{-1} influent. Scenario 3A is treating by MO with HCL/NaOH, and 3B is MO without pH control.

SUPPLEMENTAL INFORMATION

2.1 Assumptions to Develop LCA Inventory. A fraction of the total flow was treated and a fraction was bypassed such that when blended back together the final quality equaled the defined treatment goal. All treated water was assumed to reduce the contaminant concentration to 1 µg L^{-1}, which accounts for possible variability in treatment efficacy or low-level leakage. The treated portion of flow was:

$$Q_{treatment} = Q_{total} * \frac{(C_{inf} - C_{goal})}{(C_{inf} - C_{treated})} \quad (1)$$

where $Q_{treatment}$ was the flowrate being treated (gpm), Q_{total} was the total flowrate (670 gpm), C_{inf} was the influent pollutant concentration (µg L^{-1}), C_{goal} was the blended effluent pollutant target (defined as 80% of regulation, µg L^{-1}), and $C_{treated}$ was the pollutant concentration for the treated water (1 µg L^{-1}).

The mass of WBAX required to treat the functional unit was a function of the volume of treated water, sorbent density, and sorbent usage rate. The volume of treated water was the product of treated water flow rate found in Equation 1 and the project duration (70 years). The sorbent density was 38 lb ft^{-3} (Rohm & Haas 2008, Najm et al. 2014). The sorbent usage rate (ft^3 million $gallons^{-1}$) was found following (Najm et al. 2014):

$$WBAX\ Usage\ Rate\ = 1.5 * \frac{C_{inf}}{24} \quad (2)$$

The volume of SBAX used to treat the functional unit was assumed to be 750 ft^3 plus an annual replacement rate of 5%, totaling 3,375 ft^3 total. This was converted to sorbent mass using the same resin density as WBAX. The SBAX run duration was a function of the influent nitrate and sulfate levels as described(Najm et al. 2014):

$$\mathrm{BV} = 6.541 - 8307.5 * \log\left\{\left(\frac{[\mathrm{SO_4}]}{48}\right) + \left(\frac{[\mathrm{NO_3}]}{14}\right)\right\} \quad (3)$$

where BV was the number of bed volumes treated between regeneration cycles, $[SO_4]$ was the concentration of sulfate (33 mg L^{-1}), and $[NO_3]$ was the concentration of nitrate (5 mg L^{-1} as N).

The mass of MO sorbent required was based on As(V) removal capacity, assumed to be 280 µg g^{-1} as previously observed for granular ferric hydroxide(Westerhoff et al. 2005) at pH 8.5. This capacity was increased by 50% for scenarios that included pH adjustment. The required mass of MO sorbent (M_{MO}, kg) was estimated as:

$$M_{MO} = \frac{V_{total} * (C_{inf} - C_{goal})}{(1.5 * q) * 1000} \quad (4)$$

where V_{total} was the total water volume (93 billion liters), and q was the sorbent capacity (µg g^{-1}). The sorbent density for granular ferric hydroxide was 72 lb ft^{-3} (Westerhoff et al. 2005).

Transporting the sorbent from the place of manufacture to the site of usage was considered. Anion exchange resin was assumed to be produced in Hong Kong, China and traveled via transoceanic freight to Los Angeles, CA (12,000 km). It then traveled via truck to Palm Springs, CA (160 km). Metal oxide sorbent was assumed to be manufactured in Germany then travels via transoceanic freight to Houston, TX (9,000 km). It then traveled via truck to Palm Springs, CA (2,300 km). In each case, the overland truck could carry up to 5 tons per trip. The sorbent was used on-site in three vessels to allow a lead-lag-maintenance configuration. Each vessel was 10 feet in diameter and held 250 ft^3 of sorbent at 3 ft deep.

Pump energy required to overcome headloss in the sorbent bed is estimated using a headloss rate of 5.2 ft ft^{-1} (Rohm & Haas 2008) and 60% pump efficiency. Since the water pumped through two beds in series, the total headloss was 33 ft requiring 4.37 kW of pump energy. Pumping energy for water supply or distribution was not considered.

Acid and base doses required to adjust pH from 8 to 6 for treatment and back to 8 for distribution were estimated from online calculators(AQIon 2014, Water Quality & Treatment Solutions 2008). HCl and H_2SO_4 were delivered as 30% purity. NaOH, $Ca(OH)_2$, and CO_2 were delivered as 50% purity. Chemicals were transported from Los Angeles, CA to Palm Spring, CA (160 km) in trucks with 4,500 gallon capacity. Each chemical was stored on-site in one 4,500 gallon tank. In the air stripping scenario, a 26 hp blower was used per recommendation based on flowrate (Najm et al. 2014). The water was then re-pressurized up to 60 psi using a pump with 60% efficiency.

Disposal of anion exchange resin to landfill was included. Disposal of salt regeneration brine was assumed to be to sewer with no further impact. Disposal to landfill of MO sorbent, transport associated with disposal of any sorbent, and possible hazardous waste landfilling was not considered.

2.2 Matching Impact Factors to Inventory Items. Good agreement was generally found in matching impact factors available in EcoInvent to inventory items. For example, an impact factor for ‘anion exchange resin’ was matched with both weak base and strong base anion exchange inventory, and a ‘transport via transoceanic freight ship’ impact factor matched for oversea sorbent delivery. Most chemicals, including acids, salts, and bases had impact factors with matching CAS number descriptions.

Some inventory items did not have clearly corresponding impact factors. For example, no metal oxide sorbent impact factor was available, so the impact factor for magnetite was used. Magnetite is generally used for ink toner, and while not a perfect match, it was a reasonable match because both are produced from ferric chloride and hydroxide to produce ferric oxide.

Some inventory items had multiple impact factors that would have been reasonable options. The selected impact factor for overland transport was a 5-ton lorry conforming to EURO3 engine emission standards. This vehicle size was reasonable because it corresponded to on-site tank storage capacity. Chemical storage and sorbent contactor vessels used the impact factor for a similarly sized hot water tank. Electricity for pumping and air stripping used the impact factor for medium voltage electricity supply at grid with US average production and losses.

Custom impact factors were developed for specialty chemicals not found in the EcoInvent database. These were divinylbenzene, styrene-divinylbenzene copolymer, stannous chloride, aluminum chloride, and un-functionalized ion exchange copolymer. A custom impact factor was also developed for anion exchange resin to compare to the one in the database to account for wide technological options in resin synthesis and explore inventory uncertainty associated with this study. It follows a classic published recipe (Kunin 1958). These custom impact factors were derived by a weighted average of their respective stoichiometric synthesis chemicals and an assumed process efficiency of 70%. For example, divinylbenzene is industrially made using one part benzene and two parts ethylene. The custom impact factors were estimated by averaging the EcoInvent available

factors for benzene and two times the factors for ethylene, then dividing by 70%. For carcinogencity under USEtox, the calculation followed:

$$Divinylbenze = \frac{1\ part\ benzene + 2\ parts\ ethylene}{3\ parts * process\ efficiency}$$

$$= \frac{3.1455 * 10^{-8}\ \frac{CTUh}{kg\ benzene} + 2 * 2.3471 * 10^{-8}\ \frac{CTUh}{kg\ ethylene}}{3 * 0.7}$$

$$= 3.7332 * 10^{-8}\ \frac{CTUh}{kg\ divinylbenzene}$$

This and other proposed impact factors for the chemicals and anion exchange resin are in SI Table 7.1.

3.1 LCA Model Sensitivity. The model showed the greatest sensitivity to selection of pH control method, and sub-scenarios (e.g. scenarios 1A, 1B, 1C) were developed to capture this sensitivity. Theoretically, the lowest total human health impact for pH control could be achieved by pairing sulfuric acid with air stripping. However, sulfuric acid reduces water alkalinity and must be counteracted with chemical hydroxide to avoid changing the corrosion potential and causing detrimental downstream piping effects. Carbon dioxide and air stripping were exclusive partners for this reason (scenario 1C), while hydrochloric and sulfuric acid could be paired with either sodium hydroxide or lime.

The assumed influent water alkalinity highly influenced the final results for scenarios which included pH control, with a nearly direct proportionality observed. A 75% reduction (50 mg L^{-1} as $CaCO_3$) in influent alkalinity reduced the results by 71% - 74%. A 75% increase (350 mg L^{-1} as $CaCO_3$) in influent alkalinity increased the results by 71% - 75%. Intermediary changes elicited proportional changes in results. Alkalinity

is the water's ability to resist change in pH, so this result was expected since pH control chemicals are the dominant impact.

The assumed influent water nitrate and sulfate levels have a strong influence to the results of the SBAX scenario. A 75% reduction (1.3 mg L^{-1} NO_3-N and 8.3 mg L^{-1} SO_4) caused a 15% - 23% decrease in final results. A 75% increase (8.8 mg L^{-1} NO_3-N and 58 mg L^{-1} SO_4) caused a 16% to 24% increase in total results. Linear responses were observed between those points, but nitrate and sulfate levels higher than this were found to cause an exponential increase in impacts as the sorbent needed to be regenerated for more time than it was in service.

The effect of the assumed sorbent capacity was found to have little change on the final results. For both the WBAX and MO scenarios, doubling the sorbent capacity reduced impacts by only up to 3%, and a ten-fold increase in sorbent capacity only reduced the impacts by up to 6%. A 50% reduction in sorbent capacity increased the final results by less than 7%. Further reduction begins to cause more drastic changes as sorbent would be replaced very frequently, but this is not plausible as cost considerations would prevent such a low capacity sorbent from being used. Low sensitivity to sorbent capacity is because the sorption process comprised only a small percentage of the total impacts compared to pH control processes.

Custom impact factors for anion exchange resin synthesis were derived using mass relationships following a published recipe (Kunin 1958) and presented in the SI. The human health factors were 2.2 to 9.1 times higher than those found in the EcoInvent v2.2 database. Using these custom factors had the effect of increasing the total impact associated with treating Cr(VI) with WBAX by 3% - 11%, and treating Cr(VI) with

SBAX by 7% - 32%. While this was only a small change in this study, this indicates that in other treatment scenarios where the sorbent is a principal driver of life cycle impact results a custom impact factor should be used.

The type of truck assumed for chemical and sorbent land transport is inconsequential to final results. Changing the truck size (5 to 25 ton) and engine efficiency standards (EURO3 to EURO5) changed the final results by less than 1% for all scenarios. The assumed chemical and sorbent storage tank was similarly inconsequential. A scaled impact factor for a chemical storage tank was compared to that for the hot water tank and found to change the final results by less than 1%.

3.2 Dose Response Relationships. A relationship to estimate the potential number of human health cases at various drinking water equivalent levels was developed in SI Equation 1.

$$Cases_{Impact} = N_{pop} * (Slope * DWEL - Intercept) \quad \text{(SI1)}$$

$Cases_{Impact}$ is the potential number of cases for the selected pollutant, impact, and dataset (cases), N_{pop} is the study population (people), and DWEL is the drinking water pollutant concentration (µg L^{-1}). Slope and Intercept are coefficients developed for each pollutant, impact, and dataset which are found in SI Table 7.7.

No non-cancer disease cases were expected at pollutant levels at or below the reference dose under EPA IRIS methodology. The DWEL corresponding to As(V) non-cancer reference dose was 10.5 µg L^{-1}. For the 1998 Cr(VI) reference dose it was 105 µg L^{-1}, and for the 2010 Cr(VI) reference dose it was 31.5 µg L^{-1}.

4.1 Addressing Critiques of the Dose/Response Methodology. The published effect factors, slope factors and reference doses are provided with uncertainty of perhaps

an order of magnitude (USEPA 1998a, b, 2010a, b, Rosenbaum et al. 2008). The number of cancer and non-cancer cases estimated in this study from these numbers should be similarly interpreted. For example, if 6 excess cases are estimated, this result can be interpreted as anywhere between 1 and 60 cases. Embedding this uncertainty generally overestimates the actual number of disease cases. While this limits the ability of the model to predict absolute values of cancer and non-cancer cases, it is still valuable to inform the magnitude of the change in cases estimated for different treatment scenarios and to identify the most influential contributors to total health impact.

Dose-response relationships are often observed to have curved responses in the low dose range resembling an exponential increase. This study has assumed linear responses for consistency with USEtox and IRIS methodology as well as for model parity. This line would therefore overestimate the number of cases from a curved dose-response relationship.

For the non-cancer responses, all contaminant intake is assumed to come from drinking water. Drinking water does dominate arsenic intake for areas with drinking water concentrations above 10 $\mu g\ L^{-1}$ (James et al. 2015). However, ignoring any intake from food or inhalation has the effect of underestimating the expected number of non-cancer cases associated with that pollutant.

For all health benefit analysis the population is assumed to be adults with 70 kg body mass and 2 $L\ day^{-1}$ drinking water intake. Including infants as a fraction of the population with 10 kg body mass and 1 $L\ day^{-1}$ drinking water intake (Hammer and Hammer Jr. 2011) would have the effect of slightly increasing exposure and raising the expected number of cancer and non-cancer cases.

The EPA does not intend for Reference Doses to be used to inform dose-response estimations. It really should only be a threshold of “safe” or “not safe”. Also, the reference dose includes modifying factors and uncertainty factors in its derivation that make it difficult to interpret as a true point of ‘zero response’. Assuming zero response up to the level of the NOAEL would have the effect of lowering the estimated number of cases.

Material	Unit	TRACI Carcinogenicity (kg benzene-eq per kg material)	TRACI Non-Carcinogenic Toxicity (kg toluene-eq per kg material)	USEtox Carcinogenic (CTU)	USEtox Non-Carcinogenic (CTU)
divinylbenzene, at plant	kg	1.76E-04	3.46E-01	3.73E-08	4.87E-09
styrene-DVB copolymer, at plant	kg	2.20E-03	5.27E+00	3.71E-07	1.32E-07
stannous chloride, at plant	kg	1.94E-02	1.88E+02	1.25E-06	6.48E-07
aluminum chloride, at plant	kg	6.26E-03	9.37E+00	6.08E-07	3.97E-07
anion exchange resin, at plant	kg	1.85E-02	3.52E+01	1.12E-06	9.48E-07

SI Table 7.1. Custom Impact Factors.

Inventory				Impact Factor	TRACI Impacts		USEtox Impacts	
Process	Inventory Item Description	Quantity	Unit	Impact Factor Descripton	Cancer Potential (kg benzene-eq)	Non-Cancer Potential (kg toluene-eq)	Cancer Potential (cases)	Non-Cancer Potential (cases)
Sorbent	Total Sorbent Used	333,771	kg	anionic resin, at plant	2,773	3,082,543	0.0	0.1
	Naval Sorbent Delivery	4,292,786	t-km	transport, transoceanic freight ship	56	94,231	0.0	0.0
	Ground Sorbent Delivery	11,909	v-km	operation, lorry 3.5-7.5t, EURO3	1	11,997	0.0	0.0
	Sorbent Vessel	3	each	hot water tank 600l, at plant	23	39,603	0.0	0.0
	Disposal Sorbent	333,771	kg	disposal, anion exchange resin, 50% water, to municipal incineration	824	960,393	0.0	0.0
Acidification	Total HCl Usage		kg	hydrochloric acid, 30% in H2O, at plant				
	Ground HCl Delivery		v-km	operation, lorry 3.5-7.5t, EURO3				
	Total H2SO4 Usage	26,388,462	kg	sulphuric acid, liquid, at plant	25,663	40,004,908	1.6	2.2
	Ground H2SO4 Delivery	249,770	v-km	operation, lorry 3.5-7.5t, EURO3	18	251,618	0.0	0.0
	Total CO2 Usage		kg	carbon dioxide liquid, at plant				
	Ground CO2 Delivery		v-km	operation, lorry 3.5-7.5t, EURO3				
	Acid Storage Tanks	1	each	hot water tank 600l, at plant	8	13,201	0.0	0.0
Neutralization	Total NaOH Usage		kg	sodium hydroxide, 50% in H2O, production mix, at plant				
	Ground NaOH Delivery		v-km	operation, lorry 3.5-7.5t, EURO3				
	Total Ca(OH)2 Usage	11,962,769	kg	lime from lithium carbonate hydration	166,617	1,452,639,077	3.5	2.1
	Ground Ca(OH)2 Delivery	113,298	v-km	operation, lorry 3.5-7.5t, EURO3	8	114,136	0.0	0.0
	Air Stripping Electricity		kWh	electricity, medium voltage, at grid				
	Repressurize Electricity		kWh	electricity, medium voltage, at grid				
	Caustic Storage Tanks	1	each	hot water tank 600l, at plant	8	13,201	0.0	0.0
Regen-eration	Total Salt Usage		kg	sodium chloride, powder, at plant				
	Ground Salt Delivery		v-km	operation, lorry 3.5-7.5t, EURO3				
	Salt Storage Tanks		each	hot water tank 600l, at plant				
Headloss Pumping	Headloss Pump Energy	2,677,341	kWh	electricity, medium voltage, at grid	3,203	8,780,874	0.1	0.1
	Total				**199,202**	**1,506,005,783**	**5.3**	**4.5**

SI Table 7.2. Inventory and impacts for Scenario 1B (Treating Cr(VI) by WBAX with H_2SO_4 and $Ca(OH)_2$).

Inventory				Impact Factor	TRACI Impacts		USEtox Impacts	
Process	Inventory Item Description	Quantity	Unit	Impact Factor Descripton	Cancer Potential (kg benzene-eq)	Non-Cancer Potential (kg toluene-eq)	Cancer Potential (cases)	Non-Cancer Potential (cases)
Sorbent	Total Sorbent Used	333,771	kg	anionic resin, at plant	2,773	3,082,543	0.0	0.1
	Naval Sorbent Delivery	4,292,786	t-km	transport, transoceanic freight ship	56	94,231	0.0	0.0
	Ground Sorbent Delivery	11,909	v-km	operation, lorry 3.5-7.5t, EURO3	1	11,997	0.0	0.0
	Sorbent Vessel	3	each	hot water tank 600l, at plant	23	39,603	0.0	0.0
	Disposal Sorbent	333,771	kg	disposal, anion exchange resin, 50% water, to municipal incineration	824	960,393	0.0	0.0
Acidification	Total HCl Usage		kg	hydrochloric acid, 30% in H2O, at plant				
	Ground HCl Delivery		v-km	operation, lorry 3.5-7.5t, EURO3				
	Total H2SO4 Usage		kg	sulphuric acid, liquid, at plant				
	Ground H2SO4 Delivery		v-km	operation, lorry 3.5-7.5t, EURO3				
	Total CO2 Usage	43,980,770	kg	carbon dioxide liquid, at plant	94,730	136,331,589	1.4	1.9
	Ground CO2 Delivery	416,336	v-km	operation, lorry 3.5-7.5t, EURO3	30	419,417	0.0	0.0
	Acid Storage Tanks	1	each	hot water tank 600l, at plant	8	13,201	0.0	0.0
Neutralization	Total NaOH Usage		kg	sodium hydroxide, 50% in H2O, production mix, at plant				
	Ground NaOH Delivery		v-km	operation, lorry 3.5-7.5t, EURO3				
	Total Ca(OH)2 Usage		kg	lime from lithium carbonate hydration				
	Ground Ca(OH)2 Delivery		v-km	operation, lorry 3.5-7.5t, EURO3				
	Air Stripping Electricity	11,888,842	kWh	electricity, medium voltage, at grid	14,221	38,991,836	0.5	0.3
	Repressurize Electricity	11,214,780	kWh	electricity, medium voltage, at grid	13,415	36,781,114	0.5	0.3
	Caustic Storage Tanks		each	hot water tank 600l, at plant				
Regen-eration	Total Salt Usage		kg	sodium chloride, powder, at plant				
	Ground Salt Delivery		v-km	operation, lorry 3.5-7.5t, EURO3				
	Salt Storage Tanks		each	hot water tank 600l, at plant				
Headloss Pumping	Headloss Pump Energy	2,677,341	kWh	electricity, medium voltage, at grid	3,203	8,780,874	0.1	0.1
	Total				**129,284**	**225,506,799**	**2.5**	**2.7**

SI Table 7.3. Inventory and impacts for Scenario 1C (Treating Cr(VI) by WBAX with CO_2 and air stripping).

Inventory				Impact Factor	TRACI Impacts		USEtox Impacts	
Process	Inventory Item Description	Quantity	Unit	Impact Factor Descripton	Cancer Potential (kg benzene-eq)	Non-Cancer Potential (kg toluene-eq)	Cancer Potential (cases)	Non-Cancer Potential (cases)
Sorbent	Total Sorbent Used	58,173	kg	anionic resin, at plant	483	537,258	0.0	0.0
	Naval Sorbent Delivery	748,192	t-km	transport, transoceanic freight ship	10	16,424	0.0	0.0
	Ground Sorbent Delivery	2,092	v-km	operation, lorry 3.5-7.5t, EURO3	0	2,108	0.0	0.0
	Sorbent Vessel	3	each	hot water tank 600l, at plant	23	39,603	0.0	0.0
	Disposal Sorbent	58,173	kg	disposal, anion exchange resin, 50% water, to municipal incineration	144	167,387	0.0	0.0
Acidification	Total HCl Usage		kg	hydrochloric acid, 30% in H2O, at plant				
	Ground HCl Delivery		v-km	operation, lorry 3.5-7.5t, EURO3				
	Total H2SO4 Usage		kg	sulphuric acid, liquid, at plant				
	Ground H2SO4 Delivery		v-km	operation, lorry 3.5-7.5t, EURO3				
	Total CO2 Usage		kg	carbon dioxide liquid, at plant				
	Ground CO2 Delivery		v-km	operation, lorry 3.5-7.5t, EURO3				
	Acid Storage Tanks		each	hot water tank 600l, at plant				
Neutralization	Total NaOH Usage		kg	sodium hydroxide, 50% in H2O, production mix, at plant				
	Ground NaOH Delivery		v-km	operation, lorry 3.5-7.5t, EURO3				
	Total Ca(OH)2 Usage		kg	lime from lithium carbonate hydration				
	Ground Ca(OH)2 Delivery		v-km	operation, lorry 3.5-7.5t, EURO3				
	Air Stripping Electricity		kWh	electricity, medium voltage, at grid				
	Repressurize Electricity		kWh	electricity, medium voltage, at grid				
	Caustic Storage Tanks		each	hot water tank 600l, at plant				
Regen-eration	Total Salt Usage	2,750,632	kg	sodium chloride, powder, at plant	4,336	8,370,174	0.1	0.1
	Ground Salt Delivery	19,634	v-km	operation, lorry 3.5-7.5t, EURO3	1	19,779	0.0	0.0
	Salt Storage Tanks	1	each	hot water tank 600l, at plant	8	13,201	0.0	0.0
Headloss Pumping	Headloss Pump Energy	2,677,341	kWh	electricity, medium voltage, at grid	3,203	8,780,874	0.1	0.1
	Total				**8,208**	**17,946,808**	**0.2**	**0.2**

SI Table 7.4. Inventory and impacts for Scenario 2 (Treating Cr(VI) by SBAX).

Inventory				Impact Factor	TRACI Impacts		USEtox Impacts	
Process	Inventory Item Description	Quantity	Unit	Impact Factor Descripton	Cancer Potential (kg benzene-eq)	Non-Cancer Potential (kg toluene-eq)	Cancer Potential (cases)	Non-Cancer Potential (cases)
Sorbent	Total Sorbent Used	2,652,808	kg	anionic resin, at plant	8,500	16,305,221	0.2	0.7
	Naval Sorbent Delivery	25,883,380	t-km	transport, transoceanic freight ship	340	568,166	0.0	0.0
	Ground Sorbent Delivery	429,372	v-km	operation, lorry 3.5-7.5t, EURO3	31	432,549	0.0	0.0
	Sorbent Vessel	3	each	hot water tank 600l, at plant	23	39,603	0.0	0.0
	Disposal Sorbent		kg	disposal, anion exchange resin, 50% water, to municipal incineration				
Acidification	Total HCl Usage	19,742,479	kg	hydrochloric acid, 30% in H2O, at plant	71,418	150,743,697	1.5	6.3
	Ground HCl Delivery	187,005	v-km	operation, lorry 3.5-7.5t, EURO3	14	188,389	0.0	0.0
	Total H2SO4 Usage		kg	sulphuric acid, liquid, at plant				
	Ground H2SO4 Delivery		v-km	operation, lorry 3.5-7.5t, EURO3				
	Total CO2 Usage		kg	carbon dioxide liquid, at plant				
	Ground CO2 Delivery		v-km	operation, lorry 3.5-7.5t, EURO3				
	Acid Storage Tanks	1	each	hot water tank 600l, at plant	8	13,201	0.0	0.0
Neutralization	Total NaOH Usage	12,901,026	kg	sodium hydroxide, 50% in H2O, production mix, at plant	42,131	109,564,541	1.3	7.2
	Ground NaOH Delivery	122,149	v-km	operation, lorry 3.5-7.5t, EURO3	9	123,053	0.0	0.0
	Total Ca(OH)2 Usage		kg	lime from lithium carbonate hydration				
	Ground Ca(OH)2 Delivery		v-km	operation, lorry 3.5-7.5t, EURO3				
	Air Stripping Electricity		kWh	electricity, medium voltage, at grid				
	Repressurize Electricity		kWh	electricity, medium voltage, at grid				
	Caustic Storage Tanks	1	each	hot water tank 600l, at plant	8	13,201	0.0	0.0
Regen-eration	Total Salt Usage		kg	sodium chloride, powder, at plant				
	Ground Salt Delivery		v-km	operation, lorry 3.5-7.5t, EURO3				
	Salt Storage Tanks		each	hot water tank 600l, at plant				
Headloss Pumping	Headloss Pump Energy	2,677,341	kWh	electricity, medium voltage, at grid	3,203	8,780,874	0.1	0.1
	Total				**125,684**	**286,772,495**	**3.1**	**14.3**

SI Table 7.5. Inventory and impacts for Scenario 3A (Treating As(V) by MO with HCl and NaOH).

Inventory				Impact Factor	TRACI Impacts		USEtox Impacts	
Process	Inventory Item Description	Quantity	Unit	Impact Factor Descripton	Cancer Potential (kg benzene-eq)	Non-Cancer Potential (kg toluene-eq)	Cancer Potential (cases)	Non-Cancer Potential (cases)
Sorbent	Total Sorbent Used	3,979,212	kg	anionic resin, at plant	12,750	24,457,832	0.3	1.0
	Naval Sorbent Delivery	38,825,070	t-km	transport, transoceanic freight ship	510	852,249	0.0	0.0
	Ground Sorbent Delivery	644,058	v-km	operation, lorry 3.5-7.5t, EURO3	47	648,824	0.0	0.0
	Sorbent Vessel	3	each	hot water tank 600l, at plant	23	39,603	0.0	0.0
	Disposal Sorbent		kg	disposal, anion exchange resin, 50% water, to municipal incineration				
Acidification	Total HCl Usage		kg	hydrochloric acid, 30% in H2O, at plant				
	Ground HCl Delivery		v-km	operation, lorry 3.5-7.5t, EURO3				
	Total H2SO4 Usage		kg	sulphuric acid, liquid, at plant				
	Ground H2SO4 Delivery		v-km	operation, lorry 3.5-7.5t, EURO3				
	Total CO2 Usage		kg	carbon dioxide liquid, at plant				
	Ground CO2 Delivery		v-km	operation, lorry 3.5-7.5t, EURO3				
	Acid Storage Tanks		each	hot water tank 600l, at plant				
Neutralization	Total NaOH Usage		kg	sodium hydroxide, 50% in H2O, production mix, at plant				
	Ground NaOH Delivery		v-km	operation, lorry 3.5-7.5t, EURO3				
	Total Ca(OH)2 Usage		kg	lime from lithium carbonate hydration				
	Ground Ca(OH)2 Delivery		v-km	operation, lorry 3.5-7.5t, EURO3				
	Air Stripping Electricity		kWh	electricity, medium voltage, at grid				
	Repressurize Electricity		kWh	electricity, medium voltage, at grid				
	Caustic Storage Tanks		each	hot water tank 600l, at plant				
Regen-eration	Total Salt Usage		kg	sodium chloride, powder, at plant				
	Ground Salt Delivery		v-km	operation, lorry 3.5-7.5t, EURO3				
	Salt Storage Tanks		each	hot water tank 600l, at plant				
Headloss Pumping	Headloss Pump Energy	2,677,341	kWh	electricity, medium voltage, at grid	3,203	8,780,874	0.1	0.1
	Total				**16,532**	**34,779,382**	**0.4**	**1.1**

SI Table 7.6. Inventory and impacts for Scenario 3B (Treating As(V) by MO without pH control).

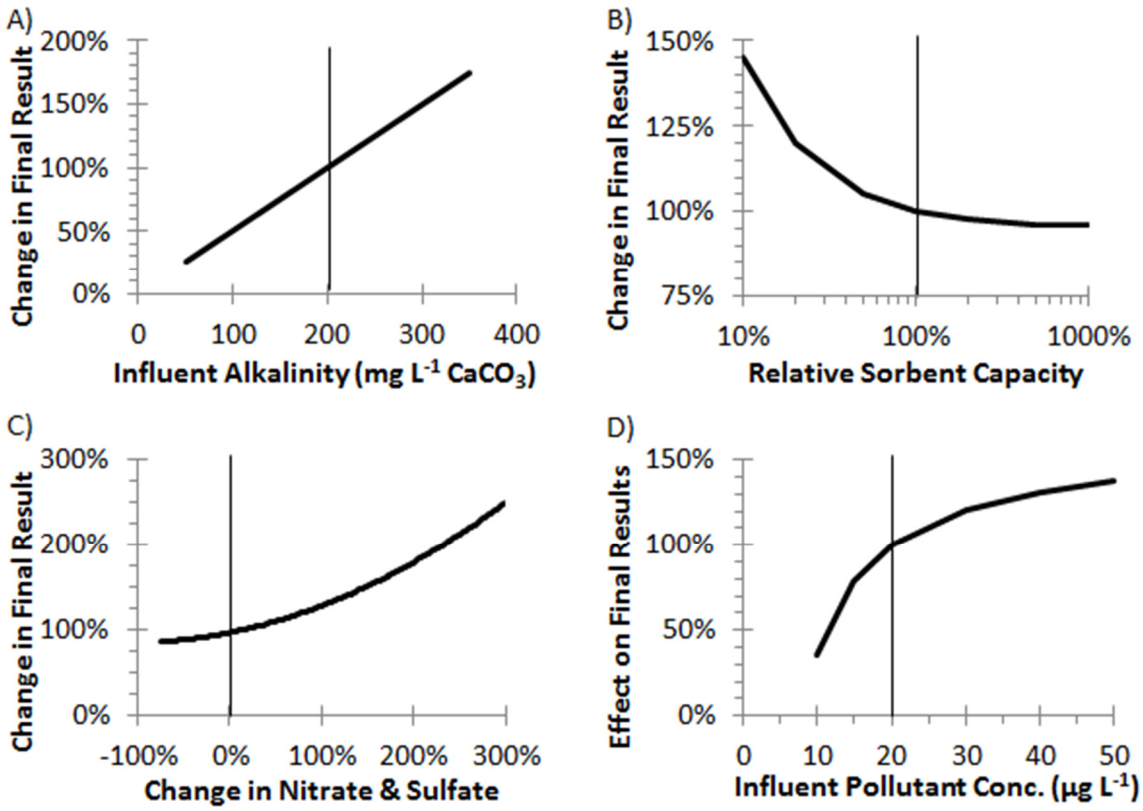

SI Figure 7.1. Sensitivity Relationships for A) influent alkalinity for treating Cr(VI) by WBAX, B) change in assumed sorbent capacity for treating As(V) by MO, C) influent nitrate and sulfate levels for treating Cr(VI) by SBAX, and D) influent pollutant concentration for treating Cr(VI) by WBAX. Vertical lines represent the base case.

Dataset	Pollutant	Impact	Slope	Intercept	Limitation
IRIS (1998)	Cr(VI)	Cancer	0	0	DWEL > 0
IRIS (2010)	Cr(VI)	Cancer	1.400 E -5	0	DWEL > 0
IRIS (1998)	Cr(VI)	Non-Cancer	6.350 E -7	6.668 E -5	DWEL > 105
IRIS (2010)	Cr(VI)	Non-Cancer	1.766 E -5	5.562 E -4	DWEL > 31.5
IRIS (1998)	As(V)	Cancer	5.000 E -5	0	DWEL > 0
IRIS (2010)	As(V)	Cancer	7.300 E -4	0	DWEL > 0
IRIS (1998)	As(V)	Non-Cancer	2.070 E -3	2.174 E -2	DWEL > 10.5
IRIS (2010)	As(V)	Non-Cancer	2.070 E -3	2.174 E -2	DWEL > 10.5
USEtox	Cr(VI)	Cancer	1.154 E -3	0	DWEL > 0
USEtox	Cr(VI)	Non-Cancer	2.597 E -6	0	DWEL > 0
USEtox	As(V)	Cancer	2.679 E -5	0	DWEL > 0
USEtox	As(V)	Non-Cancer	1.984 E -3	0	DWEL > 0

SI Table 7.7. Coefficients to calculate dose-response relationship based on the dataset, pollutant, and impact of interest given a study population and drinking water pollutant concentration (DWEL). For DWEL less than or equal to the limitation stated, the potential number of cases is zero.

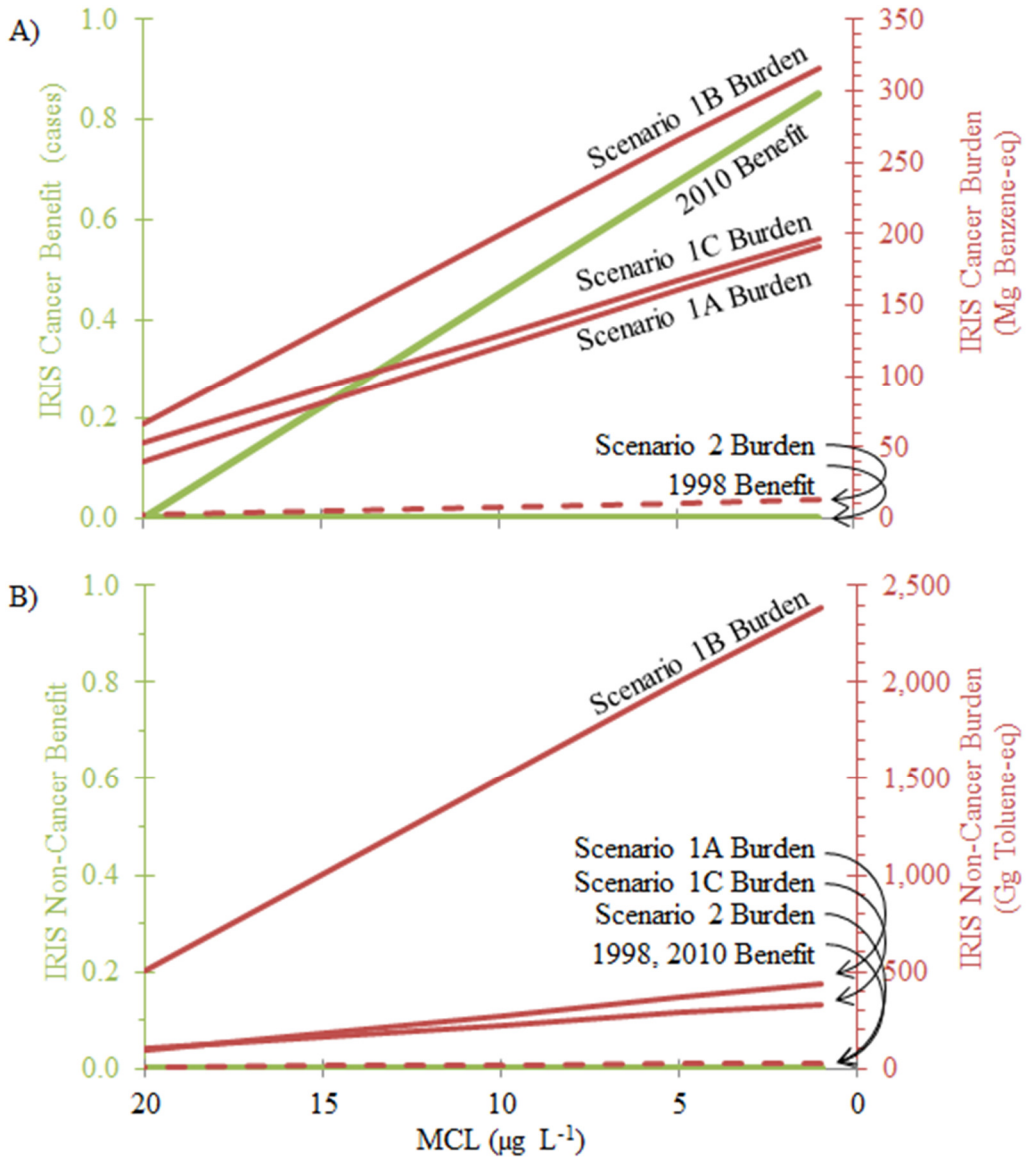

SI Figure 7.2. Tradeoffs of increasing treatment (i.e. reducing MCL) of Cr(VI) on A) cancer and B) non-cancer disease using EPA methodology for a 3,200 person population with a 20 µg L^{-1} influent. Scenario 1A is treating by WBAX with HCL/NaOH, 1B is WBAX with H_2SO_4/$Na(OH)_2$, 1C is WBAX with CO_2/air stripping, 2 is SBAX. Benefit from 1998 uses official data, while 2010 uses newer draft information. 1998 Benefit is zero in the top graph, and both benefit lines are zero in the bottom figure.

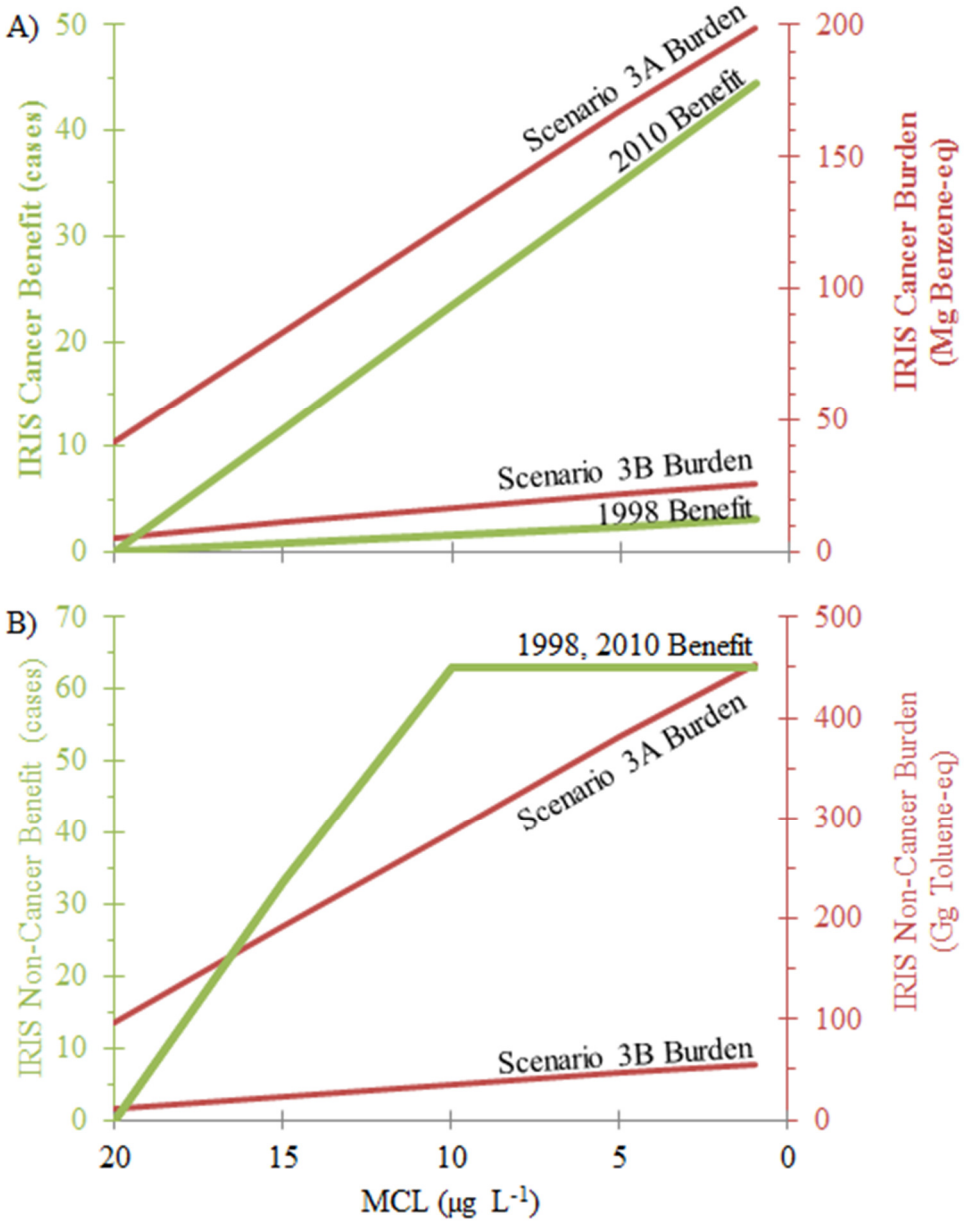

SI Figure 7.3. Tradeoffs of increasing treatment (i.e. reducing MCL) of As(V) on A) cancer and B) non-cancer disease using EPA methodology for a 3,200 person population with a 20 µg L^{-1} influent. Scenario 3A is treating by MO with HCL/NaOH, and 3B is MO with no pH control. Benefit from 1998 uses official data, while 2010 uses newer draft information. The benefit lines are coincident in the bottom figure.

CHAPTER 8

NANO-COMPOSITE SORBENT

POLLUTANT REMOVAL PERFORMANCE AND MECHANISM

1. INTRODUCTION

The goal of this chapter is to demonstrate performance of the nano-composite sorbents. Methods for synthesizing the nanocomposite sorbent infused with titanium (Ti) or iron (Fe) nanoparticles into weak base anion exchange (WBAX) have been developed as informed by sorbent characteristics and preliminary simultaneous removal capacity in Chapter 5 as well as for environmental and human health performance in Chapter 6. They now face the culminating test to demonstrate performance in challenging conditions during a long term packed bed application.

The results of this test will first verify the performance of the nano-composite sorbents and that they fulfill the goal which was outlined at the onset of the research. Secondarily, it also informs future use of the sorbent to identify key operational parameters and potential interfering constituents. Lastly, it will shine light on mechanistically understanding how the hybrid sorbents remove pollutants, and someday therefore inform how they might be regenerated.

The mechanism of removal for arsenic removal and for chromium removal is important to understand in order to maximize performance and improve any current limitations hybrid resins may have. One such current limitation with use of WBAX, and therefore nano-composite using WBAX also, is that it is unknown how it can be regenerated. It has been speculated that Cr(VI) is reduced to Cr(III) on the surface of

WBAX because visual observations show the spent resin takes on a green color characteristic of solid Cr(III).

Previous work (McGuire et al. 2007) has explored a spent WBAX commonly used for Cr treatment (SIR700). XANES demonstrates that the sorbed Cr(VI) is reduced to Cr(III). It is unknown what the electron donor is, but speculated to be the polymeric resin backbone or the ion exchange functional groups. SEM images show that the Cr(III) is distributed through the resin structure and is not localized. XRD show that the Cr(III) is amorphous. XRF showed that the resin has high affinity for Cu also. They observe that Cr removal capacity is greater at pH 6 than 7 due to the ion having a -1 charge instead of -2 and taking up fewer ion exchange sites, protonation of the weak base anion exchange groups, as well as lower competition from hydroxide ion.

Other recent work (Chaudhary and Farrell 2015) has demonstrated regenerating nano-composite sorbents embedded with iron nanoparticles that use either strong base or weak base anion exchange resins as the parent material. In that work the FeWBAX could be regenerated using only NaOH, whereas the FeSBAX required both NaOH and NaCl to regain sorption capacity. In that study the sorbents were loaded only with As, and therefore only the iron nanoparticles required regeneration. It is still unclear how the anion exchange functional sites were behaving, how it would be different if co-loaded with an anion that sorbed via ion exchange like Cr(VI), and how precipitated Cr(III) could be removed. It does validate the hope of regenerating composite sorbents, and corroborates the approach of using mixed regenerants.

This chapter aims to show if MOx-WBAX can remove hexavalent chromium and arsenic from water in challenging flow through conditions, and if so identify the removal

mechanism. It hypothesizes that during treatment of co-occuring pollutants using MOx-WBAX, the hexavalent chromium is removed by anion exchange and the arsenic is removed by metal oxide sorption. The approach is to use column testing of the Ti-WBAX and Fe-WBAX resins and compare it to that of WBAX and MO. Comparing breakthrough curves and pollutant removal capacities of the hybrid resins to standard sorbents could indicate if simultaneous removal on hybrid sorbent is competitive, additive, or even synergistic. If the hybrid resins have a similarly shaped breakthrough curve for one pollutant as the standard sorbent, that might indicate a similar removal mechanism is at work.

2. METHODOLOGY

Both the Ti-WBAX (Column A) and Fe-WBAX (Column B) were synthesized using a 10% precursor concentration solution using Amberlite PWA7 as the parent resin. For the Ti-WBAX the hydrolysis time was 24 hours with no acid post rinse. The Fe-WBAX did have an acid post rinse. Other details of synthesis are elaborated in Chapter 5. These synthesis conditions were chosen based on low environmental impacts as shown in Chapter 6 and high pollutant removal capacity as shown in Chapter 5. PWA7 (Column C) and E33 (Column D) are commercially available sorbents that were used as received.

Glass columns 1.5 cm inner diameter were prepared with glass beads, glass wool, sorbent, glass wool, and glass beads. Each column contained 20 mL of sorbent, giving a bed depth of 12 to 13 cm. This was equivalent to between 22 and 26 g of saturated sorbent. Columns were operated in downflow at a target influent pump rate of 8 mL/min,

giving a target empty bed contact time of 2.5 minutes. Pump rates did fluctuate slightly over the 2 month operation period but were monitored daily and re-adjusted as needed.

Influent was prepared by filling a 330 gallon tank with municipal tap water that had been dechlorinated with a carbon filter. It was spiked with 0.4 µM Na_2HAsO_4 (30 ppb As(V)) and 0.4 µM $K_2Cr_2O_7$ (21 ppb Cr(VI)). All four columns were operated simultaneously while drawing influent from the same tank, and were run continuously through the duration of the experiment to avoid on/off effects. The tank was refilled when it became depleted at 13,000 bed volumes and again at 25,000 bed volumes. Influent conductivity ranged between 1.27 and 1.49 mS/cm, and pH ranged from 7.9 to 8.2. In order to compare this matrix to previous experiments, batch equilibrium bottle tests were done with this water matrix and the sorbents under investigation using previously described methodology.

Influent and effluent samples were taken periodically through the column run. Metal analysis samples were acidified to 2% nitric acid, stored in a refrigerator, and analyzed for total Cr and total As by ICP-MS within 21 days. Ion analysis samples were stored in a refrigerator, filtered with a 0.7 µm glass fiber membrane, and analyzed by IC (Dionex 2000) within 21 days.

After completion of the column testing, the spent sorbents were digested to recover sorbed constituents. This was completed by removing 50 mg dry weight of sorbent from the top, one-third depth, two-third depth, and bottom of the column. Each sample was placed in a microwave digestion vessel, added 9 mL nitric acid and 1 mL hydrochloric acid, and allowed to predigest overnight. Then each sample was sealed and heated in a microwave (MARS XPRESS) at 1600 W power ramping to 175°C over 15

minutes, then holding at 175°C for 10 minutes. Digested samples were diluted to 4% acid and screened by ICPMS for 61 metals.

3. RESULTS

Cr and As breakthrough curves for each of the columns are shown in Figure 8.1. The TiWBAX removed both pollutants for the first 2,000 bed volumes (BVs). Then the As started to breakthrough sharply and reached complete exhaustion by 10,000 BVs. The Cr broke through gradually and only reached 80% exhaustion by 35,000 BVs. The FeWBAX removed both pollutants for 1,000 BVs. Then the As started to breakthrough sharply and reached exhaustion by 4,000 BVs. The Cr broke through gradually and reached exhaustion at 35,000 BVs. The WBAX was exhausted for As within 400 BVs, and broke through gradually for Cr reaching 75% exhaustion at 35,000 BVs. The MO broke through for Cr within 400 BV's and released any that was sorbed (chromatographic peaking) over the subsequent 1,000 BVs. It broke through gradually for As reaching 85% exhaustion at 35,000 BVs.

Measured as the difference between influent and effluent (area above the curve) normalized to sorbent dry weight, the TiWBAX removed 14.2 µmol/g of Cr and 5.0 µmol/g of As. The FeWBAX removed 19.0 µmol/g of Cr and 1.9 µmol/g of As. The WBAX removed 24.9 µmol/g of Cr and 0.5 µmol/g of As. The MO removed 0.0 µmol/g of Cr and 7.6 µmol/g of As.

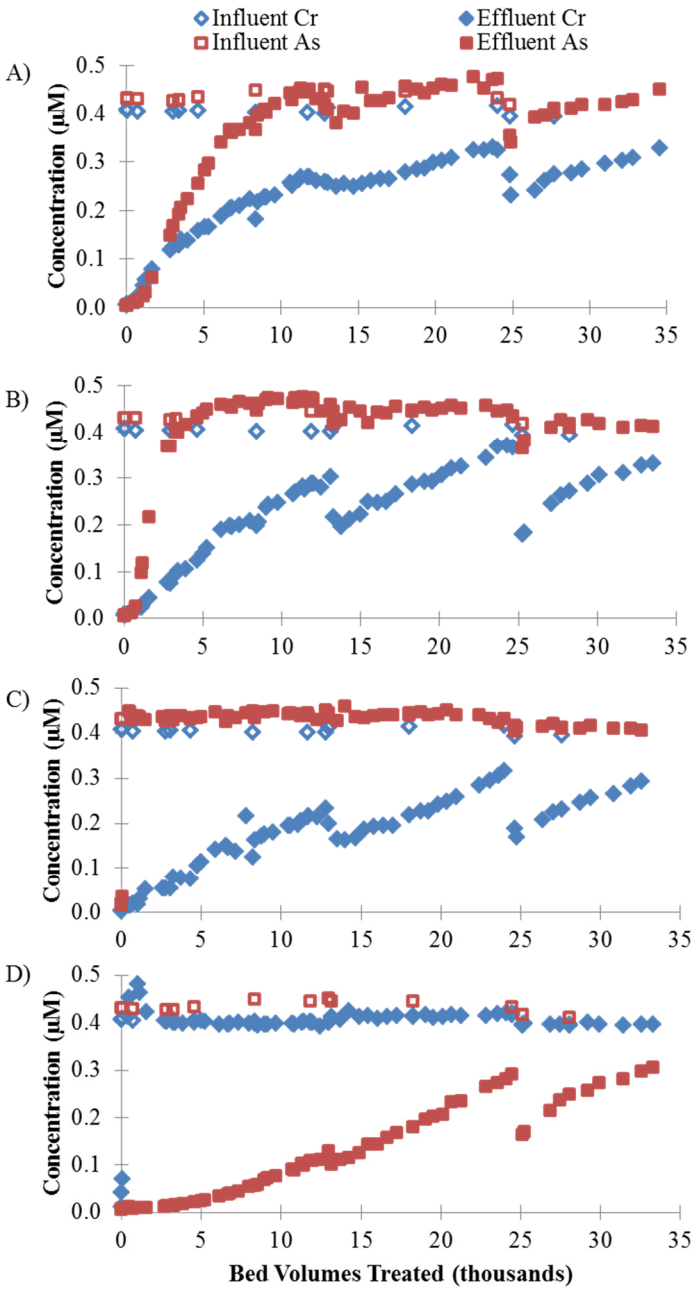

Figure 8.1. Hexavalent chromium and arsenic breakthrough curves for A) TiWBAX, B) FeWBAX, C) WBAX, and D) MO. Columns contained 20 mL of sorbent and had 2.5 minutes of empty bed contact time. Influent conductivity was 1.4 mS/cm and pH was 8.0. Columns were run continuously from the same influent tank that was refilled at 13,000 and 25,000 bed volumes.

Figure 8.2 shows the mass of metals detected in the digested raw and spent sorbents normalized to dry mass averaged for the entire column depth. Only 19 of the 61 metals were detected and are illustrated. The mass of Cr found increased from non-detect in the raw sorbent to between 0.10% (mass/mass) and 0.15% for the spent TiWBAX, FeWBAX, and WBAX. The mass of As found increased from non-detect in the raw sorbents to 0.02% in FeWBAX and 0.13% in the MO. Na, Mg, Si, and Ca were detected in all samples and generally showed slightly lower levels in the spent sorbent than in the raw sorbent. Significantly high levels of Al, V, Ni, Cu, and Zn were found in all of the spent sorbents with none in any of the raw resins. Cu in the spent sorbents had the highest mass detected of all metals (excluding Fe measured in the Fe-based sorbents), ranging from 0.33% – 2.2% of dry mass. Generally the next highest was Zn at 0.27% – 0.78% in the spent sorbents, then Al at 0.04% – 0.78% in the spent sorbents. All three were detected at higher levels than the target pollutants Cr and As. Very little Ti was found in any of the digestates, including for TiWBAX. That is to be expected since Ti is not soluble in nitric acid and a much higher mass would likely have been found with a digestion using hydrofluoric acid. The other metals of interest are nitric acid soluble.

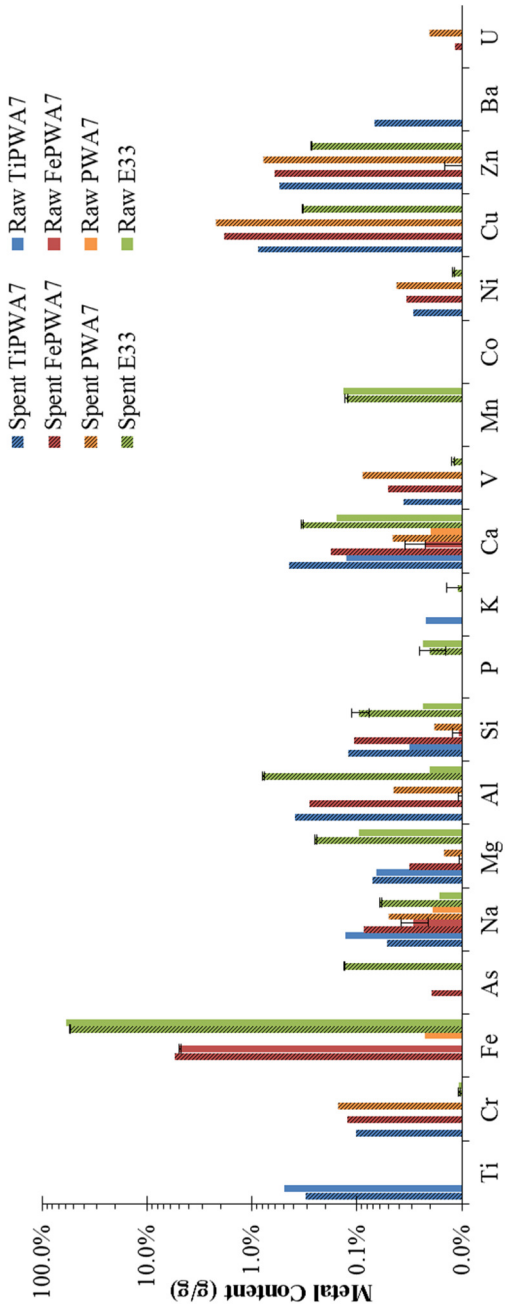

Figure 8.2. Mass of detected metals in raw and spent sorbents normalized to dry mass. Digested in nitric/hydrochloric acid by microwave heating. Another 42 metals were analyzed but not detected. Spent sorbent values are averaged over four samples taken at various column depths. Error bars show two standard deviations where triplicate sets of four samples were taken.

As a comparative experiment, batch testing was conducted with the four sorbents in the same water matrix as the column testing. This allowed comparison between column and batch testing results, as well as comparison to previous batch tests conducted in simulated groundwater or deionized water. The results of this batch test are shown in Figure 8.3. The observed data was used to generate Fruendlich isotherm parameters, then the parameters were used to calculate a sorption capacity at 0.4 µM pollutant concentration (the same as the column influent). The TiWBAX has pollutant removal capacity of 3.2 µmol/g for Cr and 3.3 µmol/g for As. The FeWBAX has pollutant removal capacity of 4.5 µmol/g for Cr and 2.3 µmol/g for As. The WBAX has pollutant removal capacity of 6.1 µmol/g for Cr and 0.0 µmol/g for As. The MO has pollutant removal capacity of 0.0 µmol/g for Cr and 3.5 µmol/g for As.

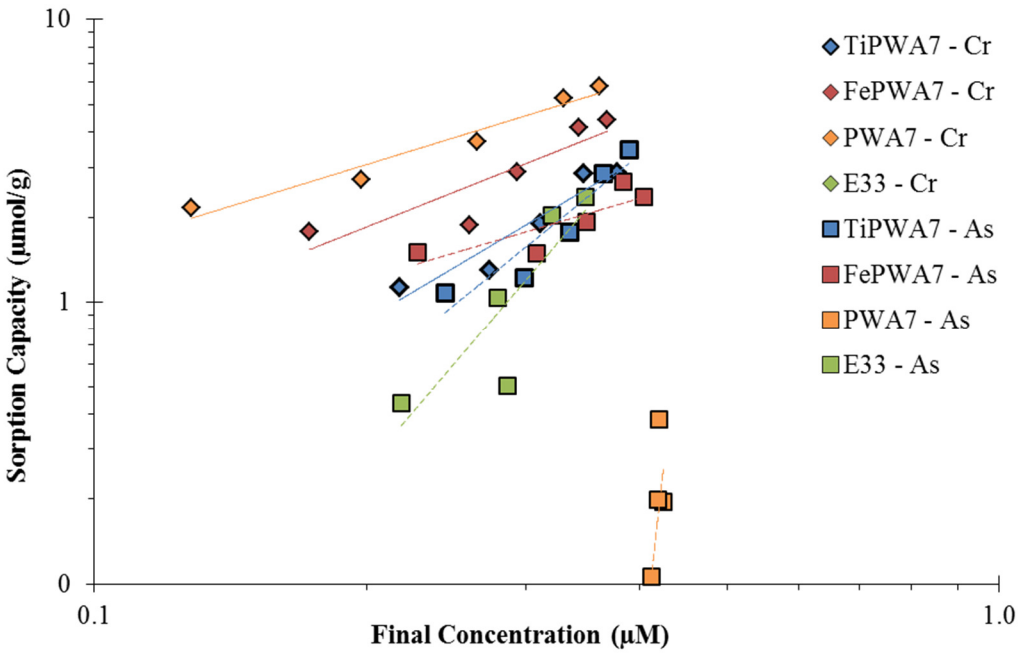

Figure 8.3. Equilibrium batch test results conducted in the same water matrix and pollutant concentrations as the column testing.

4. DISCUSSION

Both the TiWBAX and the FeWBAX showed very similar breakthrough curves as the parent WBAX in terms of shape and duration. This suggests that the primary sorption mechanism for each of the three sorbents was the same, presumably ion exchange. It also shows that the iron or titanium hybridization process does not reduce Cr removal capacity. The added metal nanoparticles do not seem to inhibit Cr sorption in any way, nor do they synergistically augment it in any way.

Adding the metal nanoparticles did successfully add As removal capacity in the TiWBAX and FeWBAX compared to the parent WBAX. This suggests that the removal mechanism for As on the hybrid resins was not ion exchange like the WBAX. However the As breakthrough curves for the hybrid sorbents did not demonstrate the same shape nor duration as the MO curve. If the removal mechanism is sorption to metal oxide like the MO, it is perhaps inhibited in some way. This apparent inhibition could be a function of metal content. The MO sorbent has 89% metal oxide content whereas the TiWBAX has 16% and the FeWBAX has 8%. The MO sorbent had 6 – 11 times more metal oxide content but only absorbed 1.5 – 4 times more As. This shows that even though the MO had a higher removal capacity the metal oxide in the hybrid sorbents was being utilized more efficiently.

4.1 Potential partial regeneration. A unique and unexpected feature of each breakthrough curve is that each shows a dip corresponding to when the influent tank was refilled. Both the Cr and As curves exhibit a decrease in the amount of pollutant in the effluent, which could be interpreted as a partial sorbent regeneration or restored pollutant

removal capacity. No significant difference in column operation, Cr or As influent concentrations, pH, or conductivity were observed before and after refilling.

It is not understood what caused this partial restoration of pollutant removal capacity, but discovering and harnessing whatever happened may be the key to unlocking the ability to regenerate and reuse hybrid resins and WBAX in general. It could inform the pollutant removal mechanism, and the ability to reuse the sorbent could reduce the overall environmental impact of its use compared to the current practice of single pass through followed by transportation and disposal.

Two possible causes of the partial regeneration are theorized and future work proposed in the following section seeks to prove or disprove them each. The first possibility is that the partial regeneration could be due to the presence of oxidants. Residual chlorine in the influent would have volatilized during long term storage in the influent tank (days to weeks). The oxidation potential of the influent water would be low as it entered the column bed, providing conditions favorable for precipitation of Cr(III) on the resin. When the tank was refilled, any residual disinfectant in the refilled water would have raised the oxidation potential that could then oxidize the precipitated Cr(III). This would open functional sites to allow for future sorption and allow access to blocked internal pores for internal diffusion. Ability to regenerate an ion exchange resin with a widely available chemical such as chlorine would be remarkable.

The second possibility is that co-occurring metals in the influent could cause the regeneration. High levels of copper and other metals were found sorbed to the spent resins (Figure 8.2). These were presumably introduced into the system from the refill tap water that came through copper pipes. This metal could have precipitated on the sorbent.

Similarly to the function of the MOx nanoparticles, the precipitated metals would create fresh sorption surface allowing additional pollutant removal.

4.2 Comparing experimental results. The mass of pollutant removed from solution in the column test can be compared to that found in the spent sorbent digestion. The TiWBAX removed 5,762 µg Cr and 2,916 µg As in column testing. Digesting recovered 6,838 µg Cr and 597 µg As (+19% and -80% error respectively). The FeWBAX removed 5,845 µg Cr and 859 µg As in column testing. Digesting recovered 6,874 µg Cr and 994 µg As (+18% and +16% error respectively). The WBAX removed 7,492 µg Cr and 231 µg As in column testing. Digesting recovered 7,640 µg Cr and 12 µg As (+2% and -95% error respectively). The MO removed 10 µg Cr and 14,241 µg As in column testing. Digesting recovered 2,872 µg Cr and 33,730 µg As (+28,620% and +137% respectively).

Generally, the mass of pollutant on the spent resin found by digestion was consistent with mass removed by the column. Error from the digestion method is attributed to the large dilutions required for analysis. This is particularly evident in the mass of Cr supposedly recovered by the MO. Even though little more than the analytical detection limit of Cr was measured, after the large dilution factor was applied it appears to be a large number compared to what was removed by the column. Error from the column method is attributed to interpolating mass removed and flow rates in between sample points. Error cannot be attributed to pollutant already sorbed to the sorbent because no Cr or As was found on the raw sorbents upon digestion.

Sorbent capacity determined by batch testing to column testing is next compared. The TiWBAX column removed 14.2 µmol/g of Cr and 5.0 µmol/g of As. Batch testing

predicts pollutant removal capacity of 3.2 umol/g for Cr and 3.3 umol/g for As. (-77% and -34% error, respectively). The FeWBAX column removed 19.0 µmol/g of Cr and 1.9 µmol/g of As. Batch testing predicts pollutant removal capacity of 4.5 umol/g for Cr and 2.3 umol/g for As (-76% and +21% error, respectively). The WBAX column removed 24.9 µmol/g of Cr and 0.5 µmol/g of As. Batch testing predicts pollutant removal capacity of 6.1 umol/g for Cr and 0.0 umol/g for As (-75% error for Cr). The MO column removed 0.0 µmol/g of Cr and 7.6 µmol/g of As. Batch testing predicts pollutant removal capacity of 0.0 umol/g for Cr and 3.5 umol/g for As (-54% error for As).

Sorption capacity demonstrated in column mode is nearly always 2 – 5 times higher than that shown in batch mode. Numerical results obtained from these two testing methods are of course not truly fairly compared because different sorption drivers are at play. For example, in column mode the pollutant concentration is continually replenished, whereas in batch it reduces as pollutant is sorbed. Kinetics and intraparticle diffusion play critical roles in column mode sorption, compared to batch testing which has been given sufficient time to reach pseudo-equilibrium conditions. However the trends demonstrated between the two methods are informative, including relative performance of the sorbents compared to eachother, and relative contaminant preference shown for each sorbent.

Lastly, batch results conducted in the dechlorinated tap water column influent are compared to previous batch tests conducted in simulated groundwater. Using the Fruendlich isotherm parameters presented in Chapter 5 and a pollutant concentration of 0.4 µM, the TiWBAX has a pollutant removal capacity in simulated groundwater of 4.6 µmol/g for Cr and 3.7 µmol/g for As. The dechlorinated tap water results are -30% and -11% relative error respectively compared to the simulated groundwater. The FeWBAX

has a pollutant removal capacity of 9.1 µmol/g for Cr and 5.2 µmol/g for As (-51% and -56% error respectively). The WBAX has a pollutant removal capacity of 19.1 µmol/g for Cr and 0.0 for As (-70% error for Cr). The MO has a pollutant removal capacity of 0.0 µmol/g for Cr and 4.1 µmol/g for As (-15% error for As).

In all cases the sorbents performed better in simulated groundwater than in dechlorinated tap water. There are multiple reasons why this could have happened. Most likely this is a function of starting concentration. The simulated groundwater batch tests were conducted with a starting concentration of 2 µM pollutants, whereas the tap water tests were conducted with a starting concentration of 0.4 µM pollutants. Even though the calculated capacities were projected to 0.4 µM in both cases, the higher starting concentration for the simulated groundwater would provide a higher gradient to drive sorption and cause higher energy sorption states. This underscores the importance of conduction batch tests at the same concentration to have truly comparable results. Another reason for the higher capacities could also be that the dechlorinated tap water would have some fraction of organic content whereas the simulated groundwater has only inorganic constituents. The organic constituents could interfere with sorption in unexplored ways.

5. FUTURE WORK

The answers to the questions that have been discovered in this dissertation are hopefully valuable in advancing the state of science for nano-composite sorbents and simultaneous pollutant removal, but also inspire further questions to address in the future. This section explores questions and proposes experiments that continue this line of

research. The focus is on further developing understanding of the pollutant removal mechanism and to explain the observed partial regeneration in order to unlock the ability to regenerate MOx-WBAX resin.

Hypotheses that can be considered in the future include:

- Hexavalent chromium is reduced to trivalent chromium on the surface of WBAX (or MOx-WBAX) and precipitated, while resin polymer is oxidized.
- MOx-WBAX can be regenerated in a three-step process of caustic rinse, a strong oxidant rinse, then an acid rinse.

5.1 Explore the removal mechanism. To explore the mechanism of removal the total ion exchange capacity could be measured via standard acid titration methodology before and after nano-metal impregnation. If the total exchange capacity has not been significantly reduced this will support the idea that the metal nanoparticles do not take up exchange sites themselves. This capacity would be compared to the pollutant removal capacity observed in column testing in the preliminary data. The removal mechanism hypothesis would be further explored by comparing the charge concentration of pollutants removed from treated water with the charge concentration of counterion introduced to the treated water from the column test. If the counterion concentration is similar to the concentration of chromate removed but not the total concentration of chromate plus arsenate removed, it would support that one pollutant is removed by a mechanism other than ion exchange (presumably by sorption).

Previous batch equilibrium tests could be further examined using a Dubinine-Radushkevich isotherm model. Using linear regression this model estimates a free energy

of sorption constant, E, which is the free energy change when 1 mole of ion is transferred to the surface of a solid (Landry et al. 2015). E values of $8 < E < 16$ kJ/mole indicate pure ion exchange mechanisms of sorption, while E values $E<8$ indicate van der Waals interactions (Alberti et al. 2012, Antonio et al. 2004, Dominguez et al. 2011, Mahramanlioglu et al. 2002)

5.2 Spent sorbent imaging. To explore the mechanism of removal and oxidation state of the sorbed pollutants, elemental mapping images of the parent resin, the hybrid resin, and spent hybrid resin could be explored by SEM and NanoSIMS. The images of the hybrid resin would describe the location of metal nanoparticles through the polymeric structure. The images of spent resin would locate where the removed pollutants ultimately reside, and correlations hopefully will emerge such that concentrations of one pollutant are coincident with locations of metal oxide nanoparticles. Other characterization tools could also be used including XAFES and XRD. This will identify the crystalline mineralogy of the embedded nanoparticles and the oxidation state of sorbed Cr and As. This would indicate if Cr(VI) is in fact reduced and precipitated on the surface as opposed to sorbed by ion exchange as Cr(VI), and if a similar process does or does not happen to As.

5.3 Jar tests for mechanism. A set of equilibrium experiments to elucidate the fundamental mechanism of pollutant removal could be conducted. First, hexavalent chromium would be mixed in a jar test with tertiary amines in different forms, such as aqueous dimethylamine or coagulant polymers with tertiary amine groups. This would be done with and without acidification, then measure results using spectrophotometry with the diphenylcarbohydrazide method to analyze reactive Cr(VI) (10-700ppb quantification

limit). It would show that chromium is reactive with tertiary amines and that tertiary amines do require acidification to become ionized and able to perform ion exchange. More importantly it would show that the tertiary amines by themselves do or do not reduce hexavalent chromium to trivalent chromium.

A similar test could be done mixing aqueous hexavalent chromium with solid trivalent chromium. The solid trivalent chromium experiment would show if adsorption and precipitation on previously sorbed chromium is a mechanism for further chromium removal. This could demonstrate what is happening on the surface of the polymeric resins after hexavalent chromium is reduced, explaining if removal after that is due to opening up the ion exchange site for future removal or if it is adsorbed directly on the precipitated metal.

Another test mixing chromium and chlorine could be conducted. The chlorine experiment would demonstrate if an oxidant can restore the reactivity of the precipitated trivalent chromium. It is discussed further in the following section since it connects to column regeneration.

A last jar test mixing hexavalent chromium and arsenic and precipitated copper could be performed. Copper is of interest since high amounts were found sorbed to the spent sorbent in the column test (see Figure 8.2). This would be done by making a solution of aqueous copper, then adding a precipitating agent. After enough time to allow some precipitation, it would be spiked with hexavalent chromium and arsenic. Reactive Cr(VI) concentration and arsenic would be measured over time. This would show if Cr(VI) or As sorbs to (or is somehow reduced by) freshly precipitated copper. Results would serve as a null hypothesis that the pollutant removal is not actually due to

precipitated metal commonly found in tap water completely inconsequential to the performance of the hybrid sorbent.

If the tertiary amine group in absence of resin is not able to reduce Cr(VI) to Cr(III), it would corroborate that the polymeric resin backbone is the electron donor. However, by itself this would not indicate why this phenomenon is observed on only WBAX and not SBAX. This implies that an unknown component of the polymeric resin backbone that is unique to WBAX does so. Product data sheets for Amberlite PWA7 and ResinTech SIR-700, two chromate specific WBAX resins known to precipitate green chromium, list the polymer structure as “cross linked polycondensate” and “epoxy polyamine” respectively. These are common descriptors used by many ion exchange resins and do not give any clue what polymeric constituents or crosslinking agents could be the unique reducing agent. As these constituents are likely proprietary information it will then be unlikely to be able to prove exactly what specific constituent is the electron donor. Carrying out these jar tests in absence of resin will at least prove or disprove that the resin backbone is vital to the reaction occurring.

If it is found that the resin is required to reduce Cr(VI) to Cr(III), an increase in DOC would be observed in the column effluent. This would need to be tested in very low DOC water since the increase would be very small compared to the amount of DOC commonly found in surface water. If it is found that the tertiary amine group itself is reduced, then an increase in ammonia would be observed in the effluent.

An additional experiment that could show the electrons are coming from the resin is to electrically ground the resin and prevent the transfer from occurring. This is the same thing that is done when imaging ion exchange resin by SEM by coating the resin in

silver epoxy to conduct electrons away and prevent image whitening. An experiment should be run by connecting the resin column to a conductor that prevents electrons from the static polymeric backbone from reaching sorbed Cr(VI). That would further show that the polymeric structure itself is the reducing agent as opposed to a surface concentration gradient.

A null hypothesis is that the chromium is reduced by organics in the bulk influent solution. This could be tested by performing the column test in highly purified water with high oxidation potential. Then if the Cr(VI) is still reduced it is shown to be inherent to the function of the sorbent. But if the Cr(VI) is not reduced under the same conditions that it would have been reduced by tap water it shows that bulk water constituents participate in the reduction reaction.

5.4 Column regeneration tests. Some column regeneration experiments could be conducted to inform the removal mechanism. A few columns of hybrid sorbents will be saturated with both arsenic and hexavalent chromium. The first experiment will be to try to regenerate them using individual solutions of chloride, caustic solution, and mixed chloride/caustic solution. If the chloride solution shows that the chromium removal capacity has been replenished without replenishing arsenic capacity, it will suggest the ion exchange was regenerated and chromium is primarily removed in this manner. Similarly, if the caustic solution regenerates the metal hydroxide surfaces such that arsenic capacity is restored but not chromium, it will suggest that is the primary mechanism of removal for that pollutant. This experiment may have a fatal flaw though if the parent WBAX is not regenerable to start with. It will work if the Cr(VI) is sorbed by

ion exchange, but will give a false negative if the Cr is reduced to Cr(III) and precipitated as previously suggested. This means that additional steps involving oxidation are needed.

Hence is the proposed hypothesis that caustic, oxidant, and acid are required to fully regenerate the column. The caustic rinse intends to strip sorbed arsenic from the metal nanoparticles and regenerate the arsenic removal capacity. Unfortunately this will also "un-functionalize" the tertiary amine ion exchange groups, similar to that observed during the hybrid synthesis process. The second rinse with strong oxidant, such as chlorine, will oxidize and remove the precipitated trivalent chromium. Lastly the acid rinse will restore the ion exchange capacity of the tertiary amine ion exchange groups for restored hexavalent chromium removal capacity. This regeneration scheme will be analyzed with life cycle assessment to verify that the environmental impact of such a chemically intense regeneration procedure is still lower than synthesizing new sorbent. Therefore the second regeneration experiment that will be run will seek to verify the effects of each step in the proposed regeneration procedure by comparing column test performance of spent sorbent that has undergone only one, two, or all three of these steps. If this procedure still does not restore Cr(VI) removal capacity, a possible salt rinse step can be added with the intent to displace the chromate from the ion exchange functional groups.

To verify that a strong oxidant such as chlorine can oxidize the precipitated Cr(III), this could be tested in the absence of the resin. Cr(III) could be precipitated in an aqueous solution using a supersaturation of salts or by causing reduced conditions through lowering the dissolved oxygen by bubbling nitrogen gas. Into various bottles will be added known doses of chlorine, including a zero dose as a control. Under reduced

conditions the equilibrium state for Cr in water is as $Cr_2O_3(s)$ which is Cr(III) and green in color. Increasing the oxidation potential of the solution by the presence of chlorine will shift the equilibrium higher to CrO_4^{-2} which is Cr(VI). I will measure the concentration of Cr(VI) spectrophotometrically.

6. CONCLUSIONS

This study has shown:

- The hybrid nano-composite sorbents that were optimized for environmental performance and sorbent characteristics can remove Cr(VI) and As(V) simultaneously from a challenging water matrix in packed bed flow through testing. It required little operational attention and no pH adjustment, confirming the applicability for use in small systems.
- The addition of iron or titanium nanoparticles does not reduce the capacity of the parent WBAX resin to sorb Cr(VI) compared to the WBAX resin.
- Similarly shaped Cr(VI) breakthrough curves demonstrated by the FeWBAX and the TiWBAX as the WBAX resin suggests that the mechanism of removal on the nano-composite sorbents is still anion exchange.
- Co-constituents in the influent also sorb to the sorbent and possibly reduce the sorbent capacity for the target pollutants. The most highly sorbed co-constituents were Cu, Zn, and organic matter from tap water (especially as compared to simulated groundwater with only inorganic constituents).

CHAPTER 9

DISSERTATION SYNTHESIS

INTRODUCTION

The purpose of this chapter is to summarize the dissertation and answer the research questions and hypotheses that have been presented. The next section "Associated Products" presents tangible accomplishments achieved while producing this research. Next, "Answering the Research Question" demonstrates how the research answered the original overarching research question. Finally, "Broader Impacts" supposes how this work can affect the water industry, science, and society. It provides concluding take away messages for different water industry stakeholders.

ASSOCIATED PRODUCTS

This work has been in development for five years. During that time it has produced deliverables, accomplishments, and been disseminated in various forms. This is a review of the tangible products and achievements that are associated with this work.

Research funding. As a graduate student I have been awarded $126,000 in research grants, $159,580 in school-sponsored fellowships, and $50,680 in private scholarships.

***Awarded research grant*.** The research presented in this dissertation was funded by the United States Environmental Protection Agency Science to Achieve Results (STAR) Fellowship for Graduate Environmental Studies. This nationally competitive fellowship supports outstanding graduate students specializing in the environmental arena. The application underwent multiple layers of review and included a five page

research proposal, a two page personal statement, three letters of recommendation, and a curriculum vitae. It was worth up to $42,000 per year for up to three years to cover tuition, expenses, and living stipend.

My grant is titled “Simultaneous Removal of Inorganic Pollutants by Sorbents for Small Drinking Water Systems”. The application was submitted to EPA-F2013-STAR-E1: Drinking Water in Fall 2012, awarded in Spring 2014, and funding began in Fall 2014. The research proposes to develop the science and technology of sorption processes for simultaneous removal of inorganic pollutants. The focus is on inorganic pollutants due to their occurrence and toxicity in groundwater. The context is small drinking water systems due to the disproportional health risk people served by these systems face. It is novel since it develops simultaneous removal of multiple pollutants instead of standard competition. As an EPA STAR fellow, the goal is to develop water treatment technology and scientific understanding, and disseminate the research results for widespread benefit to human health.

The grant included three thrusts:

1. Commercially available sorbents designed for specific pollutant removal have limited ability to simultaneously remove multiple inorganic pollutants.
2. Hybrid media synthesized by iron nanoparticle impregnation to anion exchange resin can simultaneously remove multiple inorganic pollutants.
3. Hybrid media removes As through iron adsorption and is diffusion limited, while Cr is removed through anion exchange and is capacity limited.

The first thrust sought to answer whether hope of simultaneous removal of important groundwater contaminants already exists or if it needs to be developed. This intended to have the broad impact of informing residents of small communities of their current options to provide safe drinking water. It also allowed water treatment systems that already utilize these sorbents to understand the possible side health benefits they are experiencing. The second thrust sought to answer if an anion exchange resin with a high capacity to remove one pollutant can maintain that capacity after metal oxide impregnation. This would show that simultaneous removal capacity can be cumulative or even synergistic as opposed to competitive. The impact of this finding would be to drinking water treatment systems that currently use any of these resins to know that removal of other pollutants can be achieved by use of hybrid media. The third thrust sought to answer what mechanism removes multiple pollutants in hybrid media. This answer would enable scientists to optimize resin synthesis for multiple pollutant removal. It would impact small systems by predicting performance of hybrid resins for preliminary screening without need for extensive laboratory or pilot experimentation. Results of the overall research would maximize the potential for broader impacts by widely disseminating the results through publication in peer reviewed journals, presentations at specialized conferences, and presentations for generalized audiences.

Submitted grant applications. Previous to being awarded the 2013 EPA STAR fellowship, I submitted four research grant applications for similar fellowships that were not funded. I submitted applications to each the Graduate Fellowship Research Program (GRFP) sponsored by the National Science Foundation and the STAR Fellowship for Graduate Environmental Studies sponsored by the Environmental Protection Agency in

both Fall 2010 and Fall 2011. I prepared each proposal in conjunction with my advisor Dr. Paul Westerhoff. He supplied the premise for the research project and at least one written review of the submittal materials. I carefully studied review comments from each application for the improvement of subsequent applications. I also obtained non-technical reviews before submittal from the department grant writing specialist.

Other awards. The school-sponsored fellowships I have received include the Dean's Fellowship supplied by the School of Sustainable Engineering and the Built Environment, and Research Assistant support from research grants awarded to my advisor Dr. Paul Westerhoff. These fellowships provided tuition waivers, health insurance, and a living stipend.

I have been awarded 17 private scholarships funded by generous private donors and professional associations pursuant from over 45 submitted applications. The most prominent awards are the Ron & Sharon Thomas Fellowship, the Achievement Reward for College Scientists (ARCS) Fellowship, and the AZ Water Association Scholarship. The Thomas Fellowship is intended to support a non-traditional doctoral student in ASU's Ira A. Fulton Schools of Engineering. Dr. Ron Thomas completed his doctoral degree from ASU in mechanical engineering while raising a young family. After a successful and impactful career in designing aviation instrumentation, he along with his wife Sharon provide this generous fellowship to pay it forward to other young engineers. The ARCS Foundation is a national organization that boosts American leadership and aids advancement in science and technology. The local member who sponsored my fellowship is Irene Douglas, a long-time member who has helped many graduate students and the advancement of science in Arizona. The AZ Water Association is a professional

association for water professionals that has provided many opportunities to disseminate my research, network with industry professionals, and participate in educational outreach activities. Together, these scholarships have funded personal expenses while a graduate student, allowing me to forego getting an outside job and focus on my studies. The most invaluable impact was therefore to allow me to succeed at school while still having time for my young family.

Publications. As a graduate student I have published one original research peer reviewed scientific journal article entitled "Phosphorus Recovery from Microbial Biofuel Residual Using Microwave Peroxide Digestion and Anion Exchange". The full citation is below. This paper was created as a master's thesis, grew with some additional lab work, and was further refined by co-author reviews and peer reviewer comments. The final form is also included in this document as Chapter 3.

- Gifford, M., Liu, J., Rittmann, B.E., Vannela, R., Westerhoff, P., 2015. Phosphorus Recovery from Microbial Biofuel Residual Using Microwave Peroxide Digestion and Anion Exchange. Water Research 70, 130-137. DOI:10.1016/j.watres.2014.11.052.

Many lessons were learned from this research. I learned the value of working on an interdisciplinary team to create novel research. This collaboration involved microbiologists, engineers, and ecologists and helped developed technology at the interface of all these traditional disciplines. This interdisciplinary effort did come with various challenges too. It required me to become familiar with physical laws, methods, bodies of literature, and processes that were outside my area of specialty, which took extra effort and time. It also was difficult to find the right journal for publication. While

the paper was construed around biotechnology and green energy, the core processes being investigated were water treatment. That may have contributed to the journals seeming to have difficulty finding qualified peer-reviewers, ultimately resulting in three biotechnology-focused journals declining to publish it before a water-focused journal accepted it.

It is my intent to publish the other chapters of this dissertation that contain original research in peer reviewed scientific journals. Chapters 4 through 7 are presented in this dissertation as draft manuscripts ready for review with co-authors and imminent journal submission. Chapter 8 requires some further research, story development, and manuscript preparation, but this document will still aid in its eventual publication.

Presentations. I have given eight peer reviewed scientific conference presentations related to my research as a graduate student. Two were at a national level conference (WQTC 2014, SNO 2015), one at a regional level conference (ICS 2013), and five at state level conferences (AZWater and GPSA). Presenting at these conferences has represented Arizona State University as being on the cutting edge of technology development. I have gained very valuable feedback on my research, which I have been able to use to direct the future development. It has opened networking and collaboration opportunities with other treatment professionals and testing on real world waters with public utilities. Conference presentations has been a very valuable tool to disseminate research.

In addition I have given six invited lectures and 12 poster presentations regarding my research. Invited lectures include lunch seminars on multiple university campuses. Poster presentations include local, state, and national level conferences. These lectures

are usually a longer and more casual format compared to conference talks. The poster presentations are a much more personal interaction with the audience, which allows the chance to adapt the message to his or her level of interest and understanding. They also provide an opportunity to attend conferences in more interdisciplinary settings where I would not be comfortable giving a full talk to specialists in their field of expertise, but still appreciate sharing my thoughts and hearing their input. Both of these forms of dissemination have led to good feedback guiding my research and practice presenting my data in a clear fashion.

ANSWERING THE RESEARCH QUESTION

The objective of the proposed research is to address the overarching question: *Can synthesis methods of hybrid nano-sorbents be improved to increase sustainability and feasibility to remove multiple inorganic contaminants simultaneously from groundwater compared to existing sorbents?* Here each research question and hypothesis is reviewed to clearly identify how it contributes toward answering this question, and therefore how each chapter builds upon each other to create a cohesive overall story.

Research Question 1 deals with recovering the inorganic oxygenated anion phosphate from a complex organic matrix. A hybrid nano-enabled sorbent with iron nanoparticles embedded into a strong base anion exchange resin was compared to a standard strong base ion exchange sorbent. I found that the hybrid sorbent could remove 98% of the influent phosphate in column mode, and the ion exchange sorbent captured 87%. However, the hybrid resin only released 23% of the P upon regeneration, and the ion exchange resin released 50%. This **confirmed** Hypothesis 1. From a recovery and

reuse point-of-view it is concluded that the standard sorbent worked better. But by shifting the paradigm to removal, the hybrid sorbent demonstrated a high affinity and capacity to remove inorganic contaminant even from a complex aqueous matrix. This contributes to answering the overarching research question by understanding that a hybrid sorbent has a higher capacity to remove an inorganic pollutant than an existing sorbent.

Research Question 2 then sought to quantify how well the currently available sorbents can remove multiple inorganic contaminants. Industry-leading sorbents were compared to hybrid sorbents synthesized by existing methodology for their ability to remove the oxygenated anions chromate and arsenate from a challenging groundwater matrix by via batch testing using a Simultaneous Removal Capacity (SRC). I found that the hybrid sorbents had a higher capacity to remove both pollutants simultaneously in batch mode, scoring three of the top five highest SRC scores of all sorbents tested. They also worked for a few thousand bed volumes in column mode at high influent concentrations, but struggled at low concentrations. This **confirmed** Hypothesis 2. This contributes to answering the overarching research question by verifying the potential for hybrid sorbents to remove multiple inorganic contaminants from groundwater is greater than other existing sorbents, but that the performance has opportunity to be improved.

The next questions explore if the hybrid synthesis process can be improved; first in regards to sorbent characteristics, then in regards to sustainability. Research Question 3 explored improving characteristics of the nano-composite sorbents. Various synthesis conditions were explored, such as precursor concentrations and hydrolysis times, with resulting effect on sorbent characteristics and pollutant removal ability. I found that an

acid post rinse greatly improves the ability of the Fe-WBAX sorbent to sorb chromate and arsenate. I also found that metal content and total surface area increases by increasing metal precursor concentration up to 100%. However a 10% or 50% precursor demonstrated higher pollutant removal capacity and more usable pore size distribution, inferring that too much metal blocks pores or agglomerates nanoparticles thus reducing their utility. This **rejected** Hypothesis 3. When synthesized under the correct conditions, the equilibrium chromium removal capacity had only negligible decrease while the arsenic removal capacity had significant increase compared to the parent resin. This **confirmed** Hypothesis 4. Together these findings contribute to answering the overarching question by showing how the synthesis process can be improved to increase sorbent capacity which in turn decreases environmental impact and improves multiple pollutant removal ability.

Research Question 4 anticipated the environmental and human health impacts of the hybrid sorbent life cycle normalized to the existing technology. First, the environmental impacts of using the hybrid sorbents was explored through anticipatory life cycle assessment. I found that the environmental impacts of the titanium hybrid sorbents can be reduced by altering the synthesis procedure to minimize oven heating time and chemical solvent use. The impacts of the iron sorbents could be improved by maximizing pollutant removal capacity through acid rinsing to use less sorbent to treat the same volume of water. For all environmental impact categories studied, the titanium hybrid sorbents had lower impact than the iron sorbents. This **confirmed** Hypothesis 5. The hybrid sorbents (after the environmental performance improvements) could remove multiple pollutants and therefore had a lower environmental impact for most all impact

categories than using mixed beds. This helped to answer the overarching question by proactively improving the hybrid sorbent synthesis protocol to increase sustainability.

The second part of Research Question 4 analyzed the human health impacts of treating the target groundwater contaminants. Life cycle assessment was used to compare the health burdens of producing and using processed goods to create clean water against the health benefits of drinking water with lower levels of pollutant. I found that the total number of cancer and non-cancer cases expected to be caused during the manufacture and use of water treatment energy and materials were fewer than the number of cases expected to be prevented from drinking safer water. This suggests that water treatment decreases the overall human health risk, and **confirmed** Hypothesis 6. However I also found that treatment causes significant shifts in the types and locations of those cases. The people who enjoy the health benefit of treated water are a disperse population local to the water treatment facility that avoid cancer risk. The people who bear the burden of providing that treatment are largely factory workers who produce pH control chemicals and energy required to produce them incurring non-cancer disease risk. The treatment therefore exports, concentrates, and changes the type of health risks incurred. These findings informed the overall research question by verifying that wellhead treatment of the target pollutants does provide overall benefit to human health risk, but identified that it should be done avoiding dependence on pH control chemicals to not export disease.

Research Question 5 focused on demonstrating the hybrid sorbent works for the intended purpose and shines light on the mechanism of removal for each pollutant. When employed in a packed bed flowthrough condition with challenging influent matrix, the hybrid sorbent optimized for environmental performance and sorbent characteristics

successfully removed both pollutants for a certain duration with little operational intervention and without requiring pH adjustment of the influent water. This further **confirmed** Hypothesis 4. The breakthrough for arsenic seemed to follow the same pattern as shown by metal oxide sorbents, and that for chromate followed the pattern shown by weak base anion exchange. This **supported but did not prove** Hypothesis 7. Some partial regeneration was observed by changing column influent, which may be related to increased influent copper or chlorine. The results contributed to answering the overarching question by verifying that the hybrid sorbent does demonstrate higher pollutant removal ability than existing sorbents, and because understanding how the sorbent works may illuminate further improvements to the synthesis protocol.

Looking at this work as a whole, it is clear that iron or titanium nanoparticles embedded weak base anion exchange resins do have higher affinity for and capacity to remove arsenic and chromium simultaneously from groundwater compared to existing sorbents. The synthesis methods were improved to increase sustainability through minimizing hydrolysis time and reducing mass of required sorbent. The method was improved to increase removal capacity by optimizing metal precursor concentration and using an acid post-rinse. The synthesis methods of hybrid nano-sorbents were improved to increase sustainability and ability to remove multiple inorganic contaminants simultaneously in groundwater compared to existing sorbents.

BROADER IMPACTS

The primary way that this research hopes to impact the broader community is to inspire use of different values and approaches to make water related decisions. Many of

the findings herein challenge pre-existing procedures, and those who read this may think about their own work in different ways. This applies to the focus of those who develop drinking water treatment technology, owners and operators of water treatment facilities, and regulators who decide policy that they follow.

Technology Developers. Technology developers can take away a number of findings to inspire their work. First is to strongly consider the water matrix used to test treatment efficacy. Many studies use very high pollutant concentrations and very clean water to show how well a novel technology works. This study has shown that removal efficacy can be drastically reduced in a complex organic matrix compared to deionized water (chapter 3), and in a synthetic groundwater compared to deionized water (chapter 4). A treatment method that showed high promise at lab scale with high pollutant concentration performed poorly in a field test at low pollutant concentration (chapter 4). Testing a novel technology in challenging conditions (for example, those shown in chapter 8) will inevitably not portray the technology in the best case scenario, but will give results that are dependable to those who can actually employ the technology and will avoid disappointing performance when fully deployed.

Technology developers may next take note of the potential of titanium dioxide nanoparticles as adsorbents over those of iron hydroxide. Much of the nanotechnology development has focused on iron hydroxide as a sorbent and titanium dioxide as a catalyst and photocatalyst. This work has shown that titanium dioxide is a superior nanosorbent for arsenic removal from drinking water compared to iron hydroxide. It has a higher sorption capacity for arsenic in batch equilibrium testing (chapter 5), and a longer duration before exhaustion for arsenic and chromium removal in column testing (chapter

8). Additionally, its creation and use has a lower environmental impact (chapter 6). Attention toward minimizing the energy demand in heating required for hydrolysis can continue to reduce this impact (chapter 6).

Another approach that technology developers can take away from this study is that nanocomposite sorbent synthesis processes should be specifically tailored for the application and macrostructure. Some have previously claimed that some novel method of preparing a nanoparticle would be applicable to any sorbent or porous structure for removal of any pollutant. This study has shown instead that the nanocomposite sorbent should be tailored for the specific application to reach higher removal efficiency. A nanocomposite sorbent developed for nitrate and arsenic removal did not work well for chromium and arsenic removal (chapter 4). The nanocomposite synthesis process developed with strong base anion exchange resin as the macro-material did not work well for use with a weak base anion exchange resin and additional steps were required (chapter 5).

The last suggested value that technology developers can glean to apply to their work is the viability of including sustainability metrics as design constraints. This study has demonstrated that anticipatory life cycle assessment can proactively identify critical contributions to environmental impacts during the nascent design phase of a novel technology (chapter 6). There is of course large uncertainty associated with how the technology will develop into the future and change with scale up, but no one can be better to address this uncertainty than those that are doing the development. Identifying these environmental impacts may possibly be synergistic with other design constraints such as treatment efficiency, energy usage, and cost. This study has further demonstrated that

sustainability analysis can even be used to justify the need to employ a technology for overall human health benefit (chapter 7). Technology developers can approach their work with an eye toward environmental consequences during development instead of only as an afterthought.

Treatment Facility Owners and Operators. People who own and operate water treatment facilities can acquire additional values with which to select treatment processes. It may not be necessary to install a dedicated process for each pollutant of concern. In the event that new regulation for a pollutant is enacted (such as a new hexavalent chromium rule or lowered total chromium rule), it may be possible to use the same infrastructure already installed and simply replace the sorbent media with something that can address multiple pollutants. This can simplify operation and reduce cost compared to adding a whole new contactor. This study has shown the viability of using treatment processes that address multiple pollutants simultaneously. Nanocomposite sorbents can remove both hexavalent chromium and arsenic (chapter 5 and chapter 8). This can even be done at a lower environmental footprint compared to the traditional approach of having separate dedicated processes (chapter 6). In general, owners may also shy away from treatment technologies that require high daily chemical input such as pH control in order to have the highest total benefit to the health of the customers (chapter 7).

Regulators. This research hopes to inspire values that regulators can use to decide how to enact water quality policy. The current strategy for choosing which potential contaminants to regulate and at what levels typically considers occurrence, analytical ability, and cost to treat to compliance. This research has shown that the embodied health risk in providing treatment to meet the potential regulation is non-

negligible (chapter 7). Consideration of new regulations should include not just the direct health risk avoided to the population drinking treated water, but also the indirect health risk borne by the subpopulation that creates the energy and materials required to meet the regulation.

gg

REFERENCES

Agency for Toxic Substances and Disease Registry (ATSDR) (2007) Toxicological Profile for Arsenic, Atlanta, GA.

Alberti, G., Amendola, V., Pesavento, M. and Biesuz, R. (2012) Beyond the Synthesis of Novel Solid Phases: Review on Modeling of Sorption Phenomena. Coordination Chemistry Reviews 256, 28-45.

Antonio, P., Iha, K. and Suarez-Iha, M. (2004) Adsorption of Di-2-Pyridyl Ketone Salicyloylhydrazone on Silica Gel: Characteristics and Isotherms. Talanta 64, 484-490.

ARCADIS U.S. (2013) Development of a Uniform Approach to Prepare Drinking Water Hexavalent Chromium Compliance Plans (WRF 4445) Periodic Report No. 4.

AQIon (2014) pH Calculator. Available at http://aqion.onl/

Arpke, A. and Hutzler, N. (2006) Domestic Water Use in the United States: A Life-Cycle Approach. Journal of Industrial Ecology 10(1-2), 169-184.

Baird, G.M. (2010) Water Affordability: Who's Going to Pick Up the Check? Journal AWWA 102(12), 16-23.

Balaji, T. and Matsunaga, H. (2002) Adsorption characteristics of As(III) and As(V) with titanium dioxide loaded Amberlite XAD-7 resin. Analytical Sciences 18(12), 1345-1349.

Bang, S., Pena, M.E., Patel, M., Lippincott, L., Meng, X., Kyoung and Kim, W. (2011) Removal of arsenate from water by adsorbents: a comparative case study. Environmental Geochemical Health 33, 133-141.

Batan, L., Quinn, J., Willson, B. and Bradley, T. (2010) Net Energy and Greenhouse Gas Emission Evaluation of Biodiesel Derived from Microalgae. Environmental Science and Technology 44(20), 7975-7980.

Blaney, L.M., Cinar, S. and Sengupta, A.K. (2007) Hybrid Anion Exchanger for Trace Phosphate Removal from Water and Wastewater. Water Research 41(7), 1603-1613.

Blocher, C., Niewersch, C. and Melin, T. (2012) Phosphorus Recovery from Sewage Sludge with a Hybrid Process of Low Pressure Wet Oxidation and Nanofiltration. Water Research 46(6), 2009-2019.

Blute, N.K., Wu, Y., Alspach, B., Seidel, C., Brandhuber, P. and Najm, I. (2012) Guidelines for Hexavalent Chromium Treatment Testing, Denver CO.

Bottini, A. and Rizzo, L. (2012) Phosphorus Recovery from Urban Wastewater Treatment Plant Sludge Liquor by Ion Exchange. Separation Science & Technology 47(4), 613-620.

Brandhuber, P., Frey, M., McGuire, M.J., Chao, P., Seidel, C., Amy, G., Yoon, J., McNeill, L. and Banerjee, K. (2004a) Low-Level Hexavalent Chromium Treatment Options: Bench-Scale Evaluation, AWWA Research Foundation, Denver, CO.

Brandhuber, P., Frey, M., McGuire, M.J., Chao, P., Seidel, C., Amy, G., Yoon, J., McNeill, L. and Banerjee, K. (2004b) Low-Level Hexavalent Chromium Treatment Options: Bench-Scale Evaluation, Denver CO.

Burton, F.L. (1996) Water and wastewater industries: Characteristics and energy management opportunities, St. Louis, MO.

California Code of Regulations (CCR) (2014) Title 22, Division 4, Chapter 15, Article 4, Section 64431. Available at http://www.oal.ca.gov/ccr.htm

Cantwell, J., Gehring, B. and Schepp, C. (2002) Roadmap for the Wisconsin municipal water and wastewater industry, Madison, WI. Available at http://www.seventhwave.org/sites/default/files/ww_roadmap.pdf

Chaudhary, B.K. and Farrell, J. (2015) Understanding Regeneration of Arsenate Loaded Ferric Hydroxide Based Adsorbents. Environmental Engineering Science 32(4), 353-360.

Chester, M. and Horvath, A. (2010) Life-cycle assessment of high-speed rail: The case of California. Environmental Research Letters 5(1), 1-8.

Childers, D.L., Corman, J., Edwards, M. and Elser, J.J. (2011) Sustainability Challenges of Phosphorus and Food: Solutions from Closing the Human Phosphorus Cycle. Bioscience 61(2), 117-124.

Choe, J., Bergquist, A., Jeong, S., Guest, J., Werth, C. and Strathmann, T. (2015) Performance and life cycle environmental benefits of recycling spent ion exchange brines by catalytic treatment of nitrate. Water Research 80, 267-280.

Choong, T.S.Y., Chuah, T.G., Robiah, Y., Gregory Koay, F.L. and Azni, I. (2007) Arsenic toxicity, health hazards and removal techniques from water: an overview. Desalination 217(1), 139-166.

Clarens, A.F., Resurreccion, E.P., White, M.A. and Colosi, L.M. (2010) Environmental Life Cycle Comparison of Algae to Other Bioenergy Feedstocks. Environmental Science & Technology 44(5), 1813-1819.

Coachella Valley Water District (CVWD) (2014) 2013-14 Annual Review. Available at http://www.cvwd.org/news/publicinfo/2014_06_27_2014AnnualReview_WaterQualityReport.pdf

Cordell, D., Drangert, J. and White, S. (2009) The Story of Phosphorus: Global Food Security and Food for Thought. Global Environmental Change 19(2), 292-305.

Crettaz, P., Jolliet, O., Cuanillon, J.M. and Orlando, S. (1999) Life cycle assessment of drinking water and rain water for toilets flushing. Journal of Water Supply: Research and Technology—Aqua 48(3), 73-83.

Cumbal, L. and Sengupta, A.K. (2005) Arsenic removal using polymer-supported hydrated iron(III) oxide nanoparticles: role of donnan membrane effect. Environmental Science & Technology 39(17), 6508-6515.

Cutler, D. and Miller, G. (2004) The Role of Public Health Improvements in Health Advances: The 20th Century United States, National Bureau of Economic Research, Cambridge, MA.

Dadachov, M. (2006) Novel Titanium Dioxide, Process of Making and Method of Using Same. United States Patent and Trade Office (ed).

de-Bashan, L.E. and Bashan, Y. (2004) Recent advances in removing phosphorus from wastewater and its future use as fertilizer (1997-2003). Water Research 38(19), 4222-4246.

Dennison, F., Azapagic, A., Clifft, R. and Colbourne, J. (1999) Life cycle assessment: Comparing strategic options for the mains infrastructure – Part I. Water Science and Technology 39(10-11), 315-319.

Dominguez, J., Gonzalez, T., Palo, P. and Cuerda-Correa, E. (2011) Removal of Common Pharmaceuticals Present in Surface Waters by Amberlite XAD-7 Acrylic Ester Resin: Influence of pH and Presence of Other Drugs. Desalination 269(1-3), 231-238.

Du, Q., Zhang, S., Pan, B., Lv, L., Zhang, W. and Zhang, Q. (2013) Bifunctional resin-ZVI composites for effective removal of arsenite through simultaneous adsorption and oxidation. Water Research 47(16), 6064-6074.

Dutta, P.K., Ray, A.K., Sharma, V.K. and Millero, F.J. (2004) Adsorption of arsenate and arsenite on titanium dioxide suspensions. Journal of Colloid and Interface Science 278(2), 270-275.

Elliott, T., Zeier, B., Xagoraraki, I. and Harrington, G.W. (2003) Energy use at Wisconsin's drinking water facilities, Madison, WI.

Elser, J.J., Acharya, K., Kyle, M., Cotner, J., Makino, W., Markow, T., Watts, T., Hobbie, S., Fagan, W., Schade, J., Hood, J. and Sterner, R.W. (2003) Growth Rate Stoichiometry Couplings in Diverse Biota. Ecology Letters 6(10), 936-943.

Elton, J., Hristovski, K. and Westerhoff, P. (2013) Novel Solutions to Water Pollution, pp. 223-236.

Emmerson, R., GK, Lester, J. and Edge, D. (1995) The life-cycle analysis of small scale sewage-treatment processes. Journal - The Chartered Institution of Water and Environmental Management 9, 317-325.

Erisman, J.W., van Grinsven, H., Leip, A., Mosier, A. and Bleeker, A. (2010) Nitrogen and biofuels; an overview of the current state of knowledge. Nutrient Cycling in Agroecosystems 86(2), 211-223.

Federal Register (2012) Revisions to the Unregulated Contaminant Monitoring Regulation (UCMR 3) for Public Water Systems. Available at https://www.federalregister.gov/articles/2012/07/25/C2-2012-9978/revisions-to-the-unregulated-contaminant-monitoring-regulation-ucmr-3-for-public-water-systems

Folch, J., Lees, M. and Stanley, G.H.S. (1957) A Simple Method for the Isolation and Purification of Total Lipids from Animal Tissues. Journal of Biological Chemistry 226(1), 497-509.

Frey, M.M., Seidel, C., Edwards, M., Parks, J.L. and McNeill, L. (2004) Occurrence Survey of Boron and Hexavalent Chromium, Denver CO.

Frischknecht, R., Jungbluth, N., Althaus, H.-J., Doka, G., Dones, R., Hischier, R., Hellweg, S., Nemecek, T., Rebitzer, G. and Spielmann, M. (2007) Overview and Methodology: Final Report Ecoinvent Data v2.0. Inventories, S.C.f.L.C. (ed), Dubendorf, CH.

Geider, R. and La Roche, J. (2002) Redfield revisited: Variability of C:N:P in marine microalgae and its biochemical basis. European Journal of Phycology 37(1), 1-17.

Gifford, M., Liu, J., Rittmann, B.E., Vannela, R. and Westerhoff, P. (2015) Phosphorus recovery from microbial biofuel residual using microwave peroxide digestion and anion exchange. Water Research 70, 130-137.

Griffiths-Sattenspiel, B. and Wilson, W. (2009) The Carbon Footprint of Water, Portland OR.

Guan, X., Du, J., Meng, X., Sun, Y., Sun, B. and Hu, Q. (2012) Application of titanium dioxide in arsenic removal from water: A review. Journal of Hazardous Materials 215-216, 1-16.

Hajime, W. and Murata, N. (2007) The Essential Role of Phosphatidylglycerol in Photosynthesis. Photosynthesis Research 92(2), 205-215.

Hammer, M.J. and Hammer Jr., M.J. (2011) Water and Wastewater Technology, Prentice Hall.

Hauschild, M.Z., Huijbregts, M.A.J., Jolliet, O., MacLeod, M., Margni, M., Van de Meent, D., Rosenbaum, R.K. and McKone, T.E. (2008) Building a model based on scientific consensus for Life Cycle Impact Assessment of Chemicals: the Search for Harmony and Parsimony. Environmental Science and Technology 42(19), 7032–7037.

Hawkins, T.R., Singh, B., Majeau-Bettez, G. and Stromman, A.H. (2012) Comparative Environmental Life Cycle Assessment of Conventional and Electric Vehicles. Journal of Industrial Ecology 17(1), 53-64.

Haynes, W.M., Bruno, T.J. and Lide, D.R. (eds) (2015-2016) CRC Handbook of Chemistry and Physics. CRC Press/Taylor and Francis, Boca Raton, FL. Available at www.hbcpnetbase.com

Hempel, S. (2013) The Inheritor's Powder: A Tale of Arsenic, Murder, and the New Forensic Science, W. W. Norton & Company, Inc., New York, NY.

Hristovski, K., Westerhoff, P., Moller, T., Sylvester, P., Condit, W. and Mash, H. (2008a) Simultaneous Removal of Perchlorate and Arsenate by Ion Exchange Media Modified With NanoStructured Iron Hydroxide. Journal of Hazardous Materials 152(1), 397-406.

Hristovski, K., Westerhoff, P., Moller, T., Sylvester, P., Condit, W. and Mash, H. (2008b) Simultaneous removal of perchlorate and arsenate by ion-exchange media modified with nanostructured iron (hydr)oxide. Journal of Hazardous Materials 152(1), 397-406.

Hu, X., Ding, Z., Zimmerman, A., Wang, S. and Gao, B. (2015) Batch and column sorption of arsenic onto iron-impregnated biochar synthesized through hydrolysis. Water Research 68, 206-216.

Huijbregts, M.A.J., Rombouts, L.J.A., Ragas, A.M.J. and van de Meent, D. (2005) Human-Toxicological Effect and Damage Factors of Carcinogenic and Noncarcinogenic Chemicals for Life Cycle Impact Assessment. Integrated Environmental Assessment and Management 1(3), 181-244.

Huo, Y.-X., Wernick, D.G. and Liao, J.C. (2012) Toward nitrogen neutral biofuel production. Current Opinion in Biotechnology 23(3), 406-413.

Hutson, S.S., Barber, N.L., Kenny, J.F., Linsey, K.S., Lumia, D.S. and Maupin, M.A. (2004) Estimated use of water in the United States in 2000, Denver CO.

Impellitteri, C., Patterson, C., Haught, R. and Goodrich, J. (2007) Small Drinking Water Systems: State of the Industry and Treatment Technologies to Meet the Safe Drinking Water Act Requirements, Environmental Protection Agency, Cincinnati, OH.

Ismagilov, Z.R., Tsikoza, L.T., Shikina, N.V., Zarytova, V.F., Zinoviev, V.V. and Zagrebelnyi, S.N. (2009) Synthesis and stabilization of nano-sized titanium dioxide. Russian Chemical Reviews 78(9), 873-885.

James, K., Byers, T., Hokanson, J., Meliker, J., Zerbe, G. and Marshall, J. (2015) Association between Lifetime Exposure to Inorganic Arsenic in Drinking Water and Coronary Heart Disease in Colorado Residents. Environmental Health Perspectives 123(2), 128-134.

Kaneko, T., Sato, S., Kotani, H., Tanaka, A., Asamizu, E., Nakamura, Y., Miyajima, N., Hirosawa, M., Sugiura, M., Sasamoto, S., Kimura, T., Hosouchi, T., Matsuno, A., Muraki, A., Nakazaki, N., Naruo, K., Okumura, S., Shimpo, S., Takeuchi, C., Wada, T., Watanabe, A., Yamada, M., Yasuda, M. and Tabata, S. (1996) Sequence Analysis of the Genome of the Unicellular Cyanobacterium Synechocystis sp. Strain PCC6803. II. Sequence Determination of the Entire Genome and Assignment of Potential Protein-coding Regions. DNA Research 3(3), 109-136.

Kim, W.K., Vannela, R., Zhou, C., Harto, C. and Rittmann, B.E. (2010) Photoautotrophic Nutrient Utilization and Limitation During Semi-Continuous Growth of Synechocystis sp. PCC6803. Biotechnology and Bioengineering 106(4), 553-563.

Kolen'ko, Y., Burukhin, A., Churagulov, B. and Oleynikov, N. (2003) Synthesis of nanocrystalline TiO2 powders from aquesous TiOSO4 solutions under hydrothermal conditions. Materials Letters 57(5-6), 1124-1129.

Kroschwitz, J.I. (1995) Encyclopedia of chemical technology, Wiley, New York.

Kunin, R. (1958) Ion Exchange Resins, John Wiley & Sons, New York, NY.

Landry, K., Sun, P., Huang, C. and Boyer, T. (2015) Ion Exchange Selectivity of Diclofenac, Ibuprofen, Ketoprofen, and Naproxen in Ureolyzed Human Urine. Water Research 68, 510-521.

Lee, G., Park, J. and Harvey, O.R. (2013) Reduction of Chromium(VI) mediated by zero-valent magnesium under neutral pH conditions. Water Research 47(3), 1136-1146.

Liao, P.H., Wong, W.T. and Lo, K.V. (2005) Advanced Oxidation Process Using Hydrogen Peroxide/Microwave System for Solubilization of Phosphate. Journal of Environmental Science and Health 40(9), 1753-1761.

Lin, T. and Wu, J. (2001) Adsorption of Arsenite and Arsenate within Activated Alumina Grains: Equilibrium and Kinetics. Water Research, 2049-2057.

Lindsay, D.R., Farley, K.J. and Carbonaro, R.F. (2012) Oxidation of Cr(III) to Cr(VI) during chlorination of drinking water. Journal of Environmental Monitoring 14(7), 1789-1797.

Lipps, J.P., Chen, A.S.C., Wang, L., Wang, A. and McCall, S.E. (2010) Arsenic Removal from Drinking Water by Adsorptive Media. USEPA Demonstration Project at Spring Brook Mobil Home Park in Wales, ME. Final Performance Evaluation Report, Columbus, OH.

Liu, W., Zhang, C., Zhang, J., Wang, Y. and Li, Y. (2010) Adsorptive removal of Cr (VI) by Fe-modified activated carbon prepared from Trapa natans husk. Chemical Engineering Journal 162(2), 677-684.

Lu, A., Zhong, S., Chen, J., Shi, J., Tang, J. and Lu, X. (2006) Removal of Cr(VI) and Cr(lll) from aqueous solutions and industrial wastewaters by natural clino-pyrrhotite. Environmental Science and Technology 40(9), 3064-3069.

Mahramanlioglu, M., Kizilcikli, I. and Bicer, I. (2002) Adsorption of Fluoride from Aqueous Solution by Acid Treated Spent Bleaching Earth. Journal of Fluorine Chemistry 115(1), 41-47.

Mak, M.S.H., Lo, I.M.C. and Liu, T. (2011a) Synergistic effect of coupling zero-valent iron with iron oxide-coated sand in columns for chromate and arsenate removal from groundwater: Influences of humic acid and the reactive media configuration. Water Research 45(19), 6575-6584.

Malaviya, P. and Singh, A. (2011) Physicochemical technologies for remediation of chromium containing waters and wastewaters. Critical Reviews in Environmental Science and Technology 41, 1111-1172.

Martin, B.D., Parsons, S.A. and Jefferson, B. (2009) Removal and Recovery of Phosphate from Municipal Wastewater Using a Polymeric Anion Exchanger Bound with Hydrated Ferric Oxide Nanoparticles. Water Science and Technology 60(10), 2637-2645.

Mata, T.M., Martins, A.A. and Caetano, N.S. (2010) Microalgae for Biodiesel Production and Other Applications: A Review. Renewable & Sustainable Energy Reviews 14(1), 217-232.

McGavisk, E., Roberson, A. and Seidel, C. (2013) Using Community Economics to Compare Arsenic Compliance and Noncompliance. Journal American Water Works Association 105(3), 115-126.

McGuire, M., J., Blute, N.K., Qin, G., Kavounas, P., Froelich, D. and Fong, L. (2007) Hexavalent Chromium Removal Using Anion Exchange and Reduction With Coagulation and Filtration, Denver CO.

McNeill, L., McLean, J., Edwards, M. and Parks, J. (2012) State of the Science of Hexavalent Chromium in Drinking Water.

Midorikawa, I., Aoki, H., Omori, A., Shimizu, T., Kawaguchi, Y., Kassai, K. and Murakami, T. (2008) Recovery of High Purity Phosphorus from Municipal Wastewater Secondary Effluent by a High Speed Adsorbent. Water Science and Technology 58(8), 1601-1607.

Miner, G. (2006) Standard Methods for the Examination of Water and Wastewater, 21st Edition, American Water Works Association.

Mohan, D. and Pittman, C.U. (2006) Activated carbons and low dose adsorbents for remediation of tri- and hexavalent chromium from water. Journal of Hazardous Materials 137(2), 762-811.

Mohan, D. and Pittman, C.U. (2007) Arsenic Removal from Water/Wastewater Using Adsorbents - A Critical Review. Journal of Hazardous Materials 142(1), 1-53.

Moller, J.T. (2008) Method and Sorbent for Selective Removal of Contaminants from Fluids. United States Patent and Trade Office (ed), Layne Christensen Company.

Morse, G.K., Brett, S.W., Guy, J.A. and Lester, J.N. (1998) Review: Phosphorus Removal and Recovery Technologies. The Science of the Total Environment 212(1), 69-81.

MWH (2005) Water Treatment Principles and Design, John Wiley & Sons.

Najm, I. (2013) Practical & Economic Feasibility of Implementing Cr(VI) Treatment, Water Research Foundation, Sacramento, CA.

Najm, I., Brown, N.P., Seo, E., Gallagher, B., Gramith, K., Blute, N., Wu, Y., Yoo, M., Liang, S., Maceiko, S., Kader, S. and Lowry, J. (2014) Impact of Water Quality on Hexavalent Chromium Removal Efficiency and Cost, Denver CO.

Nameni, M., Moghadam, M.R.A. and Arami, M. (2008) Adsorption of hexavalent chromium from aqueous solutionsby wheat bran. International Journal of Environmental Science and Technology 5(2), 161-168.

Noss, A. (2014) Household Income: 2013, Document ACSBR 13-02, p. 6, United States Census Bureau.

NSF International Standard / American National Standard (NSFI/AN) (2007) Drinking Water Treatment Units - Health Effects, NSF International, Ann Arbor, MI.

Owlad, M., Aroua, M.K., Daud, W.A.W. and Baroutian, S. (2009) Removal of Hexavalent Chromium-Contaminated Water and Wastewater: A Review. Water, Air, and Soil Pollution 200(1), 59-77.

Parascandola, J. (2012) King of Poisons: A History of Arsenic, Potomac Books, Inc., Dulles, VA.

Peng, C.-Y.H., Andrew S. Friedman, Melinda J. Valentine, Richard L. Larson, Gregory S. Romero, Angela M. Y. Reiber, Steve H. Korshin, Gregory V. (2012) Occurrence of trace inorganic contaminants in drinking water distribution systems. Journal of the American Water Works Association 104(3), E181-E193.

Plappally, A.K. and Lienhard, J.H. (2012) Energy requirements for water production, treatment, end use, reclamation, and disposal. Renewable and Sustainable Energy Reviews 16, 4818-4848.

Qu, X., Alvarez, P. and Li, Q. (2013) Applications of nanotechnology in water and wastewater treatment. Water Research 47(12), 3931-3946.

Racoviceanu, A.I., Karney, B.W., Kennedy, C.A. and Colombo, A.F. (2007) Life-cycle energy use and greenhouse gas emissions inventory for water treatment systems. Journal of Infrastructure Systems 13(4), 261-270.

Raluy, G., Serra, L. and Uche, J. (2005) Life Cycle Assessment of Water Production Technologies – Part 1: Life Cycle Assessment of Different Commercial Desalination Technologies. International Journal of Life Cycle Assessment 10(4), 285-293.

Rees-Nowak, D., Marston, C. and Gisch, D. (2005) Controlling Chromium. Water & Wastewater International 20(5), 21.

Ribera, G., Clarens, F., Martinez-Llado, X., Jubany, I., Marti, V. and Rovira, M. (2014) Life Cycle and Human Health Risk Assessments as Tools for Decision Making in the Design and Implementation of Nanofiltration in Drinking Water Treatment Plants. Science of the Total Environment 466-467, 377-386.

Rippka, R., Deruelles, J., Waterbury, J.B., Herdman, M. and Stanier, R.Y. (1979) GENERIC ASSIGNMENTS, STRAIN HISTORIES AND PROPERTIES OF PURE CULTURES OF CYANOBACTERIA. Journal of General Microbiology 111(MAR), 1-61.

Rittmann, B.E. (2008) Opportunities for renewable bioenergy using microorganisms. Biotechnology and Bioengineering 100(2), 203-212.

Rittmann, B.E., Mayer, B., Westerhoff, P. and Edwards, M. (2011) Capturing the lost phosphorus. Chemosphere 84(6), 846-853.

Rohm & Haas Company (2008) Product Data Sheet: Amberlite PWA7 Resin.Available at http://www.dow.com/assets/attachments/business/ier/amberlite_pw/amberlite_pwa7/tds/amberlite_pwa7.pdf

Rosenbaum, R.K., Bachmann, T.K., Gold, L.S., Huijbregts, M.A.J., Jolliet, O., Juraske, R., Koehler, A., Larsen, H.F., MacLeod, M., Margni, M., McKone, T.E., Payet, J., Schuhmacher, M., Van de Meent, D. and Hauschild, M.Z. (2008) USEtox - The UNEP/SETAC-consensus model: recommended characterisation factors for human toxicity and freshwater ecotoxicity in Life Cycle Impact Assessment. International Journal of Life Cycle Assessment 13(7), 532-546.

Sakurai, I., Shen, J., Leng, J., Ohashi, S., Kobayashi, M. and Wada, H. (2006) Lipids in Oxygen Evolving Photsystems II Complexes of Cyanobacteria and Higher Plants. Journal of Biochemistry 140(2), 201-209.

Sandoval, R., Cooper, A.M., Aymar, K., Jain, A. and Hristovski, K. (2011) Removal of arsenic and methylene blue from water by granular activated carbon media impregnated with zirconium dioxide nanoparticles. Journal of Hazardous Materials 193, 296-303.

Sarkar, S., Guibal, E., Quignard, F. and Sengupta, A.K. (2012) Polymer supported metals and metal oxide nanoparticles: Synthesis, characterization, and applications. Journal of Nanoparticle Research 14(2), 24.

Schenk, P.M., Thomas-Hall, S.R., Stevens, E., Marx, U.C., Mussgnug, J.H., Posten, C., Kruse, O. and Hankamer, B. (2008) Second Generation Biofuels: High Efficiency Microalgae for Biodiesel Production. Bioenergy Research 1(1), 20-43.

Schweitzer, G.K. and Pesterfield, L.L. (2010) The Aqueous Chemistry of the Elements, Oxford University Press, New York NY.

Sengupta, S. (2013) Novel Solutions to Water Pollution. Ahuja, S. and Hristovski, K. (eds), pp. 167-187, American Chemical Society, Washington DC.

Shah, B.A., Shah, A.V. and Singh, R.R. (2009) Sorption isotherms and kinetics of chromium uptake from wastewaterusing natural sorbent material. International Journal of Environmental Science and Technology 6(1), 77-90.

Shahadat, M., Teng, T.T., Rafatullah, M. and Arshad, M. (2015) Titanium-based nanocomposite materials: A review of recent advances and perspectives. Colloids and Surfaces B: Biointerfaces 126, 121-137.

Shastri, A.A. and Morgan, J.A. (2005) Flux Balance Analysis of Photoautotrophic Metabolism. Biotechnology 21(6), 1617-1626.

Sheng, J., Kim, H.W., Badalamenti, J.P., Zhou, C., Sridharakrishnan, S., Krajmalnik-Brown, R., Rittmann, B.E. and Vannela, R. (2011a) Effects of Temperature Shifts on Growth Rate and Lipid Characteristics of Synechocystis sp. PCC6803 in a Bench-Top Photobioreactor. Bioresource Technology 102(24), 11218-11225.

Sheng, J., Vannela, R. and Rittmann, B.E. (2011b) Evaluation of Methods to Extract and Quantify Lipids from Synechocystis PCC6803. Bioresource Technology 102(2), 1697-1703.

Singh, R., Misra, V. and Singh, R.P. (2012) Removal of hexavalent chromium from contaminated ground water using zero-valent iron nanoparticles. Environmental Monitoring and Assessment 184(6), 3643-3651.

Smith, K. (2010) Effects of a mixture of Bicarbonate, Silica and Nitrate on the Removal of Arsenic and Chromium by a Hybrid Polymer-Iron Anion Exchanger, Lehigh University.

Soh, L. and Zimmerman, J. (2011) Biodiesel Production: The Potential of Algal Lipids Extracted with Supercritical Carbon Dioxide. Green Chemistry 13(6), 1422-1429.

Speital, G., Katz, L., Chen, C.-C., Stokes, S., Westerhoff, P. and Shafieian, P. (2010) Surface Complexation and Dynamic Transport Modeling of Arsenic Removal on Adsorptive Media, Water Research Foundation.

Sterner, R.W. and Elser, J.J. (2002) Ecological Stoichiometry: The Biology of Elements from Molecules to the Biosphere, Princeton University Press, Princeton, New Jersey.

Stokes, J. and Horvath, A. (2006) Life Cycle Energy Assessment of Alternative Water Supply. International Journal of Life Cycle Assessment 11(5), 335-343.

Stokes, J. and Horvath, A. (2011) Life Cycle Assessment of Urban Water Provision: Tool and Case Study in California. Journal of Infrastructure Systems 17(1), 15-24.

Stucker, V., Ranville, J., Newman, M., Peacock, A., Cho, J. and Hatfield, K. (2011) Evaluation and application of anion exchange resins to measure groundwater uranium flux at a former uranium mill site. Water Research 45(16), 4866-4876.

Swiss Center of Life Cycle Inventories (SCLCI) (2010) EcoInvent v2.2. Available at www.ecoinvent.org

Tarantini, M. and Federica, F. (2001) LCA of drinking and wastewater treatment systems of Bologna city: Final results, Fortaleza, Brazil.

Tripathi, M. (2007) Life cycle energy and emissions for municipal water and wastewater services: Case studies of treatment plants in the USA, Ann Arbor, MI.

Tohono O'Odham Utility Authority, (TOUA) (2010) 2010 Annual Water Quality Report. Available at http://www.toua.net/water/water-quality-report/

United States Environmental Protection Agency (USEPA) (2011) Method 218.7: Determination of Hexavalent Chromium in Drinking Water by Ion Chromotography with Post Column Derivatization and UV Visible Spectroscopic Detection, Environmental Protection Agency, Cincinnati, OH.

United States Environmental Protection Agency (USEPA) Method 218.7: Determination of Hexavalent Chromium in Drinking Water by Ion Chromatography with Post-Column Derivatization and UV-Visible Spectroscopic Detection.

United States Environmental Protection Agency (USEPA) (1994) Method 200.8: Determination of Trace Elements in Waters and Wastes by Inductively Coupled Plasma - Mass Spectrometry, Washington DC.

United States Environmental Protection Agency (USEPA) (1995) Compilation of Air Pollutant Emission Factors Volume 1: Stationary Point and Area Sources, Office of Air Quality Planning and Standards, Research Triangle Park, NC.

United States Environmental Protection Agency (USEPA) (1996) Recent Developments for In Situ Treatment of Metals Contaminated Soil., Washington DC.

United States Environmental Protection Agency (USEPA) (1998a) Toxicological Review of Hexavalent Chromium (CAS No. 18540-29-9) In Support of Summary Information on the Integrated Risk Information System (IRIS), Washington DC.

United States Environmental Protection Agency (USEPA) (1998b) Toxicological Review of Inorganic Arsenic (CAS No 7440-38-2) In Support of Summary Information on the Integrated Risk Information System (IRIS), Washington DC.

United States Environmental Protection Agency (USEPA) (2000) Arsenic Occurrence in Public Drinking Water Supplies, Washington, D.C.

United States Environmental Protection Agency (USEPA) (2008) Test Methods for Evaluating Solid Waste, Physical/Chemical Methods, Washington D.C.

United States Environmental Protection Agency (USEPA) (2010a) Toxicological Review of Hexavalent Chromium (CAS No. 18540-29-9) In Support of Summary Information on the Integrated Risk Information System (IRIS) External Review Draft, Washington DC.

United States Environmental Protection Agency (USEPA) (2010b) Toxicological Review of Inorganic Arsenic (CAS No 7440-38-2) In Support of Summary Information on the Integrated Risk Information System (IRIS) External Review Draft, Washington DC.

United States Environmental Protection Agency (USEPA) (2012) Basic Information about the Arsenic Rule.

United States Environmental Protection Agency (USEPA) (2013) Basic Information about Chromium in Drinking Water.

United States Environmental Protection Agency (USEPA) (2014) Tool for the Reduction and Assessment of Chemical and Environmental Impacts.

United States Environmental Protection Agency (USEPA) (2015a) Integrated Risk Information System (IRIS).

United States Environmental Protection Agency (USEPA) (2015b) Unregulated Contaminant Monitoring Program.

United States Environmental Protection Agency (USEPA) (2015c) Unregulated Contaminant Monitoring Program.

United States Geological Survey (USGS) (2011) Mineral Commodity Summaries 2011, Reston, VA.

van de Meene, A.M.L., Hohmann-Marriott, M.F., Vermaas, W.F.J. and Roberson, R.W. (2006) The three-dimensional structure of the cyanobacterium Synechocystis sp PCC 6803. Archives of Microbiology 184(5), 259-270.

Vatutsina, O.M., Soldatov, V.S., Sokolova, V.I., Johann, J., Bissen, M. and Weissenbacher, A. (2007) A new hybrid (polymer/inorganic) fibrous sorbent for arsenic removal from drinking water. Reactive & Functional Polymers 67, 184-201.

Vermaas, W. (1996) Molecular Genetics of the Cyanobacterium Synechocystis sp. PCC 6803: Principles and Possible Biotechnology Applications. Journal of Applied Phycology 8(4-5), 263-273.

Vermaas, W.F.J. (2001) Encyclopedia of Life Sciences, pp. 245-251, John Wiley & Sons, Ltd, London.

Wang, L. and Jiang, X. (2008) Plasma-Induced Reduction of Chromium(VI) in an Aqueous Solution. Environmental Science & Technology 42(22), 8492-8497.

Water Quality & Treatment Solutions, Inc. (2008) Acid or Base Doses Needed to Change the pH of Water. Available at http://www.wqts.com/models/Acid-BaseAdditionModel2.htm

Wender, B., Foley, R., Prado-Lopez, V., Ravikumar, D., Eisenberg, D., Hottle, T., Sadowski, J., Flanagan, W., Fisher, A., Laurin, L., Bates, M., Linkov, I., Seager, T., Fraser, M. and Guston, D. (2014) Illustrating Anticipatory Life Cycle Assessment for Emerging Photovoltaic Technologies. Environmental Science & Technology 48(18), 10531-10538.

Westerhoff, P., Highfield, D., Badruzzaman, M. and Yoon, Y. (2005) Rapid Small Scale Column Tests for Arsenate Removal in Iron Oxide Packed Bed Columns. Journal of Environmental Engineering 131(2), 262-271.

Wijffels, R.H., Kruse, O. and Hellingwerf, K.J. (2013) Potential of Industrial Biotechnology with Cyanobacteria and Eukaryotic Microalgae. Current Opinion in Biotechnology 24(3), 405-413.

Wong, W.T., Chan, W.I., Liao, P.H., Lo, K.V. and Mavinic, D.C. (2006) Exploring the Role of Hydrogen Peroxide in the Microwave Advanced Oxidation Process; Solubilization of Ammonia and Phosphates. Journal of Environmental Engineering and Science 5(6), 459-465.

Yamani, J., Miller, S., Spaulding, M. and Zimmerman, J. (2012) Enhanced arsenic removal using mixed metal oxide impregnated chitosan beads. Water Research 46(14), 4427-4434.

Zhao, X., Lv, L., Pan, B., Zhang, W., Zhang, S. and Zhang, Q. (2011) Polymer supported nanocomposites for environmental application: A review. Chemical Engineering Journal 170, 381-394.

BIOGRAPHICAL SKETCH

I am an Arizonan dedicated to becoming a world leader in water resource engineering. I completed a B.S. degree in Civil Engineering with a 3.76 GPA (4.0 major GPA) in 2006 at the University of Arizona. I then worked at an engineering consultant firm for four years designing water and stormwater infrastructure for local development projects, and earned Professional Engineer licensure. I desired greater intellectual challenge and ability to work on projects with more influence in the wider world and industry. I therefore left work in August 2010 to become a graduate student in Civil and Environmental Engineering focusing in water quality and treatment processes as well as sustainable technology in the School of Sustainable Engineering and the Built Environment at Arizona State University. I completed a Graduate Certificate of Sustainable Technology and Management under the sponsorship of Dr. Brad Allenby with a capstone project entitled "Sustainable Water Management Heuristics of Native Arizonan Small Drinking Water Systems" in August 2012. I completed an M.S. degree in civil/environmental engineering under the advising of Dr. Paul Westerhoff with a thesis entitled "Phosphorus Recovery from Microbial Biofuel Residual Using Microwave Peroxide Digestion and Anion Exchange" in December 2012. I now submit this dissertation as part of requirements to complete a Ph.D. in civil/environmental engineering under the advising of Dr. Paul Westerhoff , Dr. Kiril Hristovski, and Dr. Mikhail Chester. My goal in the future is to become a well-respected water engineer who is able to work with industry and research to influence how the world provides clean and safe water.